THE
LONDON, EDINBURGH, AND DUBLIN
PHILOSOPHICAL MAGAZINE
AND
JOURNAL OF SCIENCE.

[SEVENTH SERIES.]

NOVEMBER 1931.

LXXXV. *Solutions of the Boundary-layer Equations* *. *By* V. M. FALKNER, *B.Sc., and* Miss S. W. SKAN, *of the National Physical Laboratory* †.

Introduction.

1. IT is known that when a body is immersed in a viscous fluid and the value of Reynolds' number is high the phenomena associated with viscosity occur almost wholly in a thin layer adjacent to the boundary. The boundary-layer equations, introduced by Prandtl in 1904 ‡, are so called from their application to the flow in this layer. These equations were derived from the full Navier-Stokes equations by retaining the first order terms only and using the physical conditions connected with a boundary.

In recent years much evidence has been brought forward to show that the assumptions on which the boundary-layer equations are based are very closely fulfilled over the range of Reynolds' number covered by model or full-scale aerofoils or other bodies placed in a wind-stream. The results of investigations into the flow near or at the surfaces of such

* The work described in this paper was carried out in the Aerodynamics Department of the National Physical Laboratory, and has been published by the Aeronautical Research Committee as R. & M. 1314. Permission to communicate the results has been kindly granted by the Committee.

† Communicated by E. F. Relf, A.R.C.Sc.

‡ L. Prandtl, 3rd International Mathematical Congress, Heidelberg, 1904.

bodies can be correlated with theory by finding solutions of the boundary-layer equations in terms of quantities which can easily be measured experimentally. This paper gives a particular solution and approximations to the general solution of the boundary-layer equations which may be applied with comparative ease to any case in which the pressure distribution along the boundary is known.

Notation.

2. V ≡ velocity of the general stream.
p_0 ≡ static pressure in the general stream.
p ≡ static pressure in the boundary layer.
v ≡ tangential velocity at the outer limit of the boundary layer.
q, w ≡ tangential and normal velocities in the boundary layer.
s, n ≡ distances along and normal to the boundary. The forward stagnation point is taken as the origin of s.
θ ≡ angular position of a point on the surface of a cylinder measured from the generator directed upstream.
r ≡ radius of cylinder.
ν ≡ kinematic coefficient of viscosity.
ρ ≡ density.
ψ ≡ stream function of fluid flow.
ψ_1, ϵ_1 ≡ non-dimensional functions defined by $\psi_1 = \psi s^{-\frac{1}{2}} \nu^{-\frac{1}{2}}$ and $\epsilon_1 = n s^{-\frac{1}{2}} v^{\frac{1}{2}} \nu^{-\frac{1}{2}}$.
$v_1, v_2, \ldots$ ≡ $dv/ds, d^2v/ds^2, \ldots$
l ≡ $v_1 s/v$.
$l_1, l_2, \ldots$ ≡ $dl/ds, d^2l/ds^2, \ldots$
$\mathrm{F}_1(s), \mathrm{F}_2(s)$ ≡ non-dimensional functions of s defined below.
$b_1, b_2, \ldots$; $c_1, c_2, \ldots$; m ≡ non-dimensional constants.
k ≡ constant.
F ≡ intensity of surface friction.

The Boundary-layer Equations.

3. The derivation of these equations and their transformation to a form suitable for application to an aerofoil or

boundary of any shape is described in a paper by Professor Bairstow *.

The equations are:—

$$q\frac{\partial q}{\partial s}+w\frac{\partial q}{\partial n}=-\frac{1}{\rho}\frac{\partial p}{\partial s}+\nu\frac{\partial^2 q}{\partial n^2}, \quad . \quad . \quad . \quad (1)$$

$$0=\frac{1}{\rho}\frac{\partial p}{\partial n}, \quad . \quad . \quad . \quad . \quad . \quad . \quad . \quad (2)$$

and there is also the equation of continuity,

$$\frac{\partial q}{\partial s}+\frac{\partial w}{\partial n}=0. \quad . \quad . \quad . \quad . \quad . \quad . \quad (3)$$

The physical conditions that there is no slip at the boundary and that the boundary is a stream-line are expressed by the inner boundary conditions

$$q=0, \quad w=0, \quad \text{when} \quad n\to 0,$$

and the condition that the tangential velocity becomes asymptotic to the value in the stream outside the boundary layer by the outer boundary condition

$$q/v=1 \quad \text{when} \quad n\to\infty.$$

On account of equation (2), $\frac{\partial p}{\partial s}$ becomes $\frac{dp}{ds}$.

The assumptions involved in the use of equations (1) to (3) are:—

(*a*) The flow is steady and two-dimensional.

(*b*) The boundary layer depends only upon the pressure gradient along the boundary, and is independent of the curvature of the boundary. The equations are therefore those strictly applicable to a straight boundary only.

(*c*) The pressure gradient normal to the boundary is negligible.

(*d*) The difference between the tangential and resultant velocities at the outer limit of the boundary layer is negligible.

(*e*) There are no appreciable viscous forces present in the stream except those due to the retarding action of the boundary.

* Bairstow, "Skin Friction," Journ. Roy. Aeronautical Soc., January 1925.

Previous Investigations.

4. A bibliography of previous investigations into methods of solution of these equations is given in a paper by Dr. Maccoll to the Royal Aeronautical Society*. Only those solutions which have a direct bearing upon the present work will be discussed here, the most important being that of Blasius†. Blasius simplified the equations by making $\frac{dp}{ds}=0$ (equivalent to $v=$constant), a condition approximately fulfilled at the surface of a thin flat plate placed parallel to the stream. By the introduction of the stream function ψ and the transformation of the equations by the use of the variables ψ_1, ϵ_1, and s (in the notation of this paper), instead of the system ψ, n, and s, the solution was found to be given completely by expressing ψ_1 as a function of ϵ_1 only.

It appears that Blasius' solution is a particular case of a more general solution derived by using the same transformation, but making v proportional to a power of s, *i. e.*, $v=ks^m$. Blasius' solution corresponds to $m=0$.

A solution which is applicable to the front portion of a cylinder has been given by Dr. Thom‡. This is based on the observation that near the front of a cylinder the tangential velocity in the boundary layer is independent of s. This basic condition is shown below to be one of the characteristics of the solution when the index m is made equal to unity.

A particular Solution of the Boundary-layer Equations when $v=ks^m$.

5. The procedure is similar to that adopted by Blasius. Equation (3) is satisfied by the stream function ψ where

$$q=-\frac{\partial\psi}{\partial n}, \quad \ldots\ldots\ldots \quad (4)$$

$$w=\frac{\partial\psi}{\partial s}. \quad \ldots\ldots\ldots \quad (5)$$

* Journ. Roy. Aeronautical Soc., August 1930.

† Blasius, 'Thesis,' Göttingen, 1907.

‡ Dr. Thom, "The Boundary Layer of the Front Portion of a Cylinder," Aeronautical Research Committee Reports and Memoranda, no. 1176.

As

$$p_0 + \tfrac{1}{2}\rho V^2 = p + \tfrac{1}{2}\rho v^2 = \text{const.},$$

$$\frac{1}{\rho}\frac{dp}{ds} = -vv_1, \quad . \quad . \quad . \quad . \quad . \quad . \quad . \quad (6)$$

and if

$$v = ks^m,$$

$$v_1 = mks^{m-1} = mvs^{-1},$$

and $$-vv_1 = -mv^2 s^{-1}.$$

Equations (1), (2), and (3) therefore become

$$\frac{\partial\psi}{\partial n}\cdot\frac{\partial^2\psi}{\partial s\,\partial n} - \frac{\partial\psi}{\partial s}\cdot\frac{\partial^2\psi}{\partial n^2} + \nu\frac{\partial^3\psi}{\partial n^3} - mv^2 s^{-1} = 0. \quad . \quad (7)$$

Transform this equation by using the variables s, ψ_1, and ϵ_1, instead of s, ψ, and n, where

$$\psi_1 = \psi s^{-\frac{1}{2}} v^{-\frac{1}{2}} \nu^{-\frac{1}{2}},$$

$$\epsilon_1 = n s^{-\frac{1}{2}} v^{\frac{1}{2}} \nu^{-\frac{1}{2}}.$$

The following relations are used to effect the transformation :—

$$\left(\frac{\partial}{\partial n}\right)_s = \left(\frac{\partial}{\partial \epsilon_1}\right)_s \left(\frac{\partial \epsilon_1}{\partial n}\right)_s, \quad . \quad . \quad . \quad . \quad . \quad (8)$$

$$\left(\frac{\partial}{\partial s}\right)_n = \left(\frac{\partial}{\partial s}\right)_{\epsilon_1} + \left(\frac{\partial}{\partial \epsilon_1}\right)_s \left(\frac{\partial \epsilon_1}{\partial s}\right)_n . \quad . \quad . \quad (9)$$

By using these relations the components of the terms of equation (7) are found, and after substitution and reduction this becomes

$$s\left[\frac{\partial\psi_1}{\partial\epsilon_1}\cdot\frac{\partial^2\psi_1}{\partial\epsilon_1\,\partial s} - \frac{\partial^2\psi_1}{\partial\epsilon_1^2}\cdot\frac{\partial\psi_1}{\partial s}\right]$$

$$+\left[m\left(\frac{\partial\psi_1}{\partial\epsilon_1}\right)^2 - \frac{m+1}{2}\psi_1\frac{\partial^2\psi_1}{\partial\epsilon_1^2} + \frac{\partial^3\psi_1}{\partial\epsilon_1^3} - m\right] = 0. \quad (10)$$

Subsequent analysis and calculation shows that solutions of this equation, in which ψ_1 can be expressed as a function of ϵ_1 only, can be made to satisfy the boundary conditions, and these solutions only will be considered in this paper.

As $\dfrac{\partial\psi_1}{\partial s}$ therefore becomes zero, equation (10) may be written

$$m\left(\frac{d\psi_1}{d\epsilon_1}\right)^2 - \frac{m+1}{2}\psi_1\frac{d^2\psi_1}{d\epsilon_1^2} + \frac{d^3\psi_1}{d\epsilon_1^3} - m = 0. \quad . \quad (11)$$

The transformed boundary conditions are

$$\psi_1 = 0, \quad \frac{d\psi_1}{d\epsilon_1} = 0, \qquad \text{when} \quad \epsilon_1 = 0, \quad . \quad (12)$$

and

$$\frac{d\psi_1}{d\epsilon_1} = -1, \quad \text{when} \quad \epsilon_1 \to \infty . \quad . \quad (13)$$

6. Equation (11) is apparently soluble only as a series. Let the solution be given by

$$\psi_1 = \alpha_0 + \alpha_1\epsilon_1 + \alpha_2\epsilon_1^2 + \alpha_3\epsilon_1^3 + \ldots, \quad . \quad . \quad . \quad (14)$$

where $\alpha_0, \alpha_1, \ldots$ are non-dimensional coefficients.

Condition (12) gives $\alpha_0 = 0$ and $\alpha_1 = 0$, and the series reduces to

$$\psi_1 = \alpha_2\epsilon_1^2 + \alpha_3\epsilon_1^3 + \alpha_4\epsilon_1^4 + \ldots \quad . \quad . \quad . \quad (15)$$

By substituting this series in equation (11), and equating to zero the coefficient of each power of ϵ_1, the relations between $\alpha_2, \alpha_3, \ldots$ can now be found.

These are

$$\alpha_3 = m/6,$$

$$\alpha_4 = 0,$$

$$\alpha_5 = -\frac{1}{60}(3m-1)\alpha_2^2,$$

$$\alpha_6 = -\frac{m(2m-1)}{180}\alpha_2,$$

$$\alpha_7 = \frac{-m^2(2m-1)}{2520},$$

and so on. Except for the first few, these coefficients are too complicated for general expression in terms of m, but can be evaluated for any particular value of m. Each coefficient is in terms of m and α_2, the latter of which must be found from the outer boundary condition (13).

For a flat plate $m = 0$ approximately, and it is possible to find the value of α_2 by analytical methods. Such a method is described in the paper by Professor Bairstow previously referred to. In the general case it is apparently necessary to resort to graphical methods for establishing the satisfaction of the outer boundary condition.

As

$$q/v = -\frac{d\psi_1}{d\epsilon_1} = -2\alpha_2\epsilon_1 - 3\alpha_3\epsilon_1^2 - 4\alpha_4\epsilon_1^3 - \ldots,$$

q/v can be plotted against ϵ_1 for a given value of m if a value for α_2 be assumed. The value of α_2 can be varied until the curve obtained becomes asymptotic to the line $q/v=1$. This method has been found to give the value of α_2 to close limits, as a slight variation in α_2 produces an increasingly greater variation in the shape of the curve as ϵ_1 increases. The difficulty due to the slow convergence of the series when ϵ_1 is great is fortunately avoided as the curve approaches very closely to the line $q/v=1$, while ϵ_1 is comparatively small.

Fig. 1.

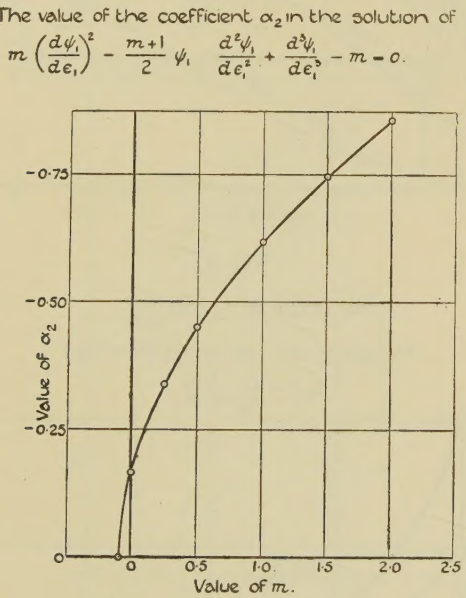

7. The solution of (11) has been found by the method outlined above for values of m ranging from $-0{\cdot}09$ to $2{\cdot}0$. These solutions are given graphically in figs. 1 and 2, fig. 1 showing the values of α_2, necessary for calculating the surface friction (see below), plotted against m, while fig. 2 gives q/v plotted against ϵ_1. It is estimated that the value of α_2 given by fig. 1 is within $0{\cdot}005$ of the correct value for values between $-0{\cdot}5$ and $-0{\cdot}85$. The possible error is increasingly greater as α_2 varies from $-0{\cdot}5$ to zero. The upper value of the range of m is limited by considerations of the values likely to occur in practice. Actually a solution is possible for any value of m beyond $2{\cdot}0$ up to ∞, the

limiting form of the curve of fig. 2 being easily seen to be the two lines $\epsilon_1 = 0$ and $q/v = 1$. The lower value of m, at which the value of α_2 becomes zero, is limited, however, by

Fig. 2.

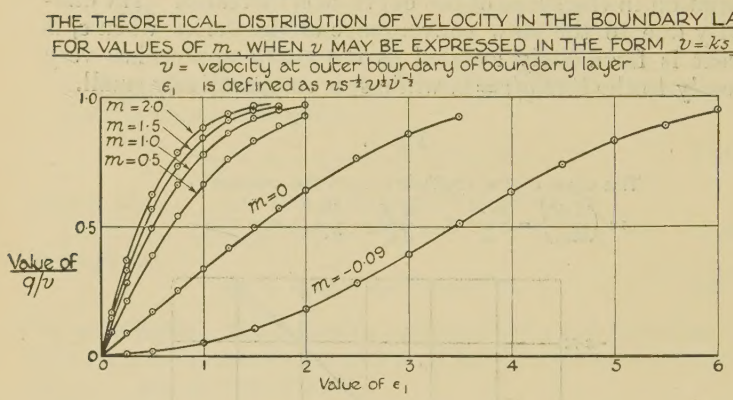

Fig. 3.

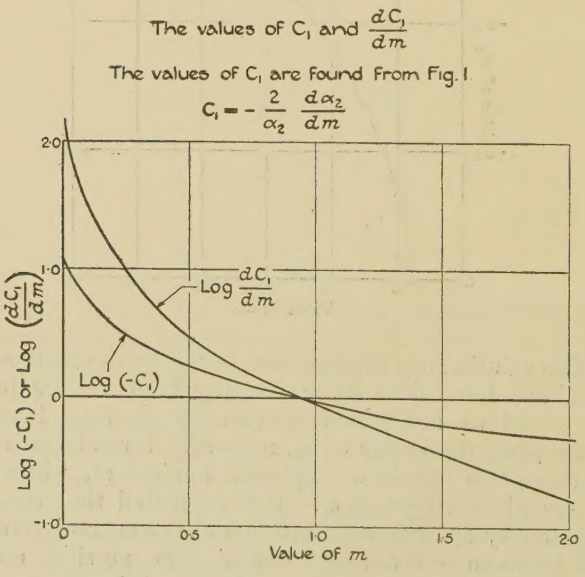

conditions imposed by the form of the equation and the boundary conditions. There is some doubt as to whether a solution is possible when m is more negative than $-0{\cdot}09$. This point is referred to again.

The solutions of equation (11) are also included in the solutions of a generalized form of equation (11) used in the approximation described below. These solutions are given numerically in Table I.* and graphically in figs. 4–8. From these figures the values of α_2 and q/v for selected values of ϵ_1 can be conveniently taken for any value of m. For this purpose the symbols $F_1(s)$ and $F_2(s)$ stand for m and $\frac{1}{2}(1+m)$ respectively.

Fig. 4.

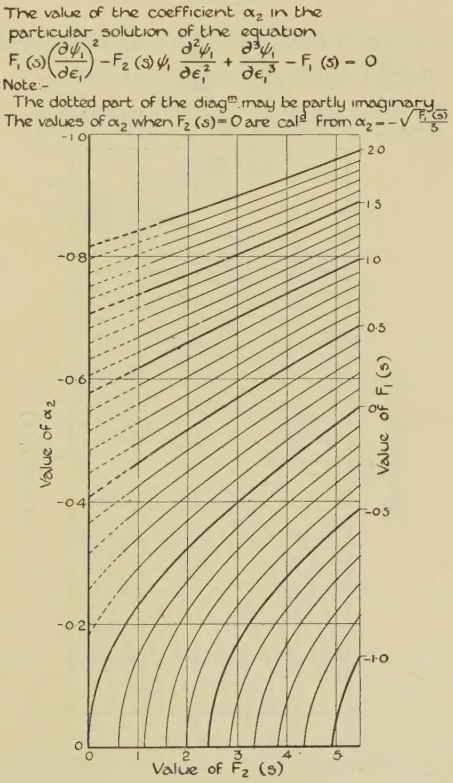

8. The surface friction depends upon the coefficient α_2. If F be the tangential force per unit area,

$$F = \rho\nu\left(\frac{\partial q}{\partial n}\right)_{n=0}.$$

* The figures from which figs. 1 and 2 were drawn are included in Table I.

As $n \to 0$, all terms in the expansion for q/v become negligible compared with the first, and therefore

$$q/v = -2\alpha_2\epsilon_1 \quad \text{and} \quad \frac{\partial q}{\partial n} = -2\alpha_2 v^{\frac{3}{2}} s^{-\frac{1}{2}} \nu^{-\frac{1}{2}},$$

from which

$$F = -2\alpha_2 \rho v^{\frac{3}{2}} \nu^{\frac{1}{2}} s^{-\frac{1}{2}}. \quad . \quad . \quad . \quad . \quad . \quad (16)$$

Fig. 5.

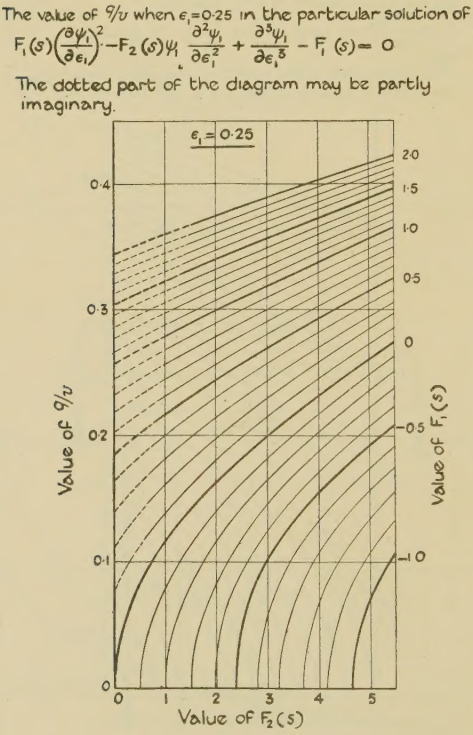

The General Equation.

9. Equation (11) is not the most general form of the boundary-layer equations, as it is derived by making v a definite function of s. The most general form is obtained when v is left arbitrary ; in this case, if similar transformations be effected to those used in the derivation of equation (10), equations (1), (2), and (3) reduce to

$$s\left[\frac{\partial\psi_1}{\partial\epsilon_1}\cdot\frac{\partial^2\psi_1}{\partial\epsilon_1\partial s}-\frac{\partial^2\psi_1}{\partial\epsilon_1^2}\cdot\frac{\partial\psi_1}{\partial s}\right]$$

$$+\left[l\left(\frac{\partial\psi_1}{\partial\epsilon_1}\right)^2-\frac{l+1}{2}\cdot\psi_1\frac{\partial^2\psi_1}{\partial\epsilon_1^2}+\frac{\partial^3\psi_1}{\partial\epsilon_1^3}-l\right]=0, \quad (17)$$

where $$l \equiv v_1 s/v.$$

Fig. 6.

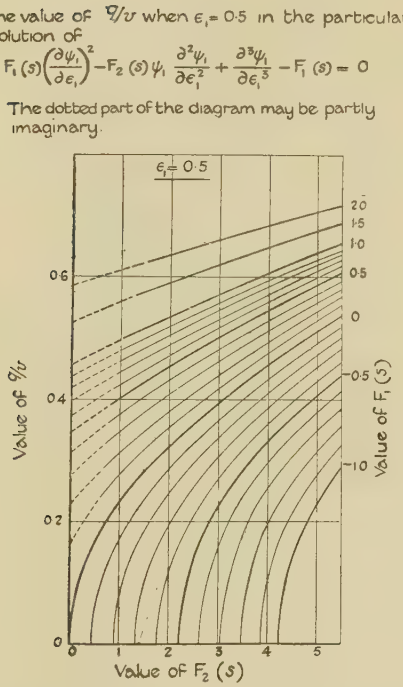

The only difference between this equation and equation (10) is that l is a function of s, whereas the corresponding quantity m is a constant.

The variable l is the slope of the curve of $\log_e v$ plotted against $\log_e s$:—

$$\frac{d(\log_e v)}{d(\log_e s)} = \frac{d(\log_e v)}{ds} \Big/ \frac{d(\log_e s)}{ds} = \frac{v_1 s}{v} = l.$$

It follows from the characteristics of the logarithmic curve

that $l \equiv m$ and is independent of s when $s \to 0$ or when v is expressed by the relation $v = ks^m$.

The values of $l_1 s$, $l_2 s^2$ ..., used below, are easily seen to be

$$\frac{d^2(\log_e v)}{d(\log_e s)^2}, \quad \frac{d^3(\log_e v)}{d(\log_e s)^3}, \quad \cdots$$

Fig. 7.

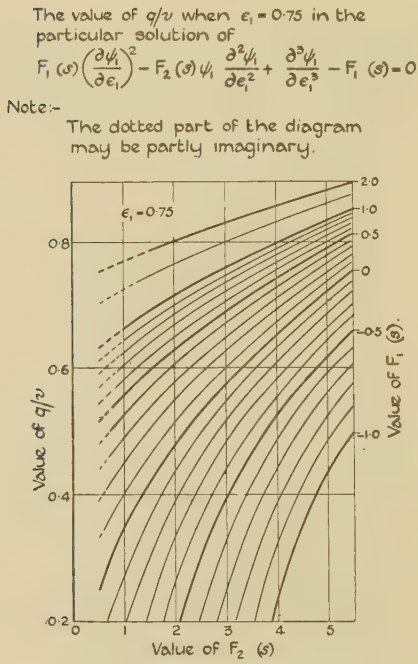

General Considerations.

10. Before detailing the methods of finding approximate solutions of equation (17) an account is given of the general considerations on which these are based.

The velocity gradient represented by $v = ks^m$ is that which occurs in two-dimensional potential flow between two straight walls meeting at an angle, v representing the fluid velocity at the wall and s being measured along either wall from the point of junction (the stagnation point when the angle of junction is less than π radians, and the point of infinite velocity when the angle is greater than π radians). By

considering the potential function of the flow * the index m can be shown to be $(\pi/\alpha - 1)$, where α is the angle between the walls. It is inferred, and it can be verified in the case of bodies for which there is a known solution of the potential equations (*e.g.*, lenticular form), that the same relation holds if the walls be curved provided that s be made small enough. If a body of any shape be placed in a stream the stagnation point can be regarded as the junction between two walls which are represented by part of the boundary and by the

Fig. 8

The value of q/v when $\epsilon_1 = 1{\cdot}0$ in the particular solution of

$$F_1(s)\left(\frac{\partial\psi_1}{\partial\epsilon_1}\right)^2 - F_2(s)\psi_1\frac{\partial^2\psi_1}{\partial\epsilon_1^2} + \frac{\partial^3\psi_1}{\partial\epsilon_1^3} - F_1(s) = 0$$

The dotted part of the diagram may be partly imaginary

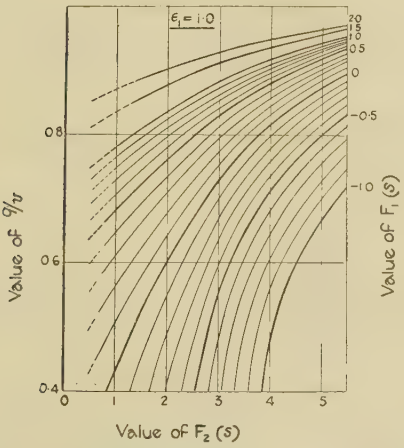

stream-line extending upstream from the stagnation point. Since, in the class of problems to which the solutions described below are applicable, the stream fulfils condition (*e*) of paragraph 3, there are no appreciable viscous forces in that part of the stream which is approaching the stagnation point. It is therefore reasonable to use as a basis for the solution the condition that the tangential velocity at the outer limit of the boundary layer is given by $v = ks^m$ as

* Glauert, 'Aerofoil and Airscrew Theory,' p. 56.

$s \to 0$. When a wedge is placed symmetrically with regard to the stream this relation is true for all values of s as the walls are straight; the solution described in § 7 is therefore directly applicable if the effect of the thickness of the layer on the velocity gradient be ignored.

Approximate Solutions.

First Approximate Solution.

11. The first part of equation (17) consists of two factors, one dependent on s and the other partly dependent on $\frac{\partial \psi_1}{\partial s}$, and vanishes either when $s=0$ or when $v=ks^m$, as in the latter case, if ψ_1 is a function of ϵ_1 only, $\frac{\partial \psi_1}{\partial s}=0$. In either case l becomes identical with m and equation (17) reduces to equation (11).

If s is very nearly zero, or if v has not deviated far from a value given by the relation $v=ks^m$, the first part of equation (17) may be considered negligible compared with the remainder. Equation (17) then reduces to

$$l\left(\frac{\partial \psi_1}{\partial \epsilon_1}\right)^2 - \frac{l+1}{2}\psi_1 \frac{\partial^2 \psi_1}{\partial \epsilon_1^2} + \frac{\partial^3 \psi_1}{\partial \epsilon_1^3} - l = 0. \quad . \quad (18)$$

The approximation called the first is that given by replacing equation (17) by (18).

12. The required particular solution of (18) satisfies the same boundary conditions as the particular solution of (11), and can be expanded in the form

$$\psi_1 = \alpha_2' \epsilon_1^2 + \alpha_3' \epsilon_1^3 + \ldots,$$

where $\alpha_2', \alpha_3', \ldots$ are functions of s only. It does not appear possible to find $\alpha_2', \alpha_3', \ldots$ as analytical functions of s, but these coefficients can be evaluated for any required value of s. Assuming for the moment that v is known for any value of s, the value of l can also be found. On assigning to l a definite value equation (18) becomes identical with equation (11), and the solution of (18) can therefore be found for as many values of s as desired by assigning to l the appropriate values, and using the solution of (11) described above (replacing m by l). The intensity of surface friction is again found by the relation given in § 8.

An example of this approximation applied to a cylinder is given below.

13. The presence of one function of s (i. e., l) in (18) suggests that the first approximation is equivalent to the identity of one only of the coefficients α_2', α_3', ... in the true * and approximate series for ψ_1. This is easily verified, as α_2', α_3', ... being functions of s only, retain their values when $\epsilon_1 \to 0$.

Let the approximate solution be

$$\psi_1 = \alpha_2' \epsilon_1^2 + \alpha_3' \epsilon_1^3 + \ldots, \quad . \quad . \quad . \quad . \quad (19)$$

and the true solution

$$\psi_1 = \alpha_2'' \epsilon_1^2 + \alpha_3'' \epsilon_1^3 + \ldots, \quad . \quad . \quad . \quad . \quad (20)$$

higher powers of ϵ_1 being neglected as ϵ_1 is to be made $\to 0$.

Considering first the true solution:

$$\frac{\partial \psi_1}{\partial \epsilon_1} = 2\alpha_2'' \epsilon_1 + 3\alpha_3'' \epsilon_1^2 + \ldots, \quad . \quad . \quad . \quad (21)$$

$$\frac{\partial^2 \psi_1}{\partial \epsilon_1^2} = 2\alpha_2'' + 6\alpha_3'' \epsilon_1 + \ldots, \quad . \quad . \quad . \quad . \quad (22)$$

$$\frac{\partial^3 \psi_1}{\partial \epsilon_1^3} = 6\alpha_3'' + \ldots, \quad . \quad . \quad . \quad . \quad . \quad . \quad . \quad . \quad (23)$$

$$\frac{\partial \psi_1}{\partial s} = \frac{d\alpha_2''}{ds} \cdot \epsilon_1^2 + \frac{d\alpha_3''}{ds} \epsilon_1^3 + \ldots, \quad . \quad . \quad (24)$$

$$\frac{\partial^2 \psi_1}{\partial \epsilon_1 \partial s} = 2\epsilon_1 \frac{d\alpha_2''}{ds} + 3\epsilon_1^2 \frac{d\alpha_3''}{ds} + \ldots \quad . \quad . \quad (25)$$

By substituting these expressions in (17), and neglecting all but the lowest power of ϵ_1, we obtain

$$6\alpha_3'' = l.$$

Similarly, by finding the corresponding derivatives for the approximate solution and substituting in (18), we obtain

$$6\alpha_3' = l;$$

$$\therefore \quad \alpha_3'' = \alpha_3' = l/6.$$

It appears, then, that the first approximation is equivalent to finding a solution satisfying the same boundary conditions as the true solution and having the coefficient α_3' identical with the corresponding coefficient in the series representing the true solution. It will be noted that the coefficient α_2',

* True refers to a true solution of the boundary-layer equations.

on which the surface friction depends, is not necessarily identical in the approximate and true solutions, and it may be supposed that the deviation of α_2' from its true value will define a limit beyond which the approximation is of no practical value.

Strictly speaking two coefficients are identical in the true and approximate solutions, as α_4 is always zero.

Second Approximate Solution.

14. Consider the equation

$$F_1(s)\left(\frac{\partial\psi_1}{\partial\epsilon_1}\right)^2 - F_2(s)\psi_1\frac{\partial^2\psi_1}{\partial\epsilon_1^2} + \frac{\partial^3\psi_1}{\partial\epsilon_1^3} - F_1(s) = 0, \quad (26)$$

where ψ_1 and ϵ_1 have the values defined in this paper and where $F_1(s)$ and $F_2(s)$ are functions of s only. The boundary conditions which must be used in finding the general solution of equation (17) are also applicable to this equation. Thus, with certain limits on the values of $F_1(s)$ and $F_2(s)$, equation (26) has a particular solution which satisfies the same boundary conditions as the required particular solution of (17). This solution of (26) will be understood by the expression "the particular solution of (26)."

The approximation called the second is that given by the assumption that the general equation (17) can be replaced by (26).

15. The necessary form of the functions $F_1(s)$ and $F_2(s)$ in (26) is readily deduced from a consideration of dimensional theory and of the limiting form assumed by equation (26) when $s\to 0$ or when l tends to a constant value (m).

If

$$F_1(s) = l + b_1 l_1 s + b_2 l_2 s^2 + \ldots, \quad . \quad . \quad . \quad . \quad (27)$$

and

$$F_2(s) = \tfrac{1}{2}[1 + l + c_1 l_1 s + c_2 l_2 s^2 + \ldots], \quad . \quad . \quad (28)$$

where $b_1, b_2, \ldots, c_1, c_2, \ldots$ are constants.

(a) The limiting form of (26) is correct when $s\to 0$ or when l tends to a constant value (m). In either case $F_1(s)$ and $F_2(s)$ reduce to l and $\frac{1}{2}(1+l)$ respectively, and the first part of equation (17) vanishes; thus (17) becomes identical with (26).

(b) $F_1(s)$ and $F_2(s)$ are arbitrary or unrestricted functions of s, for if $F_1(s)$ and $F_2(s)$ be assigned any definite values corresponding to a range of values of s, suitable values for the constants $b_1, b_2, \ldots, c_1, c_2, \ldots$ can always be found by

deducing from (27) and (28) as many relations as are required for their determination.

(*c*) $F_1(s)$ and $F_2(s)$ are non-dimensional, $b_1, b_2, \ldots$ and $c_1, c_2, \ldots$ being non-dimensional coefficients.

The second approximation may therefore be written

$$(17) \equiv (26). \quad . \quad . \quad . \quad . \quad . \quad . \quad (29)$$

16. This identity will obviously not be exact throughout the whole field, and the values of $F_1(s)$ and $F_2(s)$ must now be chosen with a view to making the approximation of practical value. Complete identity is preferable (perhaps only possible) as $\epsilon_1 \to 0$ for two reasons—firstly, the boundary-layer equations become more exact as the surface is approached, and, secondly, calculation of the surface friction is one of the most important applications of the solution. As there are two functions of (s), $F_1(s)$ and $F_2(s)$, in (26), it may be expected that two of the coefficients in the approximate and true expansions for ψ_1 in terms of ϵ_1 will be identical, α_2' and α_3' for choice.

As in the first approximation (§ 13), consider the expansion for ψ_1 in the true and approximate solutions. Let the approximate solution be

$$\psi_1 = \alpha_2'\epsilon_1^2 + \alpha_3'\epsilon_1^3 + \ldots, \quad . \quad . \quad . \quad . \quad (30)$$

and the true solution be

$$\psi_1 = \alpha_2''\epsilon_1^2 + \alpha_3''\epsilon_1^3 + \ldots, \quad . \quad . \quad . \quad . \quad (31)$$

$\alpha_2', \alpha_3', \ldots, \alpha_2'', \alpha_3'', \ldots$ being functions of s only. By substituting the expression (30) and its derivatives in (26), and neglecting all but the lowest power of ϵ_1, we obtain

$$6\alpha_3' = F_1(s).$$

Similarly, by substituting the expression (31) and its derivatives in (17), we obtain

$$6\alpha_3'' = l.$$

To make $\alpha_3' = \alpha_3''$ we put

$$F_1(s) = l; \quad . \quad . \quad . \quad . \quad . \quad . \quad (32)$$

$$\therefore \quad b_1 = b_2 = \ldots = 0.$$

The required value of $F_2(s)$ is that which will make $\alpha_2' \equiv \alpha_2''$. To determine the coefficients in the expansion for $F_2(s)$ use

is made of the identity (29). This is written in full, reduced by making use of (32), and becomes

$$s\left[\frac{\partial\psi_1}{\partial\epsilon_1}\cdot\frac{\partial^2\psi_1}{\partial\epsilon_1\partial s}-\frac{\partial^2\psi_1}{\partial\epsilon_1^2}\cdot\frac{\partial\psi_1}{\partial s}\right]$$
$$\equiv-\tfrac{1}{2}(c_1l_1s+c_2l_2s^2+\ldots)\psi_1\frac{\partial^2\psi_1}{\partial\epsilon_1^2}. \quad (33)$$

If this identity can be made exact for all values of s as $\epsilon_1\to0$, the approximate equation becomes identical with the true equation as $\epsilon_1\to0$, and it is assumed that the approximate solution becomes identical with the true solution as $\epsilon_1\to0$, *i. e.*, the value of α_2, the coefficient of the lowest power of ϵ_1, is identical in the approximate and true solutions. To investigate the conditions under which (33) becomes exact as $\epsilon_1\to0$, ψ_1 is again expanded in powers of ϵ_1. By substituting the expression for ψ_1 and its derivatives in (33), and retaining only the lowest power of ϵ_1, we obtain

$$\frac{2}{\alpha_2'}\cdot\frac{d\alpha_2'}{ds}=-(c_1l_1+c_2l_2s+\ldots), \quad . \quad . \quad . \quad (34)$$

a condition which is satisfied for all values of s by assigning appropriate values to the constants, c_1, c_2, ...

If, therefore, in equation (26) $F_1(s)$ and $F_2(s)$ be given the values l and $\frac{1}{2}(1+l+c_1l_1s+\ldots)$ respectively, where the coefficients c_1, c_2, ... are determined by relation (34), the first two coefficients of the expansion for ψ_1 in the resulting solution are identical with the first two coefficients in the true solution of equation (17). Thus the surface friction, which depends on the first coefficient α_2, can be found by the use of equation (26). Strictly speaking, the first three coefficients in the approximate and true solutions are identical, as α_4 is always zero.

17. The coefficients $c_1, c_2, \ldots$ can be evaluated from relation (34) by assuming that each term of the series is negligible compared with the preceding term as $s\to0$. Omitting all but the first term,

$$\frac{2}{\alpha_2'}\cdot\frac{d\alpha_2'}{ds}=-c_1l_1\,;$$

$$\therefore \quad c_1=\left(-\frac{2}{\alpha_2'}\cdot\frac{d\alpha_2'}{ds}\cdot\frac{1}{l_1}\right)_{s=0}=\left(-\frac{2}{\alpha_2'}\cdot\frac{d\alpha_2'}{dl}\right)_{s=} \quad . \quad . \quad (35)$$

Next, including the first two terms,

$$\frac{2}{\alpha_2'}\cdot\frac{d\alpha_2'}{ds} = -(c_1 l_1 + c_2 l_2 s),$$

$$c_2 l_2 s = \left(-\frac{2}{\alpha_2'}\cdot\frac{d\alpha_2'}{dl} - c_1\right) l_1,$$

$$c_2 = \left(\frac{l_1}{l_2}\cdot\frac{dc_1}{ds}\right)_{s=0} = \left(\frac{l_1^2}{l_2}\cdot\frac{dc_1}{dl}\right)_{s=0} \quad . \quad . \quad . \quad . \quad (36)$$

Again, including the first three terms,

$$\frac{2}{\alpha_2'}\cdot\frac{d\alpha_2'}{ds} = -(c_1 l_1 + c_2 l_2 s + c_3 l_3 s^2),$$

$$c_3 = \left[\frac{l_1^3}{l_3}\cdot\frac{d^2 c_1}{dl^2}\right]_{s=0} \quad . \quad . \quad . \quad . \quad . \quad . \quad (37)$$

Further coefficients can be found similarly.

18. The coefficients $c_1, dc_1/dl, \ldots$ can be evaluated from the known solution of (17) when $s \to 0$. Since, when $s \to 0$, l is replaceable by m, the coefficients may be written

$$c_1 = -\frac{2}{\alpha_2}\cdot\frac{d\alpha_2}{dm}, \quad . \quad . \quad . \quad . \quad . \quad (38)$$

$$c_2 = \left(\frac{l_1^2}{l_2}\right)\frac{dc_1}{dm}, \quad . \quad . \quad . \quad . \quad . \quad (39)$$

and so on.

The expressions c_1, $\dfrac{dc_1}{dm}$, ... can now be derived graphically from fig. 1, in which α_2 is plotted against m. The first two of these expressions are plotted in fig. 3. It will be noted that the coefficients $c_1, c_2, \ldots$ to be used in any problem depend entirely upon the values of $l, l_1, l_2, \ldots$ when $s=0$.

19. The series for $F_2(s)$ is evidently convergent for small values of s, but it may become divergent at large values. Even if convergence still occurs when s is large the approximate solutions, as applied to any problem, may be expected to diverge from the true solutions in some cases, as it is necessary to assume that the value of $F_2(s)$ is that found by neglecting all but the first few terms. It is only possible to find a few of the coefficients $c_1, c_2, \ldots$ with any accuracy, as these contain, not only the expressions $\dfrac{dc_1}{dm}, \dfrac{d^2c_1}{dm^2}, \ldots$, but

also $l_1, l_2 \ldots$, and the difficulty in finding such derivatives accurately by graphical means is well known. It will remain for experiment to show whether this limitation is operative before the known limit of the solution, *i. e.*, the value of s at which breakdown into turbulent flow begins.

20. It does not appear possible to find the solution of (26) unless particular values be assigned to $F_1(s)$ and $F_2(s)$. The equation has therefore been solved for a range of values of these functions likely to occur in normal problems. The method of solution is similar to that used in finding the particular solution of (11). For a definite pair of values of $F_1(s)$ and $F_2(s)$ the solution was assumed to be a series of the form

$$\psi_1 = \alpha_0 + \alpha_1\epsilon_1 + \alpha_2\epsilon_1^2 + \ldots$$

The application of the inner boundary conditions reduces this to

$$\psi_1 = \alpha_2\epsilon_1^2 + \alpha_3\epsilon_1^3 + \ldots$$

By substituting this series in the original equation the coefficients were expressed in terms of the first coefficient, α_2. The latter was then found by trial by assuming values for α_2 and demonstrating graphically the satisfaction or otherwise of the outer boundary condition $q/v = 1$ as $\epsilon_1 \to \infty$.

For each pair of values of $F_1(s)$ and $F_2(s)$ a value of α_2 and a series for ψ_1 expressible graphically as the tangential velocity in the boundary layer can be found. Table I. gives the numerical solutions for a range of values of $F_1(s)$ and $F_2(s)$. These results are most convenient for use when presented in a graphical form, and this has been done in figs. 4–8. Fig. 4 gives the values of α_2 corresponding to values of $F_1(s)$ and $F_2(s)$, and figs. 5–8 the values of q/v for a range of values of ϵ_1 from 0·25 to 1·0.

The diagrams were constructed entirely from the figures given in Table I. with the exception of fig. 4, which includes calculated values when $F_2(s) = 0$. (These values lead to incorrect or imaginary solutions: see § 22.) Each figure has been checked and faired when necessary by plotting also the lines of constant value of $F_2(s)$ and α_2 or q/v against the remaining quantities as abscissa and ordinate. The diagrams tend to become inaccurate at the greatest negative values of $F_1(s)$, owing to the increasing rate of change of α_2 and q/v with $F_2(s)$ as $F_1(s)$ becomes more negative. The general accuracy of the diagrams is estimated to be the same as that of figs. 1 and 2, referred to in § 7. It is interesting to note that the lines of constant value of $F_1(s)$ in fig. 4 appear to

TABLE

Numerical Particular Solu

$$F_1(s)\left(\frac{\partial\psi_1}{\partial\epsilon_1}\right)^2 - F_2(s)\psi_1\frac{\partial^2\psi}{\partial\epsilon_1}$$

$F_1(s)$	−1·0	−1·0	−0·75	−0·5	−0·5	−0·5	−0·25	0	0	0	0
$F_2(s)$	4·95	5·5	3·65	2·375	3·0	5·5	1·25	0·25	0·5	1·75	3·0
$-\alpha_2$	0	0·15	0	0	0·175	0·39	0	0·118	0·166	0·306	0·4

ϵ_1.											Valu
0·125	0·008	0·045	0·006	...	...	0·101	...	...	...	...	..
0·25	0·031	0·106	0·023	0·016	0·103	0·210	0·008	...	...	0·153	0·2
0·375	0·070	0·180	0·053	...	...	0·324	...	...	...	...	..
0·50	0·124	0·270	0·094	0·062	0·235	0·439	0·031	0·118	0·166	0·304	0·3
0·625	0·193	0·369	0·145	...	...	0·554	...	...	...	...	..
0·75	0·275	0,475	0·208	0·140	0·392	0·661	0·070	...	...	0·450	0·5
0·875	0·368	0·584	0·280	...	...	0·754	...	...	...	...	..
1·00	0·467	0·683	0·361	0·246	0·557	0·832	0·124	0·235	0·330	0·587	0·7
1·10	...	...	...	...	...	...	...	...	...	...	..
1·125	0·569	0·774	0·447	...	0·638	0·893	...	...	...	...	..
1·15	...	0·792	...	...	...	...	...	...	...	...	..
1·25	0·666	0·848	0·534	0·376	0·713	0·933	0·193	...	...	0·704	0·8
1·375	0·754	0·906	0·621	...	0·780	0·967	...	...	...	...	..
1·50	0·830	0·943	0·703	0·518	0·839	...	0·275	0·351	0·486	0·803	0·9
1·625	0·888	...	0·778	...	0·889	...	...	...	...	...	..
1·75	0·935	...	0·841	0·659	0·927	...	0·368	...	...	0·875	0·9
1·875	...	...	0·893								
2·00	...	...	0·934	0·784	...	...	0·467	0·463	0·630	0·925	.
2·10	...	...	0·956								
2·25	...	...	...	0·883	...	...	0·568	...	...	0·957	..
2·50	...	...	...	0·952	...	..	0·665	0·568	0·751	0·977	..
2·75	...	...	...	...	...	...	0·753	...	...	...	..
3·00	...	...	...	...	...	...	0·830	0·665	0·847		
3·25	...	...	...	...	...	...	0·890				
3·50	...	...	...	...	...	...	0·931	0·750	0·913		
3·75	...	...	...	...	...	...	0·962				
4·00	...	...	...	...	...	...	...	0 821	0·954		
4·50	...	...	...	...	...	...	...	0·877			
5·00	...	...	...	...	...	...	...	0·920			
5·50	...	...	...	...	...	...	...	0·952			
6·00	...	...	...	...	...	...	...	0·971			

[*To face page* 884.

I.

tions of the Equation

$$\frac{\partial^3 \psi_1}{\partial \epsilon_1^3} - F_1(s) = 0.$$

	0	0·05	0·5	0·5	1·0	1·0	1·0	1·0	1·5	2·0	2·0	2·0
	5·5	0·75	3·0	5·5	0·75	1·0	3·0	5·5	1·25	1·5	3·0	5·5
00	0·555	0·450	0·570	0·687	0·607	0·617	0·700	0·795	0·747	0·858	0·902	0·975

of q/v.

.	0·139	...	...	...	...	...	0·167	0·191	0·175	0·198	0·209	0·228
00	0·276	0·209	0·269	0·326	0·272	0·279	0·319	0·365	0·327	0·367	0·389	0·423
.	0·410	...	...	...	...	...	0·453	0·521	0·456	0·508	0·538	0·587
95	0·538	0·389	0·502	0·607	0·487	0·495	0·572	0·654	0·568	0·622	0·660	0·718
.	0·654	...	..	0·721	...	...	0·675	0·765	...	0·714	0·756	0·821
76	0·755	0·537	0·690	0·813	0·647	0·660	0·760	0·850	0·733	0·787	0·831	0·894
.	0·835	...	...	0·886	...	...	0·828	0·911	...	0·843	0·887	0·943
29	0·897	0·658	0·830	0·936	0·766	0·779	0·882	0·956	0·844	0·887	0·929	0·973
.	...	...	...	...	...	...	...	0·980	...	...	...	0·989
.	0·942	...	0·881	0·973	...	...	0·924	...	...	0·919	0·956	
.	...	...	...	...	...	...	...	0·985	...	...	...	0·993
44	0·971	0·754	0·920	...	0·849	0·863	0·956	...	0·913	0·946	0·977	
.	...	...	0·950	...	...	...	0·976	...	...	0·960	0·989	
17	...	0·829	0·968	...	0·906	0·919	0·991	...	0·957	0·978	0·997	
.	...	...	...	...	...	...	...	...	...	0·984	0·984	
30	..	0·884	...	...	0·944	0·956	...	...	0·977	0·991		
.	...	0·924	...	...	0·971	0·979	...	...	0·992			
.	...	0·951	...	...	0·986	0·990						
.	...	0·971	...	...	0·997							
.	...	0·982										

cut the base line $\alpha_2=0$ orthogonally, although the equation gives no simple indication that this is a definite property of the diagram.

21. There are certain limits to the values of $F_1(s)$ and $F_2(s)$ outside which the required solution of (26) apparently cannot be found. If $F_1(s)$ be considered constant, the sign of $\frac{\partial^3\psi_1}{\partial\epsilon_1^3}$ will depend to some extent on the value of $F_2(s)$, and the solutions given in this paper, which are such that, as $\epsilon_1\to\infty$, $\frac{\partial^3\psi_1}{\partial\epsilon_1^3}\to 0$ from a positive value (or, more simply, that q/v does not exceed the value 1), are not consistent with the assignation to $F_2(s)$ of any arbitrary value entirely independent of $F_1(s)$. These limits have become apparent in solving the equation. The graphical method appeared to show that, if the value of $1+\frac{1}{2}F_1(s)$ exceeded the value of $F_2(s)$ by more than a certain amount (not constant), the outer boundary condition could not be satisfied for any value of α_2. The particular solution of (26) appears to be discontinuous; the approximate boundary of discontinuity is shown in figs. 4–8, but more work would be necessary to fix its position accurately. Only those parts of the diagram given in full lines have been verified to lead to true solutions (as defined), and the remaining parts, represented by dotted lines, may lead to solutions which do not satisfy the outer boundary condition.

No attempt has been made to extend the solutions to cover positive values of α_2, owing to the great amount of work involved in the graphical application of the outer boundary condition. As α_2 becomes positive it is necessary to take a very great number of terms in the expansion for ψ_1 in order to ensure convergence to a limit, and the work becomes almost unmanageable.

22. There is one particular case in which the solution of (26) can be found analytically.

When $F_2(s)=0$, (26) reduces to

$$F_1(s)\left(\frac{\partial\psi_1}{\partial\epsilon_1}\right)^2+\frac{\partial^3\psi_1}{\partial\epsilon_1^3}-F_1(s)=0. \quad . \quad . \quad (40)$$

Multiply through by $\frac{\partial^2\psi_1}{\partial\epsilon_1^2}$, and integrate with respect to ϵ_1,

$$\frac{1}{3}F_1(s)\left(\frac{\partial\psi_1}{\partial\epsilon_1}\right)^3+\frac{1}{2}\left(\frac{\partial^2\psi_1}{\partial\epsilon_1^2}\right)^2-F_1(s)\frac{\partial\psi_1}{\partial\epsilon_1^2}+A=0.$$

The outer boundary conditions are

$$\frac{\partial^2\psi_1}{\partial\epsilon_1^2}=0, \quad \frac{\partial\psi_1}{\partial\epsilon_1}=-1, \text{ when } \epsilon_1\to\infty;$$

$$\therefore \qquad A=-\tfrac{2}{3}F_1(s).$$

The inner boundary conditions are

$$\psi_1=0, \quad \frac{\partial\psi_1}{\partial\epsilon_1}=0 \quad \text{when } \epsilon_1=0.$$

Also, when $\epsilon_1\to 0$, $\dfrac{\partial^2\psi_1}{\partial\epsilon_1^2}\to 2\alpha_2$;

$$\therefore \qquad \alpha_2=\pm\sqrt{\tfrac{1}{3}F_1(s)}. \quad . \quad . \quad . \quad . \quad . \quad . \quad (41)$$

When the negative values of α_2, calculated from this relation, are plotted in fig. 4 they lie in that part of the diagram which does not lead to true solutions, but their position confirms both the accuracy of the values of α_2 found by the graphical method and the fact that there is a true discontinuity in the solution of (26). The relation (41), with its two values for α_2, in conjunction with the appearance of fig. 4, suggests that the completed diagram may be symmetrical about the line $\alpha_2=0$. Further work would be necessary to establish or disprove the symmetry and to discover whether it extends to the line of discontinuity.

It is surmized that, if the diagram is symmetrical about the line $\alpha_2=0$, the lines of discontinuity will be arranged so that it is only possible to find one true value for α_2 corresponding to given values of $F_1(s)$ and $F_2(s)$. No explanation is offered as to the meaning of the remainder of the diagram.

23. A closer approximation to the tangential velocity in the boundary layer than that given by the second approximation can be found by using the calculated values of α_2 in the original equation (17).

Let the true solution of (17) be

$$\psi_1=\alpha_2\epsilon_1^2+\alpha_3\epsilon_1^3+\ldots.$$

By substituting this expression and its derivatives in equation (17), and equating to zero the coefficients of each power of ϵ_1, a series of equations is obtained:

$$\epsilon_1^0 : 6\alpha_3=l,$$

$$\epsilon_1 \; : \; \alpha_4=0,$$

$$\epsilon_1^2 : 2\alpha_2 s\frac{d\alpha_2}{ds}+\alpha_2^2(3l-1)+60\alpha_5=0,$$

$$\epsilon_1^3 : 4\alpha_2 s\frac{d\alpha_3}{ds} + 4\alpha_2\alpha_3(2l-1) + 120\alpha_6 = 0,$$

$$\epsilon_1^4 : 3\alpha_3 s\frac{d\alpha_3}{ds} + 3\alpha_3^2(2l-1) + 210\alpha_7 = 0,$$

and so on.

By using the values of α_2 calculated from equation (26) the true coefficients α_5, α_6 ... can be found successively from this series of equations. As, however, a new derivative which must be found by graphical means is introduced by each equation, it is probable that cumulative errors would lead to a breakdown of the process after a few of the coefficients had been determined.

Summary of Procedure.

24. The approximate solution is given by using, instead of (17), the equation

$$F_1(s)\left(\frac{\partial\psi_1}{\partial\epsilon_1}\right)^2 - F_2(s)\psi_1\frac{\partial^2\psi_1}{\partial\epsilon_1^2} + \frac{\partial^3\psi_1}{\partial\epsilon_1^3} - F_1(s) = 0, \quad (42)$$

where

$$F_1(s) = l,$$

$$F_2(s) = \tfrac{1}{2}(1 + l + c_1 l_1 s + c_2 l_2 s^2 + \ldots),$$

and

$$\frac{2}{\alpha_2}\frac{d\alpha_2}{ds} = -[c_1 l_1 + c_2 l_2 s + \ldots], \quad . \quad . \quad . \quad . \quad (43)$$

the latter relation being found from the condition that (42) is identical with (17) when $\epsilon_1 \to 0$.

Relation (43) leads to the following values for the coefficients c_1, c_2, ...

$$c_1 = -\frac{2}{\alpha_2}\cdot\frac{d\alpha_2}{dm},$$

$$c_2 = \left(\frac{l_1}{l_2}\right)_{s=0}^2\frac{dc_1}{dm},$$

and so on, where the relation between α_2 and m is that given graphically in fig. 1. The solution of (42) is given numerically in Table I. and graphically in figs. 4–8 for a range of values of $F_1(s)$ and $F_2(s)$. To apply the solution to any problem, assuming that v is known as a function of s,

(*a*) Tabulate l, l_1, l_2, ... for those values of s at which the surface friction or tangential velocity in the boundary layer is required.

(*b*) Using the value found or deduced for l when $s=0$, find the corresponding values of c_1, $\frac{dc_1}{dm}$, from fig. 3.

(*c*) Find c_2, c_3, ... by using the values of $l_1, l_2, \ldots$ when $s=0$ and the values of $\frac{dc_1}{dm}$, ... found as in (*b*).

(*d*) Tabulate $F_1(s)=l$.

(*e*) Tabulate $F_2(s)=\frac{1}{2}(1+l+c_1l_1s+\ldots)$.

(*f*) Find the value of α_2, or the tangential velocity in the boundary layer, for any required value of s by using the corresponding values found for $F_1(s)$ and $F_2(s)$ in figs. 4–8.

(*g*) The intensity of surface friction is

$$F=-2\alpha_2\rho v^{3/2}\nu^{1/2}s^{-1/2}.$$

The solution given by adopting the above procedure has been described as the second approximate solution throughout the paper. The first approximation is given when $F_2(s)$ is put equal to $\frac{1}{2}(1+l)$.

Comparison with Experiment.

25. Amongst experimental investigations of the boundary layer which have been recorded, the most suitable for comparison with theory are those of (*a*) a plate placed in a stream parallel to the wind direction, and (*b*) a cylinder placed in a stream with the axis at right angles to the wind direction.

The theoretical results used in the comparisons below are based on the measured values of the normal pressure at the surface of the body. The calculations on this basis are simpler than those which begin with the pressure due to potential flow, but it is considered that they are adequate for an initial investigation into the utility of the approximations given in this paper. The most satisfactory comparison between theory and experiment is that of the calculated and observed values of the intensity of surface friction, as this, in the general case, is the most accurate quantity derived from the second approximation. In one case the theoretical and measured values of the tangential velocity in the boundary layer are compared as a matter of interest, the values given by the second approximate solution, at finite values of s, being at best an approximation to an approximation (except when $s=0$ or $v=ks^m$, in which cases they are correct).

26. *Plate.*—An investigation into the boundary layer and surface friction of a plate placed parallel to a wind-stream was made by Burgers and Van der Hegge Zignen*. It is known that the results of this investigation are not in exact agreement with those predicted by Blasius' solution. Better agreement between theory and experiment is obtained at the front of the plate if allowance be made for the pressure drop along the plate due the shaped nose

The shape of the plate is described on p. 6 of 'Thesis Delft,' 1924 ; it is 1·2 cm. thick and is sharpened at the nose over a length of about 15 cm. with a radius of curvature of 75 cm. The two latter figures are not in entire agreement, but for the purpose of calculation the figure given for the radius for curvature is taken to be correct.

In order to estimate the true velocity gradient along the plate at the nose it is assumed that it is that due to potential flow past a body of lenticular form. This form is a special case of the generalized Joukowsky Aerofoil †, and the values of l, l_1, ... can be calculated from the known formula for v. The work is tedious when s is finite, but the values of $l_{s=0}$ and $l_{1s=0}$ have been calculated, and for the plate described are 0·042 and 0 respectively. For a wedge with the same nose-angle the values of l, l_1, ... are easily deduced as $v=ks_m$ (see § 10) :

$$l = 0{\cdot}042, \quad l_1 = l_2 = \ldots = 0$$

for all values of s. Thus the effect of the nose of the plate is to introduce a pressure drop at the nose equivalent to a value for m of 0·042 in equation (11), instead of 0, as in Blasius' solution.

The theoretical values of the tangential velocity in the boundary layer when $s=0$ are plotted in fig. 9 for $m=0{\cdot}042$ and $m=0$. For comparison the experimental values are plotted for some of the lowest values of s recorded in the experiments for the wind speeds V = 800, 1200, 1600, and 2400 cm. per second. This comparison shows that the experimental observations at the lowest values of s lie more closely to the solution obtained when $m=0{\cdot}042$ than when $m=0$. At the higher speeds the points do not always lie on curve 2, but they indicate that the slope of 2 is the more correct.

* 'Thesis Delft,' 1924.

† See Glauert, "A Generalized Type of Joukowsky Aerofoil," R. & M. 911 ; also Fage, Falkner, and Walker, "Experiments on a Series of Symmetrical Joukowsky Sections," R. & M. 1241.

27. *Cylinder.*—The experimental results used in this comparison are those given in 'Reports and Memoranda,' no. 1179, in which an investigation of the boundary layer of a 8·9-in. diameter cylinder was described ; in R. & M. 1231, in which the surface friction of this cylinder was deduced by considerations of momentum loss; and in R. & M. 1369, in which the surface friction of two cylinders, 6 in. and 3 in. diameters respectively, was measured directly by means of surface tubes similar in principle to those first used by Sir Thomas Stanton.

Fig. 9.

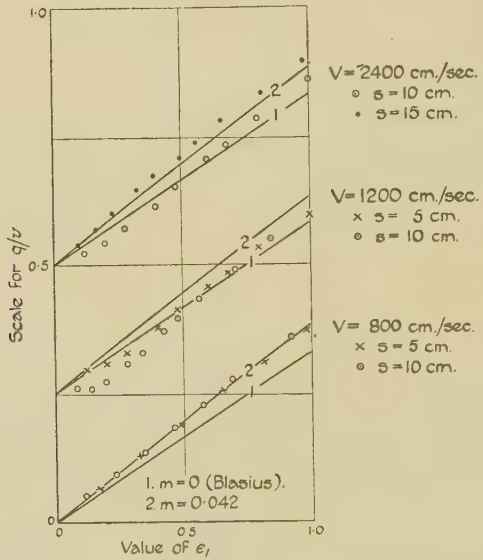

Comparison between theoretical and experimental velocity in the boundary layer near the front of Burgers' plate.

The values of l and l_1, used in the calculation of the solution, were obtained by graphical means from the experimental relations between v/V and s. It was assumed that, as $s \to 0$, the value of v/V approaches the theoretical value for potential flow ($2 \sin \theta$), and therefore $l_{(s=0)} = 1$. It was necessary to make this assumption as, near the stagnation point of a cylinder, slight experimental errors in the measurement of pressure produce a large variation in the apparent

value of l calculated graphically. Since $l_{(s=0)}=1$, the coefficient $c_1=-0{\cdot}925$. To find the coefficient c_2 we require $\left(\frac{l_1}{l_2}\right)^2_{(s=0)}$: it is again necessary to use theoretical means.

If $v/\mathrm{V}=2\sin\theta$,

$$l=\frac{v_1 s}{v}=\theta\cot\theta, \qquad \therefore\ l_{(\theta=0)}=1.$$

l may be expanded in powers of θ :

$$l=1+a_2\theta^2+a_3\theta^3+\ldots,$$

$$l_1\left(\frac{ds}{d\theta}\right)=2a_2\theta+3a_3\theta^2+\ldots,$$

$$l_2\left(\frac{ds}{d\theta}\right)^2=2a_2+6a_3\theta+12a_4\theta^2;$$

$$\therefore \qquad l_{1\,(\theta=0)}=0,$$

$$l_{2\,(\theta=0)}=2a^2\left(\frac{d\theta}{ds}\right)^2;$$

$$\therefore \quad \left(\frac{l_1^2}{l^2}\right)_{\theta=0}=0.$$

Similarly, $\left(\frac{l_1^3}{l^3}\right)_{\theta=0}=0$, and so on;

$$\therefore \quad c_2=c_3=\ldots=0.$$

It is reasonable to assume that the error involved in taking each of these coefficients to be zero is no greater than that which would be present if an attempt were made to determine their values from the measured values of the normal pressure at the circumference.

For all circular cylinder work therefore

$$l_{(s=0)}=1, \qquad c_1=-0{\cdot}925, \qquad c_2=c_3=\ldots=0.$$

These figures are also usually applicable to an aerofoil section with a rounded leading edge, as the same difficulties arise in the determination of $l_{(s=0)}$ and its derivatives.

28. Figs. 10–13 give graphically the comparison between theory and experiment for the 8·9-inch diameter cylinder of R. & M. 1179. In order to give an idea of the magnitude of the quantities involved a part of the calculation for the wind-speed 71·4 feet per second is given in Table II.

TABLE II.

Second Approximate Solution of the Boundary-layer Equations for an 8·9-inch diameter Cylinder in a 4-ft. Wind-tunnel.

$V = 71{\cdot}4$ ft. per second.

$\theta°$.	$F_1(s)$.	$c_1 l_1 s$.	$F_2(s)$.	$-\alpha_2$.	$(v/V)^{3/2}$.	$(\nu/Vs)^{1/2} \times 10^3$.	$F/\rho V^2 \times 10^3$.
0	1·000	0	1·000	0·616	0	∞	0
10	0·998	0·018	1·008	0·615	0·201	5·86	1·45
20	0·980	0·055	1·018	0·614	0·555	4·15	2·82
30	0·940	0·139	1·039	0·604	0·982	3·38	4·01
40	0·874	0·278	1·076	0·588	1·485	2·93	5·11
50	0·770	0·480	1·125	0·559	1·988	2·62	5·83
60	0·637	0·795	1·216	0·523	2·390	2·39	5·99
70	0·470	1·258	1·364	0·473	2·712	2·22	5·68
80	0·228	2·357	1·792	0·410	2·93	2·07	4·98
90	−0·310	7·580	4·135	0·362	2·94	1·95	4·16

Fig. 10.

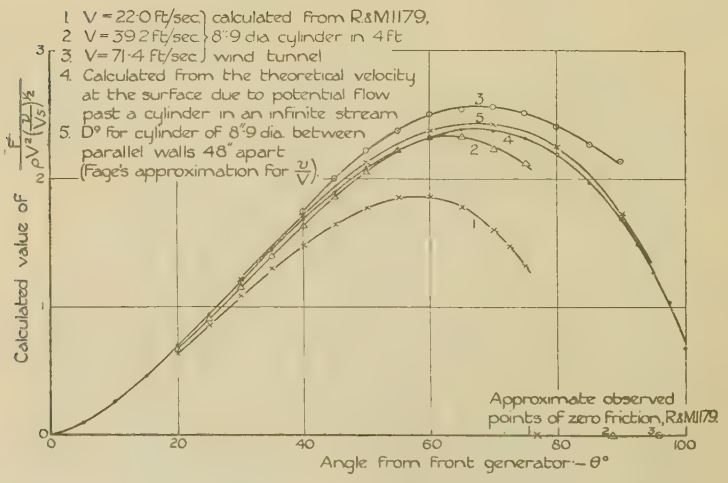

Surface friction of a circular cylinder, calculated from the experimental pressure distribution at the circumference (second approximation).

Fig. 10 gives the values of

$$\frac{F}{\rho V^2 \left(\frac{\nu}{V s}\right)^{1/2}}$$

from the second approximation, plotted against θ for three wind-speeds, 22·0, 39·2, and 71·4 feet per second. For comparison the figure includes curves calculated from the theoretical velocity at the surface due to potential flow past a cylinder in an infinite stream and an 8·9-inch diameter cylinder between parallel walls 48 inches apart, allowing for interference effects by Mr. Fage's approximate method *. The figure shows that, at the highest wind-speed, the calcu-

Fig. 11.

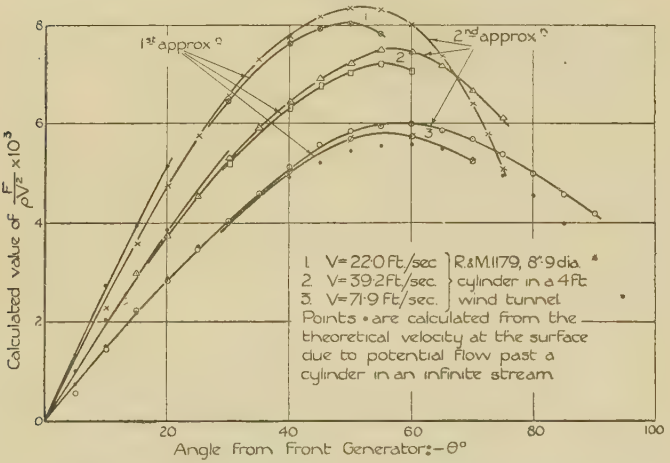

Surface friction of a circular cylinder calculated from the experimenta pressure distribution at the circumference.

lated friction is fairly close to that calculated from the velocity due to potential flow. The curves are limited partly by uncertainty as to the value of l_1, and they do not continue as far as the points at which the friction becomes zero. On the same figure the approximate observed angles at which the friction is zero are plotted.

In fig. 11 the values of $\frac{F}{\rho V^2}$, given by the first and second approximations, are plotted against θ for the same three

* Fage, "On the Two-Dimensional Flow Past a body of Symmetrical Cross-section Mounted in a Channel of Finite Breadth," R. & M 1223.

wind-speeds. This figure allows an estimate to be made of the order of difference between the two solutions.

In fig. 12 the integrals of surface friction are compared with the values deduced by Mr. Fage from the loss of momentum in the boundary layer*. As there are no experimental values below $\theta = 39°{\cdot}8$, comparison is made on the assumption that the calculated and experimental values are in agreement at $\theta = 39°{\cdot}8$.

In fig. 13 the tangential velocity in the boundary layer, calculated from the first and second approximations, is compared with the measured values given in R. & M. 1179 for

Fig. 12.

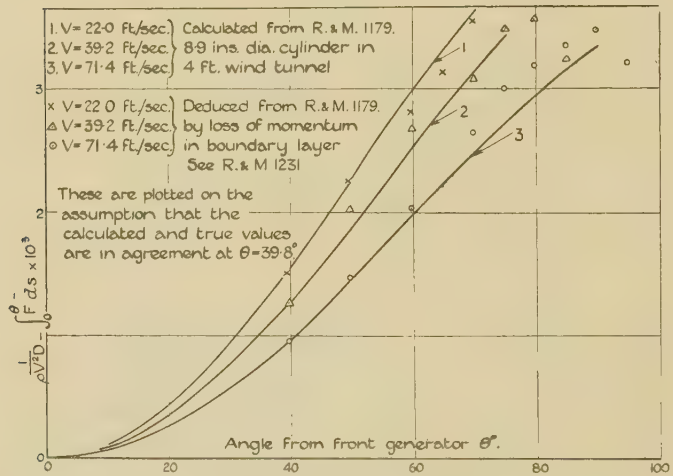

The integral of surface friction on a circular cylinder calculated from experimental pressure distribution at the circumference (second approximation).

a wind-speed of 71·4 feet per second and for several values of θ up to $79°{\cdot}8$.

In fig. 14 the calculated values of the surface friction for the 5·89-inch diameter cylinder are compared with the measured values taken from R. & M. 1369.

29. The solutions given in the paper have all been calculated from the measured values of the normal pressure appropriate to each case. As, however, the use of the equations assumes that the flow is potential beyond the limit of

* See Fage, "The Skin Friction on a Circular Cylinder," R. & M. 1231.

the boundary layer, it appears that the solutions should be calculable without reference to experiment by beginning with the normal pressure due to potential flow. To begin

Fig. 13.

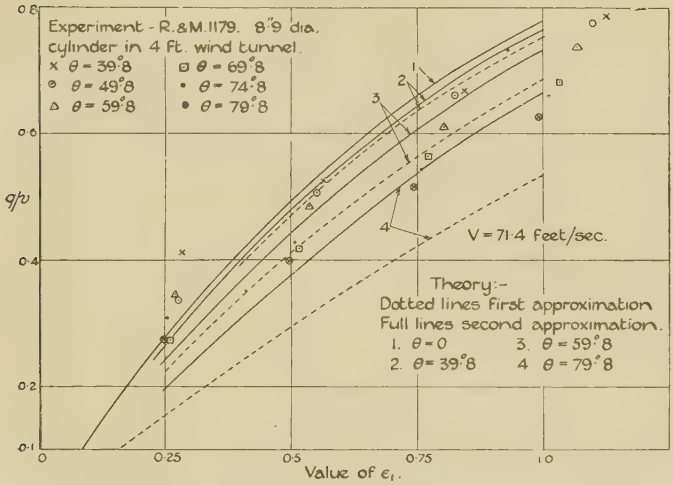

The tangential velocity in the boundary layer of a cylinder.

Fig. 14.

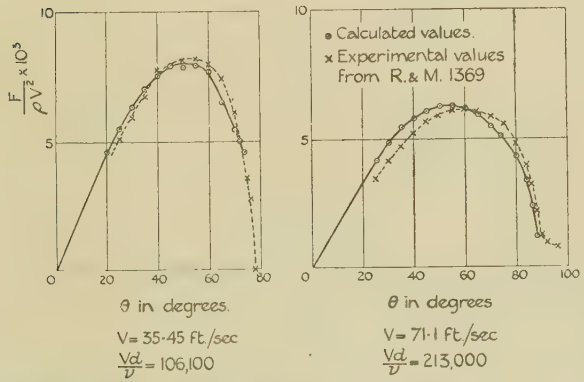

Comparison between experimental and calculated surface friction of a 5·89-inch diameter cylinder in 4-foot wind-tunnel.

with, the boundary layer must be worked out by using the data obtained from the potential pressure distribution; this layer is then converted into an equivalent change of shape

of the boundary, such that the flux at the outside of the boundary layer, assuming that the modified surface has no retarding effect, is the same as that before the change, taking account of the retarding influence of the surface. The normal pressure due to potential flow past the modified shape is then calculated by a method based on a graphical integration of Poisson's and Laplace's equation*. This cycle of operations is repeated until the calculated normal pressure at any point has converged to a definite value. It appears that in some cases convergence would be rapid. For instance, fig. 10 shows that the intensity of friction calculated from the normal pressure due to potential flow past an 8·9-inch diameter cylinder at the highest wind-speeds agrees fairly closely with that calculated from the observed normal pressures.

This method, when applicable over the whole surface of a body, would give a value for the form drag as well as for the frictional drag.

Summary.

30. A particular solution of the boundary-layer equations is given for the case where the tangential velocity at the outer limit of the boundary layer is proportional to a power of the distance measured along the boundary from the stagnation point, and the results are presented graphically for a range of values of the index. It is shown that Blasius' solution for a flat plate is a particular case of this solution. By a consideration of the necessary agreement between the solution of the equations of potential flow and that of the boundary-layer equations as the distance along the boundary from the stagnation point is decreased indefinitely, it is shown that the solution of the boundary-layer equations reduces to the particular solution described as the stagnation point is approached. This particular solution is used as a basis for two approximations of varying complexity to the solution in the general case ; the second of these gives the correct value of the surface friction. These solutions are given graphically, and the method of application to problems is described. Close agreement is found between the calculated and experimental values of the tangential velocity in the boundary layer for a flat plate and a cylinder and of the surface friction for a cylinder.

* Bairstow and Berry, "Two-Dimensional Solutions of Poisson's and Laplace's Equations," Proc. Roy. Soc. A xcv. (1919).

LXXXVI. *On an Estimation of the Height of the Heaviside Layer in Bengal.* *By* HRISHIKESH RAKSHIT, *M.Sc.*, *Khaira Research Scholar in Physics, Calcutta University* *.

Introduction.

IT is well known that the upper region of the atmosphere, ionized and rendered conducting chiefly by the ultra-violet rays from the sun, is responsible for the bending of the radio waves round the surface of the earth. A knowledge of the nature and height of this region at different places on the surface of the earth, and a record of its variation with the season and with the hour of the day or night, are of considerable importance in the study of the propagation of the radio waves. During the last few years a large number of investigators in Europe and America have made experiments to estimate the equivalent height of this region, the so-called Heaviside layer. All these experiments have, however, been carried out in the temperate zone of the Northern Hemisphere. As far as it is known no attempt has been made to estimate the height in the subtropical regions like that of India. As it is desirable to know the approximate height of this layer under as widely varying geographical, geophysical, and meteorological conditions as possible, we undertook to carry out such measurements in the subtropical climate of Bengal. The method and the results of our investigation are set forth in this communication. The observations were all made with signals from the Calcutta transmitter V.U.C. ($\lambda=370{\cdot}4$ metres) of the Indian State Broadcasting Service, with full cooperation of the transmitting staff, who maintained a constant power and wave-length all through our measurements.

Theory.

The principal methods of estimation of this height used by the previous investigators can broadly be divided into two classes :—(*a*) the angle-of-incidence method developed by Appleton and Barnett †, (*b*) the group-retardation method developed by Breit and Tuve ‡. The measurement of the angle of incidence of the downcoming waves in method (*a*) has been made in two ways § : (i.) by studying natural

* Communicated by Prof. S. K. Mitra, D.Sc.
† 'Electrician,' xcv. p. 678.
‡ Phys. Rev. xxviii. p. 554.
§ Proc. Roy. Soc. cxv. p. 297.

fading, (ii.) by studying artificial fading produced by a continuous change of wave-length of the transmitter. Method (*b*) has recently been modified by Martyn *, who increased and decreased the carrier frequency many times a second, and so heard an audible beat-note at the receiver situated at some distance from the transmitter. Appleton † has shown that, neglecting any effect of the earth's magnetic field on the propagation of the waves, all the methods described above give the same value for the height of the ionized layer, which is, however, always greater than the highest level actually attained by the ray.

For want of facility of getting a controlled wave-length change at the transmitter the method adopted in the present

Fig. 1.

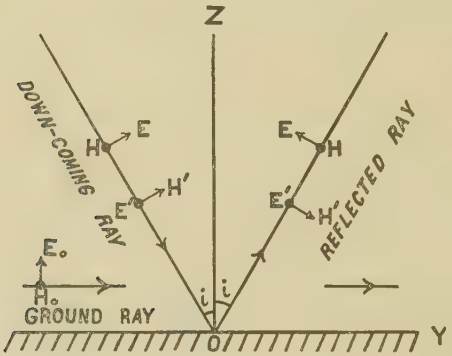

investigation was that of (*a*)i., *i. e.*, by studying the natural fading.

For the sake of convenience a brief *résumé* of the theory of this method as developed by Appleton and Barnett ‡ is given below.

Fig. 1, drawn in the plane containing the transmitter and the receiver, shows 0 as the position of the latter, where a ground ray with E_0 and H_0 as the respective amplitudes of the electric and the magnetic vectors and a downcoming ray incident at an angle i are received. The downcoming ray can be resolved into two components, one (E, H) with the electric vector in the plane of propagation, which is the

* 'Nature,' October 1930. See also R. A. Heising, I. R. E. Proc. xvi. p. 77.

† Proc. Phys. Soc. London, xli. p. 43.

‡ *Loc. cit.*

plane of the paper, and the other (E′, H′) with the electric vector perpendicular to this plane. For waves within the broadcast band the earth may be taken as approximating a perfect conductor and the downcoming ray may be represented as reflected without any appreciable loss of amplitude. We may therefore write the resultant electric and magnetic forces at 0 as

$$\left.\begin{aligned} &E_x=0,\ H_x=H_0 \sin pt+2H \sin (pt+\theta),\\ &E_y=0,\ H_y=2H' \cos i \sin (pt+\theta'),\\ &E_z=E_0 \sin pt+2E \sin i \sin (pt+\theta),\ H_z=0, \end{aligned}\right\} \quad . \quad (1)$$

where p is the angular frequency of the waves and θ and θ' are the phase differences between the ground-wave and the two corresponding components of the downcoming waves.

It is evident therefore that a vertical aerial at 0 will be acted on by an e.m.f. of amplitude proportional to E_A, where

$$E_A=\sqrt{E_0^2+4E^2 \sin^2 i+4E_0E \sin i \cos \theta}. \quad . \quad . \quad . \quad . \quad (2)$$

Similarly a loop aerial in the plane of propagation at 0 will be acted on by an e.m.f. of amplitude proportional to $\frac{d}{dt}(H_x)$; but in an electromagnetic wave the electric and magnetic forces are proportional, and hence the amplitude of this e.m.f. is proportional to E_L, where

$$E_L=\sqrt{E_0^2+4E^2+4E_0E \cos \theta}. \quad . \quad . \quad . \quad . \quad (3)$$

If the signal variations ΔE_A and ΔE_L, due to the downcoming waves, are small, so that $E_0^2>>E^2$, then for a first approximation equations (2) and (3) become

$$\left.\begin{aligned} &E_A=E_0+2E \sin i \cos \theta\\ &E_L=E_0+2E \cos \theta \end{aligned}\right\}, \quad . \quad . \quad . \quad . \quad . \quad (4)$$

and, whether the changes ΔE_A and ΔE_L are due to changes in E or θ or both, we get in each case

$$\Delta E_A : \Delta E_L=\sin i.$$

If the two aerials are coupled to two receivers which linearly amplify the input electromotive forces and rectify these amplified signals by detectors having square law characteristics, then

$$\frac{\Delta A}{\Delta L}=\frac{K_1}{K_2}\cdot\frac{\Delta E_A}{\Delta E_L}=\frac{K_1}{K_2}\cdot \sin i, \quad . \quad . \quad . \quad . \quad (5)$$

where ΔA and ΔL are the changes from the mean values of the galvanometer readings corresponding to the two aerials,

and K_1 and K_2 are constants depending on the aerial systems, on the amplification factors, and detector characteristics of the corresponding receivers.

If, therefore, by suitable adjustments $K_1 : K_2$ can be made equal to unity, then

$$\Delta A : \triangle L = \sin i. \quad . \quad . \quad . \quad . \quad . \quad (6)$$

Briefly, therefore, the method of finding the angle of incidence of the downcoming waves consists in comparing signals of fluctuating intensity, received simultaneously on a vertical and on a loop aerial in the plane of propagation.

The value of the angle of incidence being known, the effective height of the ionized layer is found from a knowledge of the distance between the transmitter and the receiver. In making the estimation it is assumed that for the distance used the downcoming ray has suffered only one deflexion from the upper atmosphere. It should also be remembered that this result is true if there is only one downcoming ray. The presence of more than one ray deflected from different layers brings in considerable errors in the result. The theory further demands that there should be no coupling between the two aerials.

Receiving Station and the Aerial Systems.

As the investigation was restricted to the use of natural fading method the site for the receiving station had to be so chosen that the ground ray was always stronger than the downcoming ray and yet the changes of signal strength were measurable with sufficient accuracy. The Hindu Academy at Daulatpur (long. 89°34′ E., lat. 22°50′ N.), situated at a distance of 76 miles from the transmitter at Calcutta, was found suitable for our purpose. It might be mentioned here that the V.U.C. aerial system is a T-antenna with the horizontal portion pointing approximately 40° E. from the North. The direction of Daulatpur with respect to the transmitter is 72° E. from the North.

For the guidance of future workers along this line the aerial systems and the receiving apparatus are described below in some detail.

The vertical aerial at the receiving station was 12 metres high, and the earth system consisted of a galvanized iron sheet buried under the ground. The aerial was tuned and magnetically coupled to one receiving set. The whole system, consisting of two tuning condensers and two variably coupled coils, was compiled into a separate unit which was

shielded and the shield earthed, the tuning and variation of coupling being made from outside.

The loop aerial consisted of a single turn of wire in the form of a triangle, and was situated in the vertical plane containing the transmitter and receiver, the height and base of the loop being 14 and 28 metres respectively. The loop circuit was completed through two tuning condensers, and the primary of a high frequency transformer, the secondary being tuned and connected to a second receiver.

Particular care was taken to eliminate the "antenna effect" of the loop. For this reason it was made of a single turn of wire completed through a H.F. shielded transformer with its centre earthed and tuned by two equal condensers. The degree of elimination of this effect can best be understood from the fact that the loop when situated in the daytime in the plane of propagation gave a deflexion of seventy divisions in the galvanometer, while in its perpendicular position the deflexion was of the order of one division only.

As in the case of vertical aerial, the assembly consisting of the H.F. shielded transformer and the three tuning condensers was compiled into another separate unit, the tuning being done from outside. To prevent any coupling between the two aerial systems the vertical aerial was situated along the vertical axis of symmetry of the loop, and both the tuning units were shielded.

Receiving and Recording Systems.

Two receivers were used, each consisting of two stages of screen-grid H.F. amplification followed by anode-bend rectification. The complete diagram of one of the receiving sets is given in fig. 2, the same components being used in the other receiver. The detector circuit will be found to be arranged in the form of a Wheatstone's bridge and without any H.T. voltage applied to the plate of the detector valve. It was so adjusted that in the absence of any signal at the input of the receiver there was no current in the galvanometer (Cambridge versatile galvanometer) whose deflexion with this arrangement indicated the presence of signals. As regards the selection of two sets of valves for the two receivers, firstly one receiver was used, and keeping the H.F. valves the same, two detector valves were selected which, with the above adjustment, gave the same deflexion in the galvanometer with a constant

signal. Then keeping the detector the same, two pairs of H.F. valves were chosen such that each pair, with either detector as selected above, gave the same galvanometer reading with a constant signal. The voltages applied to the H.F. valves were such that they worked along the straight portions of their characteristics, and hence the amplifications were assumed to be linear. Thus the rectified currents in the galvanometers were taken to be proportional to the square of the amplitude of the incoming signals.

To prevent any action between a receiver and an aerial, as well as between the receivers themselves, both of them were enclosed in two shielding boxes. It was found that with such screening of the two receivers and two aerial

Fig. 2.

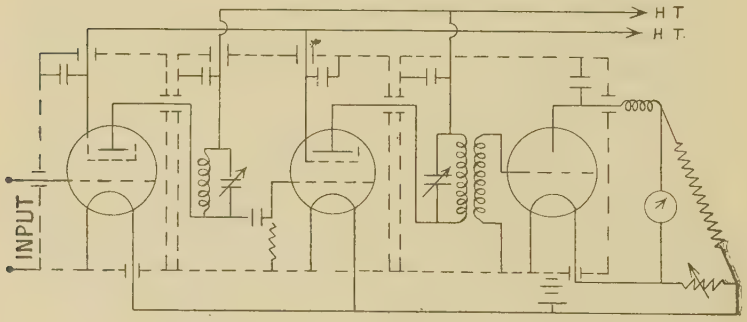

Circuit diagram of the receivers

tuning units, the presence or absence of signals in one aerial and receiver did not produce any change in the signal in the other, *i. e.*, there was no coupling between the aerials. The boxes for screening the two receivers were of the same size, for it was found that even with receivers adjusted as above the two galvanometers gave different readings with the same signal when placed in two screening boxes of unequal sizes.

The procedure for observations on a single night was as follows:—During the day, when only the ground-ray was present, the two receivers were brought to proper working conditions as described above. The coupling of the vertical aerial with the corresponding receiver was then so adjusted that the galvanometer connected to the latter gave the same reading as the galvanometer connected to the other receiver, and this final arrangement was kept undisturbed. This

ensured that $K_1 : K_2$ in equation (5) was equal to unity, and allowed the use of equation (6) for finding the angle of incidence of the downcoming waves. It now remained to make a simultaneous record of the variations of signal strength in the two receivers due to fading, from which an estimate of the angle of incidence could be made. For this purpose Appleton and his collaborators have used a photographic method employing a reflecting moving-coil galvanometer. We were, however, forced to adopt the eye-and-ear method of observation for want of facilities for taking photographic records at Daulatpur. A metronome adjusted to give a ring at the end of every five seconds was started, and the readings of the two galvanometers were simultaneously recorded by two observers just at the moment when the metronome gave the ring (the interval between successive rings was reduced to three seconds when the fluctuations of galvanometer reading became more rapid). This process was continued for about six minutes, and from the data thus obtained, two curves, one for each aerial, were drawn on the same squared paper. The ratio of the change from the normal day-value in galvanometer reading corresponding to the vertical aerial at any time to that of the other galvanometer at the same time was found for different parts of the curve, and the mean ratio was taken as the value of the sine of the angle of incidence of the downcoming waves during the six minutes period of observation. From the observations made during the day it was found that the amplifiers worked identically, and it was quite unlikely that this property of the amplifiers would change during the night ; it was for this reason that amplifiers and aerials were not interchanged during observations in the night.

Results.

From the numerous pairs of curves obtained from the data taken at different times during various nights it was found that during fading the change of galvanometer reading from the normal day-time value on the loop aerial was always greater than that corresponding to the vertical aerial. The same was also generally true for the early-morning data, though sometimes they showed the opposite effect which, as might be expected, was due to a lateral deviation of the interfering rays. All the curves obtained were not suitable for finding the angle of incidence by the use of the approximate formula (5). Fig. 3 shows a sample record, suitable for calculation, where the galvanometer

readings are exhibited as a function of time. Some of the values of sin i obtained from different parts of this pair of curves are

0·6, 0·67, 0·7, 0·57, 0·65, 0·67, 0·75, 0·67, 0·64, 0·64,

the mean value for which is 0·66.

During the period under investigation (February and March 1931) it was found that the fading began from 10 to 15 minutes before sunset and persisted throughout the night until about 10 to 15 minutes after sunrise. The records for the first part of the night were taken up to 11 P.M. with the

Fig. 3.

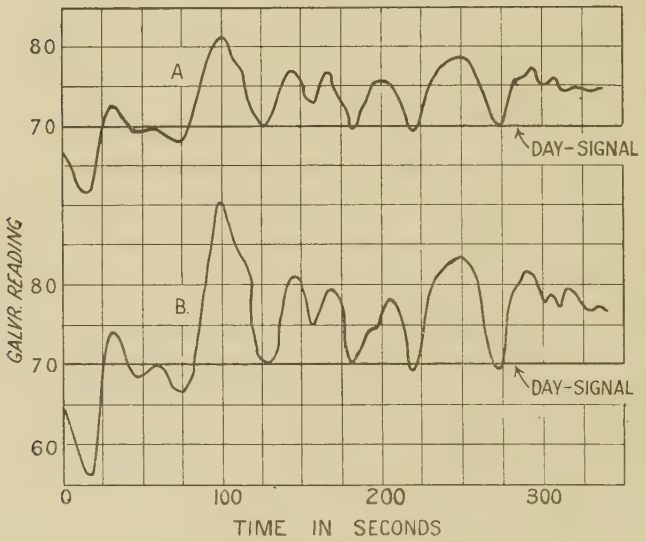

Signal fluctuations, 7.30 P.M., 20/2/31.
(A) Vertical aerial; (B) Loop aerial.

ordinary transmission from the V.U.C. station. The observed nature of variation of the intensity of fading, *i. e.*, the percentage of variation of the readings of the galvanometer with reference to the mean day-time value with the progress of night, can be divided into three types:—(*a*) in which the intensity, which is very slight near the sunset period, goes on increasing till about 8 P.M., and then diminishes to a minimum between 8 and 9 P.M., and finally goes on increasing up to the end of the period of observation; (*b*) in which the fading, which is very slight about 15 to 20 minutes before sunset, attains a maximum value within 10 to 15 minutes after sunset,

diminishes to a minimum between 8 and 9 P.M., and then goes on increasing up to the end of the period of observation; (*c*) in which the intensity, which is very slight during the sunset period, goes on increasing up to the end of the period of observation. The reduction of fading to a minimum during the middle stage is very prominent, reaching nearly the pre-sunset conditions. The percentage of occurence of the three types are: (*a*) 60 per cent., (*b*) 25 per cent., (*c*) 15 per cent. The three curves (A), (B), (C) shown in fig. 4 exhibit these effects very clearly, where the intensity of fading in the vertical aerial is plotted

Fig. 4.

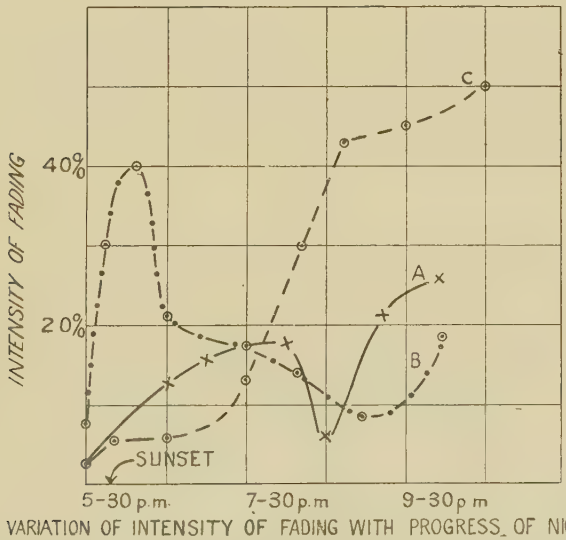

VARIATION OF INTENSITY OF FADING WITH PROGRESS OF NIGHT

against time. Records taken throughout the whole night might be expected to give further information regarding these facts. The height of the ionized layer, however, goes on increasing with the progress of the night irrespective of the changes in the intensity of fading, although the same value of the height is not obtained at the same hour every night. These are represented in the following tables:—

TABLE I.

Date, 6/2/31; Sunset at 5.44 P.M.

Time (P.M.)	5.42	5.49	6.15	7.45	8.30	9.15
Height (km.)	56	61	71	78	81	83

Table II.

Time, 7.30 P.M.

Date	6/2/31	10/2/31	13/2/31	14/2/31	15/2/31	19/2/31	20/2/31
Height (km.)	77	85	80	80	72	81	69

The observations made in the early hours of the morning, generally during the two hours before sunrise, showed a greater rapidity in the fluctuations of the galvanometer readings than during the night. No very consistent value of the ratio $\Delta A : \Delta L$ could be obtained in the interval of three minutes, which was usually required for taking one set of records (readings of the galvanometer being taken every three seconds). The records, however, generally indicated a gradual diminution in the height of the ionized layer as the hour of sunrise approached. It was also found that the intensity of fading approached zero at about 15 to 20 minutes after sunrise.

Summary and Conclusion.

Experiments for the measurement of the height of the ionized layer of the upper atmosphere in Bengal are described. The average lowest height of the ionized layer, which is obtained near about sunset, for various evenings during the month of February 1931 has been found to be 60 km. The height gradually increases with the progress of the night, reaching on an average a value of 85 km. at about 11 P.M. The corresponding lowest height, as determined by Appleton and Ratcliffe, is about 90 km. The discrepancy between the two values is not at all surprising considering the difference in the geographical positions and geophysical conditions of the two places of observation. The variation of the intensity of fading with the progress of the night can be divided into three types. These are described, and curves are drawn showing their general nature.

The observations made during the early hours of the morning generally indicated a gradual diminution in the height of the ionized layer as the hour of sunrise approached. It was also found that the intensity of fading approached zero at about 15 to 20 minutes after sunrise.

An explanation of the various phenomena observed regarding the variation of the intensity of fading with the progress of the night, and such other allied facts, will form the subject matter of a subsequent communication.

In conclusion, I wish to express my gratitude to the authorities of the Hindu Academy at Daulatpur for providing facilities to instal the receiving equipments in the open fields of the Academy ; to Mr. A. C. Nag, M.Sc., Lecturer in Physics of the Academy, for his assistance in taking observations ; to the Director, Mr. J. R. Stapleton, and the Engineer, Mr. S. C. Ray, M.Sc., of the V.U.C. station, for their cooperation in these experiments and for arranging especial early morning transmissions.

The investigation was carried out under the direction of Prof. S. K. Mitra, D.Sc., to whom I owe my sincere thanks for constant help and guidance.

Wireless Laboratory,
University College of Science,
92 Upper Circular Road,
Calcutta, India.
March 21, 1931.

LXXXVII. *Adsorption at the Surface of a Solution.* *By* W. F. Kenrick Wynne-Jones *.

AT the surface of a solution there will be, in general, an excess of some component of the system and, according to the thermodynamic treatment of Gibbs, the amount of this excess is given by the equation

$$\Gamma_{2(1)} = -\frac{\partial \sigma}{\partial \mu_2}, \quad \ldots \ldots \quad (1)$$

where $\Gamma_{2(1)}$ is the excess per unit area, σ is the surface tension, and μ_2 is the chemical potential of the adsorbed substance. If the solution is "perfect" then we may write

$$\Gamma_{2(1)} = -\frac{c}{RT} \cdot \frac{\partial \sigma}{\partial c}, \quad \ldots \ldots \quad (2)$$

where c is the concentration of the solute and other symbols have their usual significance.

This important equation has been employed by several authors, of whom Langmuir † and also Schofield and Rideal ‡ have shown from the data for dilute solutions that the behaviour of the adsorbed molecules is very similar to that

* Communicated by the Author.
† Langmuir, Journ. Amer. Chem. Soc. xxxix. p. 1848 (1917).
‡ Schofield and Rideal, Proc. Roy. Soc. A, cix. p. 57 (1925).

of the insoluble films of fatty acids studied by N. K. Adam *. In addition to their interesting studies of dilute solutions, Schofield and Rideal have also examined the adsorption in concentrated solutions of ethyl alcohol and pyridine in water and, by combining the surface tension data with vapour pressure measurements, were able for the first time to employ the exact form of the Gibbs' equation and thus to obtain values of Γ up to 100 per cent. of solute. Their results for eythl alcohol, which are reproduced as curve I in

Fig. 1.

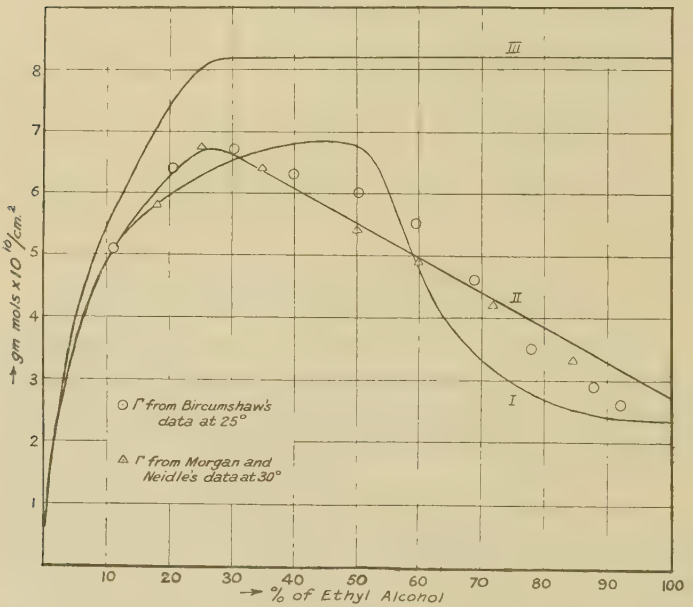

fig. 1, show that Γ reaches a maximum at 45 per cent. alcohol, and with increasing concentration falls off to less than half the maximum value. The results for pyridine (which refer to an uncharged mercury surface) give a curve of exactly the same form although, as the surface tensions were measured at 18° and the vapour pressures at 96°, there is no doubt that the actual values of Γ are less reliable. The first portion of this curve there is no difficulty in explaining, since, with increasing concentration, more and more solute will be adsorbed at the surface until, on

* N. K. Adam, 'The Physics and Chemistry of Surfaces.' Oxford University Press.

Langmuir's views, a complete unimolecular film is formed; for the subsequent decrease, however, Schofield and Rideal were unable to account, but offered two possible explanations :—

(*a*) That the orientation of the alcohol molecules changed considerably in more concentrated solution.

(*b*) That water molecules were adsorbed beneath the external alcohol layer *.

It would appear, however, that these authors have overlooked the fact that Γ, as defined by Gibbs, is not the total amount of solute at the surface, but the surface excess to which, in order to obtain the total amount, must be added the amount normally present in the absence of adsorption. This allows of a simple explanation of curve I, since what we may term the normal amount at the surface will be proportional to the concentration and, consequently, in order to maintain a unimolecular layer at the surface, as the bulk concentration increases, decreasing amounts of excess will be required. We may also express this by the equation

$$U = \Gamma + kc, \quad . \quad . \quad . \quad . \quad . \quad . \quad (3)$$

where U is the total amount present at the surface and kc the normal amount in absence of adsorption. Curve I does not quantitatively satisfy this equation if U is regarded as constant in concentrated solution. However, recalculation of Γ, using the recent vapour pressure results of Dobson † and the surface tension data of Morgan and Neidle ‡ as well as those of Bircumshaw §, gives values of Γ represented by curve II, which is evidently of the form demanded by the equation. From the latter curve we can derive values of U which are shown as curve III, the value of "k" in equation (3) being $5{\cdot}5 \times 10^{-12}$ gm. molecules per sq. cm. The constant value of U attained at concentrations higher than 30 per cent. is 8·2 gm. mol./cm.^{2}, which corresponds to a surface area per molecule of 20·3 sq. Å., in good agreement with Adam's value of 20·5 sq. Å. for the cross-section of close-packed hydrocarbon chains.

* The further hypothesis, which has apparently found favour in some quarters, that there is a complete layer of water molecules adsorbed beneath the unimolecular layer of alcohol is clearly impossible, as it would require Γ to become negative.

† Dobson, Journ. Chem. Soc. cxxvii. p. 2866 (1925).

‡ Morgan and Neidle, Journ. Amer. Chem. Soc. xxxv. p. 1856 (1913).

§ Bircumshaw, Journ. Chem. Soc. cxxi. p. 887 (1922).

With regard to the interpretation of k we may note that as c is the percentage composition, $k \times 100$ is the normal amount of solute present at the surface of the pure solute; if the adsorbed molecules extend to a depth of τ cms. into the liquid, 100 k will be equal to τ multiplied by the number of gram molecules contained in 1 c.c. of the liquid. For pure ethyl alcohol we therefore have

$$\tau = \frac{5{\cdot}5 \times 10^{-10} \times 46}{{\cdot}79} \text{ cm.} = 3{\cdot}2 \text{ Å.},$$

Fig. 2.

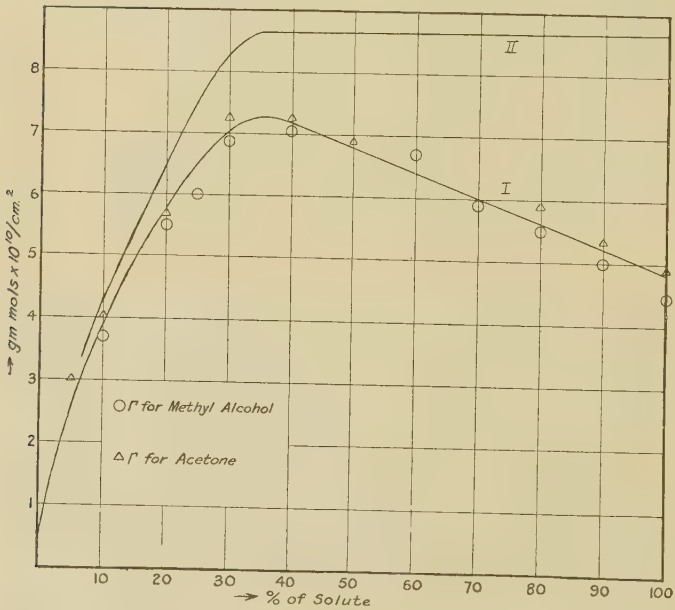

whereas, taking the density of solid alcohol to be 1·0 and the cross-sectional area to be 20·5 sq. Å., we arrive at 3·7 Å. as the length of the molecule.

The only other solutions for which both surface tension and activity data appear to be available are aqueous solutions of methyl alcohol and acetone, and for both these substances the values of Γ can be represented by curve I in fig. 2. Applying equation (3) we obtain curve II for U, the value of k being $4{\cdot}0 \times 10^{-12}$ gm. mol./cm.^{2}. From the constant value of $8{\cdot}8 \times 10^{-10}$ gm. mol./cm.^{2} that is attained by U at

concentration above 40 per cent., the area per molecule is found to be 19·5 sq. Å., while from the value of k we can deduce that τ for methyl alcohol is 1·7 Å. and for acetone 3·0 Å. On the other hand, the lengths of the molecules of these two substances calculated in the same way as that of ethyl alcohol are 2·7 Å. and 5·0 Å. respectively. Although there is some doubt as to the actual lengths of the molecules, it is evident that τ is for each substance distinctly less than the probable length of the molecule. This may be due to a certain indefiniteness in our conception of a surface, since no surface composed of molecules can be strictly plane, or it may perhaps be due to the adsorbed molecules not being completely immersed in the solution. Whatever the explanation of this may be, we can conclude from the molecular areas given below that a unimolecular layer of solute is formed at the surface of each of the solutions.

For several other substances the values of Γ calculated from equation (2) show a maximum, but this is not always

TABLE I.

Substance.	Molecular areas in square Å.		
	Calculated from U.		N. K. Adam.
Acetone	19·5		20·5
Methyl alcohol ...	19·5	±0·5	20·5
Ethyl alcohol ...	20·3		20·5

to be interpreted in the manner suggested here. Thus the data for phenol in water show a maximum which practically disappears if the activity data of Jones and Bury * are employed † ; similarly, the maximum obtained by Palitzsch ‡ for urethane is probably due to the use of the approximate equation. Bury § has also shown that the pronounced maximum for butyric acid becomes much less noticeable when activities are used in the calculation ; his values, however, still show the maximum, which is certainly to be expected at high concentrations.

* Jones and Bury, Phil. Mag. iv. p. 1125 (1927).

† The activity calculations of Goard and Rideal (J. C. S. cxxvii. p. 1668 (1925)) are difficult to understand, and the agreement between their figure of 23·8 sq. Å. for the area of the phenol molecule and Adam's value for the cross-section of the benzene nucleus is fortuitous.

‡ Palitzsch, 'Studier over Oplösningers Overfladespœnding.' Copenhagen.

§ Bury, Phil. Mag. iv. p. 980 (1927).

We may easily estimate the magnitude of the correction for the normal amount present at the surface by assuming some value for τ, the depth of the surface layer; for example, if τ is 5 Å., then for a molal solution the normal amount will be $5 \times 10^{-8} \times 10^{-3} = 5 \times 10^{-11}$ gm. mol./cm.^{2}. On the basis of this calculation we can illustrate the effect of the correction in four different cases :—

(1) If the solute is strongly capillary-active and not very soluble, a constant value of Γ is attained at concentrations below 0·1 molal and the correction is negligible. Example : *p*-toluidine in water.

(2) If the solute is moderately active and fairly soluble, Γ may reach a constant value at concentrations above 1·0 molal. The correction is appreciable and destroys the constancy of Γ. Examples : some of the higher alcohols and fatty acids in water.

(3) If the solute is active and completely miscible with the solvent a maximum may be obtained in the Γ curve, but this maximum disappears on applying the correction. Examples : ethyl alcohol, methyl alcohol, and acetone in water.

(4) If the solute is not very active but completely miscible with the solvent the values of Γ are relatively small but rise steadily, and the correction only makes the curve steeper. Examples : probably formic and acetic acids in water

Summary.

The values obtained by Schofield and Rideal for the adsorption of ethyl alcohol at the surface of its aqueous solutions are shown to refer not to the total amount present at the surface but to the surface excess. A method is suggested for the calculation of the total amount, and the values thus obtained are in accord with the conception of a unimolecular layer of alcohol at the surface of solutions containing more than 30 per cent. of alcohol. Similar results are obtained for solutions of methyl alcohol and of acetone.

I am indebted to Dr. N. K. Adam for his very helpful criticism.

The University, Reading.

LXXXVIII. *The Significance of the Compton Effect in Absolute Gamma-Ray Absorption Measurements.* *By* L. H. Clark, *Ph.D., Barnato Joel Laboratories, Middlesex Hospital, W.* 1 *.

IT has long been realized that measurements of the absorption of gamma rays of radium in different substances are complicated by the scattered radiation produced when gamma rays penetrate matter. To overcome the effects of these rays widely different methods have been used by various investigators. In their recent book, "Radiations from Radioactive Substances," Rutherford, Chadwick, and

Fig. 1.

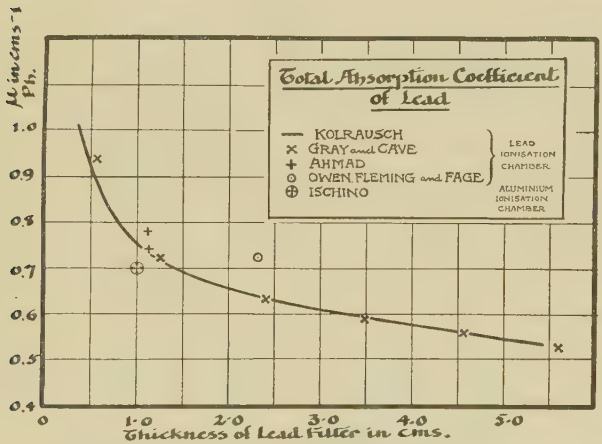

Ellis have summarized graphically the results obtained by some of these methods. Fig. 1 is taken from their book. It shows how the coefficient of absorption of gamma rays in lead varies with the thickness of lead interposed in the path of the primary beam. The results obtained by various investigators show a lack of agreement, the differences being much greater than the errors ordinarily met with in ionization measurements. With a light element, such as aluminium, forming the absorbing medium even greater discrepancies are observed. At present no particular method can be singled out as being entirely free from the effects of scattered radiation. The purpose of this investigation is to

* Communicated by Prof. Sidney Russ, C.B.E., D.Sc.

find out what factors determine the amount of scattered radiation affecting electroscopic absorption measurements, with a view to formulating the conditions under which these rays are inoperative.

Some of the scattered radiation with which one has to contend is much less penetrating than the primary gamma rays. From absorption measurements of the radiation scattered at definite angles to a beam of gamma rays, Compton [1] concluded that an increase in wave-length occurred in the scattering process. Later [2] he found that this increase in wave-length is given by the formula

$$\delta\lambda = \frac{h}{mc}(1-\cos\phi).$$

In this equation h is Planck's constant and ϕ is the angle the scattered ray makes with the primary ray. The quantities m and c are respectively the mass of the electron and the velocity of light. The rays scattered at an angle of 135° to the primary beam were reduced to half value by 0·12 cm. lead, whereas for the primary rays the corresponding value was of the order 1 cm. The scattered radiation which may affect an electroscope is heterogeneous, for rays may enter which are scattered at widely different angles to the primary rays; but even under these conditions the author [3] found that these rays are much softer than the primary beam. This fact forms the basis of the methods used in the present enquiry.

Scattered rays may originate either outside the electroscope or in its walls. Considering first those scattered radiations which originate outside the electroscope, it is to be expected that an instrument having thin walls will be more susceptible to them than one having thick walls. The procedure has been, therefore, to determine the apparent absorption of gamma rays, mainly in lead, first with a thin-walled electroscope and then with thick-walled instrument placed under otherwise identical conditions. In the first experiment the variable was the distance of the source of radiation from the electroscopes.

Experiment 1.—*The variation in the apparent transmission of gamma rays through lead with the distance of the source from* (1) *a thin-walled electroscope*, (2) *a thick-walled electroscope.*

Large quantities of radon, frequently having an initial strength of 200 millicuries, were used for these experiments.

Fig. 2 A shows the glass vessel used to contain the radon. The gas was confined to a small bulb C, 0·5 cm. in external diameter, the remainder of the vessel being filled with mercury. The bulb C was covered by a small lead cap L, the thickness of the closed end and sides of which were respectively 0·41 and 0·38 cm. The radiation from the radon was therefore first screened by this lead hood.

Fig. 2.

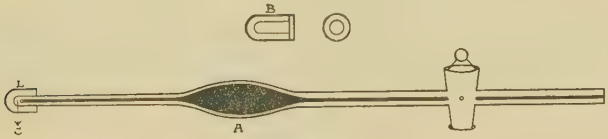

In some of the later experiments the radon was sealed in a small glass bulb, which was inserted in the lead case shown in fig. 2 B, the wall-thickness of which was 0·3 cm.

Fig. 3 represents the type of electroscope used. Two electroscopes having lead walls were used, those of one being 0·16 cm. thick, whilst those of the other were 1 cm. The external dimensions of both electroscopes were $7 \times 7 \times 7$ cm.

Fig. 3.

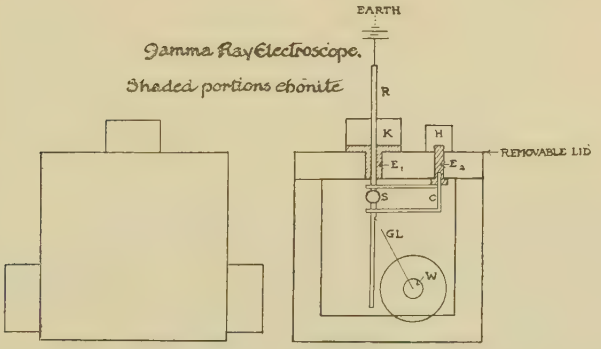

In both, the gold leaf system GL was held by a sulphur plug S, mounted at the lower end of a vertical metal rod R. An ebonite plug E_1 insulated this rod from the box, which was at earth potential. The rod R was maintained at a potential difference from earth usually of 200 volts. The charging device C consisted of a horizontal U-shaped wire mounted in an ebonite plug E_2, which could be rotated to bring the U-shaped wire into contact either with the box or

the gold leaf system. In the second position the sulphur plug was short-circuited and the gold leaf charged to the potential of the rod R. Circular mica windows W, 0·4 cm. in diameter allowed one to observe the movement of the gold leaf, which was timed over the eyepiece scale of a telemicroscope. In the case of the thick-walled electroscope the ebonite plugs were covered with lead cylinders H and K 1 cm. in thickness, as shown, and in addition the windows were surrounded by annular lead rings 1 cm. thick.

The method of experiment was as follows :—The thin-walled electroscope was mounted 25 cm. above the laboratory bench at the end of a long wooden stand used to carry the

Fig. 4.

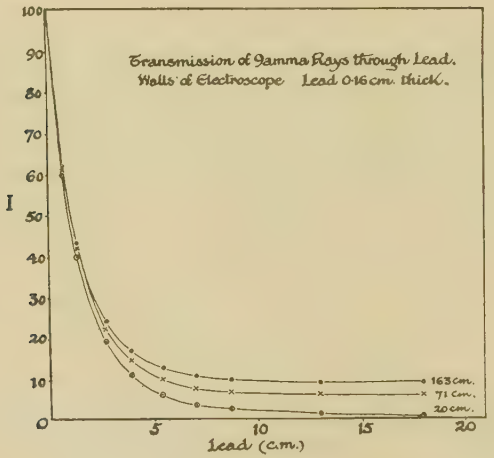

filters and the radon source. The source was set up on a level with the middle of the electroscope and maintained at a given distance from it. The apparent transmission of gamma rays through lead filters of cross-section 7 × 7 sq. cm., placed against the electroscope, was then measured. The experiment was repeated with the source placed at a number of different distances from the electroscope. The curves in fig. 4 were obtained with a thin-walled electroscope, when the distances of the sources from the electroscope were respectively 20, 71, and 163 cm. Each curve shows, for a particular distance of the source, how the ionization decreases as thicker and thicker lead filters are placed against the electroscope. The curves become less and less steep as the source is withdrawn from the electroscope. For

a distance of 163 cm. the transmission curve is practically horizontal for lead filters thicker than 13 cm., for the reduction in ionization, brought about by an additional filter 5 cm. thick, is less than one per cent. When this condition is reached it is clear that the ionization is due to radiation unaffected by the filter in the primary beam, hence this radiation cannot be entering the electroscope through the side facing the source owing to the proximity of the filter. It must therefore be scattered radiation which penetrates the other sides of the electroscope.

When the experiment is repeated with the electroscope having lead walls 1 cm. thick, no such variation with the

TABLE I.

Electroscope with walls 1 cm. thick.

Lead filter, cm.	Percentage transmission of gamma rays through lead. Distance of source from electroscope.		
	20 cm.	35·5 cm.	71 cm.
0	100	100	100
1·35.....	47·4	46·6	46·1
2·7	23·2	22·7	22·3
3·9	12·8	12·5	12·3
5·4	5·9	6·0	6·1
7·0	2·8	2·8.	3·0

distance of the source could be detected over the range tested. In this case lead filters up to 7 cm. in thickness were used, and the maximum distance of the source from the electroscope was 71 cm. The results obtained are given in Table I., which shows that the general character of the transmission of gamma rays through lead up to 7 cm. in thickness is practically the same for distances of the source from the electroscope varying from 20 to 71 cm.

The coefficients of absorption of gamma rays in lead calculated from these figures are :

For lead 0–1·35 cm. thick, $\mu = 0{\cdot}57$ cm.$^{-1}$.

„ 1·35–2·7 „ „ $\mu = 0{\cdot}54$ „

„ 2·7 –7 „ „ $\mu = 0{\cdot}49$ „

These experiments show, then, that when absorption measurements of gamma rays in lead are made by placing the filters in contact with one side of a thin-walled electroscope, scattered radiations enter the other sides of the latter, the effect of which is more pronounced the further the source is placed from the electroscope. If, however, the walls of the electroscope are made of lead 1 cm. thick, the effect of this scattered radiation appears to be practically eliminated for filters up to 7 cm. in thickness. This has been tested for distances of the source from the electroscope up to 71 cm.

The above experiments serve to show that under certain experimental conditions the effect of scattered radiation is very marked, whilst there are others in which its effect cannot be detected. It cannot be said that the conditions have been found in which the effect of scattered radiation has been entirely excluded. To gain information on this question an investigation has been made of the penetrating power of the radiations emitted by the internal walls of the electroscope. This radiation consists partly of rays similar to those incident on the electroscope and partly of radiations arising in the walls themselves as the result of irradiation. It is to be expected, however, that the composition of this internal radiation will depend upon the penetrating power of the radiation entering the electroscope. The penetrating power in aluminium of the internal radiation has therefore been measured under two conditions. In the first the effect of external scattered radiation was marked, and in the second these radiations were known by the first series of experiments to be largely eliminated. Experiments under these two conditions will now be considered.

Apparatus for measuring the penetrating power of the internal wall radiation.

Fig. 5 represents the electroscope used for these measurements and all those to be described later in the paper. It was a cube of 7 cm. side having walls of aluminium 0·001 cm. thick mounted on a cubical framework of brass 2 sq. mm. in cross-section, indicated by the shaded area in the plan drawing. The metal support for the sulphur plug S was insulated and maintained at a steady potential difference of 190 volts with respect to the electroscope. The gold leaf was charged by depressing the spring-controlled rod R until it short-circuited the sulphur bead, when it was released to return to the position shown. Three cubical lead enclosures of external measurements $10 \times 10 \times 10$ cm.

were made having walls of respective thicknesses 0·16, 0·5, and 1 cm., and means were adopted whereby the electroscope proper could be mounted centrally in each enclosure. Fig. 5 shows the electroscope mounted in the enclosure having walls 1 cm. thick. This arrangement enabled one to insert aluminium sheets between each face of the electroscope and the lead enclosure, and so to measure the penetrating power of the wall radiation. The capacity of the electroscope was maintained constant by this method of mounting. Moreover, it was arranged that in the process of changing the aluminium linings the electroscope remained fixed with respect to the telemicroscope used to measure the ionization.

Fig. 5.

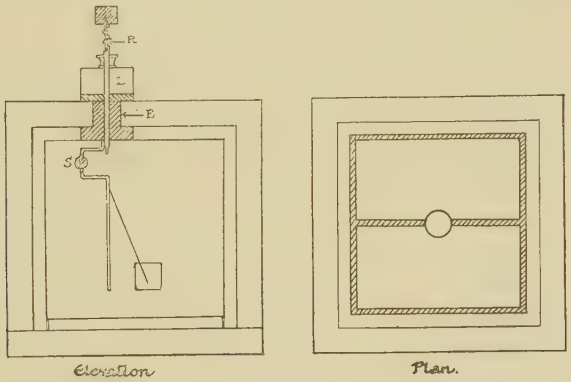

To prevent radiation entering the electroscope through the ebonite plug E it was covered with lead L 1 cm. thick; moreover, means were adopted whereby the windows through which the leaf was viewed could be blocked with lead during an ionization reading. It was found, however, that the amount of radiation entering the windows was small compared with that entering through the sides of the electroscope. It amounted to 5 per cent. of the total radiation entering the electroscope when the primary beam was filtered by 10 cm. of lead and the source was at a distance of 75 cm. from the electroscope. The natural leak of the electroscope throughout these measurements remained in the neigbourhood of 0·1 to 0·2 divisions per minute.

Strong radon sources often between 200 and 300 millicuries were used. The radon was contained in a small flat circular bulb of 2 cm. diameter, enclosed in a lead box of

wall thickness 0·33 cm. The side of this box facing the electroscope was 3·9 cm. high and 2·9 cm. wide, the thickness of the box being 1·5 cm. The area of all the filters used was the same as that of the sides of the enclosures used to screen the electroscope, viz. 10×10 sq. cm.

Now it has been seen that when absorption measurements of gamma rays in lead are made by placing the filters in contact with one side of a thin-walled electroscope (lead 0·16 cm. thick), the effect of external scattered radiation becomes more marked as the source of radiation is moved further from the electroscope. The first set of experimental

TABLE II.

Wall thickness of electroscope enclosure 0·16 cm. lead.
Primary radiation filtered by 10 cm. lead.

Thickness of aluminium lining, cm.	Distance of source from the centre of the electroscope Ionization.	
	15 cm.	75 cm.
0	100	100
0·005	—	57·9
0·018	79·0	35·9
0·036	71·7	29·8
0·072	66·5	27·1
0·205	61·6	25·5
0·41.....	59·3	24·6

conditions was therefore as follows :—The electroscope was mounted in the lead enclosure having walls 0·16 cm. thick, and a lead filter 10 cm. thick was placed in contact with the enclosure. The radon source was first placed close to the electroscope, in fact, in contact with the far side of the filter. The fall in ionization due to the insertion of aluminium linings between the enclosure and the electroscope was then measured. Lastly, the experiment was repeated with the source at 75 cm. from the centre of the electroscope, the 10 cm. filter remaining in position. The results for these two positions of the source are given in Table II.

These figures show that the penetrating power in aluminium of the internal radiation is very much less when the source is far from the electroscope than when it is close to it.

The results of the corresponding experiment made with a thick-walled enclosure are given in Table III. This is a case in which the effect of scattered radiation has been shown to be very largely eliminated.

Even in this case, however, the internal radiation is appreciably softer when the source is at 75 cm. than when it is at 15 cm. from the electroscope.

When the results of Tables II. and III. are compared two facts emerge. The first is that when the source is at a considerable distance from the electroscope the latter comes under the influence of a comparatively soft radiation, which

TABLE III.

Wall thickness of electroscope enclosure 1·0 cm. lead.
Primary radiation filtered by 10 cm. lead.

Thickness of aluminium lining, cm.	Distance of source from the centre of the electroscope. Ionization.	
	15 cm.	75 cm.
0	100	100
0·005	—	81·5
0·018	79·4	69·6
0·036	71·7	62·1
0·072	67·6	53·0
0·205	60·9	45·6

becomes more marked as the wall of the enclosure becomes thinner. The second is that when the source is placed in contact with the filter the quality of the internal radiation is independent of the wall thickness of the enclosure, *vide* column 2 of Tables II. and III. This has been found to be the case for the three enclosures of respective wall thicknesses 0·16 cm., 0·5 cm., and 1·05 cm. This second finding can only mean that under these conditions the amount of external scattered radiation entering the electroscope is negligible, even when the walls of the latter are only 0·16 cm. thick. Therefore, the ionization in the electroscope must be due to primary radiation transmitted by the 10 cm. filter.

The penetrating power of the external scattered radiation.

One is now in a position to determine the quality of the scattered radiation entering the electroscope when the source

is set at a distance of 75 cm. from it and the primary beam is filtered by 10 cm. of lead. This determination was made as follows:—The radon source was placed at 75 cm. from the centre of the electroscope shown in fig. 5, and the primary beam was filtered by 10 cm. of lead and placed in contact with the enclosure of the latter. The ionization in the electroscope was measured when it was mounted in each of the three lead enclosures. The ionization readings were corrected for any change in the sensitivity of the electroscope in transferring it from one enclosure to the next. Correction was also made for the decay of the source and for the natural leak of the electroscope, which varied from ·09 to ·22 divisions per minute. The resulting ionization values are given in the second column of Table IV., the first column of which gives the wall thickness of the lead

Table IV.

Radon at 75 cm. Wall thickness of enclosure, cm.	Primary radiation filtered by 10 cm. lead. Ionization.		
	Primary and scattered rays.	Primary rays.	Scattered rays.
$0{\cdot}16_5$.....	14·0	2·1	11·9
0·5	4·1	1·6	2·5
1·05	1·9	1·3	0·6

enclosures for which the respective ionization values were obtained. The ionization values in column 2 are due to primary radiation transmitted by the 10 cm. block, together with scattered radiation.

To find the ionization in each case due to radiation transmitted by the 10 cm. block, the above experiment was repeated with the source at 15 cm., for with this disposition the former experiments showed that the ionization is due entirely to primary radiation. These values were corrected in the manner outlined and reduced, according to the inverse square law, to determine the ionization due to transmitted radiation when the source was at 75 cm. These values are given in column 3 of Table IV. The difference between the values in columns 2 and 3 for the same enclosure gives the ionization due to external scattered radiation. Thus the figures in column 4 show how the ionization due to scattered radiation falls as the walls of the enclosure are increased

in thickness. The absorption coefficients in lead of the scattered radiation, calculated from the figures in column 4, are as follows :—

For lead 0·16–0·5 cm. thick, $\mu=4{\cdot}7$ cm.$^{-1}$.

„ 0·5 –1·0 „ „ $\mu=2{\cdot}6$ „

The external scattered radiation is heterogeneous and considerably less penetrating than the primary beam, *vide* p. 917.

In all of the experiments which have been described so far the disposition of the filter has always been the same. It has been placed in contact with one side of the electroscope, and the scattered radiation investigated has been that which has penetrated the other sides of the latter. The effect of this radiation on the apparent transmission of thick filters is to make the absorption coefficient too low. Turning now to thin lead filters a considerable amount of evidence has been accumulated in this investigation, pointing to the fact that scattered radiation affects the apparent transmission of thin lead filters, the reason being that the scattered radiation operating in this case enters the electroscope through the side facing the source. Experiments showing the presence of this forward scattered radiation and its effect upon absorption measurements will now be considered.

The effect of forward scattered radiation on the apparent transmission of gamma rays through lead.

Florance [4] showed that the apparent transmission of a thin lead filter varied with its position between the source of radiation and the electroscope. He found that the filter appeared to be more transparent when it was in contact with the source than when it was placed next to the electroscope. The author (*loc. cit.*) found that this phenomenon was also shown by filters of silver and platinum. It is unlikely that this effect is due to a change in the amount of primary radiation transmitted by a filter, brought about by moving the latter from one position to the other. It is to be expected, however, that the amount of scattered radiation entering the electroscope will depend upon this factor. If the effect here considered is due to a scattered radiation less penetrating than the primary rays, the variation in the apparent transmission of a filter with its position between the source and the electroscope will diminish as the walls of the enclosure are increased in thickness. The following

experiments were made to determine whether this is the case.

For this purpose the electroscope shown in fig. 5 was used. It could be inserted in different lead enclosures having walls 0·16 cm. and 1·0 cm. thick, respectively. The radon source was always set at a distance of 44 cm. from the electroscope. In the first set of experiments the primary beam was lightly filtered by 0·3 cm. of lead.

The apparent transmission of lead filters up to 4 cm. in thickness was found for the two positions of the filter, viz. first next to the source and then next to the electroscope. The measurements were made with the electroscope mounted first in the thin-walled enclosure and then in the enclosure

Table V.

The apparent transmission of gamma rays through 2·1 cm. of lead.

Thickness of wall of enclosure, cm.	Percentage transmission of gamma rays through 2·1 cm. of lead.		
	Filter next to the source. I.	Filter next to the electroscope. II.	Ratio $\frac{I}{II}$.
0·16	31·4	29·2	1·07
1·0	34·0	31·4	1·08

having the walls 1 cm. thick. In both cases it was found that more radiation entered the electroscope when the filter was placed next to the source than when it was in contact with the enclosure to the electroscope. Over a range of filters from 0 to 2 cm. in thickness this difference increased with the thickness of the filter. Table V. gives the results obtained with a lead filter 2·1 cm. thick.

The thin-walled enclosure was lined with aluminium 0·4 cm. in thickness and the thick-walled one with aluminium 0·2 cm. thick. A comparison of the figures given in the last column of Table V. shows that the variation in the transmission of a filter with its position between the source and the electroscope is practically unaffected by an increase of 0·8 cm. in the wall thickness of the enclosure. If, therefore, this variation is due to scattered rays they must be of greater penetrating power than those previously considered in this paper.

An attempt was made to eliminate the variation in the apparent transmission of the filter, resulting from a change in the position of the latter, by increasing the thickness of the side of the enclosure facing the source. For this purpose the thick-walled enclosure, lined with 0·2 cm. of aluminium, was used. The side of the enclosure facing the source was increased in thickness in steps up to 6 cm. by placing lead sheets against it, 10×10 sq. cm. in area. The radon source was placed 44 cm. from the centre of the electroscope, and for each additional thickness the transmission of gamma rays through 2·1 cm. of lead was measured for two positions of the latter, viz. first next to the source then next to the enclosure. Table VI. gives the results obtained when the side of the enclosure is increased in thickness to 6 cm.

TABLE VI.

Wall thickness of side of enclosure, cm.	Percentage transmission of gamma rays through 2·1 cm. of lead.		
	Filter next to the source. I.	Filter next to the electroscope. II.	Ratio $\frac{I}{II}$.
1·0	35·1	32·4	1·08
2·0	35·9	33·6	1·07
2·5	36·6	34·4	1·06
3·9	36·6	35·0	1·05
6·0	36·1	36·0	1·00

The first column of Table VI. gives the total thickness of lead forming the side of the enclosure facing the source of radiation. The second and third columns show the apparent transmission of gamma rays through 2·1 cm. of lead placed respectively next to the source and the enclosure. The last column shows that the ratio of these two values diminishes as the side of the enclosure is increased in thickness and ultimately becomes unity when the latter is 6 cm. thick. Under these conditions the transmission of gamma rays through the filter is independent of the position of the latter, and it is reasonable to suppose that only the primary radiation transmitted by the filter is operating in this case. The results obtained when the side of the enclosure is less than 6 cm. in thickness are consistent with the view that when the filter is moved from one position to the other there is a change in the amount of scattered

radiation entering the electroscope. This scattered radiation, which enters the electroscope through the side facing the radon source, is much more penetrating than the total scattered radiations falling on the other sides of the electroscope, for the latter are definitely excluded by using an enclosure having lead walls 1 cm. thick. This conclusion is in agreement with Compton's theory of scattering. On this theory the penetrating power of a scattered ray varies with the angle it makes with the primary ray, from which it originates. Rays which suffer least deviation in the scattering process are more penetrating than those scattered through large angles. Hence the scattered radiation falling

TABLE VII A.

Coefficients of absorption of gamma rays in lead.

Wall thickness of lead enclosure, cm.	Thickness of lead filter, cm.	Absorption Coefficient. Filters placed against the enclosure.
0·16	0 –0·29	0·72 cm.$^{-1}$.
	0·29–1·13	0·61 ,,
	1·13–2·13	0·53 ,,
	2·13–4·12	0·50 ,,
1	0 –2·13	0·54 ,,
	2·13–4·12	0·50 ,,

on the side of the electroscope facing the source of radiation will be richer in the more penetrating rays than that falling on all the other sides of the electroscope.

The above experiments have served to detect the presence of a forward scattered radiation which approximates in penetrating power to the primary rays when the source of radiation is only lightly filtered. The effect of this forward scattered radiation upon absorption measurements, made with the apparatus shown in fig. 5, will now be considered.

The coefficients of absorption, obtained when the electroscope was inserted in (*a*) the thin-walled enclosure, (*b*) the thick-walled enclosure, are given in Table VII A.

These values were obtained when the radon source was placed at a distance of 44 cm. from the electroscope, and the filters were placed next to the enclosure to the latter. Both enclosures were lined with aluminium, the thin-walled

enclosure with aluminium 0·4 cm. thick and the thick-walled one with aluminium 0·2 cm. in thickness.

A comparison of the results obtained with the two different lead enclosures leads to two conclusions. The first is that the apparent absorption of gamma rays in lead up to 2 cm. in thickness is appreciably greater when the measurements are made with the thin-walled enclosure than when the thick-walled enclosure is used. The second conclusion is that the absorption of gamma rays in lead between 2 and 4 cm. in thickness is independent of the wall thickness of the lead enclosure surrounding the electroscope.

When the measurements were made by placing the filters in contact with the source of radiation, the following absorption coefficients were obtained :—

TABLE VII B.

Thin-walled electroscope.	Absorption coefficient.
0 –0·29 cm. of lead.	0·67 cm.$^{-1}$.
0·29–4·12 ,,	0·51 ,,
Thick-walled electroscope.	
0 –4·12 cm. of lead.	$0·50_5$,,

With this disposition of the filters the radiation entering the electroscope appears to be more homogeneous than when the filters are placed against the enclosure to the electroscope. The radiation measured by the thin-walled electroscope still contains a soft component but it appears to be removed by 0·29 cm. of lead, whereas when the filters are placed against the enclosure 2·13 cm. of lead is required. Thus, although these results support the conclusion of Tuomikoski [5] that the penetrating power of a beam of gamma rays increases when thin filters are interposed in its path, the extent to which the penetrating power varies with the thickness of the filter is dependent upon the position of the latter. Later in this paper, *vide*, p. 933, it is contended that this process does not operate with thick filters.

A similar investigation of forward scattered radiation and its effect upon absorption measurements was made with a beam of gamma rays which was heavily filtered with lead. A powerful radon source was used which was set up at a distance of 44 cm. from the centre of the electroscope shown in fig. 5. The primary rays were filtered by a cubical block

of lead of side 10 cm. placed in contact with the source. This block of lead served to filter not only the primary rays incident on the electroscope but also the bulk of those traversing the vicinity of the latter. The apparent transmission of gamma rays through a lead filter 2·1 cm. thick was found for the two positions of the latter, viz. next to the lead block in front of the source and then next to the enclosure surrounding the electroscope. This experiment was first made with the electroscope surrounded by the thin-walled enclosure and then with the thick-walled one. Owing to the heavy filtration of the primary beam the ionization readings were small, and in consequence it was decided not to line the enclosure with aluminium. Table VIII. gives the results obtained.

TABLE VIII.

Apparent transmission of gamma rays through a lead filter 2·1 cm. thick.

Primary rays filtered by 10·3 cm. of lead.

Wall thickness of lead enclosure, cm.	Percentage transmission of radiation through 2·1 cm. of lead.	
	Filter next to source.	Filter next to electroscope enclosure.
0·16	66·0	33·8
·0.....	37·6	36·9

The results obtained with the thin-walled enclosure are the most striking. In this case the filter placed near the source appears to be nearly twice as transparent to gamma rays as when it is placed next to the enclosure. Since the fraction of the primary radiation transmitted by the filter must be the same in both positions, the observed difference must be due to scattered radiation which has access to the electroscope only when the filter is near the source. This scattered radiation has little penetrating power, for when the walls of the enclosure are increased to 1 cm. in thickness it is practically excluded, the two transmission values for the filter then differing by only 2 per cent., *vide* Table VIII. It remains to determine the direction in which this scattered radiation enters the electroscope. If it enters the latter on all sides except that facing the

source, then it is to be expected that when the filter is placed next to the enclosure it will appear more transparent when the measurement is made with the thin-walled enclosure than when the thick-walled one is used. Actually the reverse is the case, *vide* column 3 of Table VIII. It may be concluded therefore that the scattered radiation here considered falls on the side of the electroscope facing the source of radiation.

The processes operating under these experimental conditions are illustrated diagramatically in fig. 6. In the figure, E represents the electroscope and S the source, the radiation from which is filtered by a block of lead L 10 cm. thick. The radiation falling on the face AB of the enclosure may be divided roughly into three groups, indicated by the arrows P, S_1, and S_2. The arrow P represents primary radiation transmitted by the block L, whilst S_1 and S_2 indicate respectively hard and soft scattered radiation. Of these groups P and S_1 issue from the lead block L. It is clear that as the side AB of the electroscope is increased in

Fig. 6.

thickness the amount of soft scattered radiation S_2 affecting the electroscope will rapidly diminish. Hence the radiation affecting the electroscope when surrounded by the thin-walled enclosure contains more soft rays than that operating when the thick-walled enclosure is used.

Let us now consider the effect of placing a filter first in contact with the lead block at F_2 and then in contact with the enclosure at F_1. When the filter is placed at F_2 in contact with the block the relative amounts of the different groups of radiation affecting the electroscope will be sensibly the same as when the filter is removed. When the filter is in contact with the enclosure at F_1, however, it will absorb the softer group of radiations, and the amount of radiation entering the electroscope will be smaller than when the filter is at F_2. If the thickness of the wall AB of the enclosure is insufficient to absorb these softer rays, the filter will appear more transparent when near the source than when next the enclosure. Table VIII. shows this to be the case

when the walls of the enclosure are 0·16 cm. thick. If, on the other hand, the walls are by themselves sufficiently thick to absorb the softer scattered rays, a filter will appear equally transparent in the two positions F_1 and F_2. Table VIII. shows that this is practically the case when the walls of the enclosure are made 1 cm. in thickness.

It was decided to determine the coefficient of absorption in lead of gamma rays transmitted by a considerable thickness of lead. For this reason the experimental arrangement shown in fig. 7 was used. A lead hemisphere A of radius 15 cm. was mounted so that its centre was in the same horizontal plane as the centre of the electroscope E. A source of gamma radiation equivalent to 354 mg. of

Fig. 7.

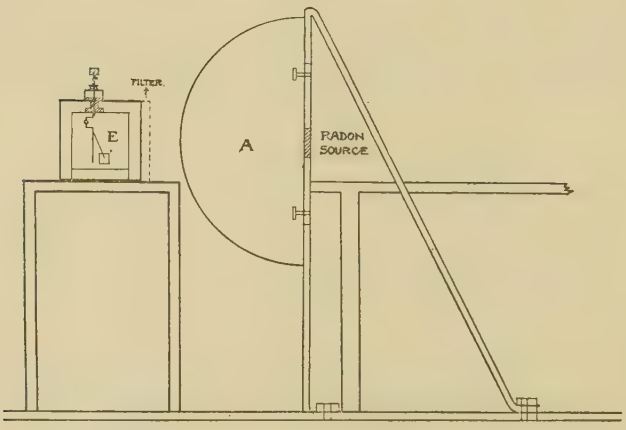

radium was placed at the centre of the vertical side of the hemisphere, the distance between the source and the centre of the electroscope being 27·5 cm. The hemisphere served to filter by 15 cm. of lead not only the primary beam to the electroscope but all those rays traversing any medium likely to scatter radiation into the electroscope. Lead filters up to 2 cm. in thickness were placed in turn against the side of the electroscope. The measurements were made in one case with the electroscope surrounded by the lead enclosure having walls 0·16 cm. thick, and in the other the thick-walled enclosure was used. The ionization readings in these experiments were small, and for this reason no aluminium linings were inserted between the enclosure and the electroscope. Curve 1 in fig. 8 was obtained with the thin-walled

enclosure, and curve 2 with the thick-walled enclosure surrounding the electroscope.

Considering first the results obtained with the thin-walled enclosure (curve 1), it is to be noted that the ionization reading for the lowest point A on this curve was 1·87 divisions per minute, only 4 per cent. of which, however, was due to the natural leak of the instrument. The absorption coefficients in lead of the radiation entering the electroscope, calculated from curve 1, were as follows :—

For filters 0–0·29 cm. thick, $\mu = 0{\cdot}75$ cm.$^{-1}$.
„ 0·29–1·13 „ „ $\mu = 0{\cdot}32$ „
„ 1·13–2·13 „ „ $\mu = 0{\cdot}25$ „

Fig. 8.

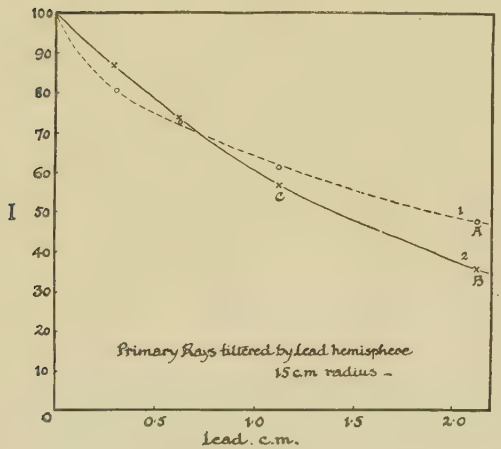

Before discussing these results the values obtained with the thick-walled enclosure will be mentioned. The ionization reading for the lowest point B on curve 2 was very small, being only five times the natural leak of the instrument, which was 0·12 divisions per minute. This point is merely included to show the general trend of the curve. The point C on the curve is more accurate, the natural leak in this case amounting to 12 per cent. of the ionization recorded with a filter 1·1 cm. thick. The radiation transmitted by lead up to 1·1 cm. thick was homogeneous, having an absorption coefficient of 0·50 cm.$^{-1}$.

When the results obtained with the two different enclosures are compared, it is clear that a considerable amount of

scattered radiation is present. The latter has a marked influence on the results obtained when the walls of the enclosure are only 0·16 cm. thick, but it is excluded when the walls are 1 cm. in thickness. The abnormally low absorption coefficients for filters thicker than 0·29 cm., obtained with the thin-walled enclosure, are undoubtedly due to the influence of soft scattered radiations entering the electroscope on all sides other than that against which the filter is placed. In spite of the influence of these rays, however, the absorption of gamma rays in 0·29 cm. of lead is appreciably greater than when the measurements are made with the thick-walled enclosure, indicating the presence of a comparatively soft forward scattered radiation.

The results of the investigation of the influence of forward scattered radiation on the apparent transmission of gamma rays through thin lead filters may be summarized as follows.

Measurements of the absorption of a beam of gamma rays in lead are influenced by forward scattered radiation. The presence of forward scattered radiation is shown by the fact that the apparent transmission of gamma rays through lead filters varies with the position of the filter between the electroscope and the source of radiation. When the initial filtration of the primary beam amounts to only 0·3 cm. of lead the forward scattered radiation is very penetrating in character. However, when the primary beam is heavily filtered by 10 cm. of lead, the bulk of the forward scattered radiation is much less penetrating, for it is excluded by making the walls of the electroscope 1 cm. in thickness. In both cases the absorption of gamma rays in thin lead filters is influenced to a marked degree by the thickness of the walls of the electroscope. Thus, the absorption of gamma radiation in thin lead filters is greater when measurements are made with a thin-walled electroscope than when one having thick walls is used. The usual explanation of this phenomenon, in the case of lightly filtered gamma radiation, is that the penetrating power of a beam of gamma rays increases rapidly when thin filters are interposed in its path. In addition to this variable there is the influence of forward scattered radiation to be contended with. Hence, the value of the absorption coefficient of lightly filtered gamma rays in lead, measured with a given instrument, will vary with the thickness of the filter and its disposition between the source and the electroscope.

When the primary beam is very heavily filtered, *e.g.* by 15 cm. of lead, the transmitted radiation is still mixed with softer components, which modify the value for the absorption

coefficient obtained with a thin-walled electroscope. Thus, in this case the absorption of the transmitted radiation in approximately 0·3 cm. of lead is given by the coefficient 0·75 cm.$^{-1}$ when an electroscope is used having walls 0·16 cm. thick. When the walls are increased to 1 cm. in thickness the transmitted radiation appears to be homogeneous, having an absorption coefficient $\mu=0·50$ cm.$^{-1}$. The presence of the softer constituent in the radiation transmitted by considerable thicknesses of lead is incompatible with the view that the penetrating power of gamma rays is increased by filtration. In this case it must be assumed, therefore, that the softer constituents are either forward scattered radiation or radiation characteristic of the filter. In this connexion the figures given in Table IX. are of interest. The table gives coefficients of absorption of the

Table IX.

Coefficients of absorption of gamma rays of radium in lead.

	Tuomikoski (*loc. cit.*).	Owen, Fleming, and Fage [6].	Ahmad [7].	Author.	
Wall thickness of electroscope	0·4 cm.	0·3 cm.	0·16 cm.	0·16 cm.	0·16 cm.
Filter thickness	0·6 ,,	0·5 ,,	0·25 ,,	0·29 ,,	0·29 ,,
Initial filtration of primary beam	0 ,,	2·3 ,,	1·0 ,,	0·3 ,,	15 ,,
Absorption coefficient.	0·70 cm.$^{-1}$	0·72 cm.$^{-1}$	0·77 cm.$^{-1}$	0·72 cm.$^{-1}$	0·75 cm.$^{-1}$

gamma rays of radium in lead obtained by different experimenters, together with details of the measurements from which the coefficients were calculated.

The table shows marked differences in the initial filtration of the primary beam used by the different experimenters, but the absorption coefficients obtained by the different methods are in fair agreement. The agreement is much better than is to be expected if the penetrating power of the gamma rays is increased upon filtration, and strongly suggests the presence of less penetrating secondary radiations, such as the experiments described require.

The minimum wave-length of gamma rays obtained by gamma ray absorption measurements.

The minimum value obtained for the coefficient of absorption of gamma rays in lead obtained in this work has

been of the order of 0·5 cm.$^{-1}$. This value has been obtained for filters between 2 and 4 cm. thick when the primary beam was filtered by 0·3 cm. of lead. The value obtained in this case is the same whether the measurements are made with an electroscope having walls 0·16 cm. thick or with one having 1 cm. walls. The value 0·5 cm.$^{-1}$ has also been obtained when the primary beam is initially screened by 15 cm. of lead, when the walls of the electroscope are sufficiently thick (1 cm.) to exclude all softer secondary radiations. It may, therefore, be concluded that the penetrating power of a beam of gamma rays does not change when the filtration of the beam is increased from 2 to 15 cm. of lead.

It was decided to estimate the effective wave-length of gamma radiation filtered by approximately 2 cm. of lead. The method used was that suggested by Compton [8] and by Ahmad, and is described by the former in his book "X-rays and Electrons." It consists in measuring the absorption of gamma rays in two elements such as lead and aluminium, which differ considerably in atomic number. The effective wave-length is calculated from these values by applying Owen's law, which states that $\mu \propto \lambda^3$, where μ is the absorption coefficient and λ is the wave-length of the absorbed radiation. The particular formula adopted by Compton to determine the effective wave-length of gamma rays has been the following :

$$\mu_e = \mathrm{K}z^3\lambda^3 + k.$$

Here μ_e is the absorption per electron. The first term represents the energy spent in true absorption and the second that spent in the scattering process. In this equation z represents the atomic number of the absorber and K and k are constants. The limitations set to this equation are that the constants K and k are the same for all elements provided the value of λ is less than the critical K absorption wave-length. Moreover, since the true absorption varies as the cube of the atomic number, the true absorption in aluminum is negligible compared with that in lead. Hence, the difference between the absorption per electron in lead and in aluminium is given by

$$\mu_{e_{\mathrm{Pb}}} - \mu_{e_{\mathrm{Al}}} = \mathrm{K}z^3{}_{\mathrm{Pb}}\lambda^3, \quad . \quad . \quad . \quad . \quad . \quad (1)$$

where $\mu_{e_{\mathrm{Pb}}}$ and $\mu_{e_{\mathrm{Al}}}$ are the respective absorption coefficients per electron in lead and in aluminium. By assuming Richtmeyer's [9] value for K, viz. $2{\cdot}24 \times 10^{-2}$, the effective

wave-length of gamma rays has been calculated from Ahmad's absorption measurements (*loc. cit.*) to be 0·0186 Å.U. A similar calculation has been made from the absorption measurements of the following experiment.

The electroscope shown in fig. 5 was mounted in the thick-walled enclosure (1 cm.), which was lined with aluminium 0·2 cm. thick. The side of the enclosure facing the source of radiation was increased in thickness to 2·5 cm. by the addition of lead 1·5 cm. thick, which was maintained in position throughout the experiment. The source of radiation was mounted at a distance of 44 cm. from the centre of the electroscope. The absorption of gamma rays in lead sheets 10×10 sq. cm. in area was then measured, the filters in each case being placed in contact with the enclosure. The measurement was repeated with aluminium filters. Table X. shows how gamma radiation is absorbed in lead and in aluminium under these experimental conditions.

TABLE X.

Absorption of gamma rays in lead and in aluminium.

Thickness of filter, cm.	Percentage transmission of gamma rays through lead.
0	100
0·33	84·8
0·62	72·8
1·13	56·1
2·1	34·1

Thickness of filter, cm.	Percentage transmission of gamma rays through aluminium.
0	100
1·0	90·2
2·0	81·2
3·5	69·4
5·0	59·8

The coefficients of absorption of gamma rays in lead and in aluminium were found to be respectively 0·511 cm.$^{-1}$ 0·102 cm.$^{-1}$. Now the absorption per electron is related to the linear absorption coefficients just given by the expression

$$\mu_e = \frac{\mu}{\rho} \cdot \frac{A}{Nz},$$

where A is the atomic weight of the filter, N is Avagadro's number, μ is the measured absorption coefficient, whilst ρ and z are respectively the density and atomic number of the absorber. Taking the value of N to be $6{\cdot}06 \times 10^{23}$ molecules per gm. molecule,

$$\mu_{e_{Pb}} = 1{\cdot}87 \times 10^{-25} \quad \text{and} \quad \mu_{e_{Al}} = 1{\cdot}29 \times 10^{-25}.$$

The effective wave-length of the most penetrating gamma rays of radium is found from equation (1) to be $0{\cdot}016_8 \times 10^{-8}$ cm. When the measurements were made with the filters placed against the source of radiation, the linear absorption coefficients of gamma rays in aluminium and lead were found to be respectively 0·092 cm.$^{-1}$ and 0·47 cm.$^{-1}$, the effective wave-length of the radiation in this case being $0{\cdot}016_5 \times 10^{-8}$ cm.

Recently Steadman [10] has carried out wave-length measurements of gamma rays from radium and its products by a refined crystal method. The two shortest wave-lengths measured by him were respectively ·039 and ·017 A.U., the latter being the more intense.

Conclusion.

It would not have been anticipated that the measurement of the absorption of the gamma rays of radium in lead, which has engaged so many experimenters, would lead to so many discordant results. This is the case in spite of the fact that each experimenter has attempted by various means to exclude the chief sources of error, viz. the effects of scattered radiation. The existing values for the coefficient of absorption of gamma rays in lead range from 0·94 cm.$^{-1}$, obtained with comparatively thin filters, to 0·25 cm.$^{-1}$, which Tuomikoski found for the radiation transmitted by 18 cm. of lead. As a result of the experiments described in this paper the view is put forward that after the gamma rays of radium have traversed approximately 2 cm. of lead they constitute a homogeneous beam of radiation. This is shown by the curve in fig. 9, obtained by plotting the coefficients of absorption of the gamma radiation transmitted by lead up to 15 cm. in thickness. It is seen that over the range of filters 2 to 15 cm. of lead the value of μ remains practically constant at 0·50 cm.$^{-1}$.

The scattered radiation with which one has to contend consists of rays which differ considerably in penetrating power. Whilst some of the rays have a penetrating power approaching that of the primary rays there are others which

are practically absorbed by 1 cm. of lead. It is found that as the primary beam is more and more heavily filtered the radiation falling on the electroscope becomes richer in easily absorbed scattered radiation. These rays may originate in the air surrounding the electroscope or in any mass of lead used to filter the primary beam. In view of these experimental findings it is suggested that measurements of the absorption of gamma rays in matter should be made with an electroscope having walls of lead at least 1 cm. in thickness. It was with an electroscope having walls of this thickness that the results given in fig. 9 were obtained. By this means the effect of soft scattered radiation may be eliminated.

Fig. 9.

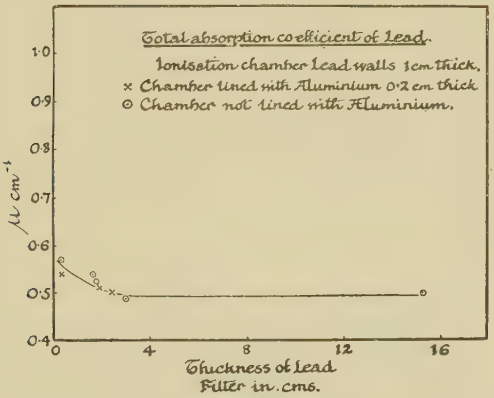

How considerable the effects of these rays may be is shown by the fact that when an electroscope is used having lead walls only 0·16 cm. thick the absorption coefficient of the radiation transmitted by 15 cm. of lead is found to vary from 0·75 cm.$^{-1}$ to 0·25 cm.$^{-1}$. In comparison the effect of scattered radiation, which is able to enter an electroscope having lead walls 1 cm. thick, is slight. These penetrating scattered rays enter the electroscope through the side facing the source of radiation. On account of this fact the gamma rays appear to be somewhat more absorbent when the filters are placed in contact with the electroscope than when they are in contact with the source of radiation. The effective wave-length of the gamma radiation determined from the absorption measurements by the method of Compton and Ahmad appears, however, to be independent

of the position of the filter. Thus the radiation filtered by 1·8 cm. of lead has an effective wave-length of $0{\cdot}016_8$ Å.U. when the filters are placed in contact with the electroscope and $0{\cdot}016_5$ Å.U. when they are placed in contact with the source. These values are in agreement with the shortest wave-length of 0·017 Å.U. observed by Steadman with crystal methods.

To avoid the effects of scattered radiation it is a common practice to line the interior walls of a gamma-ray electroscope with aluminium. The value of an aluminium lining for this purpose has been studied in this paper. In fig. 9 the crosses refer to measurements made when the electroscope was lined with aluminium 0·2 cm. thick and the circles to cases where this lining was removed. In this instance the effect of the lining is small. There are cases, however, where it exerts an appreciable influence upon absorption measurements. A thin-walled electroscope is susceptible to softer radiations than the one specified here, and the apparent penetrating power of the primary beam may be altered very considerably by increasing the filtration or the distance of the source from the electroscope. In these circumstances the insertion of an aluminium lining may have an appreciable influence on the absorption measurements.

I am much indebted to the Medical Research Council for the use of powerful radon sources, which were prepared by Mr. G. W. Spicer, B.Sc., of the Radon Department, Middlesex Hospital. I wish, also, to thank Professor Russ for his valuable advice and interest in the investigation.

References.

(1) Compton, Phil. Mag. xli. p. 749 (1921).
(2) *Loc. cit.* xlvi. 1923.
(3) Clark, Phil. Mag. ii. p. 783 (1926).
(4) Florance, Phil. Mag. ii. p. 921 (1910).
(5) Tuomikoski, *Phys. Zeits.* 1909, p. 372.
(6) Owen, Fleming, and Fage, Proc. Phys. Soc. xxxvi. p. 355 (1924).
(7) Ahmad, Proc. Roy. Soc. 1924 & 1925.
(8) Compton, "X-rays and Electrons," Appendix V. p. 390.
(9) Richtmeyer, Phys. Rev. 1921 & 1923.
(10) Steadman, Phys. Rev. xxxvi. p. 460 (1930).

LXXXIX. *The Relation between Uranium and Radium.*—Part IX. *The Period of Ionium.* *By* FREDERICK SODDY, *M.A., F.R.S.**

THE earlier Parts have appeared in the Philosophical Magazine as follows, and references in the text to these Parts are by the roman numerals.

I. 1905 [vi.] ix. p. 768.
II. With T. D. Mackenzie, 1907, [vi.] xiv. p. 272.
III. 1908 [vi.] xvi. p. 633.
IV. 1909 [vi.] xviii. p. 846.
V. 1910 [vi.] xx. p. 340.
VI. With Miss A. F. R. Hitchins, 1915 [vi.] xxx. p. 209.
VII. 1919 [vi.] xxxviii. p. 483.
VIII. With Miss A. F. R. Hitchins, 1924 [vi.] xlvii. p. 1148.

The growth of radium in the four uranium preparations purified initially very thoroughly from ionium and radium in 1905–9, has been recently redetermined as carefully as possible in order to determine the period of average life of ionium, Θ_2, as accurately as this method permits. The method involves the knowledge of the period of average life of radium, Θ_3,—for which in previous papers the value, 2375 years, has been assumed,—the products of the two periods, $\Theta_2\Theta_3$, being actually obtained by this method.

Up to 1915, the growth of radium remained too small to give anything but a gradually increasing minimum value for Θ_2, but in that year the two largest preparations indicated that the true value was not far from 10^5 years, and the next series in 1919 gave exactly this figure, viz. $\Theta_2\Theta_3 = 2{\cdot}375 \times 10^8$ (y)^2. However, the measurements in 1924 gave a value about 8 per cent. higher, and, in view of a decrease in the accepted value of Θ_3 then foreshadowed, the value $1{\cdot}1 \times 10^5$ years was suggested for Θ_2.

The measurements in 1924 showed considerable differences between the four preparations, which gave individual values between $1{\cdot}04$ and $1{\cdot}13 \times 10^5$ y. The determinations were to some extent subordinate to the problem of finding the proportion of ionium in ionium-thorium isotopes separated from the American carnotite and St. Joachimsthal pitchblende. If Θ_2 is known, the rate of growth of radium

* Communicated by the Author.

from such mixtures gives the ionium-thorium ratio. This work showed that the proportion of ionium in the case of St. J. pitchblende was considerably greater (Io : Th :: 1 : 0·9) than the ratio determined from the atomic weight of the isotopic mixture of elements, and it indicated that the preparation for which the atomic weight was determined had been contaminated by additional thorium while in process of being worked up in a thorium factory. For this preparation, the proportion of ionium was calculated to be 28·77 per cent. from the difference of the atomic weight of the mixture of isotopes from that of pure thorium on the one hand, and from that of pure ionium on the other, the latter *being assumed to be* 230, and the two former as determined by O. Hönigschmid and St. Horovitz.

The only other determination of Θ_2 at this time was that of Stefan Meyer, who measured the total α-radiation of this same preparation and obtained from it, as a maximum estimate of Θ_2, the value $1{\cdot}3 \times 10^5$ y., Θ_3 being taken as 2,280 y.* Since then, another determination has been made of Θ_3, from the rate of growth of radium from the same preparation, the proportion of ionium being taken, as in the last case, as 28·77 per cent.†. Mmes. Curie and Cotelle by this method, which does not involve the value of Θ_3, obtained for Θ_2 the value $1{\cdot}19 \times 10^5$ y.

It was of some interest, therefore, to ascertain whether the subsequent history of the uranium preparations would favour the higher values for Θ_2 obtained by other investigators, especially as the measurements in 1924 showed a trend in this direction. The result, however, has been rather to confirm the lower value. The value for $\Theta_2\Theta_3$ now obtained, $2{\cdot}44 \times 10^8$ y^2. is nearer that obtained in 1919, 2·375, than to that in 1924, 2·56.

The methods used in the present series were as described in detail (IV. 847) and subsequently modified (VI. 211). Three of the same radium standards were employed as previously. These were (1) a St. Joachimsthal pitchblende, analyzed as containing 61·23 per cent. uranium‡; (2) the radium barium chloride preparation referred to (VII. 284) as estimated by Miss Hitchins to contain 652×10^{-12} g. of radium per gram, and (3) a radium barium carbonate preparation estimated by A. Fleck to contain 12·05 milli-

* St. Meyer and E. Schweidler, "Radioaktivität," 2nd Ed. p. 389 (1927).

† Mmes. Curie and Cotelle, *Compt. rend.* cxxx. p. 1289 (1930).

‡ Compare Miss R. Pirret and F. Soddy, Phil. Mag. [vi.] xxi. p. 653 (1911).

grams of radium to the kilogram. Both of these estimates were by comparison with uranium minerals, the equilibrium ratio between radium and uranium being taken as $3{\cdot}4 \times 10^{-7}$. The last is one of the preparations referred to (VI. p. 212) in which the radium had been determined also by γ-ray measurements of a spherical sample against a radium standard, the absorption of the γ-rays in the spherical sample being evaluated. These measurements confirmed the equilibrium Ra/U ratio stated.

It is to be observed that though the Ra/U ratio enters into Rutherford's equation (VI. p. 217) for evaluating $\Theta_2\Theta_3$, viz.,

$$R/R_0 = 1/2\lambda_2\lambda_3 t^2 \quad \text{or} \quad \Theta_2\Theta_3 = 1/2(R_0/R)t^2,$$

where R is the radium grown by the uranium preparation in t years and R_0 is the quantity of radium that would be in equilibrium with the uranium,—in so far as the electroscope is calibrated by uranium minerals, the Ra/U ratio enters in the same sense both into the calibrations of the electroscope and into the measurements of radium from uranium, and is thus eliminated, the value of $\Theta_2\Theta_3$ being independent of the value used for this ratio. For the equation may be written

$$\Theta_2\Theta_3 = 1/2(U/u)t^2,$$

where U is the quantity of uranium experimented upon, and u is the quantity of uranium in a uranium mineral which contains the same amount of radium as the uranium preparation contains after t years. The calibration is effected by weighing uranium, not radium, and though, in practice, it is more convenient to express it as the number of units of radium (10^{-12} g.) required to produce unit leak (1 d.p.m.), what is actually determined is this constant divided by the Ra/U ratio, or the weight of uranium in minerals which generates the equilibrium amount of radon necessary to give unit leak in the electroscope.

Calibration of the Electroscope.

In the present series of measurement, in addition to preliminary calibrations with old standards, not included in the final results, 14 measurements have been done with 12 separate standards made of the three preparations described. The quantity of radium in the largest uranium preparation, containing 3 kilograms of uranium, is now of the order of 10^{-9} g., and it was thought that the constant might be, for this quantity, appreciably greater, owing to a lesser degree of saturation, than for the other three preparations, which

contain between 1 and 2×10^{-10} g. For this reason two sets of standards, large and small, were made up, containing quantities of radium roughly corresponding with those in the uranium preparations. The results are given in Table I.

The first column shows the nature of the standard, the second the weight used, the third the weight of contained uranium for the pitchblende standards, and the fourth

Table I.

Calibration Results.

Standard.	Weight.	U(mg.).	Ra $\times 10^{-12}$ g.	Eq. factor.	Leak d. p. m.	Constant.
$RaBaCl_2$	0·2670 g.	—	174·1	0·9963	8·83	19·65
	0·2259 g.	—	147·3	0·9963	7·76	18·91
Pitchblende..	0·835 mg.	0·5112	173·8	0·8330	7·51	19·30
				0·9946	8·77	19·72
	0·8455 mg.	0·5171	175·8	0·9889	8·69	20·01
$RaBaCO_3$	0·01547 mg.	—	186·4	0·966	9·36	19·25
			Mean of Small Standards.....			19·47
$RaBaCl_2$	1·5027 g.	—	979·6	1·0	48·98	20·00
				0·763	38·29	19·52
	1·3646 g.	—	889·6	1·0	45·42	19·59
Pitchblende..	4·38 mg.	2·682	912·0	0·8004	35·96	20·30
				1·0	45·22	20·16
	4·986 mg.	3·053	1038	0·9971	51·16	20·23
$RaBaCO_3$.....	0·0996 mg.	—	1200	0·828	49·8	19·96
	0·2094 mg.	—	2523	0·4225	54·75	19·48
			Mean of Large Standards.....			19·90

the weight of the contained radium, the Ra/U ratio $3{\cdot}4 \times 10^{-7}$ being used for the pitchblende. The fifth column shows the proportion of radon accumulated in the standard in terms of the equilibrium quantity as unity, that is, $1-e^{-\lambda\tau}$, where λ is the radioactive constant and τ is the time of accumulation of radon in the standard. The sixth column shows the leak given, in d. p. m. corrected for the natural leak, and the last column the constant, or number of units of radium equal to a leak of 1 d. p. m.

The small and large standards are shown separately in the table, and it will be seen that the expectation has been borne out, the mean of the value of the constant for the small

standards being about 2 per cent. less than the mean for the large. The value for the pitchblende standards as a group is about 2 per cent. higher than for the two radium standards which are in agreement. In making up the pitchblende standards, both filtered and unfiltered solutions of pitchblende were used, but the results for the two solutions were identical. In terms of the radium standards, the Ra/U ratio for the pitchblende would be $3{\cdot}33 \times 10^{-7}$.

The Growth of Radium from Uranium.

The results obtained with the four old uranium preparations, fully described in earlier communications (II. and IV.) are shown in Table II.

TABLE II.

Growth of Radium from Uranium.

No.	Uranium (grams).	t, (years).	t^2.	d. p m.	Ra $\times 10^{-12}$ g.	Initial.	Growth.	u (mg.).	$\Theta_2\Theta_3$ $\times 10^{-8}$.
I.	255	25·42	646·2	6·74	131·2	16	115·2	0·3389	2·431
		25·52	651·3	7·00	136·3		120·3	0·3539	[2·346]
		25·65	658·0	6·78	132·1		116·1	0·3415	2·457
II.	278	24·62	606·1	6·95	135·3	18	117·3	0·3450	2·442
		24·73	611·6	6·97	135·7		117·7	0·3462	2·455
III.	408	24·27	589·2	8·82	171·7	4	167·7	0·4933	2·437
		24·37	594·2	8·75	170·4		166·4	0·4895	2·476
IV.	3000	21·70	470·9	52·26	1040	40	1000	2·942	2·401
		21·84	477·0	52·5	1045		1005	2·956	2·420
								Mean (rejecting second).....	2·440

The first column shows the number of the preparation, the second the quantity of contained uranium, the third the age in years, the fourth the square of the age, the fifth the divisions per minute given by the radon in equilibrium with the preparation, the sixth the quantity of radium present, the seventh the quantity initially present, and the eighth the growth of radium. In the ninth column the figures in the eighth are divided by $3{\cdot}4 \times 10^{-10}$ to give the uranium (milligrams) in equilibrium with the radium, and the last column shows $\Theta_2\Theta_3$ obtained from the formula $\Theta_2\Theta_3 = 1/2(U/u)t^2$. In deriving the sixth column from the fifth, the constant of the electroscope has been taken as 19·47 for the first three preparations, and 19·9 for the last.

It will be seen that the value of $\Theta_2\Theta_3$ for all four preparations is remarkably constant. Indeed, the closeness of the agreement is greater than for the standards used for calibration, and may therefore, to some extent, be accidental. The only exception is the second measurement for the first preparation and, as a third redetermination confirmed the first, the second has been excluded in arriving at the mean. The other six measurements agree to $\pm 1{\cdot}5$ per cent. with the mean value of $\Theta_2\Theta_3$, $2{\cdot}440 \times 10^8$ (years)^2.

For the value formerly adopted for Θ_3, 2375 years, Θ_2 is 102,750 years. With the value adopted by Lord Rutherford*, $\lambda_3 = 1{\cdot}373 \times 10^{-11}$(sec.)$^{-1}$ or $\Theta_3 = 2308$ years, Θ_2 is 105,700 years. With the value adopted by Stefan Meyer and E. Schweidler† $\Theta_3 = 2280$ years, Θ_2 is 107,000 years. It is unlikely that further continuation of these measurements will lead to a more accurate determination of Θ_2, as though the quantity of radium is still only one millionth of the amount that will ultimately be produced, the further increase in the quantity of radium will not increase the accuracy of the measurements. The value for the period of average life of ionium by this method may therefore be taken as $\Theta_2 = 1{\cdot}06 \times 10^5$ years, when that of radium is 2300 years. This gives $\lambda_2 = 3{\cdot}0 \times 10^{-13}$ (sec.)$^{-1}$ and $T_2 = 73{,}500$ years. Using this value, the results of Mmes. Curie and Cotelle, on the growth of radium from the ionium-thorium preparation referred to, makes the proportion of ionium 25·63 per cent. instead of 28·77 per cent. as determined from the atomic weights. As that work, and also the estimate of Meyer on the maximum value of Θ_2 from the total α-radiation, both involve the weighing of the preparation as the oxide, it may not be out of place to mention that the author found, in connexion with the emanating power of thorium oxide many years ago, that this substance is hygroscopic and exceedingly tenacious of water, unless ignited to a temperature near the melting-point of platinum. Possibly this may in part explain the discrepancy between the two methods of estimating Θ_2.

Summary.

The continued growth of radium, according to the square of the time, from uranium preparations purified in 1905–1909, has confirmed the value for the period of ionium

* 'Radiations from Radioactive Substances,' by Lord Rutherford, J. Chadwick, and C. D. Ellis, p. 25 (1930).

† 'Radioaktivität,' St. Meyer and E. Schweidler, p. 466 (1927).

obtained by this method previously, rather than the somewhat higher values of Stefan Meyer and Mmes. Curie and Cotelle using a thorium-ionium preparation for which the proportion of ionium had been deduced from atomic weight determinations. The work gives the values

$$\Theta_2 = 1{\cdot}06 \times 10^5 \text{ years}, \quad T_2 = 73{,}500 \text{ years}, \text{ and}$$
$$\lambda_2 = 3{\cdot}0 \times 10^{-13} \text{ (sec.)}^{-1}$$

when the period of average life of radium, Θ_3, is taken as 2300 years.

Old Chemistry Department,
University Museum, Oxford.
June 10, 1931.

XC. *On the Refractivities and Optical Dispersions of Methane and of its Substituted Chlorine Derivatives.* *By* G. W. Brindley, *M.Sc., Assistant Lecturer in Physics at the University of Leeds, and* H. Lowery, *Ph.D., F.Inst.P., Head of the Department of Pure and Applied Physics, College of Technology, University of Manchester* *.

(1) *Introduction.*

THE refractivities of gaseous methane, CH_4, and of its chlorine derivatives, CH_3Cl, CH_2Cl_2, $CHCl_3$ and CCl_4, in the gaseous state are of interest from several points of view. Firstly, the series is interesting on experimental grounds because, for several members of the series, results have been obtained differing rather widely from those of previous experimenters, and in the case of methylene chloride, CH_2Cl_2, no previous determination appears to have been made. A careful investigation has therefore been made of the refractivities of CH_3Cl, CH_2Cl_2, and $CHCl_3$, and of their dispersions in the visible region of the spectrum, as part of an extended investigation of the refractivities and dispersions of gaseous compounds which will be described elsewhere. The refractivities and dispersions of CH_4 and of CCl_4 have been determined already by C. and M. Cuthbertson [1] and by H. Lowery [2]. Secondly, it has been previously shown [3] that simple relations exist between the refractivities of certain gases which appear to be connected with the number of their loosely-bound electrons. It seemed worth while, therefore, to examine the methane series from this point of

* Communicated by Prof. R. Whiddington, D.Sc., F.R.S.

view. Thirdly, it seemed possible that a consideration of the refractivities of these compounds might throw some light on the question as to whether the methane molecule is symmetrical or not. Though chemical evidence supports the view that methane contains four equal C—H linkages, there is some experimental evidence that even in the gaseous state the methane molecule may be slightly asymmetrical[4]. Mrs. Lonsdale[5] has collected a considerable amount of evidence showing that in the solid state the four bonds of a carbon atom are probably not equal but are of two kinds.

(2) *Experimental.*

The refractivities and dispersions of CH_3Cl, CH_2Cl_2, and $CHCl_3$ have been measured by one of us (H. L.) using a Jamin interferometer over a range of wave-lengths, from $\lambda = 4800$ Å.U. to $\lambda = 6708$ Å.U. The mode of experiment consisted in determining first the refractive index of the substance in the gaseous state for the wave-length $\lambda = 5461$ Å.U. (the green mercury line), the source of illumination being a mercury vapour lamp in conjunction with a Hilger monochromatic illuminator. Two parallel refraction tubes, equal in all respects, were placed between the interferometer mirrors, one tube remaining permanently evacuated and the other tube being arranged to receive the substance under experiment. Observations were made on the displacement of interference fringes in the field of view of a telescope as the substance under test gradually filled the refraction tube.

The dispersion was determined in relation to the value of the refractive index already found for $\lambda = 5461$. For this purpose a rough dispersion curve[6] was obtained, using for the dispersion points narrow bands of wave-lengths selected from a continuous spectrum, the mean wave-lengths of these bands corresponding to the accurate values of the wave-lengths to be finally employed. Exact values of the refractivities for the wave-lengths of the dispersion points were found by counting a large number of fringes (between 600 and 900) for $\lambda = 5461$ while the substance gradually entered the refraction tube and then changing the wave-length in succession to the values chosen for fixing the dispersion curve and observing for each change of wave-length the new position of the fringes relative to the fiducial line in the eye-piece of the telescope.

From these observations it is possible to find the number of fringes which would have been displaced originally had the light been of these various wave-lengths instead of $\lambda = 5461$. For a given amount of gas in the refraction

tube at constant temperature and pressure, the refractivity, $(\mu - 1)$, varies directly as the number of interference fringes displaced and also varies with the wave-length; since the refractivity has already been determined for a definite wave-length, viz., $\lambda = 5461$, and the corresponding number of interference fringes displaced has been carefully observed, all the information is available for the calculation of the refractivities for the dispersion wave-lengths.

Monochromatic illumination for the dispersion measurements was obtained by using the following sources in connexion with the Hilger monochromatic illuminator: (1) for $\lambda = 4047$, 4358, 5461 and 5770—a mercury vapour lamp; (2) for $\lambda = 4800$, 5086 and 6438—an arc between cadmium poles; (3) for $\lambda = 4602$, 6104 and 6708—an arc between carbon poles which were drilled axially and packed with lithium chloride.

In calculating the results, the observed refractivities have been reduced to the values they would have had if the number of molecules per cubic centimetre of the gas or vapour had been equal to the number of molecules per cubic centimetre of hydrogen at 0° C, and 760 mm. pressure. Cuthbertson[1] has pointed out the convenience of expressing the results in this way. The legitimacy of this method depends on the refractivity being proportional to the density and, for a given density, being independent of the temperature (both these assumptions having been justified experimentally), whereas the older method assumed that the gas laws could be applied over wide ranges of temperature and pressure, which is not justifiable. For the more perfect gases, both methods give practically the same results, but for vapours the two methods lead to results which are sometimes appreciably different and, in such cases, the density method is preferable to the older method which assumes the truth of the simple gas laws.

(3) *Results.*

(1) *Carbon Tetrachloride.* CCl_4.

The experiments on gaseous CCl_4 have already been fully described[2]. For $\lambda = 5461$, the refractive index of the gas at standard density is 1·001799. The dispersion over the range $\lambda = 4800$ to $\lambda = 6708$ can be expressed by a single term formula of the Sellmeier type,

$$(\mu - 1) = \frac{13{\cdot}543 \times 10^{27}}{7831{\cdot}7 \times 10^{27} - n^2},$$

where n is the frequency of the incident light.

(2) *Chloroform.* $CHCl_3$.

Some experiments on this substance have been described previously by one of us[7]. Further experiments, however, have been carried out, using specimens from different sources; in all cases the specimens were re-distilled before use in order that there should be no doubt about their purity. The value finally obtained for the refractive index ($\lambda = 5461$) is 1·001448 and the dispersion formula is

$$(\mu-1) = \frac{15{\cdot}391 \times 10^{27}}{10933 \times 10^{27} - n^2}.$$

Previous determinations of the refractive index of chloroform by Mascart and by Lorenz gave respectively 1·001464 and 1·001442 for $\lambda = 5893$. (See 'International Critical Tables,' vii., 1930.) The present result, therefore, confirms the value obtained by Lorenz.

(3) *Methylene Chloride.* CH_2Cl_2.

The refractivity and dispersion of this substance do not appear to have been measured previously.

Pure methylene chloride as supplied by Messrs. British Drug Houses was employed for the work, a small sealed and weighed bulb of the substance (in the liquid state) being introduced into one of the refraction tubes, which was then evacuated and sealed. The bulb of substance was afterwards broken in the refraction tube and the escaping liquid frozen by means of a suitable freezing mixture. The displacement of the interference fringes was observed as the substance was gradually allowed to vaporize completely. The weight of substance taken and the volume of the refraction tube being known, the density of the vapour producing retardation of the light could be determined,

The refractive index of gaseous methylene chloride at standard density, for $\lambda = 5461$, was found to be 1·001112, the dispersion formula being given by the expression

$$(\mu-1) = \frac{9{\cdot}1881 \times 10^{27}}{8565{\cdot}6 \times 10^{27} - n^2}.$$

(4) *Methyl Chloride.* CH_3Cl.

Mascart determined the refractive index of methyl chloride in the gaseous state for $\lambda = 5893$, and obtained a value 1·000870. (See 'International Critical Tables,' vii., 1930.) It will be seen later that this value is so very different from what we would expect for the refractive index of methyl chloride, that a new determination was necessary. The

specimen of methyl chloride used in the present experiments was obtained from a cylinder supplied by Messrs. Griffin and Tatlock. The gas was liquefied and fractionally distilled several times and was then admitted directly to the refraction tube.

The refractive index for the standard density and $\lambda = 5461$ was found to be 1·0007804, the dispersion being represented by the expression

$$(\mu - 1) = \frac{5{\cdot}8524 \times 10^{27}}{7801 \times 10^{27} - n^2}.$$

This result differs considerably from the earlier determination by Mascart, and, in view of the precautions taken in the present work and of certain numerical results given below, there is no doubt that the earlier result is inaccurate.

TABLE I.

Experimental Values of the Refractivities of Methane and its Substituted Chlorine Derivatives. $(\mu - 1) \times 10^6$.

	λ in Å.U.	CH_4.	CH_3Cl.	CH_2Cl_2.	$CHCl_3$.	CCl_4.
Li.....	6708	437·59	769·93	1098·4	1433·9	1774·0
Cd. ...	6438	438·24	771·69	1100·4	1436·2	1778·4
Li.....	6104	—	774·21	1103·7	1439·9	1784·6
Hg. ...	5770	440·29	777·15	1107·6	1443·5	1791·8
Hg. ...	5461	441·50	780·40	1112·0	1448·0	1799·0
Cd. ...	5086	443·30	785·26	1118·4	1454·7	1810·1
Cd. ...	4800	444·97	789·79	1124·0	1460·2	1819·6
Hg. ...	4602	—	793·44	1128·6	1464·6	
Hg. ...	4358	—	798·75	—	1471·3	—

(4) *Discussion of the Results.*

From both the classical and the quantum theories of dispersion it is evident that the refractivity of an atom or molecule is determined mainly by the outer loosely bound groups of electrons which are much more easily polarizable than the more tightly bound inner groups. If the deformability, α, of an atom is defined as the moment induced per unit applied field, then for gases having N atoms per unit volume,

$$(\mu^2 - 1) = 4\pi N\alpha. \quad . \quad . \quad . \quad . \quad . \quad . \quad (1)$$

According to the classical theory,

$$\alpha = \frac{e^2}{4\pi^2 m} \sum_p \frac{f_p}{p^2 - n^2}, \quad . \quad . \quad . \quad . \quad . \quad (2)$$

where f_p is the number of elastically bound electrons per atom, with natural frequency p. Then

$$(\mu^2-1) = \frac{Ne^2}{\pi m} \sum_p \frac{f_p}{p^2-n^2}. \quad . \quad . \quad . \quad . \quad . \quad (3)$$

Using the older quantum theory, Kramers and Heisenberg[8] have developed a slightly different expression for α:

$$\alpha = \frac{e^2}{4\pi^2 m} \left\{ \sum_a \frac{f_a}{n^2-n^2} - \sum_e \frac{f_e}{n_e^2-n^2} \right\}, \quad . \quad . \quad (4)$$

f_a and f_e being the average number of dispersion electrons per atom associated with the absorption and emission frequencies n_a and n_e; f_a and f_e are determined by the intensities of the corresponding absorption and emission lines. An expression essentially the same as (4) has been given by Schrödinger[9] for the case of an atom in the ground state, for which f_e is zero,

$$\alpha = 2 \sum_m \frac{(E_k - E_m) a_{km} b_{km}}{(E_k - E_m)^2 - h^2 n^2}, \quad . \quad . \quad . \quad . \quad (5)$$

where E_k is the energy of an electron in the ground state and E_m the energy in an excited state. According to modern theory, therefore, refractivity is to be thought of in terms of the probabilities of electronic transitions and of the associated frequencies arising mainly from the loosely bound 'dispersion' electrons.

The valency of the carbon atom in organic compounds has been discussed by London[10] from the point of view of his theory of homopolar valence, in which two electrons having opposite spins are associated with each homopolar linkage. According to this, carbon in its normal state should be divalent, as in CO, but in general carbon is quadrivalent, a fact which can only be reconciled with the theory if the spatial symmetry of carbon is raised when in combination with other atoms. The simplest model of the methane molecule is one in which the four hydrogen atoms are symmetrically disposed with respect to the carbon atom, each C—H linkage being formed of a pair of electrons having opposite spins, one contributed by the carbon atom and one by a hydrogen atom. These electrons will be loosely bound compared with the two K electrons of the carbon atom, and we may, therefore, regard the refractivity of methane as being due almost entirely to the eight electrons associated with the four C—H linkages, and, further, if the four linkages are similar, as chemical evidence suggests, each will contribute equally to the total refractivity of the molecule.

Similarly in CCl_4, where the linkages are also usually considered to be homopolar, the total refractivity is due to four equal contributions. Presumably, the outer electrons of the carbon atom complete rare-gas-like configurations of electrons round each chlorine nucleus, these configurations not being spherically symmetrical as in a rare-gas but distorted by the central carbon atom, the forces arising from the distortion being the forces holding the atoms together in the molecule.

It is of interest now to consider whether the refractivities of the chlorine derivatives of methane can be derived from the refractivities of the C—H and C—Cl linkages as obtained from CH_4 and CCl_4. Consider the data given in Table I. for $\lambda = 5461$ Å.U.:

$(\mu-1)$ for $CH_4 = 441{\cdot}50$ Then $(\mu-1)$ for C—H = 110.38

$(\mu-1)$ for $CCl_4 = 1799{\cdot}0$ Then $(\mu-1)$ for C—Cl = 449·75

With these values for the C—H and the C—Cl linkages, we obtain the following :—

TABLE II.

$(\mu-1)\times 10^6$, for $\lambda = 5461$ Å.U.

	Observed.	Calculated.	Percentage difference.
CH_3Cl	780·4	780·9	0·0 %
CH_2Cl_2	1112·0	1120·3	0·7 %
$CHCl_3$	1448·0	1459·6	0·8 %

TABLE III.

Comparison of Observed and Calculated Refractivities.

$(\mu-1)\times 10^6$.

	CH_3Cl.		CH_2Cl_2.		$CHCl_3$.	
λ in Å.U.	Obs.	Calc.	Obs.	Calc.	Obs.	Calc.
6708	769·93	771·70	1098·4	1105·8	1433·9	1439·9
6438	771·69	773·28	1100·4	1108·3	1436·2	1443·4
5770	777·15	778·16	1107·6	1116·0	1443·5	1453·9
5461	780·40	780·89	1112·0	1120·3	1448·0	1459·6
5086	785·26	785·00	1118·4	1126·7	1454·7	1468·4
4800	789·79	788·62	1124·0	1132·3	1460·2	1475·9

In Table III. a comparison is made between the observed and the calculated refractivities for as many wave-lengths as were used experimentally for all the gases.

The results given in Tables II. and III. show that there is quite a close agreement between the observed and the calculated refractivities throughout the visible region. The closeness of the agreement seems to justify our assumption that the refractivities of these compounds arise from the electrons associated with the C—H and C—Cl linkages and that the contributions of these linkages to the total refractivities can be calculated from CH_4 and CCl_4 respectively. If this is the case, then the electronic energy levels in the C—H linkage and the probabilities of the electrons passing to excited levels must be the same, or almost the same, for this linkage in CH_4, CH_3Cl, CH_2Cl_2, and $CHCl_3$; *i.e.*, the substitution of chlorine in methane does not appear to alter appreciably the condition of the remaining C—H linkages. Similarly, the energy levels and probabilities of excitation appear to be the same for the electrons, presumably eight

Table IV.

Comparison of the Refractivities of HCl and CCl_4.

$(\mu-1)\times 10^6$.

λ in Å.U.	HCl.	$\frac{1}{4}.(CCl_4)$.
6708	443·7	443·5
6438	444·4	444·6
5770	446·7	447·9
5461	448·0	449·7
5086	450·1	452·5
4800	451·9	454·9

altogether, associated with each C—Cl linkage and the outer shell of each chlorine atom.

In this connection it is interesting to compare the refractivities of CCl_4 and HCl both in the gaseous state.

The significance of the very close agreement between the refractivity of HCl and one quarter of the refractivity of CCl_4 shown in Table IV. is that the energy levels and excitation probabilities are the same, or almost the same, for the chlorine atom in the two molecules. It is difficult to say whether the linkage between H and Cl in HCl is homopolar or heteropolar; there seems to be no clear distinction between the two in this case. It seems probable that there will be a rare-gas arrangement of electrons round the chlorine nucleus, imbedded in which is the hydrogen nucleus which produces a lack of spherical symmetry in the electron distribution about the chlorine nucleus. The conditions in CCl_4 are

presumably rather similar ; about each chlorine nucleus there is a rare-gas distribution of electrons, whose spatial symmetry is disturbed by the central carbon nucleus, which is only partially screened by its two tightly-bound K electrons. The explanation of the results given in Tables II., III., and IV., therefore, seems to be that the energy levels and excitation probabilities of the so-called dispersion electrons are the same in the distorted outer shells of the chlorine atoms in HCl, CCl_4, $CHCl_3$, CH_2Cl_2, and CH_3Cl.

The fact that it is possible to correlate the refractivities of methane and its chlorine derivatives indicates that the four C—H linkages of methane are identical or nearly so. For if two were different from the remaining two, as Mrs. Lonsdale suggests is the case for the carbon atom in crystalline compounds, then the different linkages would have different refractivities and the close agreement shown in Tables II. and III. would not be expected.

(5) *Summary.*

The refractivities and dispersions in the visible region of the spectrum have been determined for the substituted chlorine derivatives of methane in the gaseous state, by means of a Jamin interferometer, and in all cases special precautions were taken to obtain pure compounds. The dispersion results are represented by a single term formula of the Sellmeier type, within the limits of experimental error. The results are as follows :—

$$CHCl_3 \ldots\ldots \mu-1=\frac{15{\cdot}391\times10^{27}}{10933\times10^{27}-n^2}.$$

$$CH_2Cl_2 \ldots\ldots \mu-1=\frac{9{\cdot}1881\times10^{27}}{8565{\cdot}6\times10^{27}-n^2},$$

$$CH_3Cl \ldots\ldots \mu-1=\frac{5{\cdot}8524\times10^{27}}{7801\times10^{27}-n^2}.$$

It is shown that, to within 1 per cent., the refractivities of this series of compounds can be explained by assuming a certain refractivity for the C—H and C—Cl linkages, which presumably are homopolar, derived from CH_4 and CCl_4, respectively. It is also shown that there is almost perfect agreement between $(\mu-1)/4$ for CCl_4 and $(\mu-1)$ for HCl. According to modern theory, refractivity is explained in terms of the probabilities of electrons (mainly the "dispersion" electrons) passing to excited states. The interpretation of the results given, therefore, seems to be that the

probabilities of excitation of electrons in the chlorine atom (or ion) in HCl, CCl_4, $CHCl_3$, CH_2Cl_2, and CH_3Cl are practically the same. This is also true for the C—H linkage in CH_4, CH_3Cl, CH_2Cl_2, and $CHCl_3$. It is shown that these results imply that the four C—H linkages in CH_4 are equal; this is discussed in relation to London's theory of homopolar valence.

References.

(1) C. and M. Cuthbertson, Proc. Roy. Soc. A, xcvii. p. 156 (1920).
(2) H. Lowery, Proc. Lond. Phys. Soc. xxxix. p. 421 (1927).
(3) G. W. Brindley, Phil Mag. vii. p. 891 (1929).
(4) *Cf.* Cabannes and Gauzit, *Journ. de Phys.* vi. p. 182 (1925).
(5) K. Lonsdale, Phil. Mag. vi. p. 433 (1928).
(6) *Cf.* C. and M. Cuthbertson, Proc. Roy. Soc. A, lxxxiii. p. 152 (1909).
(7) H. Lowery, Proc. Lond. Phys. Soc. xl. p. 26 (1927).
(8) Kramers and Heisenberg, *Zeits. f. Physik*, xxxi. p. 681 (1926).
(9) E. Schrödinger, *Ann. der Physik*, lxxxi. p. 109 (1926).
(10) F. London, *Zeits. f. Physik*, xlvi. p. 455 (1928).

XCI. *Surface-tension of different Dilutions of Boys' Soap Solution.*

By L. D. Mahajan, *M.Sc., Professor of Physics, Mohindra College, Patiala* *.

IN 1878 Prof. W. Gibbs † showed that within very wide limits the surface-tension of soap solutions as determined by capillary tubes is almost independent of strength.

In 1890 Lord Rayleigh ‡ proved beyond doubt that the surface-tension of soap solutions changes with the freshness of the surface formed. From observations upon a jet of liquid issuing from an elliptical aperture he concluded that the addition of a little oleate of soda does not change the surface-tension if the surface be fresh, proving thereby that the change in the tension is due to external agency.

In 1920 M. G. White and J. W. Marden § found the surface-tension of various soap solutions and their emulsifying powers, and found that, unlike the solutions of sodium hydrate

* Communicated by the Author.

† Gibbs, W., Connecticut Acad. Trans. iii. part 2 (1877–78).

‡ Rayleigh, "On the Tension of recently formed Liquid Surfaces," Proc. Roy. Soc. xlvii. pp. 127–140, 281–287 (1890).

§ White, M. G., and Marden, J. W., 'Journal of Physical Chemistry,' xxiv. pp. 617–629 (Nov. 1920).

(Na . OH) and many other salts, soap solutions diminish in surface-tension as they increase in concentration. Thus they concluded that the emulsifying power is closely connected with the surface-tension.

In 1922 A. L. Narayan and G. Subrahmanyam * showed from experimental data by using a bubble method that the surface-tension of soap solutions is the same for all concentrations between very wide limits.

In 1924 very dilute colloidal solutions were tried by P. L. Du Nouy †, who showed that a drop increases with dilution and shows a maximum at a given concentration varying between 10^{-4} and 10^{-5} generally. He writes also that certain colloids (saponin for instance) do not show any drop at high concentration, and when such solutions are stirred their surface-tension rises.

A large number of other papers have been published on the surface-tensions of colloidal solutions, but owing to the various methods used certain facts have still been overlooked so far. The purpose of this paper is to review briefly the results obtained by using a different method, namely the Warren's surface-tension balance ‡, which is the most sensitive method for finding a series of results with different concentrations and at different temperatures. The results have also been found by using a weighing method §, and compared with those obtained by the former method. In all the experiments mentioned in this paper, the Boys' soap solution ‖ is used.

Method.

The Boys' soap solution (standard) was prepared in stock and kept in a cool and dark place. By mixing different quantities of the same with water fresh dilutions of different concentrations were prepared whenever required.

* Narayan, A. L., and Subrahmanyam, G., "The Surface-tension of Soap Solutions for Different Concentrations," Phil. Mag. (6) xliii. pp. 663–668 (1922).

† Du Nouy, P. L., "Surface-tension of Colloidal Solutions and Dimensions of certain Organic Molecules," Phil. Mag. xlviii. pp. 264–270 (Aug. 1924) ; Du Nouy, P. L., "A New Determination of the Constant N of Avogadro, based on its Definition," Phil. Mag. xliii. pp. 664–669 (Oct. 1924) ; Du Nouy, P. L., "The Surface-tension of Colloidal Solutions and the Size of some Colloidal Molecules," J. Exp. Med. 1924.

‡ Warren, E. L., "Surface-tension Balance," Phil. Mag. (7) iv. pp. 358–386 (1927).

§ "Weighing Method." See 'Properties of Matter,' by Poynting and Thomson, p. 161.

‖ Boys' soap solution contains 2·5 per cent. sodium oleate and 25 per cent. glycerine.

The capillary method was not used, for it is difficult in the first place to find a capillary tube of sufficiently uniform cross-section, and when one has been found the calibration, the cleaning, and keeping clean, of this tube are no small matters. Moreover, difficulty is experienced in measuring accurately the height of ascent of the liquid in the tube. Furthermore, the elaborate thermostatic arrangements to keep the temperature constant and to measure the angle of contact are still more difficult in performing the experiment. Hence some easier and more accurate methods were used, namely, (i.) the surface-tension balance, and (ii.) the weighing method.

The glassware, containers, flasks, beakers, pipettes, jets, etc. were freshly boiled for two hours in a cleaning solution ($H_2SO_4 + K_2Cr_2O_7$), rinsed in specially prepared distilled water, and dried. The greatest care was taken in handling the solutions under experiment, so as not to disturb their surfaces.

The experiments were performed in a dark and cool room. The temperature of the room was kept fairly constant. The exposure of the solution to the light and heat rays was avoided as far as possible. The arrangements of the apparatus and theory are given in full detail in Phil. Mag. (August 1927).

In the case of weighing method (ii.), from a smooth jet of burette a known number of drops were dropped into a weighed beaker. Knowing the radius a of the jet and mean weight w of the drop, the surface-tension T of the liquid was calculated from the following formula :—

$$w = \pi a \mathrm{T},$$

where π is a certain constant.

Since the above formula was not very accurate, the results were compared with water (distilled) at a known temperature. Thus many constants of the formula were eliminated, and the results obtained were quite concordant with those of the first one. The following relation was used :

$$\frac{w_1}{w'} = \frac{\pi . a . \mathrm{T}_1 . c}{\pi . a . \mathrm{T}' . c} = \frac{\mathrm{T}_1}{\mathrm{T}'},$$

where w_1 is the weight of one drop of the solution and w' is the weight of one drop of water. T_1 is the surface-tension of the solution and T' is the surface-tension of water ; c and π are the constants in the formula, and a is the radius of the jet.

Observations.

The following set of observations was taken with the weighing method :—

TABLE I.

No.	Amount of Boys' soap solution in the dilution.	Room temp.	Surface-tension in dynes per cm.
1	100·0 per cent.	21°·0 C.	32·96 dynes per cm.
2	70·0 ,,	,,	32·20 ,,
3	50·0 ,,	,,	30·98 ,,
4	40·0 ,,	,,	30·00 ,,
5	20·0 ,,	,,	27·53 ,,
6	15·0 ,,	,,	27·20 ,,
7	10·0 ,,	,,	29·01 ,,
8	5·0 ,,	,,	30·20 ,,
9	0·0 ,,	,,	73·72 ,,

The following sets of observations were taken with the surface-tension balance method :—

TABLE II.

No.	Amount of Boys' soap solution in the dilution.	Room temp.	Surface-tension in dynes per cm.
1	100·0 per cent.	30°·0 C.	31·821 dynes per cm.
2	50·0 ,,	,,	31·618 ,,
3	30·0 ,,	,,	30·812 ,,
4	20·0 ,,	,,	29·902 ,,
5	15·0 ,,	,,	29·813 ,,
6	10·0 ,,	,,	32·111 ,,
7	7·0 ,,	,,	34·836 ,,
8	0·0 ,,	,,	71·586 ,,

TABLE III.

No.	Amount of Boys' soap solution in the dilution.	Room temp.	Surface-tension in dynes per cm.
1	75·0 per cent.	30°·0 C.	31·714 dynes per cm.
2	50·0 ,,	,,	31·613 ,,
3	30·0 ,,	,,	30·810 ,,
4	20·0 ,,	,,	29·900 ,,
5	15·0 ,,	,,	29·810 ,,
6	10·0 ,,	,,	32·110 ,,
7	7·0 ,,	,,	34·840 ,,

One curve is drawn showing the relation between the concentration of the Boys' soap solution in the dilution and its surface-tension in the accompanying figure.

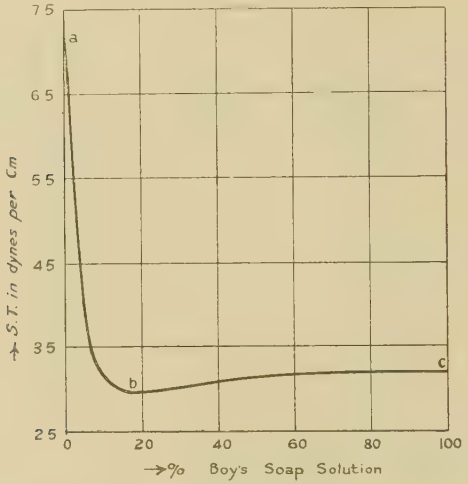

Discussion.

The curve in the figure shows that the relation is a very interesting one. The surface-tension of the dilution falls very rapidly as the amount of Boys' soap solution added to water is increased from zero to 5·0 per cent. From 5·0 per cent. to 15·0 per cent. it falls comparatively slowly ; then after 15·0 per cent. the further addition of Boys' soap solution increases the surface-tension instead of decreasing it as in many other salt solutions, but this increase of surface-tension is very slow.

The part *ab* of the curve shows that the greater the concentration of the Boys' soap solution the less is the surface-tension. This part of the curve agrees with the results obtained by White and Marden. The part *bc* shows that the greater the concentration the greater is the surface-tension. This increase of surface-tension with concentration in dilute solutions is the reverse of that given by the said scientists.

It is also evident from the curve that the surface-tension of the soap-solutions is not independent of the strength of the soap-solution (*i. e.*, the strength of the sodium oleate in the solution), and hence throws much light on the results obtained by Lord Rayleigh and A. L. Narayan and G. Subrahmanyam. The latter showed that within very wide limits the surface-tension of the soap solutions is independent of the strength of sodium oleate in the solutions.

Further the part *ab* of the curve also agrees with the results of P. L. Du Nouy, who found that the size of the drop increases with dilution, *i. e.*, the less the concentration the greater is the surface-tension, for the size of the drop depends upon the surface-tension ; but the part *bc* will show the reverse phenomena.

A marked minimum in surface-tension is also apparent in the same curve at 15·0 per cent. concentration of the Boys' soap solution, or 0·375 per cent. sodium oleate in the dilution. This marked minimum in surface-tension may be explained thus :—It occurs only when the quantity of sodium oleate in the dilution is just sufficient to form a monolayer of particles on the surface of water. When the quantity of sodium oleate in the dilution is greater than that required to form a monolayer on the water surface the surface-tension of the dilution increases with the concentration of sodium oleate, *i. e.*, the greater the concentration the greater will be the surface-tension ; but when the quantity of the sodium oleate is less than that required to form a monolayer, the surface-tension of water predominates, which is far greater than that of the soap solutions. Hence the surface-tension again increases with decrease of concentration of sodium oleate, *i. e.*, the less the concentration the greater will be the surface-tension.

Conclusion.

The results obtained are very encouraging and throw much light on the previous papers on the same problem.

Physics Laboratory,
Mohindra College,
Patiala (India).
22nd April 1931.

XCII. *Classical and Modern Gravitational Theories.*

To the Editors of the Philosophical Magazine.

Gentlemen,—

IN the January 1931 issue of your Magazine, in the article by Mr. A. Press on "Classical and Modern Gravitational Theories" we find on pages 118 and 119 the following statement :—

"As a matter of fact, in the earlier paper (*l.c.* pp. 642–643) a very important error was shown to have crept into the

Lorentzian analysis, due to disregarding the essential limitations under which $\operatorname{div}\rho\mathbf{u}$ could be equated to $d\rho/dt$. As a result the invariant transformations made so much of in General Relativity Theory fall by the wayside."

On looking up the earlier paper mentioned above, entitled "Classical and Modern Electromagnetic Theories" published in the 'Philosophical Magazine' of November 1929, we find that instead of ρu, Mr. Press always uses $\rho u'$, where u' has the components u_x, u_y, and u_z in equation (27), while in equation (32) it has the components u_x', u_y', and u_z'. This tends to introduce confusion, but does not prevent one from detecting several serious errors both in the mathematics and in its interpretation.

His equation (27) is

$$\operatorname{div}\rho u' = \frac{\partial}{\partial x}(\rho u_x) + \frac{\partial}{\partial y}(\rho u_y) + \frac{\partial}{\partial z}(\rho u_z), \quad . \quad . \quad (27)$$

and equation (32) is

$$\frac{d\rho}{dt} = u_x' \cdot \frac{\partial \rho}{\partial x} + u_y' \cdot \frac{\partial \rho}{\partial y} + u_z' \cdot \frac{\partial \rho}{\partial z}. \quad . \quad . \quad . \quad (32)$$

Mr. Press then states:

"Equation (32) has now to be correlated with (27). Yet in order that (27) and (32) should be equivalent we must specify

$$\left.\begin{aligned} u_x' &= f_x(y, z, t) \text{ and independent of } x, \\ u_y' &= f_y(x, z, t) \quad \text{,,} \quad \text{,,} \quad \text{,,} \ y, \\ u_z' &= f_z(x, y, t) \quad \text{,,} \quad \text{,,} \quad \text{,,} \ z. \end{aligned}\right\} . \quad . \quad (33)$$

These are very serious limitations. Only when (33) are satisfied can we write (32) in the form

$$\frac{d\rho}{dt} = \frac{\partial}{\partial x}(\rho u_x') + \frac{\partial}{\partial y}(\rho u_y') + \frac{\partial}{\partial z}(\rho u_z'). \quad . \quad (27')."$$

Let us now examine the foregoing statements of Mr. Press. On equating the right-hand members of equations (27) and (32), (assuming that the primed and unprimed velocity components are intended to be treated as identical) we find $\rho \operatorname{div} u' = 0$, which does not mean that we must specify (33), for the latter conditions are not necessary, although they may be sufficient to make $\rho \operatorname{div} u' = 0$.

Furthermore Mr. Press's interpretation of (33) is incorrect, for he states:

"Surely this is equivalent to regarding the movement

of the whole aggregation of charges + and − as partaking of a rigid body movement."

On the contrary, it is apparent from an inspection of the first equation (33), $u_x' = f_x(y, z, t)$, that different charges in a plane perpendicular to the x-axis must have different values of u_x' or that the motion of the system is like that of a deformable body.

Mr. Press then charges Lorentz with the error of ignoring these "limitations" in the latter's use of the equation $\frac{d\rho}{dt} = \operatorname{div} \rho u'$. We find, however, that Mr. Press likewise proceeds to ignore these very "serious limitations" when he goes on to derive the "two equations fundamental to electrodynamics," for he makes his equation (27″), $\frac{d\rho}{dt} = \operatorname{div} \rho u'$, the starting point in his derivation.

If we ignore this strange inconsistency and try to check the mathematics we find that the term curl $\rho u'$ in equation (38) is incorrectly equated to zero. The following is Mr. Press's reasoning :—

'Yet from (27″) $\rho u'$ cannot have curl, since it already has divergence and note must be taken of (33)."

In the first part of this statement we are asked to believe that a vector having a divergence can for that reason have no curl. This is obviously false. In the second part of the above statement we are told that curl $\rho u'$ is zero in view of (33). We see, however, that (33) are not necessary, and it is therefore not necessary that curl $\rho u'$ shall vanish.

Mr. Press calls attention to the fact that equation (35), $\frac{d}{dt}\mathbf{d} + \rho \mathbf{u}' = \operatorname{curl} \mathbf{h}$, is one of Lorentz's "fundamental equations," while in his work it is made a "derived" equation. Although it is true that this equation is derived by Mr. Press from his equation (28′),

$$\operatorname{div}\left(\frac{d\mathbf{d}}{dt} + \rho \mathbf{u}'\right) = 0, \quad . \quad . \quad . \quad . \quad . \quad (28')$$

it is apparent from the nature of the derivation that one need not interpret equation (35) as a fundamental equation of electromagnetism unless the vector $\mathbf{h}$ is identified in some way with magnetic field intensity. Mr. Press's "derived" equation is a defination of a certain vector $\mathbf{h}$, since this vector is introduced merely to satisfy condition (28′). There is

nothing in the derivation nor in the definition given which allows us to connect h with the magnetic field intensity.

Mr. Press's fundamental equation is $\frac{d\rho}{dt} = \text{div}\,\rho\mathbf{u}'$, which implies the conservation of charge, but it does not tell us anything about the connexion between electricity and magnetism. His derived fundamental equation (35) has therefore no physical significance other than that it is consistent with the familiar equation of continuity.

The second fundamental equation derived by Mr. Press is obviously in conflict with experience, since, according to $-\frac{1}{c}\frac{dh}{dt} = \text{curl}\,\mathbf{d}$, we may say that the total induced electromotive force about a circuit due to a varying magnetic flux interlinking the circuit depends upon the material of the circuit. Such a theoretical result is not surprising in view of the error committed in neglecting curl $\rho u'$ and the unjustified shift in symbols from **D** in (41) to **d** in (42).

The College of the City of New York
Department of Physics,
Convent Avenue and 139th Street.
February 17, 1931.

Respectfully yours,
Alexander Marcus.

XCIII. *A Precise Experimental Determination of Energy of Excitation by Electron Impact in Helium.* *By* J. E. Roberts, *Ph.D.*, *and* R. Whiddington, *F.R.S.*, *Leeds* *.

ALTHOUGH the theory of spectra has given a fairly complete and accurate analysis of the energy levels in the helium atom, the corresponding results from direct experiments on electron impacts are not so satisfactory. In particular the result of the impact of an electron of moderately high velocity—*i. e.*, with energy well above the excitation energy—with a helium atom is somewhat uncertain. The usual critical potential methods of Franck and Hertz and Foote and Mohler † have been applied with some success to the problem. In these methods the velocity of an electron beam in the gas is increased until the critical energy for excitation is reached, this energy then being

* Communicated by the Authors.
† Mohler, Bull. Nat. Res. Coun. ix. p. 120 (1924).

measured. By this means all the accepted lower spectroscopic states of the atom have been identified. On the other hand, when electrons of 40 to 200 volts energy are used the question of the relative probabilities of excitation of the various states for such electronic impact velocities has to be taken into consideration. Determinations of the most probable energy losses of these faster electrons have been made by Dymond * and by McMillen † with rather discordant results. Other gases have been studied by a number of investigators in a similar way.

In most of the experimental methods so far used for the determination of critical electron energies in gases there are a number of factors which tend to make the results inconsistent and unsatisfactory. Considerable corrections have to be made in some cases for the inevitable velocity distribution of the primary electrons and for contact potentials in the apparatus which are difficult to measure directly. This is particularly the case in the older experiments where current-potential curves are obtained. Two methods have been used in the past to correct these effects:—

(*a*) If the electron velocity is sufficiently high to give double collisions, then the voltage difference between the peaks in the curves representing single and double collisions should give the correct excitation potential. The accuracy of this method is considerably reduced by the fact that the double collision effects are much smaller than the single. Moreover, when there are a number of prominent resonance potentials the double collision effects become complex and difficult to unravel.

(*b*) On the other hand, it is a common practice to introduce a small quantity of mercury or one of the rare gases into the apparatus and to measure its critical potentials at the same time as those of the gas being investigated. The potentials for the inert gas are then calculated from spectroscopic data and the necessary corrections estimated. Apart from the relative nature of the method, which in itself is unattractive in some ways, this procedure, although often successful, is open to the criticism that no account can be taken of the relative probabilities of excitation of the states of the inert gases in the fixing of their critical potentials. For example, in the case of helium the lowest calculated potential is 19·77 volts, but it is very doubtful whether this would be *clearly* shown in current potential curves. Corrections of

* Dymond, Phys. Rev. xxix. p. 433 (1927).
† McMillen, Phys. Rev. xxxvi. p. 1034 (1930).

this type often amount to 5 to 10 per cent. of the whole measured potential. In more recent work of this type Glockler * has used direct methods of estimating corrections, thereby increasing the accuracy of the measurements. Further, it has been shown by Rudberg † that unless very special precautions are taken the contact potentials change considerably during the course of an experiment. This might well explain a number of discrepancies in critical potential work.

In the cases where actual energy losses of electrons are investigated other difficulties arise. It is usual to measure the voltage separation between the primary electrons and those which have suffered inelastic collisions with gas molecules. This measurement is often rendered difficult owing to the large intensity of the primary beam, and hence the impossibility of an accurate determination of the "zero" voltage. In most previous experiments ‡ the energy loss has been estimated from the differences in voltage between the primary and the "loss" electrons. As this consisted in finding the difference between two comparatively large quantities, high accuracy could not be obtained. The experiments to be described in this paper were made in an attempt to overcome most of these difficulties and to reach an accuracy hitherto unattained in electron work.

The choice of a gas for such an investigation was of some importance. It was clear that a monatomic gas would be far more convenient than a diatomic, owing to the comparative simplicity of the states. A number of investigations in this laboratory § (some unpublished) have shown that the magnetic spectrum of electrons in diatomic gases show much broader lines—or bands—than the corresponding spectra in monatomic gases. This effect is due to the complex nature of the molecular electronic state, the excitation of the vibrational levels giving an extended energy spectrum of the exciting electrons. Such broadening of the loss "lines" would inevitably slightly reduce the accuracy of measurement. Diatomic gases were therefore ruled out for calibration experiments of the type projected. The obvious

* Glockler, Phys. Rev. xxxiii. p. 175 (1929).

† Rudberg, Proc. Roy. Soc. A. cxxix. p. 628 (1930).

‡ McMillen, *loc. cit.*; Jones and Whiddington, Phil. Mag. vi. p. 889 (1928); Roberts and Whiddington, Proc. Leeds Phil. Soc. ii. p. 12 (1929); Proc. Leeds Phil. Soc. ii. p. 46 (1930).

§ Jones and Whiddington, Phil. Mag. vi. p. 889 (1928); Roberts and Whiddington, Proc. Leeds Phil. Soc. ii. p. 12 (1929); Proc. Leeds Phil. Soc. ii. p. 46 (1930).

monatomic gas for our purpose was atomic hydrogen, but difficulties of technique made this virtually impossible. Argon has been investigated to some extent * by the authors, and it has been pointed out that the observed "loss lines" cannot be assigned to single spectroscopic transitions with any certainty. Helium alone, therefore, seemed to have a sufficiently simple system of energy levels to be suitable for accurate determination and interpretation by this method. An added advantage was that the known critical potentials are so large that the results were not likely to be affected by any possible impurities.

Experimental.

The experimental method was very similar to that used for other gases and described in previous papers. Electrons

Fig. 1.

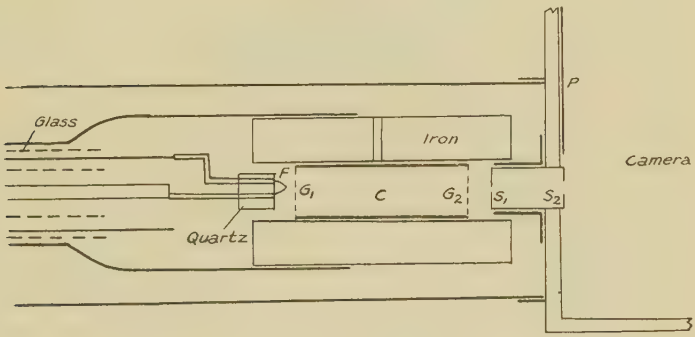

Collision space and slits.

from a pure tungsten filament F (fig. 1) were accelerated to a platinum grid G_1 at a potential of 120 volts and passed into a field-free iron-clad collision chamber C containing helium at a pressure of about 0·01 mm. of mercury. This collision space was 2·5 cm. in length, with diameters 0·6 cm. (internal) and 1·4 cm. (external), and was bounded at both ends by grids. The iron, however, extended beyond the grids at each end, shielding the filament at one end and the first slit of the camera at the other. After traversing the collision space the electrons passed through two slits, the first, S_1, 0·05 mm. and the second, S_2, 0·5 mm. wide. Although the presence of the iron prevented accurate focussing, the

* Roberts and Whiddington, *loc. cit.*

narrow slits made it possible to pass a sharp beam of electrons travelling in the forward direction into the highly evacuated camera. The camera consisted of a brass box, $7\frac{1}{2} \times 9\frac{1}{2} \times 4\frac{1}{2}$ cm., with a slot covered by a ground-on cap for the insertion of films. The slits were fitted on the ends of a tube 7 mm. long, protruding from the side of a camera. Thus, by arranging the end of the cylindrical iron shield to fit over this tube the electron beam and slits were automatically placed in line. The collision space was insulated from the camera in order that a retarding potential could be introduced between them at will. A transverse magnetic field of 12 gauss, produced by means of a pair of large Helmholtz coils, bent the electrons on to an oiled photographic film, and so produced a magnetic energy spectrum of the electrons entering the camera. A general diagram of the collision space and slits is given in fig. 1.

A very pure sample of helium was used *, the gas entering the apparatus through a fine needle valve and passing over phosphorus pentoxide and through a large liquid-air trap before reaching the collision space. Nothing in the spectra investigated could be attributed to impurities in the gas.

The magnetic spectrum contained as usual a very strong line corresponding to electrons with the full primary velocity, together with fainter lines corresponding to electrons which had lost energy in collisions with gas atoms. The problem was to determine accurately the loss of energy which these lines represent. Clearly no errors due to velocity distribution in the primary electrons or to contact potentials will be present so long as these effects are constant during an exposure. The only effects of these potentials would be to broaden the lines slightly and to move the whole spectrum along the film, and as only differences were measured, such a shift would not be observed. However, there was always the possibility of changes in the potential difference between filament and camera during an exposure. Rudberg †, in similar work, found drifts in potential of more than 1 volt during the taking of a set of readings, and suggests the contamination of the slits as a cause of the change. In the present work care was taken to keep the metal parts in the path of the beam as clean as possible. Observations were nevertheless made to discover possible changes. To detect any such shift a very fine line was put on some con-

* Helium kindly presented by the Linde Air Products Company, New York City.

† Rudberg, *loc. cit.*

venient part of the film before the main exposure by means of a short exposure with an accurately known retarding voltage. After the main run the voltage was set again to exactly the same value and the short exposure repeated. In general the resultant line was sharp and single. Any broadening or doubling of this line was an indication of a shift of potential during the exposure, and in such a case the whole film was rejected. Even after careful cleaning of the apparatus small shifts were often detected, but it has been found that this effect could be completely eliminated by running the apparatus in the absence of gas and with zero retarding potential for some time before commencing the actual experiment. The single photographic example here

Fig. 2.

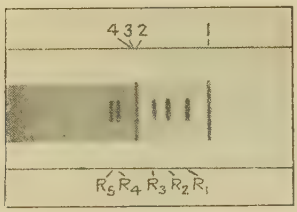

(1) Full velocity line (intensity reduced).
(2) Loss line.... 21·24 volts.
(3) Loss line.... 23·19 „
(4) Loss line.... 23·84 „
(Very faint in reproduction.)

Reference lines.

R_1.....	5·96 volts.
R_2.....	11·96 „
R_3.....	15·85 „
R_4.....	25·76 „
R_5.....	27·77 „

reproduced (fig. 2) illustrates a typical spectrum and reference lines.

In the method finally adopted, after taking many hundred photographs the "full" line was neglected and the values of the energy losses were estimated by means of fine reference lines placed on the film, using very short exposures with accurately known retarding voltages. Instead of the usual method of reducing the primary velocity of the electrons a retarding potential produced by a bank of heavy batteries was introduced between the collision space and the camera. This voltage was in general kept at zero for the main exposure and then varied for the short exposure reference lines. The great advantage of this method was that the value of this retarding potential, which really produced artificial "loss" lines, could be accurately measured on a

standardized low-reading voltmeter. Errors in voltage measurement were therefore reduced to a minimum, probably not more than 0·01 volt.

The procedure, then, was first to expose the film to the beam with the full primary velocity of 120 volts for five to ten minutes with the apparatus completely evacuated. When conditions were perfectly steady the helium was introduced into the collision chamber at a pressure of about 0·01 mm., and a short exposure (5–10 secs.) made with a retarding potential of, say, 6 volts. The voltage was again restored to 120 volts and the main exposure of five to ten minutes made. Without changing the conditions in any way whatever the first short exposure was repeated, and then two similar reference lines with accurately measured retarding potentials were put on the film, one on either side of the loss line. If, as was usual, in the resultant photograph the line at 6 volts "loss" was single and sharp, the film was regarded as satisfactory.

Measurement of Films.

The problem now resolved itself into a question of measuring with great accuracy the separations of the loss line and the reference line—similar, in fact, to the ordinary measurement of optical spectra. As the photographs showed one very prominent loss line accompanied by fainter lines our attention was concentrated in the first place on obtaining the value of the main loss. The subsidiary losses were then referred to this. In order to obtain the highest possible accuracy all the measurements were made on a sensitive microphotometer constructed in the workshop of the laboratory. Usually it was unnecessary to obtain a complete photometric curve of the film, only the peak intensity positions being required. By this method the probable error in the fixing of the positions of the peaks was reduced to $\pm 0{\cdot}001$ mm., representing approximately 0·003 volts.

Preliminary measurements showed that the dispersion varied slightly along the spectrum, as might be expected. It was essential, therefore, if the value of the loss was to be interpolated between the reference lines to place these lines as near to the loss lines as was compatible with easy measurement. Experience showed that reference lines about 3 volts distant on either side of the loss gave the most satisfactory results. It was then possible, assuming a linear voltage-separation law, to obtain the value of the loss by linear interpolation between the reference lines. Finally,

a small correction amounting to +0·02 volts was then made for deviation from the linear of the voltage-separation law *.

The following is a typical set of readings referring to one film :—

Primary voltage 119·2.

Thermionic emission 70 microamps.

Exposure for loss line 10 minutes.

Exposure for reference lines 10 seconds.

Retarding potentials for reference lines, 18·07 volts, 24·03 volts.

Microphotometer readings :—

18·07 ref. line.	Loss line.	24·03 ref. line.
17·9219	18·0142	18·0996
17·9215	18·0141	18·0995
17·9216	18·0142	18·0994
Mean... 17·9217	Mean... 18·0142	Mean... 18·0995

Whence value of loss (measured) = 21·16 volts.

,, ,, (corrected) = 21·18 volts.

* If V, V_1, and V_2 are the absolute voltages of the "loss" and reference line electrons respectively, and l, l_1, and l_2 the diameters of the corresponding beam paths, we have

$$V=kl^2, \quad V_1=kl_1^2, \quad \text{and} \quad V_2=kl_2^2,$$

where k is a constant for the apparatus. Hence

$$(V_2-V_1)=k(l_2^2-l_1^2),$$

and the dispersion over the V V_1 range is given by

$$D=\frac{(V_2-V_1)}{(l_2-l_1)}=k(l_2+l_1).$$

The actual voltage measured is the difference between V_2 and V. Hence the measured value of

$$(V_2-V)=D(l_2-l)=k(l_2+l_1)(l_2-l).$$

If, however, we do not assume linearity for the voltage-separation law, the correct value for (V_2-V) is given by

$$(V_2-V)_{\text{correct}}=k(l_2+l(\ -l).$$

Hence the error in (V_2-V) is given by

$$E=k(l_2+l)(l_2-l)-k(l_2+l_1)(l_2-l)$$
$$=k(l_2-l)(l-l_1),$$

i. e., $$E=(\sqrt{V_2}-\sqrt{V})(\sqrt{V}-\sqrt{V_1}).$$

Inserting the values used in the present experiments, this correction necessitates the addition of 0·02 volts to the loss measured.

The values of the subsidiary losses were estimated by reference to the calculated mean value of the main loss. This was done most satisfactorily by measuring the separations of the peaks in the photometric curves described in the next section. As the dispersion was known for the range the losses could then be found by adding the differences to

Fig. 3.

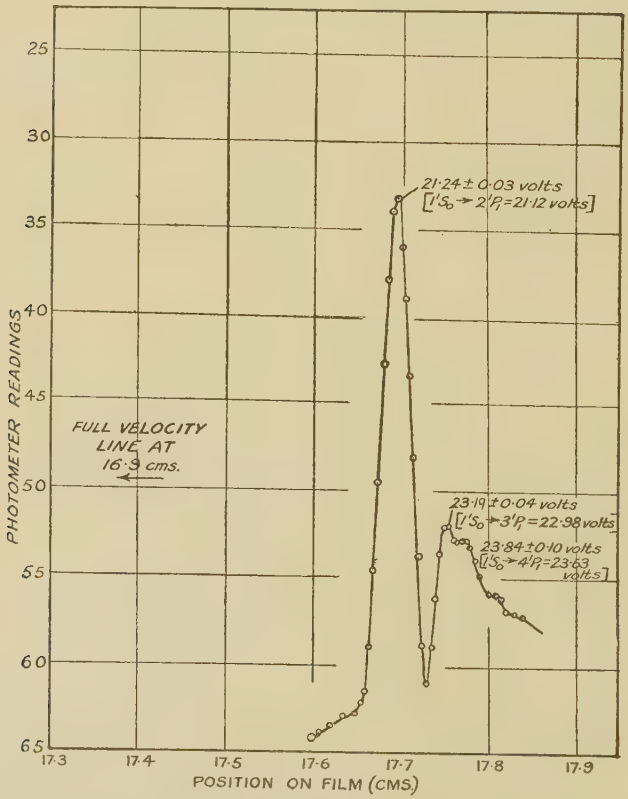

the main loss. The accuracy here was naturally not quite so great owing to the comparative smallness of the peaks.

Energy Losses.

Perhaps the clearest idea of the observed energy losses can be obtained from the photometric curves of the films, a typical one of which is reproduced in fig. 3.

Blank experiments with no gas in the apparatus showed that in general, under these conditions only a full velocity

line was obtained. The curves show that, in addition to the full velocity peak, the only other factor of any importance is the group of peaks corresponding to an energy loss of just over 20 volts. This is strong evidence against the presence of impurity lines, as previous experiments have shown that the usual impurities in helium give loss lines or bands in the region of 8 to 14 volts.

The measurements described in the preceding section refer to the main peak shown in the curves. From a series of spectra chosen before measurement for their clarity and freedom from reference line shift a mean value for this main peak, with its probable error, was obtained of

$$21{\cdot}24 \pm 0{\cdot}03 \text{ volts.}$$

This is a result on which great reliance can be placed, as in the spectra used for the determination the average deviation from the mean was less than 0·1 volt. For the less prominent losses the values estimated were

$$23{\cdot}19 \pm 0{\cdot}04 \text{ volts,}$$

$$23{\cdot}84 \pm 0{\cdot}10 \text{ volts.}$$

These figures are shown in comparison with others in Table III. It can be seen from the curves that there are distinct signs of other smaller peaks representing higher losses, but even with the large scale which the microphotometer made possible these could not be measured with any accuracy.

A point of some interest in this case of helium is the rapid falling off in the intensity of the shading beyond the loss lines on the low velocity side. As usual, there is no peak corresponding to the ionization potential. The feeble "ionization shading," however, seems to indicate (1) that the probability of excitation of the higher states and of ionization is small for 120 volts electrons, and (2) at these speeds the ionizing electron gives up very little of its energy to the ejected electron in the form of translational energy.

Intensities of Lines.

Although no accurate intensity measurements have so far been made, superficial observation of the relative intensities of the loss lines leads to the obvious though unexpected result that the first loss, 21·24 ($1^1S_0 \longrightarrow 2^1P_1$), is many times stronger than the second, 23·19 ($1^1S_0 \longrightarrow 3^1P_1$), the difference being even more marked for the higher members of the

series. We estimate that the ratio of the intensities of the first and second losses is at least 20. It is difficult to reconcile this value with the estimates (presumably visual) of the relative intensities of the corresponding helium ultra-violet spectrum lines. Compton and Boyce * under similar experimental conditions give the ratio for the first two members of the principal series in emission as 2, and for the first and third members as 2·2, values clearly much lower than ours. A comparison is given in Table I.

In this connexion it should be remembered that two conditions affect the intensities of the ultra-violet lines, whilst

Table I.

Transition.	Wave-length obs.	Intensity.	Loss, obs.	Intensity.
$1^1S_0 \rightleftharpoons 2^1P_1$	584·41	20	21·24	20
$1^1S_0 \rightleftharpoons 3^1P_1$	537·04	10	23·19	1
$1^1S_0 \rightleftharpoons 4^1P_1$	522·25	9	23·84	—

only one of them affects the electron lines. The relative intensity of the two ultra-violet lines would depend on :

(*a*) The relative numbers of the two types of excited atoms—*i. e.*, the probabilities of the two excitations from the ground state.

(*b*) The probabilities of the transitions to the ground state.

Clearly only the first condition will affect the electron lines.

Our experiments seem to indicate that the probabilities of excitation of the 2^1P_1 and 3^1P_1 from the ground state are in the ratio of about 20 to 1. From the spectroscopic evidence it would appear that the second condition then becomes effective, virtually in the opposite direction, and decreases the relative intensity of the lower energy line. It is not impossible that a large number of transitions from the 2^1P_1 state to some other state than the ground state—*e. g.*, 2^1S_0—may account for the comparatively low intensity of the transition $2^1P_1 - 1^1S_0$, but there is no experimental evidence for this up to the present. If we assume the ratio

* K. T. Compton and J. C. Boyce, Journ. Franklin Inst. ccv. p. 497 (1928).

of the exciting transitions to be 20, and of the spectrum intensities to be 2, then it is clear that the ratio of the numbers of the *emitting* transitions $2^1P_1 \rightarrow 1^1S_0$ and $3^1P_1 \rightarrow 1^1S_0$ must be 0·1, or, expressed in another way, the higher energy transition is far more probable than the lower. There is no adequate theory to account for this result. From a theoretical point of view, on a radial model of the atom, the relative intensities of various transitions are given by the integral

$$I = \left[\int_0^\infty r R_{nl}(r) . R_{n'l'}(r) . r^2 dr \right]^2,$$

where $R_{nl}(r)$ and $R_{n'l'}(r)$ are the radial factors of the wave functions for the initial and final states respectively. For helium this integral is far too complicated to be calculable, but for the comparable case of the Lyman series in hydrogen we have *

$$I \propto \frac{(n-1)^{2n-1}}{n(n+1)^{2n+1}},$$

where n is the total quantum number of the initial state. For the first two members of the series the ratio of the intensities should be 3·2 as compared to the experimental result (in helium) of 0·1. In spite of the general unsatisfactoriness of comparing different cases the discrepancy is too large to be ignored completely. Whilst, owing to the crudeness of the measurements, it is impossible to draw any very definite conclusions from this result, it seems necessary to suggest, tentatively at any rate, that the probabilities of transitions from the higher levels of a series may be much greater than is indicated by spectroscopic work and by the simple theory.

Interpretation of Energy Loss Values.

Quite a number of experimenters have investigated the energy levels of helium by various methods, and their results are tabulated in Tables II. and III. The first attack on the problem was made by Horton and Davies †, who obtained one critical potential at 20·4 volts and ionization at 25·6 volts. This was quickly followed by the classical work of Franck and Knipping ‡. These workers found four distinct critical potentials, and gave values with an accuracy of about

* Condon and Morse, 'Quantum Mechanics,' p. 107.
† Horton and Davies, Proc. Roy. Soc. xcv. p. 408 (1919).
‡ Franck and Knipping, *Zs. f. Phys.* i. p. 320 (1920).

$\pm 0{\cdot}25$ volts. In the light of the more recent knowledge of the helium spectrum all these potentials can be connected with those predicted from the spectrum. However, Franck * later suggested a further contact potential correction of 0·8 volt which, applied to the earlier experimental results, brought the three higher potentials into better agreement with the newly interpreted helium spectrum. The agreement, considering the accuracy of measurement, is certainly remarkable, and becomes more so when the then unknown triplet level at 19·77 is added to the spectrum levels. This result is very surprising when one examines the current potential curves of Franck and Knipping. Probability considerations suggest that in general the higher singlet states would be more easily excited than the 19·77 triplet state. The curves, however, indicate that the first observed break (according to the interpretation the 19·77 potential) is very strong and the higher excitations relatively feeble. At the same time no definite conclusion can be drawn from this owing to the scanty knowledge of the mechanism of excitation by electrons near the critical voltage.

Dymond †, using a more precise critical potential method, obtained a value $20{\cdot}9 \pm 0{\cdot}15$ for the main potential in helium. He points out that in such a method a rather high value might be expected, and connects his results with the predicted spectroscopic level at 20·55. The more recent work of Glockler ‡ represents perhaps the most rigorous attack on the problem from this angle, the results agreeing to some extent with the earlier work of Franck. It should be pointed out that these experiments are still open to the objections outlined in our first section. Presently these results will be considered further.

During the course of researches on electron scattering in gases both Dymond § and McMillen ‖ have measured the energy losses in helium of electrons of 50–150 volts. Dymond gives 20·58 as the approximate value for the most prominent energy loss, but apparently lack of resolving power prevents the determination of other losses. On the other hand McMillen observed three losses, the lowest and most prominent being considerably greater than that suggested by Dymond. These results, together with those

* Franck, *Zs. f. Phys.* xi. p. 155 (1922).
† Dymond, Proc. Roy. Soc. cvii. p. 291 (1925).
‡ Glockler, Phys. Rev. xxvii. p. 423 (1926); xxxiii. p. 175 (1929).
§ Dymond, Phys. Rev. xxix. p. 433 (1927).
‖ McMillen, *loc. cit.*

obtained in the present experiments and the first five pectroscopic levels, are included in Table III.

It can be seen from these tables that the present results represent a considerable advance in general, from the point of view of accuracy, on previous work of this nature.

TABLE II.

Horton and Davies.	Franck and Knipping.	Franck (corrected).	Dymond.	Glockler.
		19·75±0·25		19·90±0·02
20·4	20·45±0·25	20·55 „	20·9±0·15	20·57±0·06
	21·25 „	21·2 „		
	21·9 „	22·9 „		
	23·6 „			

TABLE III.

Spectroscopic * levels.	Dymond (100 v. electrons).	McMillen (50–150 v. electrons).	Present experiments.
19·77			
20·55	20·58±0·1		
21·12		21·50±0·15	21·24±0·03
22·98		23·63±0·15	23·19±0·04
23·63		24·45±0·15	23·84±0·10

* Int. Crit. Tables, vi. p. 69.

We have from spectroscopic data the five possible energy losses given in column 1 of Table III., representing the following transitions from the ground state :—

$1^1S_0 \rightarrow 2^3S_1$, $1^1S_0 \rightarrow 2^1S_0$, $1^1S_0 \rightarrow 2^1P_1$, $1^1S_0 \rightarrow 3^1P_1$, $1^1S_0 \rightarrow 4^1P_1$ (fig. 4).

There can be little doubt that the main loss in our experiments corresponds to the first transition of the principal series $1^1S_0 \rightarrow 2^1P_1$. This is in definite agreement with the result of McMillen as opposed to that of Dymond. Accepting this interpretation of the most prominent loss, the subsidiary losses are then assigned to the higher members of the same

series, the transitions being $1^1S_0 \rightarrow 3^1P_1$ and $1^1S_0 \rightarrow 4^1P_1$. The agreement with the spectroscopic values is good, though even better agreement is suggested if we measure the separations between the peaks and compare them with the predicted separations of the principal series. Between the main loss peak and the first subsidiary peak we have a separation of

Fig. 4.

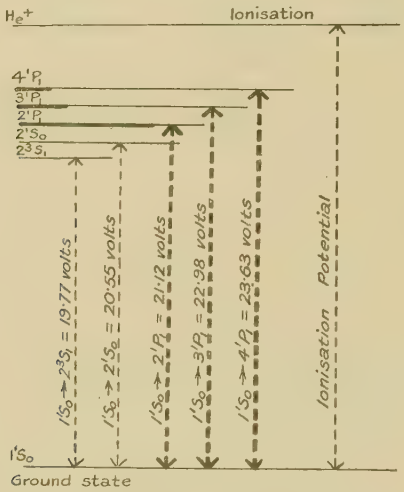

Energy Levels in Helium.

TABLE IV.

Loss.	Differences (obs.).	Differences (calc.).	Spectroscopic value.	Interpretation.
21·24	1·95	1·86	21·12	$1^1S_0 \rightarrow 2^1P_1$
23·19	0·65	0·65	22·98	$1^1S_0 \rightarrow 3^1P_1$
23·84			23·63	$1^1S_0 \rightarrow 4^1P_1$

1·95 volts, the predicted difference being 1·86 volts; whilst in the case of the two subsidiary peaks the experimental and spectroscopic separations are both 0·65 volt. This interpretation of the subsidiary losses may be used to support the original interpretation of the main loss. A summary of the losses and the proposed interpretation is given in Table IV.

It would seem then that when electrons of moderately high velocity strike the helium atom only the principal series is excited to any extent. The energy loss spectrum would therefore show lines due to the first few levels, and then a fainter shading extending beyond the ionization potential. It might be expected that there would be indistinct peaks corresponding to the principal levels beyond 4^1P_1. Such indications have been observed in our photometric curves.

In almost all of our experiments there have been no signs of energy losses less than the main loss of 21·24 volts. Only in the most intense photographs was it possible to detect a very slight trace of such losses. Further, the photometric curve of the main loss was in general found to be perfectly symmetrical. In this we are in agreement with Dymond and McMillen, who only found slight indications of a lower loss when using rather slower electrons. The absence of the 19·77 volt loss is in accord with recent theoretical developments, for it has been known for some time that there were differences in the mode of excitation of singlet and triplet states, and Massey and Mohr * have calculated excitation probabilities for helium. They show that for high electron velocities the excitation of the triplet states is very feeble, and as the 19·77 loss would be due to a transition $1^1S_0 \rightarrow 2^3S_1$ it is not surprising that in our experiments it is not observed. The absence of the excitation of the 2^1S_0 state is not so easily explained. We might expect the probability of excitation to be somewhat less than for the 2^1P_1 state ($S \rightarrow S$ transition instead of $S \rightarrow P$), but our experiments actually indicate that for 120 volt electrons the probability of excitation of the ^1S series is negligible compared to that of the ^1P series.

Comparison with Spectroscopic Term Values.

It will be noticed that our loss values are all slightly above the spectroscopic values. Glockler † finds a similar discrepancy in his more recent interpretation of the helium critical potentials. Taking all possible precautions he obtained a series of Franck and Lenard current-potential curves, the average of these curves giving an accurate value for the first critical potential. Unfortunately, as in previous work, corrections for contact potentials amounting to more than 1 volt had to be applied before the critical potentials could be estimated. In both types of experiment (Franck and Lenard) the observed critical potential was higher

* Massey and Mohr, 'Nature,' Feb. 14, 1931.
† Glockler, *loc. cit.*

than the spectroscopic value by an amount greater than the calculated error. The mean discrepancy was 0·13 volt, as compared with our 0·12. The probable errors in these quantities are, of course, comparatively large, and they actually refer to different excited states, but the agreement of the three types of experiment is interesting. Glockler further obtains curves of the primary electron velocity distribution. He then suggests that the high value of the observed critical potential is due to the fact that the probability of excitation of the particular state reaches a sharp maximum slightly above the spectroscopic level. Using the experimental electron-velocity distribution curve, and assuming various arbitrary probability functions, it is possible to construct Franck-Lenard differential curves. Glockler finds that the best fit with experimental results is obtained when a probability distribution having a maximum 0·18 volt above the theoretical critical point is used. This result is in qualitative agreement with the earlier work of Dymond.

It is clear that the present results, whilst not disproving Glockler's theory, cannot be explained on the same assumptions, since the energy lost at impact by a high-speed electron should not be affected in any way by the probability distribution near the critical potential as considered by Glockler.

Our experiments indicate then that the true critical energy for electron impact is slightly higher than the spectroscopic value—*i. e.*, energy other than the spectroscopic term energy is being lost by the electron. It is difficult to visualize any mechanism whereby this loss could occur. Hertz* showed that small quantities of energy were lost in elastic impacts between electrons and atoms, the changes being in accordance with the rules for the impact of elastic spheres. If we make the assumption that the atoms are stationary (this is justified owing to the relatively high speed of the electrons) the maximum possible elastic energy loss can be calculated from ordinary mechanics†.

* Hertz, *Ver. d. Deutsch. Phys. Ges.* xix. p. 268 (1917).

† If u and u' are the electron velocities before and after impact, and V the velocity of the atom after impact, we have

$$\mathrm{V}=\frac{m(u+u')}{\mathrm{M}}.$$

Equating energies,

$$mu^2=\mathrm{M}\left[\frac{m(u+u')}{\mathrm{M}}\right]^2+mu'^2,$$

$$\mathrm{M}mu^2=mu^2+2m^2uu'+m^2u^2+\mathrm{M}mu'^2.$$

The fractional loss for *direct impact* comes out to $f=4m/M$, where m and M are the masses of the electron and atom, and substituting the values of M and m we get $f=0{\cdot}0005$, or in the case of electrons of 120 volts primary energy a loss of 0·06 volt. In a similar calculation K. T. Compton * obtains as the average energy loss for impacts at all angles a value $f=2m/M$.

Although such an "elastic" loss is of the correct order of magnitude, it is obvious that it holds only for large scattering angles—in the extreme case for 180° scattering. For the extremely small scattering angles used in the present experiments the corresponding loss would be negligible †. Multiple collisions might increase the elastic energy loss, but in the present experiments this possibility is excluded owing to the low gas pressure used. At present there seems to be no obvious explanation of the phenomenon.

Acknowledgment.

The senior author acknowledges with gratitude the provision of a research assistant (J. E. R.) by the Department of Scientific and Industrial Research, without whose assistance this work would not have been possible; he also records, with thanks, the fact that some of the apparatus was purchased out of a grant made by the Royal Society.

Summary.

Electronic excitation experiments have hitherto been liable to three main sources of error associated with:

(1) The velocity distribution in the primary electron stream.

Solving this equation,

$$u'=\frac{u[-m^2\pm Mm]}{m^2+mM}.$$

For the maximum energy loss on direct impact

$$u'=u\left[\frac{M-m}{M+m}\right].$$

Fractional energy loss

$$=\frac{mu^2-mu'^2}{mu^2}=\frac{4Mm}{(M+m)^2}.$$

We may neglect m in comparison with M:

$$f=\frac{4m}{M}.$$

* K. T. Compton, Phys. Rev. xxii. p. 333 (1923).

† The loss varies with $\cos^2\theta$, where θ is the angle between the electron path and the path of the atom after impact.

(2) Uncontrollable contact potentials between the electrodes.

(3) The measurement of the energy of the impacting electrons.

Experiments are described which successfully overcome these difficulties and result in a much higher accuracy of measurement than heretofore.

The method used is a modification of the magnetic spectrum apparatus already used by Jones and Whiddington, in which on a single photograph are recorded traces of the main electron stream, and of the other, less intense, streams of lower energy resulting from excitation of the helium atom.

Using 120 volt electrons in helium, only the principal series excitations were observable, the losses, their origin, and the comparable values calculated from spectroscopy being included in the following table :—

Observed value of excitation potential.	Interpretation.	Calculated value from spectroscopy.
21·24±0·03	$1^1S_0 \rightarrow 2^1P_1$	21·12
23·19±0·04	$1^1S_0 \rightarrow 3^1P_1$	22·98
23·84±0·10	$1^1S_0 \rightarrow 4^1P_1$	23·63

The photographs furnish no evidence for the direct excitation of the 2^3S_1 and 2^1S_1 states, while the intensities of the excitation lines which are observed do not accord with the optical spectra. The values obtained are all slightly higher than the spectroscopic values, but no explanation can be given.

Physics Laboratories,
University of Leeds.

XCIV. *An X-ray Investigation of some Copper-Aluminium Alloys.* *By* G. D. Preston, *B.A., National Physical Laboratory* *.

[Plates XIX. & XX.]

THE investigation, the results of which are described below, deals with that part of the copper-aluminium system containing from 31 to 50 atomic per cent. of

* Communicated by Sir J. E. Petavel, K.B.E., D.Sc., F.R.S.

aluminium. The lower limit coincides with the boundary of the well-known γ phase, the structure of which has been worked out by Bradley †. According to the original X-ray investigation carried out by Jette, Phragmen, and Westgren ‡, this phase field extends from the limit assigned above up to 44 atomic per cent. aluminium, and is then followed in the constitutional diagram by the compound $CuAl_2$. Stockdale §, however, as the result of a very careful thermal and micrographical investigation of these alloys, interpolated another phase, which he denoted by η, extending from 43 to 50 atomic per cent. aluminium, the limits of existence of the γ phase (δ in Stockdale's notation) being placed at 31 and 41 atomic per cent. of aluminium. The present paper contains an account of two new phases which have been examined by the Laue and oscillating crystal methods.

CuAl.

A small fragment from an ingot of composition 30 per cent. aluminium by weight, annealed at 602° C. and quenched from that temperature, was examined by the Laue method. When suitably orientated with respect to the incident X-ray beam this specimen yielded a photograph symmetrical about two perpendicular lines. By rotating the crystal about axes parallel to these lines through angles of 90° another pair of photographs showing the same type of symmetry, V_h, was obtained. These photographs are reproduced in fig. 1 (Pl. XIX.); they show that the symmetry of the crystal is orthorhombic. Gnomonic projections of the Laue diagrams gave approximate values for the axial ratios $a:b:c = 1:3:2$. These projections are shown in fig. 2. The choice of axial ratios is to some extent arbitrary, and the values given above are those which lead to simple values for the indices of the observed reflexions. In fig. 2 (*a*) every alternate line of the net, corresponding to even values of k/h and l/h, has been drawn. If the "a" axis were doubled so that the axial ratios become $a:b:c = 2:3:2$, the net on this projection would be as shown in the figure, but with the values of k/h and l/h halved. In the other projections the effect of the new axial ratios will be to interpolate lines halving the net parallel to a vertical line in fig. 2 (*b*) and to a horizontal line in fig. 2 (*c*). So far as the simplicity of the resulting indices are concerned this change would appear to be permissible.

* Phil. Mag. vi. p. 878 (1928).
† Journ. Inst. Met. xxxi. p. 193 (1924)
‡ *Ibid.* p. 275.

Fig. 2 *a*).

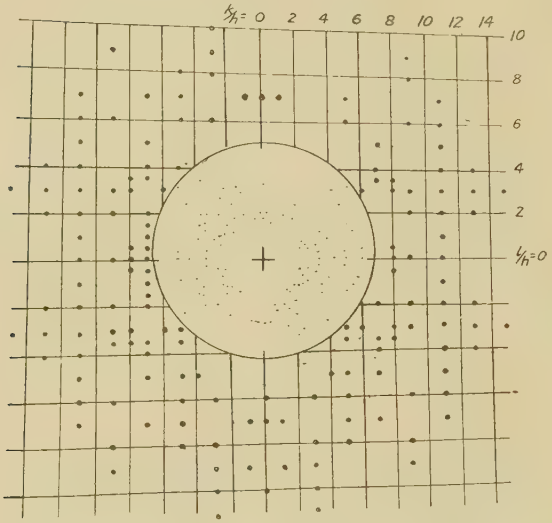

Gnomonic Projection of CuAl Crystal.

X-rays parallel [100].
001] vertical.

Fig. 2 (*b*).

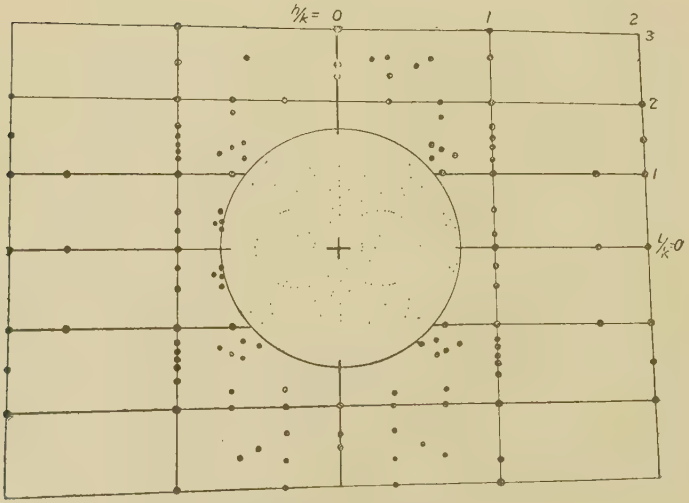

Gnomonic Projection of CuAl Crystal.

X-rays parallel [010].
[001] vertical.

The specimen was examined by the oscillating crystal method, but the presence of stray crystals in the fragment makes the interpretation of the results difficult. Photographs were taken with radiation from an iron target, the range of oscillation being 16°, six photographs being required to cover a range of 90°. The goniometer adjustment only allowed photographs to be obtained with the crystal oscillating about [001] and about [010], the range of adjustment being insufficient to bring [100] parallel to the axis of oscillation. The separation of the "layer" lines on these photographs showed that the spacings were approximately $c=8{\cdot}5$ Å. and

Fig. 2 (c).

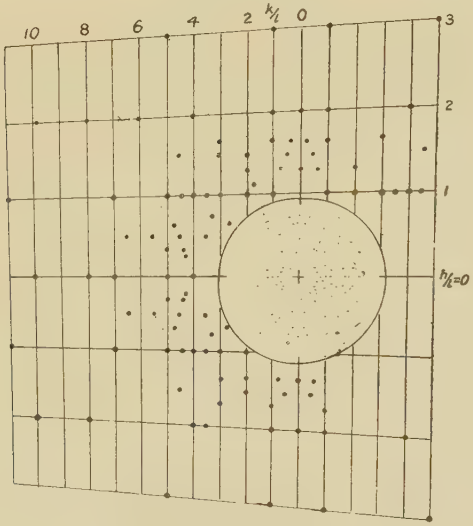

Gnomonic Projection of CuAl Crystal.

X-rays parallel [001].
[100] vertical.

$b=12$ Å., the remaining spacing being inferred to be about 4·1 Å. Owing to the failure to obtain photographs in which the axis of oscillation is parallel to the a axis of the crystal, this figure for the (100) spacing may be in error by a factor of 2 ; if so, the axial ratios will be $a:b:c=2:3:2$ approximately. The crystal was unfortunately lost in an attempt to remount it with the "a" direction parallel to the axis of oscillation and no other crystal of sufficient perfection could be isolated. A unit of these dimensions ($a=4{\cdot}1$, $b=12{\cdot}0$, $c=8{\cdot}5$ Å.) should give reflexions on one or more of

TABLE I.

CuAl. FeK Radiation.

hkl.	I.	*hkl.*	I.	*hkl.*	I.
020	M.	082	M.	335	M.
021	M.W.	310	S.	400	V.V.S.
002	M.S.	311	S.	138	S.
110	S.	083	W.	420	S.
111	S.	155	M.	421	M.
022	S.	205	M.	0(12)0	S.
040	W.	330	S.	316	M.
003	M.S.	136	M.W.		
130	S.	263	M.W.		
023	S.	190	M.W.		
132	M.W.	332	M.		
113	M.S.	007	W.		
043	W.	313	S.		
150	S.	192	M.		
200	V.S.	027	W.		
024	M.S.	0(10)0	M.S.		
133	V.S.	350	V.S.		
151	S.	156	M.S.		
060	S.	333	V.V.S.		
061	W.	206	V.S.		
220	S.	117	M.S.		
221	M.	351	V.S.		
202	S.	282	S.		
222	S.	193	S.		
044	V.W.	225	W.		
005	M.	283	S.		
134	W.	334	M.W.		
240	M.W.	008	S.		
203	S.	371	S.		
063	W.	207	M.		
223	S.	1(11)0	V.S.		
080	V.W.	372	M.W.		
154	W.	2(10)0	M.S.		
135	M.W.				
081	M.W.				
224	S.				
006	S.				
260	V.S.				

the photographs from over 300 different planes, but of these possible reflexions only the 89 given in Table I. could be detected in all the expected places, the absence of the

remainder being due to the complexity of the structure. The spurious reflexions from small stray crystals associated with the one under examination have been partly eliminated by careful comparison of the *b* and *c* photographs (*i. e.*, the photographs in which the axis of oscillation is parallel to *b* and *c* respectively). Most of these stray reflexions do not fall on the "layer" lines, and are thus easily recognized, but some fall on or very near to the "layer" lines and may be

TABLE II.

hkl.	I.	*hkl.*	I.
112	W.	281	W.
131	W.	0(10)1	M.
042	V.W.	127	M.
210	M.W.	1(10)0	M.W.
201	W.	352	M.
211	W.	147	W.
053	W.	353	W.
231	W.	246	W.
153	M.	325	V.W.
115	W.	1(11)1	S.
242	W.	227	W.
243	V.W.	2(10)0	M.S.
261	W.	2(10)1	S.
026	V.W.	1(11)2	M.W.
181	S.	401	M.
244	W.	411	M.W.
312	W.	138	S.
225	V.W.	381	M.S.
331	V.W.	402	S.
272	M.		
235	M.		
146	W.		
280	M.		

recorded as reflexions from the crystal under examination. Each plane (*hkl*) appears in general on two of the *b* photographs and on two of the *c* photographs if it belongs to the crystal under examination, so that by comparing the *b* and *c* photographs many of these spurious reflexions from stray crystals may be eliminated. The cases in which doubt arises are forty-two in number, and are given in Table II. The probability is that all these reflexions are spurious, but the possibility that some of them are not cannot be neglected. As regards the determination of the lattice, the presence in Table I. of

intense reflexions from planes (110), (130), (150), etc., where h, k, and l are neither all even nor all odd, excludes Γ_0'' the face-centred orthorhombic lattice. The body-centred lattice Γ_0''' is excluded by the intense reflexions recorded in Table I. from planes where $(h+k+l)$ is odd, such as (111), (023), (133), etc. The lattice Γ_0' is characterized by the halving of the spacings (hkl) when $h+k$ is odd. All the planes recorded in Table I. satisfy this condition, but there are fourteen in Table II. which violate it. Reference to the

Table III.

hkl.	I (calc.).	*h'k'l'*.	I (obs.).
100	256	130	S.
		003	M.S.
110	1764	200	V.S.
		133	V.S.
		060	S.
111	256	203	S.
		063	W.
200	1764	260	V.S.
		006	S.
210	256	330	S.
		136	M.W.
		263	M.W.
		190	M.W.
211	1764	333	V.V.S.
		193	S.
		206	V.S.
		066	(off film)
220	1764	400	V.V.S.
		266	(off film)
		0(12)0	S.

tables of Astbury and Yardley * shows that the following space groups are possible if the reflexions violating this condition in Table II. are regarded as spurious: C_{2v}^{11}, C_{2v}^{12} (with a change of axes), V^6 or V_h^{19}, in which Γ_0' is the underlying lattice. If weight is attached to the planes recorded in Table II. the most probable group would appear to be V_h^4, characterized by the halving of the spacing (okl) when k is odd, the halving of (hol) when h is odd, and the halving of (hko) when $(h+k)$ is odd. These conditions are violated only by (053) and (210). C_{2v}^4 or V_h^5, characterized by the

* Phil. Trans. Roy. Soc. A, ccxxiv. p. 233 (1924).

halving of (*hol*) when h is odd, satisfy all the observed conditions.

The dimensions of the unit were determined by means of a powder photograph recording the reflexions at large angles, the indices to be ascribed to these being inferred from the strong reflexions recorded in the oscillating crystal photographs. Reflexions of the K_α doublet of chromium were observed for the planes ($3\bar{5}0$), (351), (282), and (333), the values of a, b, and c being

$$\begin{aligned} a &= 4{\cdot}087 \pm {\cdot}005 \text{ Å}, \\ b &= 12{\cdot}00 \pm {\cdot}02 \text{ Å}, \\ c &= 8{\cdot}635 \pm {\cdot}01 \text{ Å}, \end{aligned}$$

giving $a : b : c = 1 : 2{\cdot}94 : 2{\cdot}11$.

The volume of the unit is $423{\cdot}5 \times 10^{-24}$ cm.^{3}, and if 16 molecules, CuAl, are associated with it, the density is 5·65 gm./cm.^{3}, a value close to that given by Jette, Phragmen, and Westgren *.

There is a very interesting similarity between this structure and the γ phase Cu_9Al_4. Bradley has pointed out that the cubic structure of the γ phase of side 8·7 Å. is approximately equivalent to twenty-seven body-centred cubes of side 2·90 Å., but that instead of containing 54 atoms it contains 52. In the present case a is $2{\cdot}89\sqrt{2}$ Å., *i. e.*, the diagonal of the face of a cube of side 2·89, b is nearly $3a$, and $3 \times 2{\cdot}89$ (8·67) is very nearly c. Putting $2{\cdot}89 = a_0$, the orthorhombic unit has sides $a = a_0\sqrt{2}$, $b = 3a_0\sqrt{2}$, and $c = 3a_0$, while its volume $abc = 18a_0^3$. It should contain 36 atoms, and apparently contains 32 as stated above. This similarity to the body-centred cube is not confined to the dimensions of the unit but is also apparent in the X-ray spectra. The most intense lines observed are those which would arise from the body-centred unit, and the variations of intensity correspond to those which would be observed from a unit with copper atoms at the corners and aluminium atoms at the centres of the cubes. If (*hkl*) is a plane in the small body-centred cubic unit, the corresponding plane ($h'k'l'$) in the orthorhombic unit is given by

$$\begin{aligned} h' &= h + k, \\ k' &= 3(h - k), \\ l' &= 3l. \end{aligned}$$

If copper atoms are placed at the corners and aluminium atoms at the centre of the small cube, the intensity of the

* Journ. Inst. Met. xxxi. p. 205 (1924).

reflexion from the plane (hkl) will be proportional to $(z_1-z_2)^2$ if $(h+k+l)$ is odd and to $(z_1+z_2)^2$ if $(h+k+l)$ is even, where z_1 and z_2 are the atomic numbers of copper and aluminium. These values (256 and 1764) are included in Table III. under I (calc.), the observed intensities appearing in the last column. The planes for which $(h+k+l)$ is even are in general very strong and those for which $(h+k+l)$ is odd weak or medium. This suggests that the atoms are arranged in the structure close to the points of a body-centred cubic unit, but that the distribution of copper and aluminium atoms among these points is not quite that of the small body-centred unit.

Fig. 4.

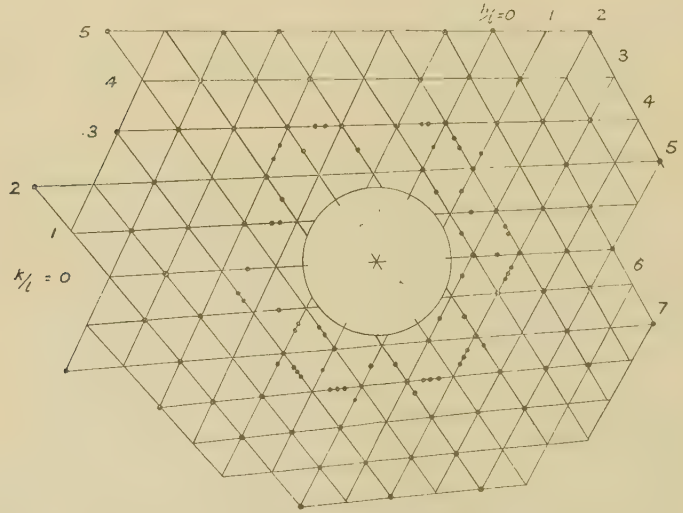

Gnomonic Projection 25·4 weight per cent. Aluminium.
X-rays parallel [0001.]

Alloy containing 25·4 *weight per cent. Aluminium.*

A fragment from an ingot of composition 25·4 per cent. by weight of aluminium which had been annealed at 575° C. and quenched from that temperature was examined by the Laue and oscillating crystal methods. The Laue photograph, when the crystal had been suitably orientated, showed a six-fold symmetry (D_{6h}) with two-fold axes at right-angles to it. The photographs are reproduced in fig. 3 (Pl. XX.). Gnomonic projections of these photographs gave a value of $c:a = 1{\cdot}23$; the projection of the photograph

with six-fold symmetry is reproduced in fig. 4. The oscillating crystal photographs were taken with iron radiation, the range of oscillation being 16° in each photograph. When the *c* axis is parallel to the axis of oscillation, two photographs are sufficient to cover all the possible planes owing to the six-fold symmetry; thus, if in the first two photographs the line [10$\bar{1}$0] oscillates from 0°–16° and from

TABLE IV.

25·4 weight per cent. Aluminium. FeK Radiation.

H.K.	L=0.	L=1.	L=2.	L=3.	L=4.
10	—	—	—	M.S.	—
11	—	M.W.	—	—	—
20	M.	—	M.	—	V.S.
21	—	W.	—	M.	—
30	—	—	—	—	—
22	S.	—	—	—	—
31	V.W.	W.	—	W.	—
40	S.	—	M.	—	S.
32	—	—	—	M.S.	—
41	—	W.	—	—	—
50	—	M.W.	—	M.S.	—
33	M.W.	—	—	—	—
42	W.	—	M.	—	S.
51		W.	—	M.S.	—
60	S.	—	—	—	—
43	M.	W.	—	S.	—
52	M.S.? 44$\bar{8}$0 β	S.	—	V.W.	—
61	W.	W.	—	—	—
44	V.S.	W.	—	—	—
70	—	W.	—	—	—
53	—	—	—	—	—
62	M.	—	—	—	—

14°–30° to the X-ray beam, then an oscillation from 30°–46° will reproduce the second photograph but with the right- and left-hand sides interchanged. Four photographs were taken with a view to eliminating reflexions from stray crystals. The results of these are summarized in Table IV. From the separation of the layer lines the value of *ac* is found to be about 10 Å., so that "*a*" is approximately 8·1 Å. The Laue photograph, showing symmetry of the type D_{6h}, shows that the crystal belongs to one of the groups D_{3h}, C_{6v}, D_6, or D_{6h}.

The presence of planes of the type $(ho\bar{h}l)$ and $(hh2\bar{h}l)$ when l is odd reduces the choice of groups to D^1_{3h}, C^1_{6v}, D^1_{6h}, or one of the groups D_6.

A more accurate determination of the dimensions of the unit was effected by the powder method, the result being $a=8{\cdot}08$ Å., $c=1{\cdot}23_5$, giving a volume of 562×10^{-24} cm.^{3}. The density is in the neighbourhood of 5·98/cm.^{3}, and calculation shows that the most probable composition is $Cu_{24}Al_{18}$ (24·2 weight per cent. Al) or $Cu_{23}Al_{21}$ (28 weight per cent. Al).

This unit is again closely related to the body-centred cubic unit of side 2·89, referred to above in connexion with CuAl. A simple cube of side a_0 can be referred to a set of hexagonal axes of length $a=a_0\sqrt{2}$ and height $ac=a_0\sqrt{3}$. The axial ratio $c=\sqrt{3}/\sqrt{2}=1{\cdot}225$, so that the volume of the unit is $\sqrt{3}/2$, $a^3c=3a_0^3$, and the coordinates of the cube corners are (000) $(\frac{1}{3}\,\frac{2}{3}\,\frac{1}{3})$ and $(\frac{2}{3}\,\frac{1}{3}\,\frac{2}{3})$ within the hexagonal unit. Since the side $a=8{\cdot}08$ Å.$=2\sqrt{2}\times2{\cdot}86$ Å., we must suppose that the unit we are concerned with is not three times the volume of the small body-centred unit but twenty-four times, the value of a in terms of a_0 being $2a_0\sqrt{2}$ while $ac=2a\sqrt{3}$. This large unit should contain 48 atoms and therefore four or six are missing if the composition is that stated above. As in the case of CuAl, the similarity of the hexagonal and cubic structures is shown in the X-ray spectrum. Planes (hkl) of the cubic unit are connected with (HK.L) of the hexagonal unit by the relations

$$\mathrm{H}=2\,(h-l),$$
$$\mathrm{K}=2\,(k-h),$$
$$\mathrm{L}=2\,(h+k+l).$$

The results of a comparison of the two units are shown in Table V., and as in the case of CuAl we find that, when $(h+k+l)$ is even, a very intense reflexion is recorded from the corresponding plane (HK.L).

Specimens from an ingot of the same composition (25·4 weight per cent. aluminium), annealed at 618° C. and at 545° C. respectively and quenched from those temperatures, yielded Laue photographs which were identical with one another and with those obtained from the specimen annealed at and quenched from 575° C. The hexagonal structure thus exists at all these temperatures.

The investigation, the results of which have been described above, was undertaken with two definite objects. Firstly,

the existing X-ray and metallographic researches on this region of the copper aluminium constitutional diagram were not in agreement. The work of Jette, Phragmen, and Westgren * indicated a range of existence of the cubic γ phase (Cu_9Al_4), extending from 16 to 25 weight per cent. of Al. Stockdale †, however, reported a phase, which he denoted by η, extending from 43 to 50 atomic per cent. aluminium in addition to a phase (δ in his notation) extending from 31 to 41 atomic per cent. aluminium (16 to 23 weight per cent.). The alloy containing 25 weight per cent. aluminium (44 atomic per cent.) according to Stockdale

TABLE V.

hkl.	I (calc.).	HK.L.	I (obs.).
100	256	$20\bar{2}2$	M.
110	1764	$20\bar{2}4$	V.S.
		$22\bar{4}0$	S.
111	256	0006	(off film)
		$40\bar{4}2$	M.
200	1764	$40\bar{4}4$	S.
210	256	$22\bar{4}6$	(off film)
		$42\bar{6}2$	M.
211	1764	$20\bar{2}8$	(off film)
		$60\bar{6}0$	S.
		$42\bar{6}4$	S.
220	1764	$40\bar{4}8$	(off film)
		$44\bar{8}0$	V.S.

should be in the η field. The X-ray photographs of Jette, Phragmen, and Westgren placed it in the cubic γ field, and they did not report any other phase between this and $CuAl_2$.

More recently Westgren and Phragmen ‡ have reported a difference between the powder photographs of the γ phase and of alloys with 35 to 40 atomic per cent. aluminium. Some of the lines of the γ phase split up into multiplets as the aluminium concentration increases, indicating a change of symmetry of the crystal. At still higher aluminium

* Journ. Inst. Met. xxxi. p. 193 (1924).

† *Ibid.*

‡ Metallwirtshaft, vii. p. 700 (June 1928); Trans. Am. Inst. Mining and Metallurgical Engineers, Tenth Annual Lecture (February 1931).

concentrations these authors have found an orthorhombic structure, which they identify as CuAl, and state that it has a unit containing 1500 atoms, but details of the preparation of this alloy and the evidence on which this conclusion is based have not been published.

The results of the present investigation show that the cubic γ phase has a homogeneity range extending from 31 to 35·5 atomic per cent. aluminium. This is followed by a hexagonal phase which exists in the neighbourhood of 43 atomic per cent. aluminium, and then by an orthorhombic phase which is probably CuAl. The hexagonal phase certainly exists over an extended range of temperature and it seems probable that it does not decompose during cooling to room temperatures. The difficulty of obtaining equilibrium at temperatures below 500 C. leaves this point in doubt. The orthorhombic phase, on the other hand, exists at 600° C. (it has been identified in crystals obtained from ingots annealed at 602° and 592° C.), but probably undergoes a transformation during cooling to room temperature. Attempts have been made to gain further information by powder photographs of alloys annealed at different temperatures. The diffraction lines are invariably very broad and the photographs obscured by much scattered radiation, while the similarity of the X-ray diffraction patterns, referred to above, makes the identification of the phases by the powder method a very difficult process. The results are so unsatisfactory that they will not be referred to here. It is clear, however, that the constitutional diagram is more complex than previous workers have supposed.

The second object of the present investigation was to adduce evidence in support of a view put forward by Dr. W. Rosenhain concerning the nature of intermetallic compounds. Dr. Rosenhain suggested that neighbouring phases in a constitutional diagram might arise from definite molecular groups of atoms held together by other atoms, the range of existence (in concentration) of the phase being supposed to be due to the possibility of replacing the binding atoms by atoms of either element, while the "molecule" or group remained unchanged from phase to phase. At the inception of the investigation it was hoped that a complete solution of the hexagonal and orthorhombic structures might be obtained in which atomic groupings could be identified. This has not proved possible. The complexity of the structures, combined with the imperfection of the experimental evidence (which is largely due to failure to obtain a single crystal), has rendered the task of placing the atoms in the

units insoluble. Nevertheless, it is felt that certain broad conclusions, not inconsistent with Dr. Rosenhain's view, may be drawn from the results. The numerical relationships between the parameters of the cubic γ phase and of the hexagonal and orthorhombic structures described above (to which may be added the body-centred cubic β phase of side 5·83 Å. described by Persson* and by Obinata†), are, no doubt, only an expression of the constancy of "atomic radii" as we pass from phase to phase. The similarity of the X-ray diffraction pattern is, however, on quite another footing. It implies that, so far as their spatial arrangement, irrespective of kind, is concerned, the atoms lie at or near to the points of a body-centred cubic lattice of side about 2·88 Å. The differences of symmetry arise from a change in the arrangement of the two kinds of atom associated with the points of the lattice. If this interpretation of the X-ray evidence is justified, it appears that in the range of composition dealt with we have a state of affairs in some respects analogous to the structure of silicates as given by W. L. Bragg and West‡.

Acknowledgments.

I have great pleasure in expressing my thanks to Dr. Marie L. V. Gayler for the preparation and heat treatment of the specimens used in this work.

May 1931.

XCV. *The Steady Motion of Two Doublets.* *By* M. A. Higab, *M.Sc., Ph.D., Lecturer in Applied Mathematics in the Egyptian University, Cairo* §.

THE mutual action of two doublets is discussed in standard books on magnetism, where their mutual energy is given. The object here is to discuss the dynamical problem more generally. The equations of motion are difficult to integrate, so we shall confine our attention to steady motion.

It will be seen that, in fact, the steady motion can be very general even in the case where the doublets are supposed to

* *Zeit. f. Phys.* lvii. p. 115 (1929).
† 'Nature,' cxxvi. p. 809 (1930).
‡ Proc. Roy. Soc. cxiv. p. 450 (1927).
§ Communicated by the Author.

be equal dynamically. The classification of the possible steady motions is a problem of some difficulty, and this classification is the main task of the present paper.

The following assumptions are made :—

(*a*) The doublets are treated as rigid bodies, equal in mass and moment of inertia ;

(*b*) Each doublet has kinetic symmetry about its axis of figure ;

(*c*) Each doublet carries an electric charge placed at its centre of gravity.

Let

m be the mass of each doublet,

M_1, M_2 their magnetic moments, which are taken to be positive,

e_1, e_2 the electric charges, where $e_1 e_2 \neq 0$,

b_1, b_2 their centres of gravity,

b the middle point of the line $b_1 b_2$,

r the distance $b_1 b_2$.

Take a set of axes $b(XYZ)$ fixed in space, and let θ, ϕ be the polar angles of the line $b_1 b_2$ referred to these axes.

Through b_1 take two other sets of axes, as follows :—

(a) $b_1(X_1 Y_1 Z_1)$ parallel to the set of axes fixed in space,

(b) $b_1(A_1 B_1 C_1)$ fixed in the body and moving with it.

Let θ_1, ϕ_1, ψ_1 be the Eulerian angles of the moving system referred to the fixed ones.

Through b_2 take two sets of axes similar to those through b_1. Let these be $b_2(X_2 Y_2 Z_2)$ and $b_2(A_2 B_2 C_2)$.

Let θ_2, ϕ_2, ψ_2 be the corresponding Eulerian angles.

Let A, B, C be the moments of inertia of each doublet about its own axes; but since we have assumed that there is kinetic symmetry about the axes of figure, then we must have $A = B$ for each doublet.

We shall assume that θ, θ_1, θ_2 are always positive.

Equations of Motion.

The kinetic energy of the system is

$$\begin{aligned} T = m/4[\dot{r}^2 + r^2\dot{\theta}^2 + r^2 \sin^2\theta \dot{\phi}^2] \\ + A/2\,[\dot{\theta}_1^2 + \sin^2\theta_1 \dot{\phi}_1^2 + \dot{\theta}_2^2 + \sin^2\theta_2 \dot{\phi}_2^2] \\ + C/2\,[(\dot{\psi}_1 + \dot{\phi}_1 \cos\theta_1)^2 + (\dot{\psi}_2 + \dot{\phi}_2 \cos\theta_2)^2]. \end{aligned}$$

The potential energy is

$$\mathrm{V}=\frac{e_1e_2}{r}+\frac{\mathrm{M}_1\mathrm{M}_2}{r^3}[\cos\theta_1\cos\theta_2+\sin\theta_1\sin\theta_2\cos(\phi_1-\phi_2)]$$
$$-\frac{3\mathrm{M}_1\mathrm{M}_2}{r^3}[\cos\theta_1\cos\theta+\sin\theta\sin\theta_1\cos(\phi-\phi_1)]$$
$$\times[\cos\theta\cos\theta_2+\sin\theta\sin\theta_2\cos(\phi-\phi_2)].$$

We have nine equations of motion, two of which are

$$\frac{d}{dt}(\dot\psi_1+\dot\phi_1\cos\theta_1)=0,$$
$$\frac{d}{dt}(\dot\psi_2+\dot\phi_2\cos\theta_2)=0\ ;$$
$$\therefore\quad \dot\psi_1+\dot\phi_1\cos\theta_1=n_1,$$
$$\dot\psi_2+\dot\phi_2\cos\theta_2=n_2,$$

where n_1 and n_2 are constants.

This means that the angular momenta of the doublets about their axes of symmetry are constants.

Using the above equations to simplify the remaining ones, we get the equations of motion to be

$$\frac{m}{2}(\ddot r-r\dot\theta^2-r\sin^2\theta\dot\phi^2)$$
$$=\frac{e_1e_2}{r^2}+\frac{3\mathrm{M}_1\mathrm{M}_2}{r^4}[\cos\theta_1\cos\theta_2+\sin\theta_1\sin\theta_2\cos(\phi_1-\phi_2)]$$
$$-\frac{9\mathrm{M}_1\mathrm{M}_2}{r^4}[\cos\theta\cos\theta_1+\sin\theta\sin\theta_1\cos(\phi-\phi_1)]$$
$$\times[\cos\theta\cos\theta_2+\sin\theta\sin\theta_2\cos(\phi-\phi_2)],\qquad .\quad (1)$$

$$\frac{m}{2}\frac{d}{dt}(r^2\dot\theta)-\frac{m}{2}r^2\sin\theta\cos\theta\dot\phi^2$$
$$=\frac{3\mathrm{M}_1\mathrm{M}_2}{r^3}[-\sin\theta\cos\theta_1+\cos\theta\sin\theta_1\cos(\phi-\phi_1)]$$
$$\times[\cos\theta\cos\theta_2+\sin\theta\sin\theta_2\cos(\phi-\phi_2)]$$
$$+\frac{3\mathrm{M}_1\mathrm{M}_2}{r^3}[\cos\theta\cos\theta_1+\sin\theta\sin\theta_1\cos(\phi-\phi_1)]$$
$$\times[-\sin\theta\cos\theta_2+\cos\theta\sin\theta_2\cos(\phi-\phi_2)],$$
$$.\quad .\quad .\quad (2)$$

$$\frac{m}{2\sin\theta}\frac{d}{dt}(r^2\sin^2\theta\dot{\phi})$$
$$= -\frac{3M_1M_2}{r^3}\sin\theta_1\sin(\phi-\phi_1)$$
$$\times[\cos\theta\cos\theta_2+\sin\theta\sin\theta_2\cos(\phi-\phi_2)]$$
$$-\frac{3M_1M_2}{r^3}\sin\theta_2\sin(\phi-\phi_2)$$
$$\times[\cos\theta\cos\theta_1+\sin\theta\sin\theta_1\cos(\phi-\phi_1)], \quad (3)$$

$$A\ddot{\theta}_1-A\sin\theta_1\cos\theta_1\dot{\phi}_1^2+Cn_1\sin\theta_1\dot{\phi}_1^2$$
$$= -\frac{M_1M_2}{r^3}[-\sin\theta_1\cos\theta_2+\cos\theta_1\sin\theta_2\cos(\phi_1-\phi_2)]$$
$$+\frac{3M_1M_2}{r^3}[-\cos\theta\sin\theta_1+\sin\theta\cos\theta_1\cos(\phi-\phi_1)]$$
$$\times[\cos\theta\cos\theta_2+\sin\theta\sin\theta_2\cos(\phi-\phi_2)], \quad . \quad (4)$$

$$A\ddot{\theta}_2-A\sin\theta_2\cos\theta_2\dot{\phi}_2+Cn_2\sin\theta_2\dot{\phi}_2^2$$
$$= -\frac{M_1M_2}{r^3}[-\cos\theta_1\sin\theta_2+\sin\theta_1\cos\theta_2\cos(\phi_1-\phi_2)]$$
$$+\frac{3M_1M_2}{r^3}[\cos\theta\cos\theta_1+\sin\theta\sin\theta_1\cos(\phi-\phi_1)]$$
$$\times[-\cos\theta\sin\theta_2+\sin\theta\cos\theta_2\cos(\phi-\phi_2)], \quad . \quad (5)$$

$$\frac{1}{\sin\theta_1}\frac{d}{dt}(A\sin^2\theta_1\dot{\phi}_1+Cn_1\cos\theta_1)$$
$$= \frac{M_1M_2}{r^3}\sin\theta_2\sin(\phi_1-\phi_2)+\frac{3M_1M_2}{r^3}\sin\theta\sin(\phi-\phi_1)$$
$$\times[\cos\theta\cos\theta_2+\sin\theta\sin\theta_2\cos(\phi-\phi_2)], \quad . \quad (6)$$

$$\frac{1}{\sin\theta_2}\frac{d}{dt}(A\sin^2\theta_2\dot{\phi}_2+Cn_2\cos\theta_2)$$
$$= -\frac{M_1M_2}{r^3}\sin\theta_1\sin(\phi_1-\phi_2)+\frac{3M_1M_2}{r^3}\sin\theta\sin(\phi-\phi_2)$$
$$\times[\cos\theta\cos\theta_1+\sin\theta\sin\theta_1\cos(\phi-\phi_1)]. \quad . \quad (7)$$

Steady Motion.

Steady motion is that in which the distance between the centres of gravity of the two magnets is constant, and the lines b_1b_2, b_1C_1, b_2C_2 revolve round the axes bZ, b_1Z_1

b_2Z_2 respectively with the same angular velocity, which we shall call ω. Thus we must have

$$\dot{r}=0, \qquad \dot{\theta}=\dot{\theta}_1=\dot{\theta}_2=0,$$
$$\dot{\phi}=\dot{\phi}_1=\dot{\phi}_2=\omega.$$

Hence $r=a$, where a is constant; θ, θ_1, θ_2 are constants which we shall denote by α, β, γ respectively, where $0\leq\alpha\leq\pi$, $0\leq\beta\leq\pi$, $0\leq\gamma\leq\pi$.

We shall adopt the symbols δ, ϵ for the constant angles $\phi_1-\phi$, $\phi_2-\phi$ respectively.

Substituting these values in the equations of motion, we get the equations of steady motion to be

$$-\frac{m}{2}\sin^2\alpha\,\omega^2$$
$$=\frac{e_1e_2}{a^3}+\frac{3M_1M_2}{a^5}[\cos\beta\cos\gamma+\sin\beta\sin\gamma\cos(\delta-\epsilon)]$$
$$-\frac{9M_1M_2}{a^5}[\cos\alpha\cos\beta+\sin\alpha\sin\beta\cos\delta]$$
$$\times[\cos\alpha\cos\gamma+\sin\alpha\sin\gamma\cos\epsilon], \quad . \quad . \quad (1)$$

$$-\frac{m}{4}\sin 2\alpha\,\omega^2$$
$$=\frac{3M_1M_2}{a^5}[-\sin\alpha\cos\beta+\cos\alpha\sin\beta\cos\delta]$$
$$\times[\cos\alpha\cos\gamma+\sin\alpha\sin\gamma\cos\epsilon]$$
$$+\frac{3M_1M_2}{a^5}[\cos\alpha\cos\beta+\sin\alpha\sin\beta\cos\delta]$$
$$\times[-\sin\alpha\cos\gamma+\cos\alpha\sin\gamma\cos\epsilon], \quad . \quad . \quad (2)$$

$$0=\sin\beta\sin\delta[\cos\alpha\cos\gamma+\sin\alpha\sin\gamma\cos\epsilon]$$
$$+\sin\gamma\sin\epsilon[\cos\alpha\cos\beta+\sin\alpha\sin\beta\cos\delta], \quad . \quad . \quad (3)$$

$$\sin\beta[-A\cos\beta\omega^2+Cn_1\omega]$$
$$=-\frac{M_1M_2}{a^3}[-\sin\beta\cos\gamma+\sin\gamma\cos\beta\cos(\delta-\epsilon)]$$
$$+\frac{3M_1M_2}{a^3}[-\cos\alpha\sin\beta+\sin\alpha\cos\beta\cos\delta]$$
$$\times[\cos\alpha\cos\gamma+\sin\alpha\sin\gamma\cos\epsilon], \quad . \quad . \quad . \quad (4)$$

$$\sin\gamma[-A\cos\gamma\omega^2+Cn_2\omega]$$
$$=-\frac{M_1M_2}{a^3}[-\cos\beta\cos\gamma+\sin\beta\cos\gamma\cos(\delta-\epsilon)]$$

$$+\frac{3M_1M_2}{a^3}[\cos\alpha\cos\beta+\sin\alpha\sin\beta\cos\delta]$$
$$\times[-\cos\alpha\sin\gamma+\sin\alpha\cos\gamma\cos\epsilon], \quad . \quad . \quad (5)$$

$$0=\sin\gamma\sin(\delta-\epsilon)-3\sin\alpha\sin\delta[\cos\alpha\cos\gamma+\sin\alpha\sin\gamma\cos\epsilon], \quad . \quad . \quad (6)$$

$$0=\sin\beta\sin(\delta-\epsilon)+3\sin\alpha\sin\epsilon[\cos\alpha\cos\beta+\sin\alpha\sin\beta\cos\delta]. \quad . \quad . \quad (7)$$

The following types of steady motion are to be considered separately :—

I. Statical configurations defined by $\omega=0$,

II. $\omega\neq0$, $\sin\alpha=0$, $\sin\beta\neq0$, $\sin\gamma\neq0$,

III. $\omega\neq0$, $\sin\alpha\neq0$, $\sin\beta=0$, $\sin\gamma=0$ simultaneously,

IV. $\omega\neq0$, $\sin\alpha\neq0$, $\sin\beta=0$, $\sin\gamma\neq0$,

V. $\omega\neq0$, $\sin\alpha\neq0$, $\sin\beta\neq0$, $\sin\gamma\neq0$, axes of the doublets in one plane $\alpha=\pi/2$,

VI. $\omega\neq0$, axes of the doublets in one plane $\sin\alpha\neq0$, $\cos\alpha\neq0$, $\sin\beta\neq0$, $\sin\gamma\neq0$,

VII. $\omega\neq0$, axes of the doublets not in one plane $\sin\alpha\neq0$, $\sin\beta\neq0$, $\sin\gamma\neq0$, $\alpha=\pi/2$,

VIII. $\omega\neq0$, axes of the doublets not in one plane $\sin\alpha\neq0$, $\cos\alpha\neq0$, $\sin\beta\neq0$, $\sin\gamma\neq0$,

Cases I., II., III., IV., V. are simple to deal with, and for this reason they are not to be discussed in this paper.

Type VI.

The most general steady motion with the axes of the doublets in one plane is defined by $\omega\neq0$, $\sin\alpha\neq0$, $\cos\alpha\neq0$, $\sin\beta$ and $\sin\gamma$ not zero simultaneously. $\sin\delta=0$, $\sin\epsilon=0$ simultaneously.

The following cases arise :—

VI. (*a*) $\delta=0$, $\epsilon=0$,
VI. (*b*) $\delta=0$, $\epsilon=\pi$,
VI. (*c*) $\delta=\pi$, $\epsilon=\pi$,
VI. (*d*) $\delta=\pi$, $\epsilon=0$.

The conditions for steady motion in these cases are shown in the following table :—

Equations of steady motion when axes of the doublets are in one plane.

Case VI. (*a*).	Case VI. (*b*).	Case VI. (*c*).	Case VI. (*d*).	
$-\frac{m}{2}a\sin^2\alpha\,\omega^2=\frac{e_1e_2}{a^2}$	$-\frac{m}{2}a\sin^2\alpha\,\omega^2=\frac{e_1e_2}{a^2}+\frac{3M_1M_2}{a^4}$	$-\frac{m}{2}a\sin^2\alpha\,\omega^2=\frac{e_1e_2}{a^2}$	$-\frac{m}{2}a\sin^2\alpha\,\omega^2=\frac{e_1e_2}{a^2}$	
$+\frac{3M_1M_2}{a^4}\cos(\beta-\gamma)-\frac{9M_1M_2}{a^4}$	$\times\cos(\beta+\gamma)-\frac{9M_1M_2}{a^4}$	$+\frac{3M_1M_2}{a^4}\cos(\beta-\gamma)-\frac{9M_1M_2}{a^4}$	$+\frac{3M_1M_2}{a^4}\cos(\beta+\gamma)-\frac{9M_1M_2}{a^4}$	
$\times\cos(\alpha-\beta)\cos(\alpha-\gamma).$	$\times\cos(\alpha-\beta)\cos(\alpha+\gamma).$	$\times\cos(\alpha+\beta)\cos(\alpha+\gamma).$	$\times\cos(\alpha+\beta)\cos(\alpha-\gamma).$	(1)
$-\frac{m}{4}a^2\sin 2\alpha\,\omega^2$	$-\frac{m}{4}a^2\sin 2\alpha\,\omega^2$	$-\frac{m}{2}a^2\sin 2\alpha\,\omega^2$	$-\frac{m}{2}a^2\sin 2\alpha\,\omega^2$	
$=-\frac{3M_1M_2}{a^3}\sin(2\alpha-\beta-\gamma).$	$=-\frac{3M_1M_2}{a^3}\sin(2\alpha-\beta+\gamma).$	$=-\frac{3M_1M_2}{a^3}\sin(2\alpha+\beta+\gamma).$	$=-\frac{3M_1M_2}{a^3}\sin(2\alpha+\beta-\gamma).$	(2)
$-\frac{A}{2}\sin 2\beta\,\omega^2+Cn_1\omega\sin\beta$	$-\frac{A}{2}\sin 2\beta\,\omega^2+Cn_1\omega\sin\beta$	$-\frac{A}{2}\sin 2\beta\,\omega^2+Cn_1\omega\sin\beta$	$-\frac{A}{2}\sin 2\beta\,\omega^2+Cn_1\omega\sin\beta$	
$=\frac{M_1M_2}{a^3}\sin(\beta-\gamma)+\frac{3M_1M_2}{a^4}$	$=\frac{M_1M_2}{a^3}\sin(\beta+\gamma)+\frac{3M_1M_2}{a^3}$	$=\frac{M_1M_2}{a^3}\sin(\beta-\gamma)-\frac{3M_1M_2}{a^3}$	$=\frac{M_1M_2}{a^3}\sin(\beta+\gamma)-\frac{3M_1M_2}{a^3}$	
$\times\sin(\alpha-\beta)\cos(\alpha-\gamma).$	$\times\sin(\alpha-\beta)\cos(\alpha+\gamma).$	$\times\sin(\alpha+\beta)\cos(\alpha+\gamma).$	$\times\sin(\alpha+\beta)\cos(\alpha-\gamma).$	(3)
$-\frac{A}{2}\sin 2\gamma\,\omega^2+Cn_2\omega\sin\gamma$	$-\frac{A}{2}\sin 2\gamma\,\omega^2+Cn_2\omega\sin\gamma$	$-\frac{A}{2}\sin 2\gamma\,\omega^2+Cn\,\omega\sin\gamma$	$-\frac{A}{2}\sin 2\gamma\,\omega^2+Cn_2\omega\sin\gamma$	
$=-\frac{M_1M_2}{a^3}\sin(\beta-\gamma)+\frac{3M_1M_2}{a^3}$	$=\frac{M_1M_2}{a^3}\sin(\beta+\gamma)-\frac{3M_1M_2}{a^3}$	$=-\frac{M_1M_2}{a^3}\sin(\beta-\gamma)$	$=\frac{M_1M_2}{a^3}\sin(\beta+\gamma)+\frac{3M_1M_2}{a^3}$	
$\times\cos(\alpha-\beta)\sin(\alpha-\gamma).$	$\times\cos(\alpha-\beta)\sin(\alpha+\gamma).$	$-\frac{3M_1M_2}{a^3}\cos(\alpha+\beta)\cos(\alpha+\gamma).$	$\times\cos(\alpha+\beta)\sin(\alpha-\gamma).$	(4)

It appears at first sight that there are four distinct cases, but in reality there are not, for if we substitute $(\pi-\alpha)$ for α in case VI. (a) we get case VI. (c). Similarly, if we substitute $(\pi-\alpha)$ for α in case VI. (b) we get case VI. (d). Thus it is only necessary to consider cases VI. (a) and VI. (b).

Case VI. (a).

The following subcases are to be considered separately :—

(i.) $n_1=n_2=0$,
(ii.) $n_1=+n_2$,
(iii.) $n_1=-n_2$,
(iv.) $n_1\neq n_2$.

Case VI. $(a$, i.$)$ $n_1=n_2=0$.

The equations for steady motion are

$$-\frac{m}{2}a\sin^2\alpha\,\omega^2=\frac{e_1e_2}{a^2}+\frac{3M_1M_2}{a^4}\cos(\beta-\gamma)$$
$$-\frac{9M_1M_2}{a^4}\cos(\alpha-\beta)\cos(\alpha-\gamma), \quad . \quad (1)$$

$$\frac{m}{4}a^2\sin 2\alpha\,\omega^2=\frac{3M_1M_2}{a^3}\sin(2\alpha-\beta-\gamma), \quad . \quad . \quad . \quad . \quad (2)$$

$$-\frac{A}{2}\sin 2\beta\,\omega^2=\frac{M_1M_2}{a^3}\sin(\beta-\gamma)$$
$$+\frac{3M_1M_2}{a^3}\sin(\alpha-\beta)\cos(\alpha-\gamma), \quad . \quad . \quad . \quad (3)$$

$$-\frac{A}{2}\sin 2\gamma\,\omega^2=-\frac{M_1M_2}{a^3}\sin(\beta-\gamma)$$
$$+\frac{3M_1M_2}{a^3}\cos(\alpha-\beta)\sin(\alpha-\gamma). \quad . \quad , \quad . \quad (4)$$

The equations (3), (4) are satisfied if $\beta=\gamma$, *i. e.*, if the doublets are parallel.

Putting $\beta=\gamma$, the equations (2), (3) give

$$a^2=-\frac{4A}{m}\frac{\sin 2\beta}{\sin 2\alpha}.$$

Thus for given values of m, M_1, M_2, A, α, $\beta(=\gamma)$ we can interpret the equation just found as determining a^2, the equation (3) with $\beta=\gamma$ as determining ω^2, and the

equation (1) as determining e_1e_2; but α, β are subject to the conditions that

$$\sin(2\alpha-2\beta)/\sin 2\beta \quad \text{and} \quad \sin 2\alpha/\sin 2\beta$$

are both negative simultaneously.

These conditions are satisfied if

(i.) $0<\beta<\pi/2, \quad \pi/2<\alpha<\pi, \quad \pi/2<\alpha-\beta<\pi,$

(ii.) $\pi/2<\beta<\pi, \quad 0<\alpha<\pi/2, \quad \pi/2<\beta-\alpha<\pi.$

If $\beta\neq\gamma$, then from (2), (3), and (4) we get

$$-\tan(\beta+\gamma)\cos(\beta-\gamma) = 3\sin(2\alpha-\beta-\gamma),$$

$$\mathrm{A}\sin(\beta+\gamma)\cos(\beta-\gamma) = m/4\,a^2\sin 2\alpha,$$

$$\mathrm{A}\cos(\beta+\gamma)\omega^2 = \frac{\mathrm{M}_1\mathrm{M}_2}{a^3}.$$

Thus for given values of m, M_1, M_2, A, β, γ the first of the equations just found determines α, the second determines a^2, and the third determines ω^2; but α, β, γ are subject to the conditions that

$$\sin 2\alpha/\sin(\beta+\gamma)\cos(\beta-\gamma) \quad \text{is negative}$$

and

$$\cos(\beta+\gamma) \quad \text{is positive.}$$

These conditions are satisfied if

(i.) $0<\beta+\gamma<\pi/2, \quad \pi/2<\alpha<\pi$;

(ii.) $3\pi/2<\beta+\gamma<2\pi, \quad 0<\alpha<\pi/2, \quad 0<\beta-\gamma<\pi/2.$

In this case steady motion is possible.

Case VI. (a, ii.) $n_1=+n_2=n$.

The equations for steady motion are

$$-\frac{m}{2}a\sin^2\alpha\,\omega^2 = \frac{e_1e_2}{a^2} + \frac{3\mathrm{M}_1\mathrm{M}_2}{a^4}\cos(\beta-\gamma) - \frac{9\mathrm{M}_1\mathrm{M}_2}{a^4}\cos(\alpha-\beta)\cos(\alpha-\gamma), \quad (1)$$

$$\frac{m}{4}a^2\sin 2\alpha\,\omega^2 = \frac{3\mathrm{M}_1\mathrm{M}_2}{a^3}\sin(2\alpha-\beta-\gamma), \quad . \quad . \quad (2)$$

$$-\frac{\mathrm{A}}{2}\sin 2\beta\,\omega^2 + Cn\omega\sin\beta = \frac{\mathrm{M}_1\mathrm{M}_2}{a^3}\sin(\beta-\gamma) + \frac{3\mathrm{M}_1\mathrm{M}_2}{a^3}\sin(\alpha-\beta)\cos(\alpha-\gamma), \quad (3)$$

$$-\frac{A}{2}\sin 2\gamma\,\omega^2+Cn\omega\sin\gamma=-\frac{M_1M_2}{a^3}\sin(\beta-\gamma)$$
$$+\frac{3M_1M_2}{a^3}\cos(\alpha-\beta)\sin(\alpha-\gamma). \quad (4)$$

The equations (4) and (5) are satisfied by $\beta=\gamma$. Thus for given values of M_1, M_2, a, ω, α, $\beta(=\gamma)$ the equations (1) and (2) with $\beta=\gamma$ can be interpreted as determining e_1e_2 and m respectively, the equation (3) with $\beta=\gamma$ determines n, but α and β are subject to the condition that

$$\sin(2\alpha-2\beta)/\sin 2\alpha \quad \text{is positive.}$$

This condition is satisfied if

(i.) $0<\alpha<\pi/2$, $0<\alpha-\beta<\pi/2$, $\pi/2<\beta-\alpha<\pi$;

(ii.) $\pi/2<\alpha<\pi$, $\pi/2<\alpha-\beta<\pi$, or $0<\beta-\alpha<\pi/2$.

Hence steady motion is possible.

If $\beta\neq\gamma$ the equations (3) and (4) give

$$\omega^2=-\frac{M_1M_2}{2a^3A}$$
$$\times\left[\frac{2\cos^2(\beta-\gamma)/2+3\sin(2\alpha-\beta-\gamma)\cot(\beta+\gamma)/2}{\sin\beta\sin\gamma}\right].$$

$$-A\omega^2\cos(\beta+\gamma)\cos\frac{(\beta-\gamma)}{2}+Cn\omega\cos\frac{(\beta+\gamma)}{2}$$
$$=-\frac{M_1M_2}{a^3}\cos\frac{(\beta-\gamma)}{2}.$$

Thus for given values of M_1, M_2, A, α, β, γ, a the first of the equations just found determines ω^2, the second determines n, the equation (1) determines e_1e_2 and the equation (2) determines m; but α, β, γ are subject to the conditions that

$$\sin(2\alpha-\beta-\gamma)/\sin 2\alpha \quad \text{is positive,}$$

$$2\cos^2(\beta-\gamma)/2+3\sin(2\alpha-\beta-\gamma)\cot(\beta+\gamma)/2 \quad \text{is negative.}$$

As an example for which both conditions are satisfied we have

$$\alpha=150^\circ, \qquad \beta=5^\circ, \qquad \gamma=10^\circ.$$

Thus we see that steady motion is possible.

Case VI. (a, iii.) $n_1=-n_2$.

Let $n_1=n$, $n_2=-n$.

The equations for steady motion are

$$-\frac{m}{2}a\sin^2\alpha\,\omega^2=\frac{e_1e_2}{a^2}+\frac{3M_1M_2}{a^4}\cos(\beta-\gamma)$$
$$-\frac{9M_1M_2}{a^4}\cos(\alpha-\beta)\cos(\alpha-\gamma), \quad (1)$$

$$\frac{m}{4}a^2\sin 2\alpha\,\omega^2=\frac{3M_1M_2}{a^3}\sin(2\alpha-\beta-\gamma), \quad . \quad . \quad (2)$$

$$-\frac{A}{2}\sin 2\beta\,\omega^2+Cn\omega\sin\beta=\frac{M_1M_2}{a^3}\sin(\beta-\gamma)$$
$$+\frac{3M_1M_2}{a^3}\sin(\alpha-\beta)\cos(\alpha-\gamma), \quad (3)$$

$$-\frac{A}{2}\sin 2\gamma\,\omega^2-Cn\omega\sin\gamma=-\frac{M_1M_2}{a^3}\sin(\beta-\gamma)$$
$$+\frac{3M_1M_2}{a^3}\cos(\alpha-\beta)\sin(\alpha-\gamma). \quad (4)$$

The equations (3) and (4) give

$$\omega^2=-\frac{M_1M_2}{2Aa^3}$$
$$\times\left[\frac{2\sin^2(\beta-\gamma)/2+3\sin(2\alpha-\beta-\gamma)\tan(\beta+\gamma)/2}{\sin\beta\sin\gamma}\right],$$

and

$$-A\sin\frac{(\beta-\gamma)}{2}\cos(\beta+\gamma)\omega^2+Cn\omega\sin\frac{(\beta+\gamma)}{2}$$
$$=-\frac{M_1M_2}{a^3}\sin\frac{(\beta-\gamma)}{2}.$$

Thus for given values of M_1, M_2, A, C, a, α, β, γ the first of the equations just found determines ω^2, the second determines n, the equations (1) and (2) determine e_1e_2 and m respectively; but α, β, γ are subject to the conditions that

$$\sin(2\alpha-\beta-\gamma)/\sin 2\alpha \quad \text{is positive}$$

and

$$2\sin^2(\beta-\gamma)/2+3\sin(2\alpha-\beta-\gamma)\tan(\beta+\gamma)/2$$

is negative.

As an example which satisfies both conditions we have

$$\alpha=170^\circ, \qquad \beta=80^\circ, \qquad \gamma=79^\circ.$$

Hence steady motion is possible.

Case VI. (*a*, iv.) $n_1 \neq n_2$.

The equations for steady motion are

$$-\frac{m}{2}a\sin^2\alpha\,\omega^2 = \frac{e_1e_2}{a^2} + \frac{3M_1M_2}{a^4}\cos(\beta-\gamma) - \frac{9M_1M_2}{a^4}\cos(\alpha-\beta)\cos(\alpha-\gamma), \quad (1)$$

$$\frac{m}{4}a^2\sin 2\alpha\,\omega^2 = \frac{3M_1M_2}{a}\sin(2\alpha-\beta-\gamma), \quad . \quad . \quad . \quad . \quad (2)$$

$$-\frac{A}{2}\sin 2\beta\,\omega^2 + Cn_1\omega\sin\beta = \frac{M_1M_2}{a^3}\sin(\beta-\gamma) + \frac{3M_1M_2}{a^3}\sin(\alpha-\beta)\cos(\alpha-\gamma), \quad (3)$$

$$-\frac{A}{2}\sin 2\gamma\,\omega^2 + Cn_2\omega\sin\gamma = -\frac{M_1M_2}{a^3}\sin(\beta-\gamma) + \frac{3M_1M_2}{a^3}\cos(\alpha-\beta)\sin(\alpha-\gamma). \quad (4)$$

For given values of M_1, M_2, A, C, a, ω, α, β, γ the equations (1), (2), (3), (4) determine e_1e_2, m, n_1, n_2 respectively ; but α, β, γ are subject to the condition that

$$\sin(2\alpha-\beta-\gamma)/\sin 2\alpha \quad \text{is positive.}$$

This condition is satisfied if

(i.) $0<\alpha<\pi/2$, $0<2\alpha-\beta-\gamma<\pi$;

(ii.) $0<\alpha<\pi/2$, $\pi<\beta+\gamma-2\alpha<2\pi$;

(iii.) $\pi/2<\alpha<\pi$, $\pi<2\alpha-\beta-\gamma<2\pi$;

(iv.) $\pi/2<\alpha<\pi$, $0<\beta+\gamma-2\alpha<\pi$.

Hence steady motion is possible.

Case VI. (*b*).

The following cases are to be discussed separately :—

(i.) $n_1=n_2=0$;

(ii.) $n_1=+n_2$;

(iii.) $n_1=-n_2$;

(iv.) $n_1\neq n_2$.

Case VI. (*b*, i.) $n_1 = n_2 = 0$.

The equations for steady motion are

$$-\frac{m}{2}a\sin^2\alpha\,\omega^2 = \frac{e_1e_2}{a^2} + \frac{3M_1M_2}{a^4}\cos(\beta+\gamma) - \frac{9M_1M_2}{a^4}\cos(\alpha-\beta)\cos(\alpha+\gamma), \quad (1)$$

$$\frac{m}{4}a^2\sin 2\alpha\,\omega^2 = \frac{3M_1M_2}{a^3}\sin(2\alpha-\beta+\gamma), \quad . \quad . \quad . \quad . \quad (2)$$

$$-\frac{A}{2}\sin 2\beta\,\omega^2 = \frac{M_1M_2}{a^3}\sin(\beta+\gamma) + \frac{3M_1M_2}{a^3}\sin(\alpha-\beta)\cos(\alpha+\gamma), \quad (3)$$

$$-\frac{A}{2}\sin 2\gamma\,\omega^2 = \frac{M_1M_2}{a^2}\sin(\beta+\gamma) - \frac{3M_1M_2}{a^3}\cos(\alpha-\beta)\sin(\alpha+\gamma). \quad (4)$$

The equations (3) and (4) are satisfied by $\gamma = \pi - \beta$. In this case the equations (2) and (3) give

$$a^2 = -4A/m\sin 2\beta/\sin 2\alpha.$$

Thus for given values of m, M_1, M_2, A, α, and β we can interpret the equation just found as determining a^2, the equations (1) and (3) with $\gamma = \pi - \beta$ as determining e_1e_2 and ω^2 respectively ; but α, β are subject to the conditions that

$$\sin(2\alpha-2\beta)/\sin 2\beta \quad \text{is positive}$$

and

$$\sin 2\alpha/\sin 2\beta \quad \text{is negative.}$$

These conditions are satisfied if

(i.) $0<\beta<\pi/2$, $\pi/2<\alpha<\pi$, $0<\alpha-\beta<\pi/2$;

(ii.) $\pi/2<\beta<\pi$, $0<\alpha<\pi/2$, $0<\beta-\alpha<\pi/2$.

Hence steady motion is possible.

If $\gamma \neq \pi - \beta$ the equations (2), (3), and (4) give

$$-\tan(\beta-\gamma)\cos(\beta+\gamma) = 3\sin(2\alpha-\beta+\gamma),$$

$$-A\sin(\beta-\gamma)\cos(\beta+\gamma) = m/4\,a^2\sin 2\alpha,$$

$$A\cos(\beta-\gamma)\omega^2 = \frac{M_1M_2}{a^3}.$$

Thus for given values of m, M_1, M_2, A, β, γ the first of the equations just found determines α, the second determines a^2, the third determines ω^2, and the equation (1) determines e_1e_2; but α, β, γ are subject to the condition that

$$\sin 2\alpha/\sin(\beta-\gamma)\cos(\beta+\gamma) \quad \text{is negative,}$$
$$\cos(\beta-\gamma) \quad \text{is positive.}$$

These conditions are satisfied if

(i.)	$0<\beta-\gamma<\pi/2$,	$0<\beta+\gamma<\pi/2$,	$\pi/2<\alpha<\pi$;
(ii.)	$0<\beta-\gamma<\pi/2$,	$3\pi/2<\beta+\gamma<2\pi$,	$\pi/2<\alpha<\pi$;
(iii.)	$0<\gamma-\beta<\pi/2$,	$\pi/2<\beta+\gamma<3\pi/2$,	$\pi/2<\alpha<\pi$;
(iv.)	$0<\beta-\gamma<\pi/2$,	$\pi/2<\beta+\gamma<3\pi/2$,	$0<\alpha<\pi/2$;
(v.)	$0<\gamma-\beta<\pi/2$,	$0<\beta+\gamma<\pi/2$,	$0<\alpha<\pi/2$;
(vi.)	$0<\gamma-\beta<\pi/2$,	$3\pi/2<\beta+\gamma<2\pi$,	$0<\alpha<\pi/2$.

Hence steady motion is possible.

Case VI. (b, ii.) $n_1=+n_2=n$.

The equations for steady motion are

$$-\frac{m}{2}a\sin^2\alpha\,\omega^2=\frac{e_1e_2}{a^2}+\frac{3M_1M_2}{a^4}\cos(\beta+\gamma)$$
$$-\frac{9M_1M_2}{a^4}\cos(\alpha-\beta)\cos(\alpha+\gamma), \quad (1)$$

$$\frac{m}{4}a^2\sin 2\alpha\,\omega^2=\frac{3M_1M_2}{a^3}\sin(2\alpha-\beta+\gamma), \quad . \quad . \quad . \quad . \quad (2)$$

$$-\frac{A}{2}\sin 2\beta\,\omega^2+Cn\omega\sin\beta=\frac{M_1M_2}{a^3}\sin(\beta+\gamma)$$
$$+\frac{3M_1M_2}{a^3}\sin(\alpha-\beta)\cos(\alpha+\gamma), \quad (3)$$

$$-\frac{A}{2}\sin 2\gamma\,\omega^2+Cn\omega\sin\gamma=\frac{M_1M_2}{a^3}\sin(\beta+\gamma)$$
$$-\frac{3M_1M_2}{a^3}\cos(\alpha-\beta)\sin(\alpha+\gamma). \quad (4)$$

From (3) and (4) we get

$$\omega^2=\frac{M_1M_2}{2Aa^3}\left[\frac{2\cos^2(\beta+\gamma)/2+3\sin(2\alpha-\beta+\gamma)\cot(\beta-\gamma)/2}{\sin\beta\sin\gamma}\right]$$

$$-A\cos\frac{\beta+\gamma}{2}\cos(\beta-\gamma)\omega^2+Cn\omega\cos\frac{\beta+\gamma}{2}=-\frac{M_1M_2}{a^3}\cos\frac{\beta+\gamma}{2}.$$

Thus for given values of M_1, M_2, a, C, A, α, β, γ the first of the equations just found determines ω^2, the second determines n, the equations (1) and (2) determine e_1e_2 and n respectively; but α, β, γ are subject to the conditions that

$$\sin(2\alpha-\beta-\gamma)/\sin 2\alpha \quad \text{is positive}$$

$$2\cos^2(\beta+\gamma)/2+3\sin(2\alpha-\beta-\gamma)\cot(\beta-\gamma)/2$$

is positive.

As an example for which both these conditions are satisfied we have

$$\alpha=30°, \qquad \beta=15°, \qquad \gamma=10°.$$

Thus steady motion is possible.

Case VI. (b, iii.) $n_1=-n_2$.

Let $n_1=n$ and $n_2=-n$.

The equations for steady motion are

$$-\frac{m}{2}a\sin^2\alpha\,\omega^2=\frac{e_1e_2}{a^2}+\frac{3M_1M_2}{a^4}\cos(\beta+\gamma)$$
$$-\frac{9M_1M_2}{a^4}\cos(\alpha-\beta)\cos(\alpha+\gamma), \quad (1)$$

$$\frac{m}{4}a^2\sin 2\alpha\,\omega^2=\frac{3M_1M_2}{a^3}\sin(2\alpha-\beta+\gamma), \quad . \quad . \quad . \quad . \quad (2)$$

$$-\frac{A}{2}\sin 2\beta\,\omega^2+Cn\omega\sin\beta=\frac{M_1M_2}{a^3}\sin(\beta+\gamma)$$
$$+\frac{3M_1M_2}{a^3}\sin(\alpha-\beta)\cos(\alpha+\gamma), \quad (3)$$

$$-\frac{A}{2}\sin 2\gamma\,\omega^2-Cn\omega\sin\gamma=\frac{M_1M_2}{a^3}\sin(\beta+\gamma)$$
$$-\frac{3M_1M_2}{a^3}\cos(\alpha-\beta)\sin(\alpha+\gamma). \quad (4)$$

The equations (3) and (4) are satisfied by $\gamma=\pi-\beta$.

Thus for given values of M_1, M_2, A, C, a, ω, α, β the equations (1), (2), (3) with $\gamma=\pi-\beta$ determine e_1e_2, m, n; but α, β are subject to the condition that

$$\sin(2\alpha-2\beta)/\sin 2\alpha \quad \text{is negative.}$$

This condition is satisfied if

(i.) $0<\alpha<\pi/2, \quad 0<\beta-\alpha<\pi/2$;

(ii.) $\pi/2<\alpha<\pi, \quad 0<\alpha-\beta<\pi/2.$

Hence steady motion is possible.

If $\gamma\neq\pi-\beta$ the equations (3) and (4) give

$$\omega^2=\frac{M_1M_2}{2Aa^3}\left[\frac{2\sin^2(\beta+\gamma)/2+3\sin(2\alpha-\beta+\gamma)\tan(\beta-\gamma)/2}{\sin\beta\sin\gamma}\right]$$

and

$$-A\sin\frac{\beta+\gamma}{2}\cos(\beta-\gamma)\omega^2+Cn\omega\sin\frac{\beta-\gamma}{2}=-\frac{M_1M_2}{a^3}\sin\frac{\beta+\gamma}{2}.$$

Thus for given values of M_1, M_2, A, C, a, α, β, γ the first of the equations just found determines ω^2, the second determines n, the equations (1) and (2) determine e_1e_2 and m respectively ; but α, β, γ are subject to the conditions that

$$\sin(2\alpha-\beta+\gamma)/\sin 2\alpha \quad \text{is positive}$$

and

$$2\sin^2(\beta+\gamma)/2+3\sin(2\alpha-\beta+\gamma)\tan(\beta-\gamma)/2$$

is positive.

As an example for which both these conditions are satisfied we have

$$\alpha=60^\circ, \qquad \beta=25^\circ, \qquad \gamma=10^\circ.$$

Hence steady motion is possible.

Case VI. (*b*, iv.) $n_1\neq n_2$.

The equations for steady motion are

$$-\frac{m}{2}\omega^2a\sin^2\alpha=\frac{e_1e_2}{a^2}+\frac{3M_1M_2}{a^4}\cos(\beta-\gamma)-\frac{9M_1M_2}{a^4}\cos(\alpha-\beta)\cos(\alpha+\gamma), \quad (1)$$

$$\frac{m}{4}a^2\sin 2\alpha\,\omega^2=\frac{3M_1M_2}{a^3}\sin(2\alpha-\beta+\gamma), \quad . \quad . \quad . \quad . \quad (2)$$

$$-\frac{A}{2}\sin 2\beta\,\omega^2+Cn_1\omega\sin\beta=\frac{M_1M_2}{a^3}\sin(\beta+\gamma)+\frac{3M_1M_2}{a^3}\sin(\alpha-\beta)\cos(\alpha+\gamma), \quad (3)$$

$$-\frac{A}{2}\sin 2\gamma\,\omega^2+Cn_2\omega\sin\gamma=\frac{M_1M_2}{a^3}\sin(\beta+\gamma)$$
$$-\frac{3M_1M_2}{a^3}\cos(\alpha-\beta)\sin(\alpha+\gamma). \quad (4)$$

For given values of M_1, M_2, A, C, a, ω, α, β, γ the equations (1), (2), (3), and (4) determine e_1e_2, m, n_1, and n_2 respectively; but α, β, γ are subject to the conditions that

$$\sin(2\alpha-\beta+\gamma)/\sin 2\alpha \quad \text{is positive.}$$

This condition is satisfied if

(i.) $\quad 0<\alpha<\pi/2, \qquad 0<2\alpha-\beta+\gamma<\pi;$

(ii.) $\quad \pi/2<\alpha<\pi, \qquad \pi<2\alpha-\beta+\gamma<2\pi.$

Hence steady motion is possible.

Type VII.

The most general type of steady motion is defined by

$$\omega\neq 0, \quad \sin\alpha\neq 0, \quad \sin\beta\neq 0, \quad \sin\gamma\neq 0, \quad \sin\delta=0, \quad \sin\epsilon\neq 0.$$

As a special case take $\alpha=\pi/2$.

Putting $\alpha=\pi/2$ in the equations for steady motion, two distinct cases arise which are to be discussed separately:

Case VII. (*a*) $\quad \delta=\pi/2, \qquad \epsilon=\pi/2;$

Case VII. (*b*) $\quad \delta=\pi/2, \qquad \epsilon=-\pi/2.$

Case VII. (*a*).

The following sub-cases arise:—

(i.) $\quad n_1=n_2=0;$

(ii.) $\quad n_1=+n_2;$

(iii.) $\quad n_1=-n_2;$

(iv.) $\quad n_1\neq n_2.$

Case VII. (*a*, i.) $\quad n_1=n_2=0.$

In this case two other cases arise, namely, we get either

$$\beta+\gamma=\pi \quad \text{or} \quad \beta-\gamma=\pm\pi/2.$$

If $\beta+\gamma=\pi$ the equations for steady motion reduce to

$$-\frac{m}{2}a\omega^2=\frac{e_1e_2}{a^2}-\frac{3M_1M_2}{a^4}\cos 2\beta,$$

$$\omega^2=\frac{2M_1M_2}{Aa^3}.$$

The first of these equations determines e_1e_2, and the second determines ω^2, when m, M_1, M_2, a, and β are given.

If $\gamma=\beta+\pi/2$ the equations for steady motion reduce to

$$e_1e_2=-m/2\ a^3\omega^2,$$

$$\omega^2\sin 2\beta=\frac{2M_1M_2}{Aa^3}.$$

The first of these equations determines e_1e_2, and the second determines ω^2; but β is subject to the condition that $\sin 2\beta$ is positive, *i. e.*, $0<\beta<\pi/2$.

If $\gamma=\beta-\pi/2$ the equations for steady motion reduce to

$$e_1e_2=-m/2\ a^3\omega^2,$$

$$\omega^2\sin 2\beta=-\frac{2M_1M_2}{Aa^3}.$$

As in the previous case, $\sin 2\beta$ must be a negative, *i. e.*, $\pi/2<\beta<\pi$.

Case VII. (*a*, ii.) $n_1=+n_2=n$.

The equations for steady motion are

$$-\frac{m}{2}a\omega^2=\frac{e_1e_2}{a^2}+\frac{3M_1M_2}{a^4}\cos(\beta-\gamma), \quad . \quad . \quad (1)$$

$$-\frac{A}{2}\sin 2\beta\,\omega^2+Cn\omega\sin\beta=\frac{M_1M_2}{a^3}\sin(\beta-\gamma), \quad . \quad (2)$$

$$-\frac{A}{2}\sin 2\gamma\,\omega^2+Cn\omega\sin\gamma=-\frac{M_1M_2}{a^3}\sin(\beta-\gamma). \quad (3)$$

The equations (2) and (3) are satisfied by $\beta=\gamma$.

Putting $\beta=\gamma$, the equations reduce to

$$-\frac{m}{2}a\omega^2=\frac{e_1e_2}{a^2}+\frac{3M_1M_2}{a^4},$$

$$\omega=\frac{Cn}{A\cos\beta}.$$

The first of these equations determines e_1e_2, and the second determines ω, when m, a, M_1, M_2, C, n, A are given.

If $\beta \neq \gamma$ the equations (2) and (3) give

$$\omega^2 = \frac{2M_1M_2}{Aa^3} \frac{\cos^2(\beta-\gamma)/2}{\sin\beta \sin\gamma}$$

and

$$n = \frac{A\omega}{C} \cos\frac{(\beta+\gamma)}{2} \frac{\cos(\beta-\gamma)}{\cos(\beta-\gamma)/2}.$$

Thus for given values of m, M_1, M_2, A, C, β, γ, a the first of the equations just found determines ω^2, the second determines n, and equation (1) determines e_1e_2. In this case steady motion is always possible.

Case VII. (a, iii.) $n_1 = -n_2$.

Let $n_1 = n$ and $n_2 = -n$.

The equations for steady motion are

$$-\frac{m}{2}a\omega^2 = \frac{e_1e_2}{a^2} + \frac{3M_1M_2}{a^4}\cos(\beta-\gamma), \quad . \quad . \quad (1)$$

$$-\frac{A}{2}\sin 2\beta\,\omega^2 + Cn\omega\sin\beta = \frac{M_1M_2}{a^3}\sin(\beta-\gamma), \quad . \quad (2)$$

$$-\frac{A}{2}\sin 2\gamma\,\omega^2 - Cn\omega\sin\gamma = -\frac{M_1M_2}{a^3}\sin(\beta-\gamma). \quad (3)$$

The equations (2) and (3) are satisfied by $\beta+\gamma=\pi$.

Putting $\gamma = \pi - \beta$, the equations for steady motion reduce to

$$-\frac{m}{2}a\omega^2 = \frac{e_1e_2}{a^2} - \frac{3M_1M_2}{a^4}\cos 2\beta, \quad . \quad . \quad (1')$$

$$A\cos\beta\,\omega^2 - Cn\omega = \frac{2M_1M_2}{a^3}\cos\beta. \quad . \quad . \quad . \quad . \quad (2')$$

Thus for given values of m, M_1, M_2, A, C, a, ω, β the equation (1') determines e_1e_2 and (2') determines n.

If $\beta+\gamma \neq \pi$ the equations (2) and (3) give

$$\omega^2 = \frac{2M_1M_2}{Aa^3} \frac{\sin^2(\beta-\gamma)/2}{\sin\beta\sin\gamma}$$

and

$$n = \frac{A\omega}{C}\sin\frac{\beta+\gamma}{2} \frac{\cos(\beta-\gamma)}{\sin(\beta-\gamma)/2}.$$

Thus for given values of m, M_1, M_2, A, C, a, β, γ the first of the equations just found determines ω^2, the second determines n, and equation (1) determines e_1e_2. In this case steady motion is always possible.

Case VII. (a, iv.) $n_1 \neq n_2$.

The equations for steady motion are

$$-\frac{m}{2}a\omega^2 = \frac{e_1e_2}{a^2} + \frac{3M_1M_2}{a^4}\cos(\beta-\gamma), \quad . \quad . \quad (1)$$

$$-\frac{A}{2}\sin 2\beta\,\omega^2 + Cn_1\omega\sin\beta = -\frac{M_1M_2}{a^3}\sin(\beta-\gamma), \quad . \quad (2)$$

$$-\frac{A}{2}\sin 2\gamma\,\omega^2 + Cn_2\omega\sin\gamma = -\frac{M_1M_2}{a^3}\sin(\beta-\gamma). \quad (3)$$

For given values of m, M_1, M_2, A, C, ω, β, γ the equations (1), (2), and (3) determine e_1e_2, n_1, and n_2. In this case steady motion is always possible.

Case VII. (b).

The following subcases are to be discussed separately :—

(i.) $n_1 = n_2 = 0$;
(ii.) $n_1 = +n_2$;
(iii.) $n_1 = -n_2$;
(iv.) $n_1 \neq n_2$.

Case VII. (b, i.) $n_1 = n_2 = 0$.

In this case we get either $\beta = \gamma$ or $\beta+\gamma = \pi/2$ or $3\pi/2$. If $\beta = \gamma$ then steady motion is impossible, since ω^2 must be positive. If $\beta+\gamma = \pi/2$, then

$$\omega^2 = -\frac{2M_1M_2}{Aa^3\sin 2\beta},$$

which is positive if $\pi/2 < \beta < \pi$; but in this case γ is negative. Hence steady motion is impossible. Also, if $\beta+\gamma = 3\pi/2$, then

$$\omega^2 = \frac{2M_1M_2}{Aa^3\sin 2\beta},$$

which is positive if $0 < \beta < \pi/2$; but in this case γ is greater than π. Hence steady motion is impossible.

Case VII. (*b*, ii.) $n_1 = +n_2 = n$.

The equations for steady motion are

$$-\frac{m}{2}a\omega^2 = \frac{e_1e_2}{a^2} + \frac{3M_1M_2}{a^4}\cos(\beta+\gamma), \quad . \quad . \quad (1)$$

$$-\frac{A}{2}\sin 2\beta\,\omega^2 + Cn\omega\sin\beta = \frac{M_1M_2}{a^3}\sin(\beta+\gamma), \quad . \quad (2)$$

$$-\frac{A}{2}\sin 2\gamma\,\omega^2 + Cn\omega\sin\gamma = \frac{M_1M_2}{a^3}\sin(\beta+\gamma). \quad . \quad (3)$$

The equations (4) and (5) are satisfied by $\beta = \gamma$.

Putting $\beta = \gamma$, the equations for steady motion become

$$-\frac{m}{2}a\omega^2 = \frac{e_1e_2}{a^2} + \frac{3M_1M_2}{a^4}\cos 2\beta$$

$$A\cos\beta\,\omega^2 - Cn\omega = -\frac{2M_1M_2}{a^3}\cos\beta.$$

Thus for given values of m, a, ω, M_1, M_2, A, C, β the first equation determines e_1e_2, the second determines n. Hence steady motion is possible.

If $\beta \neq \gamma$ the equations (2) and (3) give

$$\omega^2 = -\frac{2M_1M_2}{Aa^3}\frac{\cos^2(\beta+\gamma)/2}{\sin\beta\sin\gamma},$$

which is negative. Hence steady motion is impossible.

Case VII. (*b*, iii.) $n_1 = -n_2$.

Let $$n_1 = +n \quad \text{and} \quad n_2 = -n.$$

The equations for steady motion are

$$-\frac{m}{2}a\omega^2 = \frac{e_1e_2}{a^2} + \frac{3M_1M_2}{a^4}\cos(\beta+\gamma), \quad . \quad . \quad (1)$$

$$-\frac{A}{2}\sin 2\beta\,\omega^2 + Cn\omega\sin\beta = \frac{M_1M_2}{a^3}\sin(\beta+\gamma), \quad . \quad (2)$$

$$-\frac{A}{2}\sin 2\gamma\,\omega^2 - Cn\omega\sin\gamma = \frac{M_1M_2}{a^3}\sin(\beta+\gamma). \quad . \quad (3)$$

The equations (2) and (3) give $\gamma = \pi - \beta$.

Putting $\gamma=\pi-\beta$, the equations for steady motion reduce to

$$-\frac{m}{2}a\omega^2=\frac{e_1e_2}{a^2}-\frac{3M_1M_2}{a^4}\cos 2\beta,$$

$$\omega=\frac{Cn}{A\cos\beta}.$$

Thus for given values of m, M_1, M_2, a, A, C, n, β the first equation determines e_1e_2 and the second determines ω. Hence steady motion is possible.

If $\gamma\neq\pi-\beta$ the equations (2) and (3) give

$$\omega^2=-\frac{2M_1M_2}{Aa^3}\frac{\sin^2(\beta+\gamma)/2}{\sin\beta\sin\gamma},$$

which is negative. Hence steady motion is impossible.

Case VII. (*b*, iv.) $n_1\neq n_2$.

The equations for steady motion are

$$-\frac{m}{2}a\omega^2=\frac{e_1e_2}{a^2}+\frac{3M_1M_2}{a^4}\cos(\beta+\gamma), \quad . \quad . \quad (1)$$

$$-\frac{A}{2}\sin 2\beta\,\omega^2+Cn_1\omega\sin\beta=\frac{M_1M_2}{a^3}\sin(\beta+\gamma), \quad . \quad (2)$$

$$-\frac{A}{2}\sin 2\gamma\,\omega^2+Cn_2\omega\sin\gamma=\frac{M_1M_2}{a^3}\sin(\beta+\gamma). \quad . \quad (3)$$

For given values of m, M_1, M_2, a, C, A, ω, β, γ the equations (1), (2), and (3) determine e_1e_2, n_1, and n_2. Hence steady motion is possible.

Type VIII.

The most general steady motion is defined by

$$\omega\neq0, \quad \sin\alpha\neq0, \quad \cos\alpha\neq0, \quad \sin\beta\neq0, \quad \sin\gamma\neq0, \quad \sin\delta=0,$$
$$\text{and} \quad \sin\epsilon\neq0.$$

Considering the equations for steady motion on pp. 997, 998, we find that the equations (3), (6), and (7) are not independent ; so we will reject equation (3).

From (6) and (7) we get

$$\cot\beta=\frac{2\sin(\delta-\epsilon)}{3\sin 2\alpha\sin\epsilon}-\tan\alpha\cos\delta, \quad . \quad . \quad . \quad (i.)$$

$$\cot\beta=\frac{2\sin(\delta-\epsilon)}{3\sin 2\alpha\sin\delta}-\tan\alpha\cos\epsilon. \quad . \quad . \quad . \quad (ii.)$$

Thus for given values of M_1, M_2, A, C, a, ω we can put α, δ, and ϵ any angles we like; then the equations (i.) and (ii.) determine β and γ respectively, the equations (1), (2), (4), and (5), p. 997, determine $e_1 e_2$, m, n_1, and n_2 respectively; but α, β, γ, δ, and ϵ are subject to the condition that

$$\sin 2\alpha(\cos\delta\cos\epsilon - \cot\beta\cot\gamma) + \cos 2\alpha(\cot\gamma\cos\delta + \cot\beta\cos\epsilon)$$

is negative. This condition is satisfied if $\cos\alpha\sin\delta\sin\epsilon$ is positive. Hence steady motion is possible.

In conclusion, the writer wishes to thank Professor S. Brodetsky, of Leeds University, under whose supervision the above work has been done.

Summary.

The steady motion of two electrified doublets moving under each other's action is classified and discussed. The conditions for steady motion are found in each case.

XCVI. *Note on a Problem in the Conduction of Heat.* *By* C. E. Wright *.

THE effect of a steady source of heat at one end of an infinite bar, whose other end is kept at zero temperature, was suggested by Prof. G. D. West as having approximate applications to many simple physical circumstances. Reference to usual sources did not disclose any complete discussion, and the following treatment, based on Kelvin's † formula (a reference suggested by Prof. Lees), for an instantaneous source of heat, may be of interest.

An instantaneous source, of amount σ acting at time $t=0$ on one end of a (semi-) infinite bar, assumed not to radiate, gives

$$v = \frac{\sigma}{\sqrt{a\pi}} e^{-\frac{x^2}{4at}} t^{-\frac{1}{2}},$$

* Communicated by the Author.

† The quotation from Kelvin is in Rayleigh, 'Collected Papers,' vi. p. 51; Kelvin, "Compendium of Fourier Mathematics," Encyc. Brit. 1880; or 'Collected Papers,' ii. p. 44.

where v is temperature at distance x from the source of heat and a is the constant in the equation of conductivity

$$\frac{\partial^2 v}{\partial x^2} = \frac{1}{a}\frac{\partial v}{\partial t}; \quad a = \mathrm{K}/c\rho$$

[K = conductivity, c = specific heat, ρ = density].

From this, by integration, the effect of a steady source supplying quantity σ per unit time, starting at $t=0$, is given by

$$v = \frac{\sigma}{\sqrt{a\pi}}\int_0^t \frac{e^{-\frac{x^2}{4a(t-t')}}}{(t-t')^{\frac{1}{2}}}dt'. \quad . \quad . \quad . \quad . \quad (1)$$

The integral may be transformed in various ways. Thus, $x^2 = 4a(t-t')\beta^2$, with β as new variable, transforms (1) to

$$v = \frac{\sigma x}{a\sqrt{\pi}}\int_{\frac{x}{2\sqrt{at}}}^{\infty x} \frac{e^{-\beta^2}d\beta}{\beta^2}, \quad . \quad . \quad . \quad . \quad . \quad (2)$$

where ∞x is used to indicate the effect at $x=0$ on the upper limit.

A further transformation by means of the identity

$$\int_0^1 e^{-p\beta^2}dp = -\left[\frac{e^{-\beta^2}}{\beta^2} - \frac{1}{\beta^2}\right]$$

gives

$$v = -\frac{\sigma x}{a\sqrt{\pi}}\int_{\frac{x}{2\sqrt{at}}}^{\infty x} d\beta\left[\int_0^1 e^{-k\beta^2}dk - \frac{1}{\beta^2}\right]$$

$$= 2\sigma\sqrt{\frac{t}{a\pi}} - \frac{\sigma x}{a\sqrt{\pi}}\int_0^1 dk\int_{\frac{x}{2\sqrt{at}}}^{\infty x} e^{-k\beta^2}d\beta. \quad . \quad (3)$$

From this it is clear that when $x=0$, $v \propto t^{\frac{1}{2}}$; also, if $\frac{x}{2\sqrt{at}} \to 0$, $v = \mathrm{A} - \mathrm{B}x$, where A, B are functions of t only, from which the approach to the steady state may be seen.

On the other hand, from (1) it follows that the total heat in the bar, $\int_0^\infty v\,dx$, is given by

$$\frac{\sigma}{\sqrt{a\pi}}\int_0^t dt\int_0^\infty \frac{e^{-\frac{x^2}{4a(t-t')}}}{(t-t')^{\frac{1}{2}}}dx = \sigma t,$$

a verification of the initial hypothesis, since σ is the amount of heat supplied in unit time.

Again, from the formula (2), by using the identity

$$\frac{d}{du}\left(\frac{1}{u}\cdot e^{-u^2}\right) = -\frac{1}{u^2}e^{-u^2} - 2e^{-u^2},$$

the result takes the form

$$v = 2\sigma\sqrt{\frac{t}{a\pi}}\,e^{-\frac{x^2}{4at}} - \frac{\sigma x}{a\sqrt{\pi}}\int_{\frac{x}{2\sqrt{at}}}^{\infty} e^{-u^2}du. \quad . \quad . \quad (5)$$

If in this x^2 is put $= 4ak^2t$, the result takes the form

$$\frac{v\sqrt{a\pi}}{2\sigma\sqrt{t}} = e^{-k^2} - k\int_k^{\infty} e^{-u^2}du$$

$$= e^{-k^2} - \tfrac{1}{2}k\sqrt{\pi}[1-\Theta(k)], \quad . \quad . \quad (6)$$

in which $\Theta(k)$ is the tabulated function $\frac{2}{\sqrt{\pi}}\int_0^k e^{-u^2}du$, and $k^2 = x^2/4at$.

It will be seen that $v/\sqrt{t}$ is a function of $x/\sqrt{t}$ only. Let the function $e^{-k^2} - k\int_k^{\infty} e^{-u^2}du$ be denoted by $f(k)$; the graph of $f(k)$ is given in fig. 1, which has been plotted from the data below, obtained by aid of Dale's "Five-figure Tables of Mathematical Functions."

k.	$f(k)$.	k.	$f(k)$.
0·0	1·00	1·1	0·1814
0·1	0·9114	1·2	1415
0·2	8230	1·3	1086
0·3	7354	1·4	0·0817
0·4	6492	1·5	603
0·5	5663	1·6	438
0·6	4870	1·7	312
0·7	4128	1·8	218
0·8	3444	1·9	149
0·9	2826	2·0	100
1·0	2285		

This diagram gives an almost immediate view of the space distribution of temperature at any given *time*; it is only necessary to use values of k as values of $x/2a\sqrt{t}$, at the same time values of $f(k)$ are read as values of $v\sqrt{a\pi}/2\sigma\cdot\sqrt{t}$:

that is, the one graph gives v as a function of x with scales which are always uniformly divided, but which both depend on t. Alternatively the graphs of $v\sqrt{a\pi}/2\sigma$ against $x/2\sqrt{a}$ for given values of t are similar curves, similarly situated, whose scales are proportional to $\sqrt{t}$.

The time distribution of temperature at a given point is not so conveniently indicated; but it may be noted that,

Fig. 1.

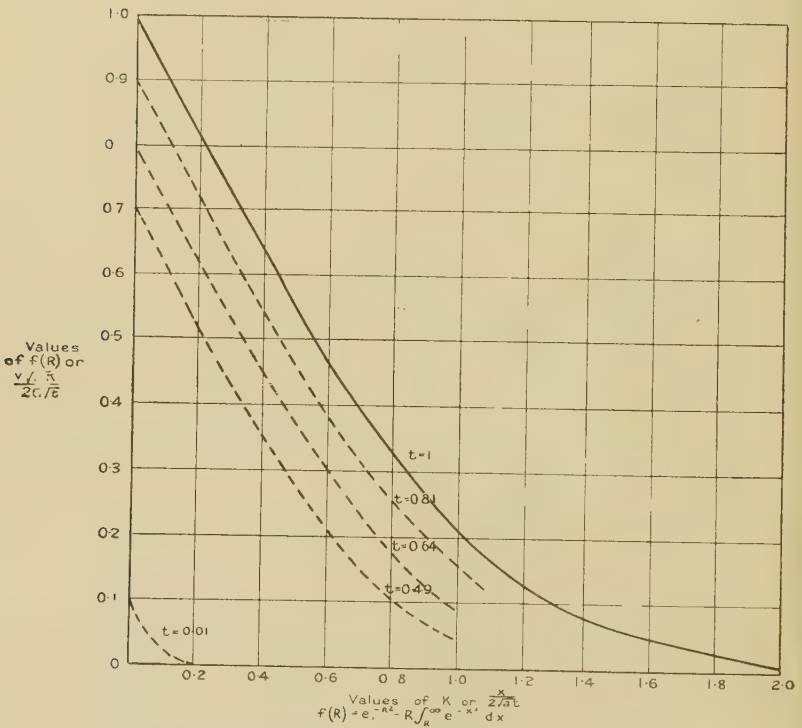

for given values of x, fig. 1 gives $v/\sqrt{t}$ plotted as a function of $1/\sqrt{t}$.

Unfortunately values near $t=0$ are not conveniently shown on any graph of reasonable size; but for $x=0$, $v \propto \sqrt{t}$, and hence the v, t graph is parabolic, whilst for other small values of x this graph will retain the same general shape.

In fig. 1 the scales marked refer to the continuous curve. For the dotted curves, which have been roughly

derived from the former, the scale is in all cases $k=x/2\sqrt{a}$, $f(k)=v\sqrt{a\pi}/2\sigma$; the values of t are given on the curves ($t=1$ corresponds to the continuous curve).

In fig. 2 are given the parabolic graph for $x=0$ and a sketch of the graph for $x=2\sqrt{a}$, the few points actually plotted being derived from the table for $f(k)$ by assigning values to $\sqrt{t}$.

Fig. 2.

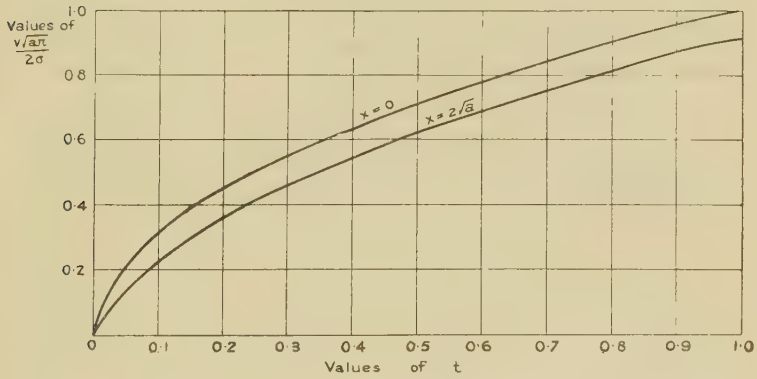

A more complete discussion near $t=0$ would require tables for $\int_k^\infty e^{-k^2}dk$ for values of k outside the usual range. It is doubtful whether any points of interest are lost by this omission.

Blackheath,
May 13th, 1931.

XCVII. *The Temperature Coefficient of the Dielectric Constant of Water.* *By* R. T. Lattey, O. Gatty, *and* W. G. Davies *.

FOR the calculation of the heat of dilution of electrolytic solutions by the use of Bjerrum's formula [4], an accurate knowledge of the temperature coefficient of the dielectric constant of the solvent is required. It has been pointed out by Lange and Robinson [20] that existing data are hardly consistent enough to give us the required information, and it appeared to us that it would be of interest to add the

* Communicated by the Authors.

results of our own experiments on the subject. The method used by us was essentially that described by Lattey and Gatty [21], with certain improvements in technique which we hope shortly to describe elsewhere. The condensers which we used were designed rather to detect changes in dielectric constant than to yield absolute values, and we therefore calibrated them by taking the dielectric constants of certain liquids as known from the work of others. Even if we have taken a faulty value for the dielectric constant of water at a fixed temperature our conclusions will not be invalidated, since it is $\frac{1}{D} \cdot \frac{dD}{dt}$ which is wanted and not simply $\frac{dD}{dt}$.

1. *The Absolute Dielectric Constant of Water.*

All available data in the neighbourhood of 18° C. were collected and corrected to 18° C. by using the equation

$$\log_{10} D = \log_{10} D_0 - 0{\cdot}002\,t.$$

TABLE I.

Dielectric Constant of Water at 18° C.

Ratz [24]	80·43	Sack [25]	80·85
Cole [6]	80·45	Errera [11]	81·02
Kockel [19]	80·53	Palmer [23]	81·03
Heerwagen [16]	80·54	Turner [26]	81·07
Cohn and Zeeman [5]	80 58	Wyman [27]	81·11
Alimova [2]	80·65	Drake, Pierce, and Dow [9]	81·17
Novosilzew [22]	80·68	Franke [12]	81·19
Devoto [8]	80·71	Coolidge [7]	81·23
Drude [10]	80·76		

MEAN ..... 80·82

Since the range of temperature is small, a slight inaccuracy in the temperature coefficient would not introduce serious error.

It was clear that the majority of the values centred round 80·4 to 81·2, and an average of data between these limits was therefore adopted as the most probable value (Table I.).

2. *The Temperature Coefficient.*

When existing series of values for the changes in dielectric constant with temperature were examined, it was clear that the formula suggested by Abegg [1] was the simplest by which the results could be compared with the required degree of accuracy,

$$D = D_0 . e^{-at} \quad \text{or} \quad \log_{10} D = \log_{10} D_0 - \mu at.$$

Three condensers were calibrated, using nitrobenzene, water, and a 10 per cent. solution of sugar as substances of known dielectric constant in order to eliminate the capacity

TABLE II.

Sugar Solutions at Frequencies corresponding to Wave-lengths in Air of 75, 85, 125, 180, and 200 metres.

Temp.	10 per cent. solution.	20 per cent. solution.
9·4°	81·48	78·71
18·0	(78·24) *	(75·70) *
18·4	78·28	75·62
19·1	78·44	75·27
19·7	77·58	75·22
20·0	(77·52) *	(75·00) *
26·4	75·42	72·61
28·0	(74·71) *	(72·25) *
31·2	73·43	71·24
37·0	71·52	69·13
46·5	68·58	66·55
57·9	65·00	62·80
64·2	62·80	60·95
74·2	60·11	
85·4	57·37	

Temp.	10 per cent. solution.	20 per cent. solution.
	Harrington (14)	
18°	76·10	74·12
	Astin (3)	
18°	77·93	75·52
	Fürth (13)	
20°	79·50	74·00
	Kniekamp (18)	
28°	74·63	72·32

* Interpolated.

Sugar Solutions at Rounded Temperatures for Comparison with Values given by Kockel [19]. (The values given by Kockel have been multiplied by 80·81/80·53 to bring them to the same standard for pure water as we have adopted.)

	10 per cent. solution.		20 per cent. solution.	
Temp.	Davies.	Kockel.	Davies.	Kockel.
0°	84·99	85·86	82·34	83·13
10	81·17	81·75	78·58	79·02
20	77·52	77·84	74·99	75·12
30	74·03	74·11	71·57	71·41
40	70·70	70·57	68·31	67·88
50	67.51	67·19	65·18	64·53
60	64·48	63·98	62·21	61·35
70	61·58	60·91	59·36	58·31
80	58·80	58·00	56·65	55·43
90	56·16	55·22	54·07	52·70

of leads and earth capacities from the observed capacity. Nitrobenzene had already been examined by Lattey and Gatty [21]; the sugar solution was examined at various

temperatures and various frequencies in large condensers calibrated by the use of benzene (Hartshorn and Oliver [15]), nitrobenzene, and water. The results are shown in Table II. together with those of other observers. Good agreement with Kniekamp's [18] values at 28°, with Astin's [3] at 18°, and with Kockel's [19] values between 10° and 60° C. will be noted.

The same condensers were used for both the series quoted in Table III. The conductance of the purest water at high

TABLE III.

D SERIES.

Temp.	D obs.	D calc.	Diff.
14·0°	82·57	82·33	+0·24
20·0	80·25	80·08	+0·17
31·7	75·54	75·87	−0·33
39·5	73·07	73·185	−0·115
46·0	71·15	71·025	+0·125
53·0	68·27	68·77	−0·50
63·0	65·44	65·68	−0·24
74·5	62·34	62·27	+0·07
81·3	60·57	60·345	+0·225

G SERIES.

Temp.	D obs.	D calc.	Diff.
15·6	82·22	81·72	+0·50
21·45	79·70	79·545	+0·155
26·25	77·71	77·80	−0·09
33·9	75·28	75·13	+0·15
42·05	72·54	72·33	+0·21
*(54·2	69·49	68·385	+1·10)
61·15	66·84	66·225	+0·615
72·4	62·86	62·73	+0·13
80·15	60·57	60·67	−0·10

* Neglected in calculation of coefficient.

temperatures makes observations difficult, and this is especially the case when the condenser has a large capacity, and we therefore made no attempt to go beyond 80° C.

In each case the value quoted is a mean of values obtained in more than one condenser at various temperatures within a degree or so of that quoted.

The series given under the heading D was obtained after the whole lay-out of the circuit had been improved in every detail, and we have therefore given double weight to the

results in deducing the temperature coefficient. As will be seen from Table III., the results are in good agreement with the formula

$$\log_{10} D = 1{\cdot}94361 - 0{\cdot}002{,}004{,}5\, t$$

or

$$\log_e D = \log_e 87{\cdot}824 - 0{\cdot}004{,}515\, t.$$

In order to facilitate comparison, the results of other observers have each been multiplied by a factor such that D_{18} is always 80·82.

In Table IV. are shown our values for the dielectric constant of water, side by side with those of other observers

TABLE IV

Dielectric Constant of Water at Rounded Temperatures.

np.	Kockel (19).	Coolidge (7).	L., G., & D.	Wyman (27).	Iwanow (17).	Drake, Pierce, & Dow (9).	Drude (10).
0 ...	88·225	87·69	(87·825)	87·69	87·76	88·06	87·57
...	84·01	83·83	83·86	83·82	83·85	83·98	83·76
...	80·05	80·08	80·08	80·08	80·10	80·13	80·11
...	78·155	78·25	78·25	78·27	78·29	78·28	78·34
...	76·315	76·43	76·465	76·49	76·56	76·52	76·61
...	72·80	72·89	73·02	73·02	73·14	73·14	73·27
...	69·49	...	69·725	69·70	69·94	70·03	70·10
...	66·37	...	66·58	66·51	66·91	67·15	67·16
...	63·42	...	63·58	63·45	63·94	...	64·48
...	60·64	...	60·71	60·54	61·21		
...	58·025	...	(57·97)	57·77	58·51		
...	55·545	...	(55·355)	55·13			

at rounded temperatures. Many more series could be quoted, but have been omitted because of their complete disaccord with our results and with those of Kockel (19) and Coolidge (7), both of whom give evidence in their published papers of having observed all the precautions necessary to obtaining accurate results.

In Table V. and in the figure are shown our values of $\frac{d \log D}{d \log T}$, side by side with those of certain other observers. It will be seen that in the neighbourhood of 20° C. there is quite good agreement between our values and those of Drake, Pierce, and Dow (9), of Coolidge (7), of Ivanow (17), and of Wyman (27), and this renders it probable that at 25° C. the value $-\frac{d \log D}{d \log T} = 1{\cdot}376$ is not far from correct.

TABLE V.

Values of $-\frac{d \log D}{d \log T}$ for Water.

Temp.	Kockel (19).	Coolidge (7).	L., G., & D.	Wyman (27).	Ivanow (17).	Drake, Pierce, & Dow (9).
0° ...	1·344	1·216	...	1·228	1·247	1·275
10 ...	1·377	1·284	1·306	1·284	1·286	1·308
20 ...	1·408	1·354	1·352	1·343	1·336	1·339
25 ...	1·423	1·390	1·376	1·371	1·354	1·355
30 ...	1·438	1·425	1·398	1·398	1·371	1·370
40 ...	1·467	1·498	1·445	1·456	1·420	1·400
50 ...	1.493	...	1·491	1·509	1·452	1·428
60 ...	1·521	...	1·537	1·559	1·482	1·456
70 ...	1·546	...	1·583	1·611	1·527	
80 ...	1·570	...	1·629	1·657	1·552	
90 ...	1·593	...	...	1·702	1·595	
100 ...	1·615	...	...	1·737		

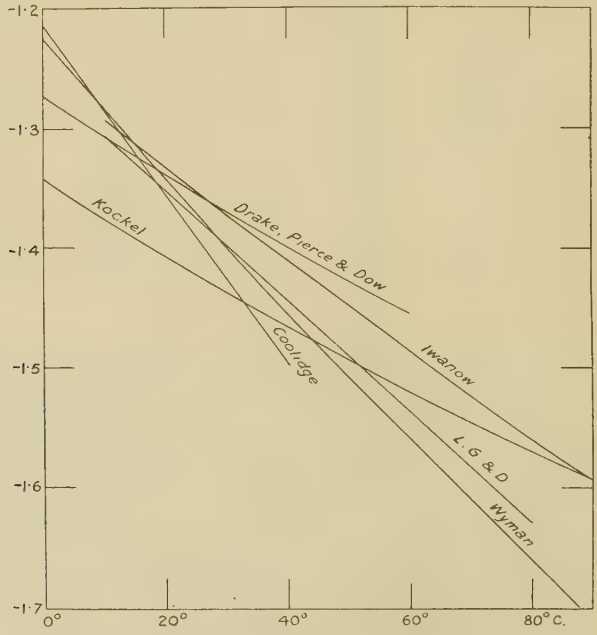

References.

(1) Abegg, *Wied. Ann.* lx. p. 54 (1897).
(2) Alimova (see *Ann. d. Phys* ii. p. 535 (1929).
(3) Astin, Phys. Rev. xxxiv. p. 300 (1929).
(4) Bjerrum, *Zeit. phys. Chem.* cix. p. 145 (1926). See also Gatty, Phil. Mag. xi. p. 1082 (1930).

(5) Cohn and Zeeman, *Wied. Ann.* lvii. p. 15 (1896).
(6) Cole, *Wied. Ann.* lvii. p. 290 (1896).
(7) Coolidge, *Wied. Ann.* lxix. p. 125 (1899).
(8) Devoto. *Gazetta*, lx. p. 208 (1930).
(9) Drake, Pierce, and Dow, Phys. Rev. xxxv. p. 613 (1930).
(10) Drude, *Wied. Ann.* lix. p. 17 (1896).
(11) Errera, *Journ. de Phys.* v. p. 304 (1924).
(12) Franke, *Wied. Ann.* l. p. 163 (1893).
(13) Fürth *Phys. Zeit.* xxv. p. 676 (1924).
(14) Harrington, Phys. Rev. viii. p. 581 (1916).
(15) Hartshorn and Oliver, Proc. Roy. Soc. cxxiii. p. 664 (1929).
(16) Heerwagen, *Wied. Ann.* xlviii. p. 35 (1893); xlix. p. 272 (1893).
(17) Ivanow, *Ann. d. Phys.* lxv. p. 481 (1921.
(18) Kniekamp, *Zeit. f. Phys.* li. p. 95 (1928).
(19) Kockel, *Ann. d. Phys.* lxxxvii. p. 417 (1925).
(20) Lange and Robinson, Journ. Amer. Chem. Soc. lii. p. 2811 (1930).
(21) Lattey and Gatty, Phil. Mag. vii. p. 985 (1929).
(22) Novosilzew, *Ann. d. Phys.* ii. p. 515 (1929).
(23) Palmer, Phys. Rev. xvi. p. 267 (1903).
(24) Ratz, *Zeit. phys. Chem.* xix. p. 94 (1896).
(25) Sack, *Phys. Zeit.* xxvii. p. 206 (1926); xxviii. p. 199 (1927).
(26) Turner, *Zeit. phys. Chem.* xxxv. p. 385 (1900).
(27) Wyman, Phys. Rev. xxxv. p. 623 (1930).

Electrical Laboratory,
Oxford.

XCVIII. *On Curve-Fitting by means of Least Squares.* By W. R. Cook, *M.Sc.**

DR. DEMING † has recently given an account of the application of the method of Least Squares to the problem of curve-fitting when errors arise in more than one variable. The same method, in two variables, was formulated and used in the Research Department, Woolwich, and it became necessary to investigate the errors which are likely to arise in the parameters of the equation connecting the variables. The results, which are set out below, are similar to those ordinarily used when the error is in one variable only. For the problem in hand, the probable error of observations of one variable was known, while that of observations of the other variable could only be estimated roughly. The question arose as to whether the original observations would yield any indication of the relative weights to be attached to the two variables. A relation was found which allows a test to be made of the correctness of the assumed weights, pro-

* Communicated by Prof. H. R. Hassé, M.A., D.Sc.
† Deming, Phil. Mag. vol. ii. no. 68, p. 146 (Jan. 1931).

vided the data are extensive or the observations can be repeated a number of times—a condition which was fulfilled in the actual case.

Derivation of the "Normal" Equations.

These (for two variables) will be given briefly, since the resulting relations are used. The general case is dealt with by Deming.

Observations are made of two variables y, x, with the result

$$y_1, y_2, \dots y_n,$$

$$x_1 x_2, \dots x_n.$$

The y's are assumed to have the same, unknown, precision constant h_1; that of all the x's is the unknown h_2. Let the true values of the quantities y_i, x_i, be ξ_i, η_i $(i=1, 2, \dots n)$, and suppose the equation connecting them to be

$$f(\xi_i, \eta_i, a, b, c, \dots) = 0. \quad . \quad . \quad . \quad . \quad (1)$$

There will be n such equations involving m parameters $a, b, c, \dots$. If the errors of observation follow the normal law, the *à posteriori* probability that the true values ξ_i, η_i lie between ξ_i, η_i and $\xi_i+d\xi_i$, $\eta_i+d\eta_i$, $(i=1, 2, \dots n)$, respectively, will be

$$\frac{h_1^n h_2^n}{\pi^n} \exp\left[-h_1^2 \sum_1^n (\xi_i-y_i)^2 - h_2^2 \sum_1^n (\eta_i-x_i)^2\right] \times d\xi_1 d\xi_2 \dots d\xi_n d\eta_1 d\eta_2 \dots d\eta_n \Big/ \int_{-\infty}^{+\infty} \dots \int_{-\infty}^{+\infty} \frac{h_1^n h_2^n}{\pi^n} \exp\left[-h_1^2 \sum_1^n (\xi_i-y_i)^2 - h_2^2 \sum_1^n (\eta_i-x_i)^2\right] \times d\xi_1 d\xi_2 \dots d\xi_n d\eta_1 d\eta_2 \dots d\eta_n, \quad (2)$$

provided that, *à priori*, all values of ξ_i, η_i, are equally likely. The most probable values of ξ_i, η_i make (2) a maximum.

If equation (1) is not linear in $\xi_i, \eta_i, a, b, c, \dots$, we may determine, by some means, approximate values Y_i, X_i, A, B, C, ... Writing

$$\xi_i = Y_i + \delta y_i \; ; \quad \eta_i = X_i + \delta x_i,$$

$$a = A + \delta a \; ; \quad b = B + \delta b, \text{ etc.},$$

$$f(Y_i, X_i, A, B, C, \dots) \equiv f_i \quad (i=1, 2 \dots n),$$

we have n equations of the type

$$f_i + f_{Y_i}' \delta y_i + f_{X_i}' \delta x_i + f_{A_i}' \delta a + f_{B_i}' \delta b + \dots = 0. \quad . \quad (3)$$

If Δy_i, Δx_i, Δa, Δb, ..., are the most probable values of δy_i, δx_i, δa, δb, ..., we have to make

$$h_1^2 \sum_1^n (Y_i - y_i + \Delta y_i)^2 + h_2^2 \sum_1^n (X_i - x_i + \Delta x_i)^2 \quad . \quad . \quad (4)$$

a minimum, subject to the n equations,

$$f_i + f'_{Y_i} \Delta y_i + f'_{X_i} \Delta x_i + f'_{A_i} \Delta a_i + f'_{B_i} \Delta b + \ldots = 0. \quad . \quad (5)$$

Using Lagrangian multipliers $\lambda_1, \lambda_2, \ldots \lambda_n$, the result of making (4) a minimum is

$$\sum_1^n \lambda_i f'_{A_i} = \sum_1^n \lambda_i f'_{B_i} = \sum_1^n \lambda_i f'_{C_i} = \ldots = 0, \quad . \quad . \quad (6)$$

$$h_1^2 (Y_i - y_i + \Delta y_i) + \lambda_i f'_{Y_i} = 0, \quad . \quad . \quad . \quad . \quad . \quad (7)$$

$$h_2^2 (X_i - x_i + \Delta x_i) + \lambda_i f'_{X_i} = 0 \quad (i = 1, 2, \ldots n). \quad (8)$$

Combining equations (7) and (8),

$$\lambda_i \left(\frac{f'^2_{Y_i}}{h_1^2} + \frac{f'^2_{X_i}}{h_2^2} \right) + (Y_i - y_i) f'_{Y_i} + (X_i - x_i) f'_{X_i} + f'_{Y_i} \Delta y_i + f'_{X_i} \Delta x_i = 0.$$

Substituting from (5) and writing

$$\gamma_i^{-1} = f'^2_{Y_i} + \frac{h_2^2}{h_1^2} f'^2_{X_i},$$

$$-\lambda_i = \gamma_i h_1^2 \{ f'_{A_i} \Delta a + f'_{B_i} \Delta b \ldots + f_i + (Y_i - y_i) f'_{Y_i} + (X_i - x_i) f'_{X_i} \}.$$

. . . (9)

Using these values of λ_i in (6), dividing throughout by h_1^2, and abbreviating by means of

$$a_{11} = \sum_1^n \gamma_i f'^2_{A_i}, \qquad a_{12} = \sum_1^n \gamma_i f'_{A_i} f'_{B_i} = a_{21},$$

$$a_{22} = \sum_1^n \gamma_i f'^2_{B_i}, \quad \text{etc.},$$

we obtain the symmetrical "normal" equations :—

$$a_{11} \Delta a + a_{12} \Delta b + a_{13} \Delta c + \ldots = -\sum_1^n \gamma_i \{ (Y_i - y_i) f'_{Y_i} + (X_i - x_i) f'_{X_i} + f_i \} f'_{A_i},$$

$$a_{21} \Delta a + a_{22} \Delta b + a_{23} \Delta c + \ldots = -\sum_1^n \gamma_i \{ (Y_i - y_i) f'_{Y_i} + (X_i - x_i) f'_{X_i} + f_i \} f'_{B_i},$$

$$a_{31} \Delta a + a_{32} \Delta b + a_{33} \Delta c + \ldots = -\sum_1^n \gamma_i \{ (Y_i - y_i) f'_{Y_i} + (X_i - x_i) f'_{X_i} + f_i \} f'_{C_i}, \text{ etc.}$$

These equations determine the most probable values Δa, Δb, Δc, ... They simplify when the observed values are taken as the first approximations, for, in this case, the bracket on the right reduces to f_i. The values of Δa, Δb, ... are then used to find λ_i and hence, to find the most probable corrections Δy_i, Δx_i, to the approximations, by means of equations (7) and (8). If necessary, we may then proceed to a second approximation, using

$$Y_i' = Y_i + \Delta y_i, \quad X_i' = X_i + \Delta x_i, \quad A' = A + \Delta a, \quad \text{etc.}$$

It will be seen that it is only the ratio of h_1 to h_2, entering the equations by means of γ_i, which is used to determine Δa, Δb, ... Δy_i, Δx_i, and some estimate of this ratio is necessary to effect a solution of the "normal" equations. In the case where f represents a straight line, γ_i is a constant and disappears from the above equations. The solution must then be carried to a second approximation.

Consideration of Errors.

Transformations.

The method followed is essentially that used by Burnside *. Using equations (7) and (8), we may write

$$\begin{aligned}\phi &= h_1^2 \sum_1^n (\xi_i - y_i)^2 + h_2^2 \sum_1^n (\eta_i - x_i)^2 \\ &= h_1^2 \sum_1^n (\delta y_i - \Delta y_i)^2 + h_2^2 \sum_1^n (\delta x_i - \Delta x_i)^2 + \sum_1^n \lambda_i^2 \frac{f'^2_{Y_i}}{h_1^2} + \sum_1^n \lambda_i^2 \frac{f'^2_{X_i}}{h_2^2} \\ &\qquad - 2 \sum_1^n \lambda_i \{ f'_{Y_i} (\delta y_i - \Delta y_i) + f'_{X_i} (\delta x_i - \Delta x_i) \}.\end{aligned}$$

It is seen that, by means of (3) and (5),

$$\begin{aligned}&\sum_1^n \lambda_i \{ f'_{Y_i} (\delta y_i - \Delta y_i) + f'_{X_i} (\delta x_i - \Delta x_i) \} \\ &\qquad = -(\delta a - \Delta a) \sum_1^n \lambda_i f'_{A_i} - (\delta b - \Delta b) \sum_1^n \lambda_i f'_{B_i} - \dots,\end{aligned}$$

and is therefore zero, by equations (6).

Hence, writing

$$\delta y_i - \Delta y_i = \Delta' y_i ; \quad \delta x_i - \Delta x_i = \Delta' x_i ; \quad \delta a - \Delta a = \Delta' a, \text{ etc.},$$

we have

$$\phi = h_1^2 \sum_1^n \Delta' y_i^2 + h_2^2 \sum_1^n \Delta' x_i^2 + \sum_1^n \lambda_i^2 \frac{f'^2_{Y_i}}{h_1^2} + \sum_1^n \lambda_i^2 \frac{f'^2_{X_i}}{h_2^2}. \qquad (10)$$

* Burnside, 'Theory of Probability.'

The probability of getting observations y_i, x_i, lying between y_i, x_i, and $y_i + dy_i, x_i + dx_i$ $(i = 1, 2, \ldots n)$, is

$$\delta p = \frac{{h_1}^n {h_2}^n}{\pi^n} e^{-\Phi} dy_1 dy_2 \ldots dy_n dx_1 dx_2 \ldots dx_n. \quad (11)$$

We may express $y_1, y_2, \ldots y_n, x_1, x_2 \ldots x_n$, in terms of $\Delta' a$, $\Delta' b$, $\Delta' x_i$, $\Delta' y_i$, λ_i, $(i = 1, 2, \ldots n)$ by a linear transformation by means of equations (3), (7), (8), and the "normal" equations.

Further, the n variables $\Delta' y_i$ can be expressed in terms of $\Delta' x_i$, $\Delta' a$, $\Delta' b$, etc., by means of equations (3) and (5),

$$-\Delta' y_i = \frac{1}{f'_{Y_i}} \{ f'_{X_i} \Delta' x_i + f'_{A_i} \Delta' a + f'_{B_i} \Delta' b + \ldots \}. \quad (12)$$

The n λ's are connected by means of m equations (6). Finally, then, we may transform the $2n$ variables y_i, x_i $(i = 1, 2, \ldots n)$ to m quantities $\Delta a, \Delta b, \ldots$, n quantities $\Delta' x_i$ $(i = 1, 2, \ldots n)$, and $n - m$ independent variables obtained from n λ's and the equations (6). Choice of the latter variables leads to two cases of interest.

(A) We may choose $n - m$ quantities θ_j, such that

$$\sum_1^n \lambda_i^2 \frac{f'^2_{Y_i}}{{h_1}^2} + \sum_1^n \lambda_i^2 \frac{f'^2_{X_i}}{{h_2}^2} = \frac{1}{{h_1}^2} \sum_1^n \frac{\lambda_i^2}{\gamma_i} = \sum_1^{n-m} {h_1}^2 \theta_j^2.$$

(B) We may choose $n - m$ quantities ζ_j, such that

$$\sum_1^n \lambda_i^2 \frac{f'^2_{Y_i}}{{h_1}^2} = {h_1}^2 \sum_1^{n-m} \zeta_j^2,$$

and, at the same time,

$$\sum_1^n \lambda_i^2 \frac{f'^2_{X_i}}{{h_2}^2} = {h_1}^2 \sum_1^{n-m} (k_j - 1) \zeta_j^2,$$

the k's being constants.

Probable error of Δa, *etc.*

Dealing with case (A), the transformation

$$y_i, x_i \longrightarrow \Delta' a, \Delta' b, \ldots, \Delta' x_i, \theta_i,$$

being linear, the expression (11) for the probability δp becomes

$$\delta p = J \frac{{h_1}^n {h_2}^n}{\pi^n} \exp \Big[-{h_1}^2 \sum_1^{n-m} \theta_j^2 - {h_2}^2 \sum_1^n \Delta' x_i^2 - {h_1}^2 \sum_1^n \frac{1}{f'^2_{Y_i}} \{ f'_{X_i} \Delta' x_i + f'_{A_i} \Delta' a + \ldots \}^2 \Big] \ldots d(\Delta' x_i) d(\Delta' a) d(\Delta' b) \ldots d\theta_i \ldots$$

where J is the constant Jacobian of the transformation. δp expresses the probability that $\Delta' x_i$ lies between $\Delta' x_i$ and $\Delta' x_i + d(\Delta' x_i)$, $\Delta' a$ lies between $\Delta' a$ and $\Delta' a + d(\Delta' a)$, etc., θ_j lies between θ_j and $\theta + d\theta_j$, $(i=1, 2, \ldots n)$, $(j=1, 2, \ldots n-m)$. Since

$$\int_{-\infty}^{+\infty} \exp\Big[-h_2{}^2\Delta' x_i{}^2 - h_1{}^2 \frac{1}{f'^2_{Y_i}} \{f'_{X_i}\Delta' x_i + f'_{A_i}\Delta' a + f'_{B_i}\Delta' b + \ldots\}^2\Big] d(\Delta' x_i)$$
$$= k \exp\left[-\gamma_i h_1{}^2 (f'_{A_i}\Delta' a + f'_{B_i}\Delta' b + \ldots)^2\right],$$

k being a constant; then

$$\int_{-\infty}^{+\infty} \cdots \int_{-\infty}^{+\infty} \exp\Big[-h_2{}^2 \sum_1^n \Delta' x_i{}^2 - h_1{}^2 \sum_1^n \frac{1}{f'^2_{Y_i}} \{f'_{X_i}\Delta' x_i + f'_{A_i}\Delta' a + \ldots\}^2\Big] \times d(\Delta' x_1) d(\Delta' x_2) \ldots d(\Delta' x_n)$$
$$= k' \exp\Big[-h_1{}^2 \sum_1^n \gamma_i \{f'_{A_i}\Delta' a + f_{B_i}{}'\Delta' b + \ldots\}^2\Big].$$

Now

$$\int_{-\infty}^{+\infty} \exp\left[-(at+b)^2 - d\right] dt = \frac{\sqrt{\pi}}{a} \exp\left[-d\right],$$

and is proportional to e raised to a power obtained by making a maximum, with respect to t, the original value of the power of e in the integrand. This may be used to find

$$\int_{-\infty}^{+\infty} \cdots \int_{-\infty}^{+\infty} \exp\Big[-h_1{}^2 \sum_1^n \gamma_i \{f'_{A_i}\Delta' a + f'_{B_i}\Delta' b + \ldots\}^2\Big] \times d(\Delta' b) d(\Delta' c). \quad . \quad . \quad . \quad (13)$$

Making

$$f = h_1{}^2 \sum_1^n \gamma_i \{f'_{A_i}\Delta' a + f'_{B_i}\Delta' b + \ldots\}^2$$

a maximum with respect to $\Delta' b$, $\Delta' c$, etc., we obtain the equations

$$\left.\begin{aligned} \sum_1^n \gamma_i f'_{B_i} \{f'_{A_i}\Delta' a + f'_{B_i}\Delta' b + f'_{C_i}\Delta' c + \ldots\} = 0, \\ \sum_1^n \gamma_i f'_{C_i} \{f'_{A_i}\Delta' a + f'_{B_i}\Delta' b + f'_{C_i}\Delta' c + \ldots\} = 0, \\ \text{etc.} \end{aligned}\right\} \quad . \quad (14)$$

Since f is homogeneous in $\Delta'a$, $\Delta'b$, etc., and

$$\frac{\partial f}{\partial(\Delta'b)} = \frac{\partial f}{\partial(\Delta'c)} = \ldots = 0,$$

$$f_{\max.} = h_1^2 \Delta'a \sum_1^n \gamma_i f'_{A_i} \{f'_{A_i} \Delta'a + f'_{B_i} \Delta'b + \ldots\}. \quad . \quad (15)$$

The value of $\Delta'a$ resulting from equations (14) and (15) is, clearly,

$$\Delta'a = \frac{A_{11}}{D} \cdot \frac{f_{\max.}}{h_1^2 \Delta'a},$$

where A_{11} is the minor of a_{11} in the determinant of the a's, formed from the "normal" equations, and D is the value of the determinant. Hence

$$f_{\max.} = h_1^2 \frac{D}{A_{11}} \Delta'a^2$$

and the value of the expression (13) is proportional to

$$\exp\left[-h_1^2 \frac{D}{A_{11}} \Delta'a^2\right].$$

The value of

$$\int \ldots \int \exp\left[-h_1^2 \sum_1^{n-m} \theta^2\right] d\theta_1 d\theta_2 \ldots d\theta_{n-m},$$

where the integral is taken over the domain, for which

$$\alpha^2 \leq \sum_1^{n-m} \theta_j^2 \leq (\alpha + d\alpha)^2,$$

is proportional to

$$\exp\left[-h_1^2 \alpha^2\right] \alpha^{n-m-1} d\alpha.$$

Hence the probability that α lies between α and $\alpha + d\alpha$, and, simultaneously, that $\Delta'a$ lies between $\Delta'a$ and $\Delta'a + d(\Delta'a)$ is proportional to

$$\exp\left[-h_1^2 \frac{D}{A_{11}} \Delta'a^2 - h_1^2 \alpha^2\right] . \alpha^{n-m-1} d\alpha\, d(\Delta'a).$$

Integrating this expression with respect to α, over the range from 0 to $+\infty$, will leave us with the distribution of $\Delta'a$ given in terms of the unknown h_1. This may be avoided by transforming to new variables s, t, such that

$$\sqrt{\frac{D}{A_{11}}} . \Delta'a = t \; ; \quad h_1 \alpha = s,$$

where

$$\frac{\partial(\alpha, \Delta'a)}{\partial(s, t)} = \sqrt{\frac{A_{11}}{D}} \cdot \frac{s}{h_1^2}.$$

The probability that t lies between t and $t+dt$, while s lies between s and $s+ds$, is then proportional to

$$s^{n-m}\exp\left[-s^2(1+t^2)\right]ds\,dt.$$

Hence the probability that s lies between s and $s+ds$ is proportional to

$$s^{n-m-1}\exp\left[-s^2\right]ds,$$

and the probability that t lies between t and $t+dt$ is proportional to

$$\frac{dt}{(1+t^2)^{\frac{n-m+1}{2}}}.$$

Since

$$s = h_1\alpha = h_1\left[\sum_1^{n-m}\theta_j^2\right]^{1/2}$$

$$= \sqrt{h_1^2\sum_1^n(\mathrm{Y}_i-y_i+\Delta y_i)^2+h_2^2\sum_1^n(\mathrm{X}_i-x_i+\Delta x_i)^2}$$

and

$$st = h_1\sqrt{\frac{\mathrm{D}}{\mathrm{A}_{11}}}(\delta a-\Delta a)$$

$$= h_1\sqrt{\frac{\mathrm{D}}{\mathrm{A}_{11}}}\text{ (true value—most probable value) of }\delta a,$$

we may conclude, finally, that

(1) the probability that

$$h_1\sqrt{\sum_1^n(\mathrm{Y}_i-y_i+\Delta y_i)^2+\frac{h_2^2}{h_1^2}\sum_1^n(\mathrm{X}_i-x_i+\Delta x_i)^2}$$

lies between s_1 and s_2 is

$$\frac{\int_{s_1}^{s_2}s^{n-m-1}\exp\left[-s^2\right]ds}{\int_0^{\infty}s^{n-m-1}\exp\left[-s^2\right]ds}, \qquad \ldots \quad (16)$$

and (2) the probability that

$$\frac{\sqrt{\frac{\mathrm{D}}{\mathrm{A}_{11}}}(\delta a-\Delta a)}{\sqrt{\sum_1^n(\mathrm{Y}_i-y_i+\Delta y_i)^2+\frac{h_2^2}{h_1^2}\sum_1^n(\mathrm{X}_i-x_i+\Delta x_i)^2}}$$

lies between $\pm t$ is

$$\frac{\int_{-t}^{+t} \frac{dt}{(1+t^2)^{\frac{n-m+1}{2}}}}{\int_{-\infty}^{+\infty} \frac{dt}{(1+t^2)^{\frac{n-m+1}{2}}}} \quad . \quad . \quad . \quad . \quad (17)$$

The probable value of

$$h_1^2 \sum_1^n (Y_i - y_i + \Delta y_i)^2 + h_2^2 \sum_1^n (X_i - x_i + \Delta x_i)^2,$$

defined by

$$\frac{\int_0^\infty s^2 (s^{n-m-1} \exp[-s^2])\, ds}{\int_0^\infty s^{n-m-1} \exp[-s^2]\, ds},$$

is

$$\frac{\Gamma\left(\frac{n-m+2}{2}\right)}{\Gamma\left(\frac{n-m}{2}\right)} = \frac{n-m}{2}, \quad . \quad . \quad . \quad . \quad (18)$$

while the most probable value of s, defined by

$$\frac{\partial}{\partial s}(\delta p) = 0,$$

is given by

$$2s^{n-m} - (n-m-1)s^{n-m-2} = 0,$$

$$s^2 = \frac{n-m-1}{2}. \quad . \quad . \quad . \quad . \quad . \quad (19)$$

If s lies between

$$\sqrt{\frac{n-m}{2}} \quad \text{and} \quad \sqrt{\frac{n-m}{2}} + ds$$

with a probability $\frac{1}{2}$, so that ds measures the zone within which s is as likely to fall as not, and if ds is small, we have, approximately,

$$\left(\frac{n-m}{2}\right)^{\frac{n-m-1}{2}} \exp\left[-\frac{n-m}{2}\right] ds = \frac{1}{2}\int_0^\infty s^{n-m-1} \exp[-s^2]\, ds.$$

Hence

$$ds = \frac{\Gamma\left(\frac{n-m}{2}\right) e^{\frac{n-m}{2}}\, 2^{\frac{n-m-1}{2}}}{4(n-m)^{\frac{n-m-1}{2}}}.$$

Similarly, if the value found, Δa, is as likely as not to differ from the true value δa by an amount t, then t is given by the equation

$$t = \sqrt{\frac{A_{11}}{D}} \sqrt{\sum_1^n (Y_i - y + \Delta y_i)^2 + \frac{h_2^2}{h_1^2} \sum_1^n (X_i - x_i + \Delta x_i)^2} \cdot \gamma,$$

where γ is given by

$$\int_{-\gamma}^{+\gamma} \frac{dt}{(1+t^2)^{\frac{n-m+1}{2}}} = \frac{1}{2} \int_{-\infty}^{+\infty} \frac{dt}{(1+t^2)^{\frac{n-m+1}{2}}}.$$

The usual theory gives (18) as the value of

$$h_1^2 \sum_1^n (Y_i - y_i + \Delta y_i)^2,$$

if the errors of observation are confined wholly to the y's, while the probability for $\Delta' a$ is translated to mean that the weight of Δa is D/A_{11}. The expressions (17) and (18) reduce to those of Burnside * for the special case of n observations of a quantity whose true value is y. In this case there is just one parameter to be dealt with, so that $m = 1$.

Probable value of $h_1^2 : h_2^2$.

Returning to the transformation (B), the probability that $\sum_1^{n-m} \zeta_j^2$ lies between β^2 and $(\beta + d\beta)^2$ is proportional to

$$\int \dots \int \exp\left[- \sum_1^{n-m} k_j \zeta_j^2 \right] d\zeta_1 d\zeta_2 \dots d\zeta_{n-m},$$

the integral being taken over the domain

$$\beta^2 \leq \sum_1^{n-m} \zeta_j^2 \leq (\beta + d\beta)^2. \quad . \quad . \quad . \quad (20)$$

The probable value of β^2 is defined by

$$\frac{\int_0^\infty \beta^2 d\beta \int \dots \int \exp\left[- \sum_1^{n-m} k_j^2 \zeta_j^2 \right] d\zeta_1 d\zeta_2 \dots d\zeta_{n-m}}{\int_0^\infty d\beta \int \dots \int \exp\left[- \sum_1^{n-m} k_j^2 \zeta_j^2 \right] d\zeta_1 d\zeta_2 \dots d\zeta_{n-m}},$$

* Burnside, *loc. cit.*

the inner integrals being taken over the domain (20), and may be written

$$\frac{\int_0^\infty \dots \int_0^\infty \sum_1^{n-m} \zeta_j^2 \exp\left[-\sum_1^{n-m} k_j^2 \zeta_j^2\right] d\zeta_1 d\zeta_2 \dots d\zeta_{n-m}}{\int_0^\infty \dots \int_0^\infty \exp\left[-\sum_1^{n-m} k_j^2 \zeta_j^2\right] d\zeta_1 d\zeta_2 \dots d\zeta_{n-m}}.$$

But

$$\int_0^\infty z^2 \exp\left[-kz^2\right] dz = \frac{1}{2k} \int_0^\infty \exp\left[-kz^2\right] dx,$$

and hence the probable value of β^2 is

$$\sum_1^{n-m} \frac{1}{2k}.$$

From the transformation

$$\sum_1^n \lambda_i^2 \frac{f'^2_{Y_i}}{h_1^2} \rightarrow \sum_1^{n-m} \zeta_i^2 \; ; \quad \Sigma \lambda_i^2 \frac{f'^2_{X_i}}{h_2^2} \rightarrow \sum_1^{n-m} (k_i - 1)\zeta_i^2,$$

the k's are given * as the roots of the discriminant of

$$(1-k) \sum_1^n \lambda_i^2 \frac{f'^2_{Y_i}}{h_1^2} + \sum_1^n \lambda_i^2 \frac{f'^2_{X_i}}{h_2^2},$$

i. e., of

$$\sum_1^n \frac{\lambda_i^2}{\gamma} - k \sum_1^n \lambda_i^2 f'^2_{Y_i}.$$

Making use of the relations between the λ's, expressed by equations (6), the equation for k may be written as the following determinant equated to zero :—

$$\begin{vmatrix}
\gamma_1^{-1} - k f'^2_{Y_1}, & 0, & 0, \dots & 0, & f'_{A_1}, & f'_{B_1}, & f'_{C_1}, \dots \\
0, & \gamma_2^{-1} - k f'^2_{Y_2}, & 0, \dots & 0, & f'_{A_2}, & f'_{B_2}, & f'_{C_2}, \dots \\
\dots & \dots & \dots & \dots & \dots & \dots & \dots \\
0, & 0, & 0, \dots & \gamma_n^{-1} - k f'^2_{Y_n}, & f'_{An}, & f'_{Bn}, & f'_{Cn}, \dots \\
f'_{A_1}, & f'_{A_2}, & f'_{A_3}, \dots & f'_{An}, & 0, & 0, & 0, \dots 0 \\
f'_{B_1}, & f'_{B_2}, & f'_{B_3}, \dots & f_{Bn}, & 0, & 0, & 0, \dots 0 \\
\dots & \dots & \dots & \dots & \dots & \dots & \dots
\end{vmatrix}$$

* Burnside and Panton, 'Theory of Equations.'

This may be reduced to

$$\left|\begin{matrix} \sum_1^n \frac{f'^2_{A_i}}{\gamma_i^{-1}-kf'^2_{Y_i}}, & \sum_1^n \frac{f'_{A_i}f'_{B_i}}{\gamma_i^{-1}-kf'^2_{Y_i}}, & \sum_1^n \frac{f'_{A_i}f'_{C_i}}{\gamma_i^{-1}-kf'^2_{Y_i}}, & \dots, & \dots, & \dots \\ \sum_1^n \frac{f'_{B_i}f'_{A}}{\gamma_i^{-1}-kf'^2_{Y_i}}, & \sum_1^n \frac{f'^2_{B_i}}{\gamma_i^{-1}-kf'^2_{Y_i}}, & \dots & , \dots, & \dots, & \dots \\ \sum_1^n \frac{f'_{C_i}f'_{A_i}}{\gamma_i^{-1}-kf'^2_{Y_i}}, & \dots, & \dots & , \dots, & \dots, & \dots \\ \cdot & \cdot & \cdot & \cdot & \cdot & \cdot \\ \cdot & \cdot & \cdot & \cdot & \cdot & \cdot \end{matrix}\right| \quad (21)$$

$$\times$$

$$(\gamma_1^{-1}-kf'^2_{Y_1})(\gamma_2^{-1}-kf'^2_{Y_2}) \dots (\gamma_n^{-1}-kf'^2_{Y_n}) = 0.$$

Putting $k=0$, the absolute term is $D\{\gamma_1\gamma_2\dots\gamma_n\}^{-1}$; differentiating the expression (21), with respect to k, and, afterwards, putting $k=0$, the coefficient of k in (21) is

$$D[\gamma_1\gamma_2\dots\gamma_n]^{-1}\left\{-\sum_1^n \gamma_1 f'^2_{Y_i} + \frac{A_{11}}{D}\sum_1^n \gamma_i^2 f'^2_{Y_i} f'^2_{A_i} \right.$$
$$\left. + 2\cdot\frac{A_{12}}{D}\sum_1^n \gamma_i^2 f'^2_{Y_i} f'_{A_i} f'_{B_i} + \frac{A_{22}}{D}\sum_1^n \gamma_i^2 f'^2_{Y_i} f'^2_{B_i} + \dots\right\}.$$

Hence the probable value of β^2, *i.e.*, of $h_1^2\sum_1^n(Y_i - y_i + \Delta y_i)^2$ is

$$\frac{1}{2}\left\{\sum_1^n \gamma_i f'^2_{Y_i} - \frac{A_{11}}{D}\sum_1^n \gamma_i^2 f'^2_{Y_i} f'^2_{A_i} - 2\frac{A_{12}}{D}\sum_1^n \gamma_i^2 f'^2_{Y_i} f'_{A_i} f'_{B_i} - \dots\right\}.$$

If the observations are repeated a number of times under the same conditions we should expect h_1^2/h_2^2 to approximate to

$$\frac{\sum_1^n(X_i - x_i + \Delta x_i)^2}{\sum_1^n(Y_i - y_i + \Delta y_i)^2} \times \frac{\left\{\sum\gamma_i f'^2_{Y_i} - \frac{A_{11}}{D}\sum\gamma_i^2 f'^2_{Y_i} f'^2_{A_i} - \dots\right\}}{\left\{\sum\gamma_i f'^2_{X_i} - \frac{A_{11}}{D}\sum\gamma_i^2 f'^2_{X_i} f'^2_{A_i} - \dots\right\}\frac{h_1^2}{h_2^2}}. \quad . \quad . \quad . \quad (22)$$

Writing $H_1^2 : H_2^2$ for the probable value of the ratio, we have the probable value given in terms of the true value $h_1^2 : h_2^2$, by

$$\frac{H_1^2}{H_2^2} = \left(\frac{n-m}{\frac{h_1^2}{h_2^2}\left\{\sum\gamma_i f'^2_{X_i} - \frac{A_{11}}{D}\sum_n \gamma_i^2 f'^2_{X_i} f'^2_{A_i} - \dots\right\}} - 1\right)$$
$$\times \frac{\sum(X_i - x_i + \Delta x_i)^2}{\sum(Y_i - y_i + \Delta y_i)^2}. \quad (23)$$

We may, therefore, use this relation, by substituting the assumed value of $h_1^2 : h_2^2$ for its true value, in expression (23), and comparing the value of $H_1^2 : H_2^2$ with the assumed value of $h_1^2 : h_2^2$. From a theoretical standpoint, an infinite number of observations will be required to determine the true value of $h_1^2 : h_2^2$ from this relation, but, practically, if the ratio of factors, such as

$$\Sigma\gamma_i^2 f'^2_{X_i} f'^2_{A_i}, \quad \Sigma\gamma_i f'^2_{A_i}, \quad \text{etc.},$$

varies slowly with the value of $h_1^2 : h_2^2$, as is often the case, it will be possible to determine $h_1^2 : h_2^2$ within sufficiently narrow limits from a reasonable amount of data.

Numerical Example.

An illustration of the use of the above relation was constructed in the following way. The curve

$$p(v-b) = a,$$

with $b = \cdot 98$, $a = 9 \cdot 8$, was plotted, the scale of v being twice that of p. Over a selected point on the curve, a pencil was held and then released; the mark made by the pencil was taken as an "observed" point.

It seemed advisable to test whether the errors, involved in such a procedure, follow the Gaussian law. To this end, 121 attempts were made to drop the pencil on a definite mark. The target, analysed by dividing it into equal strips, symmetrical about the bull, and counting the number of hits per strip, gave the following result:—

TABLE I.

Range for X.	No. of hits.	Range for Y.	No. of hits.	Theoretical distribution.
−·25−−·35	2	−·25−−·35	1	1
−·15−−·25	5	−·15−−·25	9	8
−·05−−·15	30	−·05−−·15	28	29
+·05−−·05	45	+·05−−·05	47	46
+·05−+·15	29	+·05−+·15	26	29
+·15−+·25	10	+·15−+·25	6	8
+·25−+·35	0	+·25−+·35	4	1
Totals.....	121		121	122

The distribution is reasonably symmetrical. We may determine the precision index from the number of hits between $-\cdot05$ and $+\cdot05$, by means of

$$\frac{2}{\sqrt{\pi}}\int_0^{\cdot05\,h} e^{-x^2}\,dx = \frac{46}{121},$$

whence $h=\cdot7$.

The theoretical distribution with this value of h is shown in column 5 of the above table. The general agreement with the observed distribution shows that, without serious error, we may take the normal law to apply to the attempts to hit the curve

$$p(v-\cdot98) = 9\cdot8.$$

With the scale ratio 1 : 2, we should expect the value of $h_p^2 : h_v^2$ to be 1 : 4.

Since, with a small number of observations, a single large error might, of itself, determine the order of the ratio

$$\Sigma(\Delta p)^2 : \Sigma(\Delta v)^2,$$

and yield a false result, thirty points were taken.

TABLE II.

p.	v.	p.	v.	p.	v.
5·19	2·86	3·25	4·06	2·15	5·43
4·76	3·01	3·25	4·14	2·03	6·01
4·70	3·10	3·22	3·95	1·89	5·78
4·32	3·22	3·00	4·25	1·89	6·18
3·99	3·37	2·86	4·58	1·81	6·60
3·95	3·40	2·65	4·73	1·75	6·87
3·75	3·58	2·51	4·80	1·50	7·30
3·67	3·63	2·46	4·92	1·49	7·47
3·66	3·74	2·30	5·37	1·41	7·72
3·62	3·83	2·25	5·17	1·32	8·00

The approximations $b=1\cdot05$, $a=9\cdot39$, were obtained by passing the curve through the points ($p=5\cdot19$, $v=2\cdot85$), and ($p=1\cdot41$, $v=7\cdot72$), and the first approximations to the true values of p, v were taken as the observed values.

The ratio $h_p^2 : h_v^2$ was assumed to be unknown. The normal equations were solved for the three values 1, $\frac{1}{4}$, $\frac{1}{9}$,

of this ratio. The resulting values of Δa, Δb, and the ratios $H_p^2 : H_v^2$, are given in the following table:—

TABLE III.

Assumed value of $h_p^2 : h_v^2$.	Δa.	Δb.	Probable value of $H_p^2 : H_v^2$, $h_p^2 : h_v^2$.	$9{\cdot}39 + \Delta a$.	$1{\cdot}05 + \Delta b$.
1 : 1	·361	−·040	1 : $1{\cdot}4_5$	9·75	1·010
1 : 4	·408	−·066	1 : 4·1	9·80	·984
1 : 9	·433	−·074	1 : 12	9·82	·976

Hence, as far as we can tell from the analysis of 30 points, the ratio $h_p^2 : h_v^2$ is $\frac{1}{4}$. It will be noted that this value of the ratio gives the closest approximation to the curve from which the "observed" points were obtained.

My thanks are due to the Ordnance Committee for their courtesy in granting permission for publication.

XCIX. *A Balance Method of Measuring Sound Transmission.*

By A. E. KNOWLER, *M.Sc., A.Inst.P. (Physics Department, National Physical Laboratory, Teddington, Middlesex)**.

IN a recent paper† a description was given of the measurement of the transmission of sound through a partition by a method which involves the reduction of the sound from loud speakers to threshold intensity. When there is any extraneous noise this is found to be a difficult and trying procedure. Readings are apt to be very inconsistent, so it is necessary to take a large number.

As an improvement, the present method has been evolved in which two sounds are adjusted to equality.

The partition under test separates two reverberant rooms, each of which contains a loud-speaker, and in one of which is situated the observer. The loud-speaker in the observer's room is in series with a variable shunt.

The loud-speakers are switched on alternately. The sound from one is reduced by the partition ; that from the other is reduced by the shunt. The shunt is then adjusted until the two sounds appear equal.

The observer then goes in the other room, the shunt is connected in series with the other loud-speaker, and another balance is made.

* Communicated by Dr. G. W. C. Kaye, O.B.E.

† Knowler, Phil. Mag. pp. 342-44 (August 1930).

The shunt is of such a design that the effect of transferring a plug from the left to the right-hand side of the shunt box is to introduce one resistance in series with the loud-speaker and another one in parallel. The values of these are so chosen that the combined resistance of the loud-speaker and shunt is constant, and that the intensity reductions are $\frac{1}{2}$, 1, 2, 2, 5, 10, 20, 20, 20 decibels. The reduction can thus be varied by $\frac{1}{2}$ decibel steps from $\frac{1}{2}$ to 80 decibels. As it is essential that the load shall be constant, a compensating resistance is included in series with the loud-speaker and is reduced as the frequency rises.

The size of the test partitions was 15 ft. by 9 ft. Each of the rooms measured approximately 16 ft. by 7 ft. by 10 ft. high, and had an absorbing power of about 70 sq. ft. of open window, corresponding to a reverberation period of 0·8 seconds.

Suppose that the partition under test separates two rooms, A and B, and that the observer listens in B.

Let I_A, I_B be the intensity of sound in A and B respectively; Q, Q′ the rate of emission of energy from the loud-speakers in A and B, when adjusted for equality of loudness in the observer's room.

v the velocity of sound in air.

R the reading of the shunt box when the sounds are equalized.

a_A, a_B, the absorbing power of the rooms A and B.

then $$R = 10 \log_{10} Q/Q',$$

or $$Q' = Q10^{-R/10}.$$

Now $$I_A = \frac{4Q}{va_A},$$

and $$I_B = \frac{4Q}{va_B}.$$

Thus the reduction factor of the partition expressed in decibels is given, under the conditions of the test, by :—

$$10 \log_{10} I_A/I_B = 10 \log_{10} (a_B/a_A\, 10^{R/10}) = R + \log_{10} a_B/a_A.$$

If, when the experiment is repeated with the rooms interchanged, so that the observer now listens in room A, the balance reading of the shunt box is R′, the reduction factor is given by

$$R' + \log_{10} a_A/a_B.$$

Eliminating a_A/a_B, the reduction factor of the partition in decibels equals

$$\frac{R+R'}{2}.$$

To avoid stationary-wave effects with consequent variation of loudness from point to point the source of sound used in these experiments was a "warbling tone" record with an electrical pick-up and amplifier. The frequencies were 300 ± 50, 600 ± 50, 1200 ± 50, 2400 ± 50.

Moving-coil loud speakers were used because the relationship between electrical input an acoustic output is known with greater certainty for a moving-coil instrument than for an electromagnetic one.

Since the observer, by moving from room to room, changed the absorbing power of the rooms, a slab of material having equivalent absorbing power was introduced to compensate for his absence.

Measurements were made on the following partitions :—

(1) 7/16 in. fibre board, fixed to 3 in. by $1\frac{1}{2}$ in. studding with studs on 2 ft. centres and struts on 2 ft. 6 in. centres.

(2) Fibre board fixed to both sides of this studding.

(3) Specimen (2) with one of the fibre boards rendered with lime mortar $\frac{1}{2}$ in. thick.

(4) Specimen (2) with both the fibre boards rendered.

(5) A $4\frac{1}{2}$ in. Fletton brick wall set in cement mortar.

Results are shown in fig. 1. The manner in which curves for partitions (1) to (4) tend toward different minima at the lower frequencies suggests that as the mass per unit area increases the resonant frequency of the partition decreases. This is to be expected if the stiffness is reasonably constant.

In fig. 2 the reduction factor of each partition is plotted against the logarithm of the mass per unit area.

Other workers * have shown that if the logarithm of the mass per unit area of single, non-porous, homogeneous partitions be plotted against their reduction factors the points lie near a straight line. The points for some other types of construction do not fall near this straight line. Such an example is found in the results quoted here. The double

* Chrisler and Snyder, 'Bur. of Standards J. of Research,' ii. pp. 541-559 (Jan. 1929).

fibre board (No. 4) which is rendered on both sides has a reduction factor rather greater than that of a $4\frac{1}{2}$ inch brick

Fig. 1.

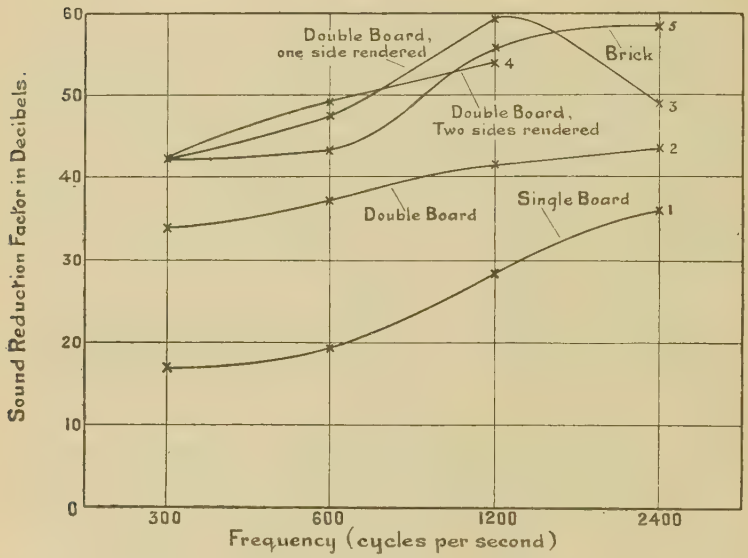

Fig. 2.

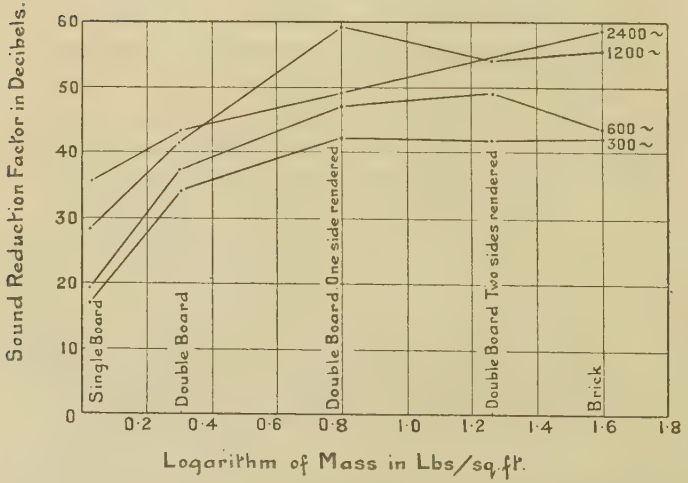

wall, although the former has not much more than half its mass. It is therefore, a good type of construction from the standpoint of sound insulation.

C. *Flame Temperatures.* *By* W. T. David, *Sc.D.*, W. Davies, *B.Sc.*, *and* J. Jordan, *M.Sc.**

THE temperature of an open flame, such as that produced in the bunsen burner, has been measured in various ways by different workers, and the general agreement in the results recently obtained † appears to justify the definition which is usually given to flame temperature as that which a solid, immersed in the flame, will eventually attain, provided that the presence of the solid in any part of the flame does not alter the conditions there. It is usually assumed that if the solid is sufficiently small to cause no sensible cooling of the gas in its neighbourhood the final temperature of the solid will be that of the flame, but the validity of this assumption must depend on whether the flame gases are in the normal state ; for if this is not the case the solid may produce other than a purely thermal disturbance in its neighbourhood in virtue of a catalytic or other kind of surface effect.

Several workers have compared the measured flame temperatures according to the above definition, with the calculated temperatures based on the heat of combustion of the gaseous mixture supplied to the burner and the specific heats of the products of combustion. But since the measured temperatures are by no means uniform throughout the flame (due probably to lack of homogeneity resulting from imperfectly mixed gases supplied to the burner, and also to infiltration of secondary air from the surrounding atmosphere) the comparison of the measured and calculated temperatures for any given mixture is somewhat uncertain.

In the course of our work on temperature measurements during the explosive combination of gaseous mixtures in closed vessels we have been able to measure the temperatures reached by fine platinum-rhodium wires in the flames of certain mixtures, while combustion was proceeding at constant pressure as in the open flame. It is well known that when an inflammable gaseous mixture is ignited at the centre of the containing vessel the flame spreads outwards and travels a considerable

* Communicated by the Authors.

† Griffiths and Awbery, Proc. Roy. Soc. A, cxxiii. p. 401 (1929) ; Jones and others, J. Am. Chem. Soc. liii. no. 3, p. 869.

part of the distance between the centre and the walls of the vessel before there is a sensible increase of pressure. If, therefore, the thermometer wire is placed near the point of ignition and it is thin enough to follow the changes in the temperature of the gas with sufficient rapidity it will, during this time, reach the same temperature as it would in the open flame of a perfectly homogeneous mixture of the same composition.

The rate at which the flame travels outwards is practically constant for any given mixture during the period of constant pressure burning, and, therefore, the time available for recording the temperature of the wire before the pressure rises depends on the size of the explosion vessel. The results given in this paper were obtained in spherical vessels up to 18 inches diameter, and the range of mixtures for which these temperatures could be measured was therefore limited. We are now making arrangements to extend the range by increasing the size of our vessels.

The view impressed upon us by the experiments we describe in the following sections is that the temperature of a flame as measured by a solid of small heat capacity (such as a metal wire) or by the spectral line reversal method when certain salts are introduced into the flame, is not necessarily, or indeed generally, that which corresponds with the mean translational energy of the molecules constituting the flame, and this confirms the view we arrived at as the result of earlier experiments *.

Description of Apparatus and Method of Calibrating Platinum-Rhodium Wires.

Two spherical explosion vessels were used in these experiments, one of which was 6 inches in diameter, and the other 18 inches in diameter. The platinum-rhodium thermometer wires were ·0005 inch diameter, and were fused at their ends to thick platinum-rhodium leads which passed into the explosion vessel through a gas-tight holder T as shown in fig. 1. The holder also carried a pair of duplicate leads similarly disposed within the explosion vessel, and the external terminals of each pair of leads were connected to the opposite arms of a slide wire bridge, thus making use of Callendar's

* Phil. Mag. pp. 402–14 (March 1930).

method of compensation for the effects of temperature changes in the leads.

A torsion string galvanometer G, the natural period of which was 1/50th second, was connected as shown in fig. 1, and sufficient resistance was placed in series with the compensating leads to balance the bridge when the sliding contact was at the middle point of the wire, and the thermometer was at room temperature. The

Fig. 1.

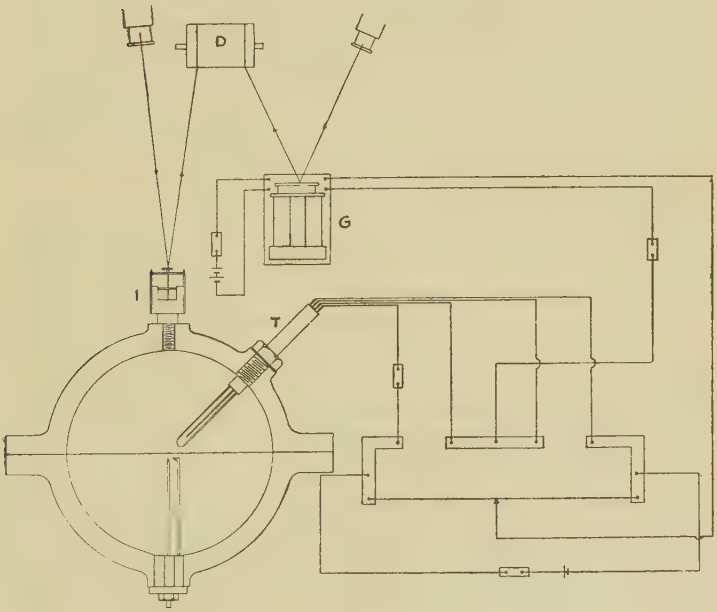

sliding contact was then left in this position and the changes in the resistance of the thermometer wire during the explosion were obtained from a continuous record of the galvanometer deflections on a photographic film mounted on the revolving drum D. The pressure rise during the explosion was simultaneously recorded on the same film by means of the optical indicator I which was fitted with a light spring so as to be sensitive to small changes of pressure.

The temperature scale for each wire used was determined directly by recording the deflections of the galvanometer

when the wire was placed in an electric furnace at various temperatures up to a maximum of 1180° C., giving a range which includes practically all the temperatures measured in the experiments described in this paper.

The furnace temperature was indicated by a standard thermocouple, and for the determination of each point on the calibration curve the wire was placed as close to the junction of this couple as was possible without actually touching it. The wire during this process of calibration was mounted on its usual leads, and was in every respect in the same condition as when placed in the explosion vessel. It was never in the furnace for more than 3 seconds, a time insufficient to allow of any appreciable heating of the comparatively thick leads. During the whole of this time a photographic record of the galvanometer was taken, and it was found to remain quite constant *.

In a previous paper we stated that platinum-rhodium wires of ·001 inch diameter were capable of following rapidly fluctuating temperatures without appreciable lag. This we confirm in regard to the temperatures attained by wires by the time the maximum explosion pressure is reached, except in those cases in which the time of explosion is extremely small. But for purposes of measuring temperatures during the pre-pressure period we find that ·0005 inch diameter wires rise in temperature more rapidly as the flame passes over them, and indeed, record slightly higher temperatures during this period than the ·001 inch wires. It is impracticable to use still thinner wires, and we have accordingly confined ourselves in our present experiments to wires of ·0005 inch diameter.

Results of Experiments.

A typical record traced from an actual film is shown in fig. 2. P_0P_0 is the line of zero pressure, reckoned from the initial pressure in the vessel before ignition,

* In our earlier experiments the ends of the compensating leads were joined by a short length of ·0005 inch wire, but we found that our final temperatures were almost exactly the same as in experiments in which this compensating wire was omitted. As the flame front did not simultaneously envelope the thermometer and compensating wires we decided to dispense with the latter for the purpose of the experiments described in this paper.

and T_0 T_0 is the line of zero temperature corresponding to the resistance of the wire at room temperature. The pressure scale is shown on the left, and the time scale is drawn below the diagram. The points A indicate the moment of the passage of the spark. Almost immediately afterwards the flame passed over the wire and its temperature increased rapidly to B. The temperature remained practically constant while the flame continued to travel outwards until the pressure began to rise at C and then increased again because of the further heating of the gas at the centre of the explosion vessel owing to the adiabatic compression produced as a result of the burning of the outer layers.

The temperatures recorded by the wires during the pre-pressure period in a mixture of 12 per cent. hydrogen

Fig. 2.

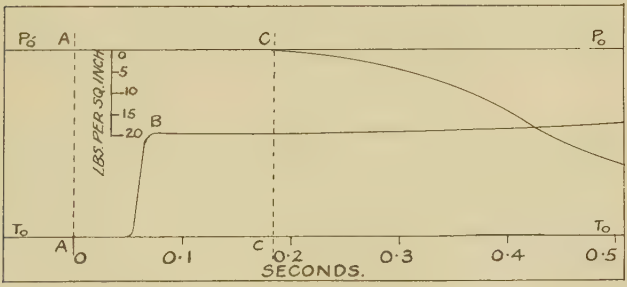

and air in the 18 inch sphere, and in a mixture of 14 per cent. carbon monoxide and air in the 6 inch sphere, are shown in figs. 3 and 4 respectively. The horizontal broken line on each diagram represents the temperature calculated on the basis of the heats of combustion and the specific heats of the products.

In both these experiments the pre-pressure period lasted for over 1/10th second *, but comparatively little cooling was indicated by the wires, although in the hydrogen experiment the wire temperature was throughout this period considerably higher than the

* There is doubtless a small rise of pressure during this period, but the very sensitive pressure indicator which we have employed shows that it must be less than 1/50 lb. per sq. inch. Adiabatic compression due to an increase of pressure of this order can have no appreciable effect upon the temperature of the gas first ignited.

Fig. 3.

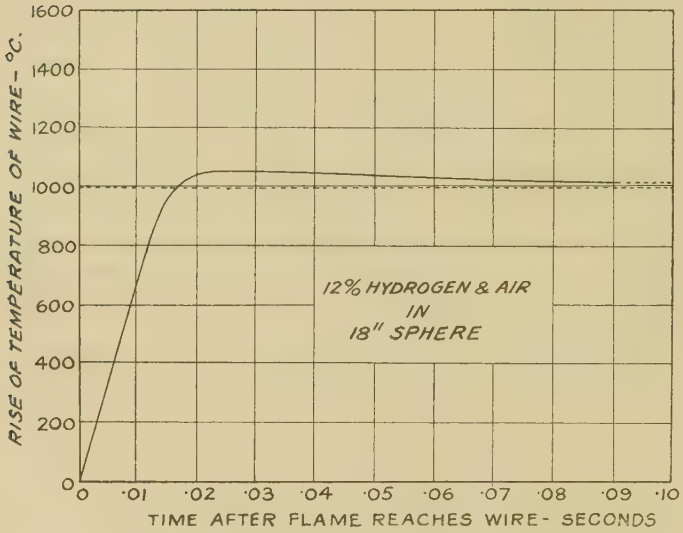

Fig. 4.

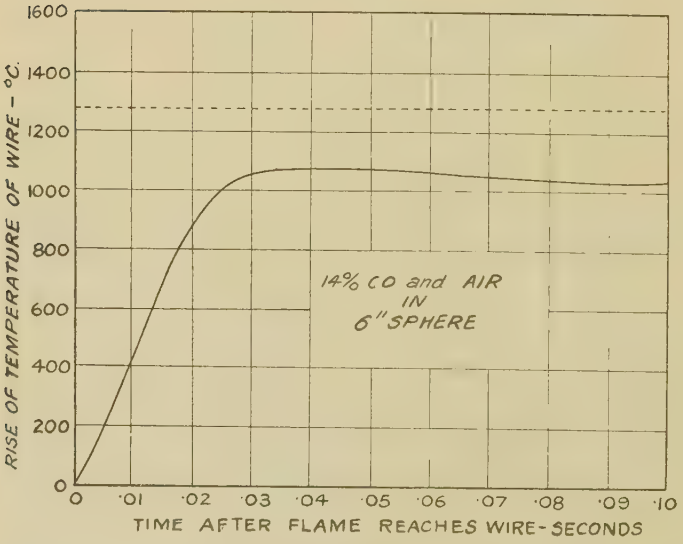

calculated temperature for the mixture. In the carbon monoxide experiment reference to fig. 4 shows that the wire temperature was far below the calculated temperature.

Apart from the lack of agreement between the measured and the calculated temperatures it might be thought that the temperature of the wire would remain constant during the pre-pressure period, because at first sight it would appear that the wire lies within an adiabatic enclosure as soon as the flame surrounds it. But since gas flames are highly transparent to their own radiation, heat loss must proceed by this means from the gas at the centre after the moment of ignition practically unimpeded, and therefore an appreciable amount of cooling actually

Fig. 5.

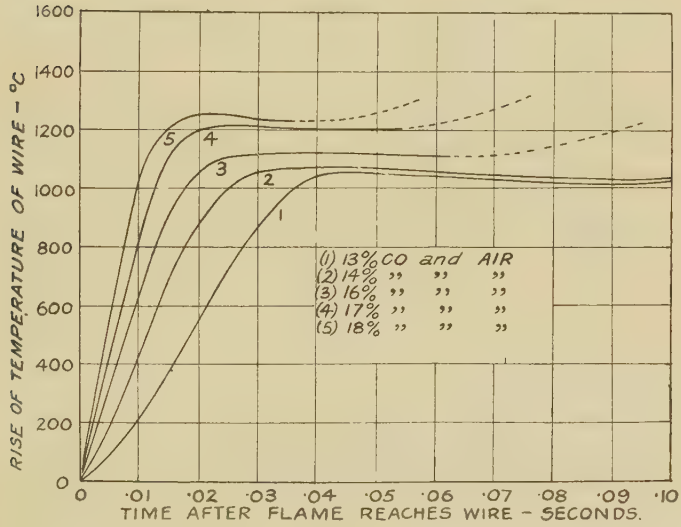

occurs in the gas surrounding the wires during pre-pressure periods lasting as long as those shown in figs. 3 and 4.

The temperatures recorded by the wire during the pre-pressure period in a series of carbon monoxide and air mixtures * fired in the 6 inch sphere are shown in fig. 5, and in fig. 6 the measured temperatures are compared with the gas temperatures calculated on the basis of the heat of combustion and the specific heats at constant

* In this series of experiments a small amount of hydrogen was substituted for an equivalent amount of carbon monoxide to obtain a more uniform rate of flame propagation. This substitution has been allowed for in calculating the ideal temperatures.

pressure of the products *. In figs. 7 and 8 similar results are shown for a series of hydrogen and air mixtures fired

Fig. 6.

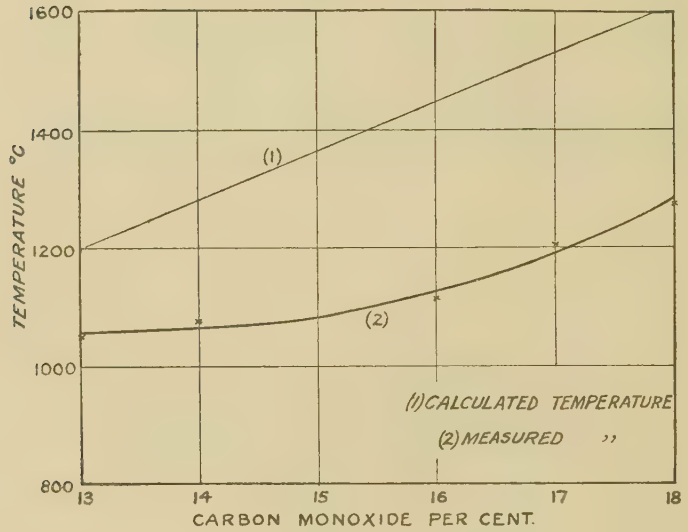

Fig. 7.

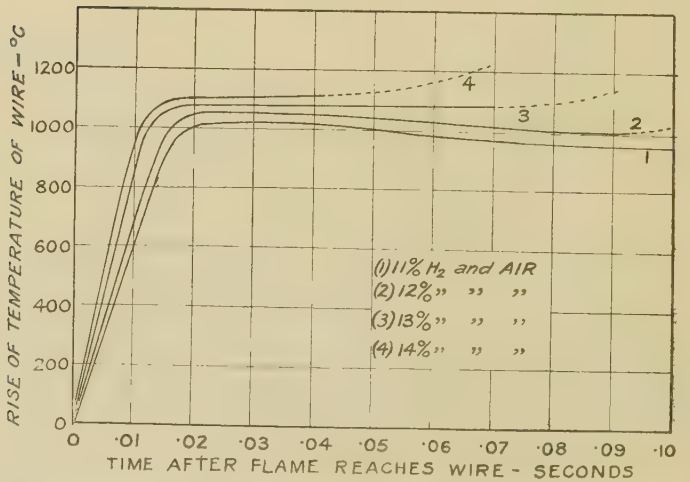

* The specific heats are taken from the tables published by Partington and Shilling in "The Specific Heats of Gases" (Benn 1924). The temperatures measured are well under 1400° C., and at such temperatures the specific heat values are generally accepted as being reasonably accurate.

in the 18 inch sphere. The full line portions of the wire temperature curves in figs. 5 and 7 relate to the temperatures shown by the wire during the pre-pressure period. The dotted portions of these curves relate to the temperatures shown by the wires after compression begins.

An examination of the measured and calculated temperatures given in figs. 6 and 8 shows that, for both the carbon monoxide and for the hydrogen mixtures, the rate of increase of the measured temperature with mixture strength is less than that of the calculated

Fig. 8.

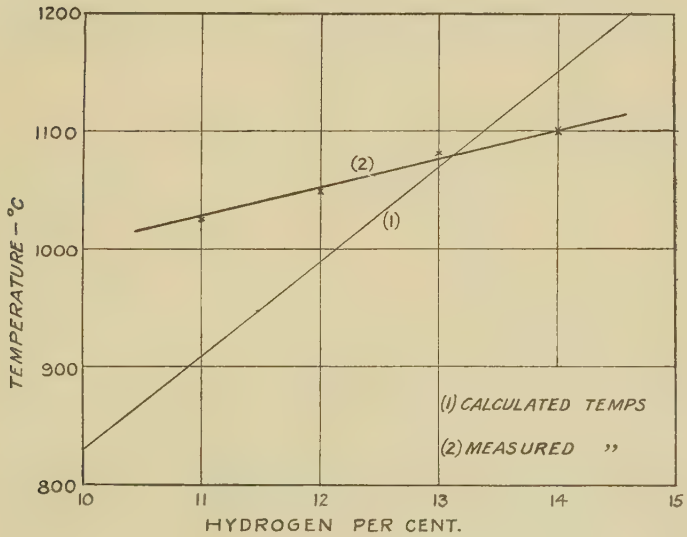

temperatures. We have for a long time thought, as a result of some earlier unpublished experiments, that this was probably so, and it was partly in consideration of this that we adopted the view that platinum thermometers immersed in flames do not record the temperature corresponding to their mean molecular translational energy.

Perhaps the most remarkable feature of the hydrogen experiments as shown in fig. 8 is that the wire temperatures in the weaker mixtures are considerably above the calculated temperatures. Precisely the same results were obtained when we substituted thin gold wires for

the platinum-rhodium wires, and to these we make further reference in a later section.

We think it may be of interest to include in this paper two records which are typical of many we have obtained relating to slow explosions in which the flame enveloped the thermometer wire for some time (as shown by A B figs. 9 and 10) and then rose above it, leaving it in uninflamed gas. Referring to fig. 9, it will be noticed that the flame leaves the wire before, and in fig. 10 some little time after, the beginning of the rise of pressure. In the former case, the wire on emerging from the inflamed portion falls back to the original temperature of the gaseous mixture, whilst in the latter the temperature falls to that corresponding to the adiabatic compression

Fig. 9.

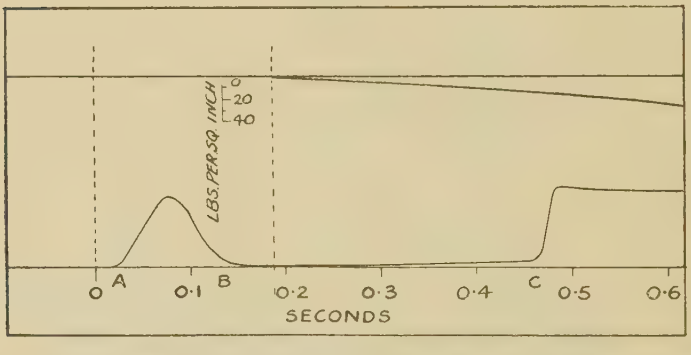

of the uninflamed portion of the mixture. In both cases the effects of further adiabatic compression is shown by the temperature rise during the intervals of time B C and the temperatures recorded by the wire during B C in each case are in close agreement with those calculated on the assumption of adiabatic compression of the uninflamed gas. These records seem to prove that the changes in the resistance of the wire are due entirely to temperature changes in the wire itself.

Discussion of Results.

The rise of temperature in the wire during the pre-pressure period in closed vessel explosions was precisely of the same general character in our experiments as that indicated by Hopkinson * who, so far as we are aware,

* Proc. Roy. Soc. A, lxxvii. p. 387 (1906).

made the only previous attempt to measure the temperatures at this stage of the explosion by means of a platinum wire.

The rapidity with which the wire is heated to a steady temperature during the pre-pressure period led Hopkinson to believe that combustion was instantaneously complete in any layer of gas as soon as the flame reached it. This view, however, is now no longer tenable because, as in our carbon monoxide and air experiments, the wire temperatures were very much lower than the ideal temperatures calculated on the basis of the generally accepted values of the specific heats *.

The mixture strengths we used were weaker than those generally employed in open flames, but we made some

Fig. 10.

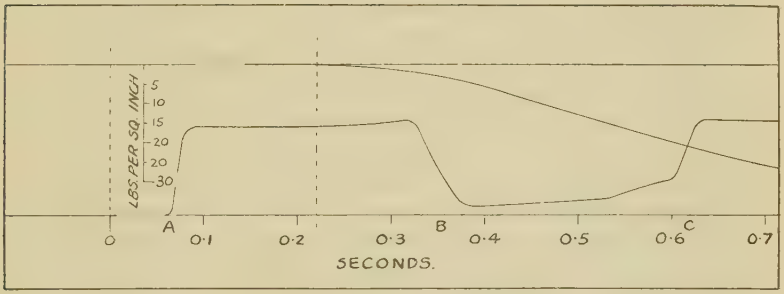

experiments with a mixture of 25 per cent. CO and air in the 18 inch sphere which corresponds to one of the weakest mixtures used by Griffiths and Awbery † in their open flame temperature measurements by the sodium line reversal method. They stated that this method yielded results in agreement with those obtained by means of rhodium wires in the flame when heated electrically to compensate for conduction and radiation losses. Our measurements gave a temperature for this mixture of 1660° C., whereas the temperature measured by them for the same mixture in the open flame was 1580° C. The calculated temperature for this mixture, assuming complete combustion, is about 2000° C., so that the

* See footnote p. 1050. It should be pointed out that these values were not established when Hopkinson made his experiments.

† Proc. Roy. Soc. A. lxxiii. p. 401 (1929).

measured temperatures in both cases are far below the ideal *.

We think the reason why the temperature found by Griffiths and Awbery is below that measured by us may be due to two causes. In the first place, as pointed out by them, they may not have measured the temperature at the hottest point in the flame and, secondly, the flame may have been cooled to some extent by the infiltration of secondary air. On the whole, therefore, the agreement between our results and theirs may be regarded as being satisfactory and lends support to the view that our direct method of calibration automatically compensates for conduction losses from the wire to the cold leads.

The results of some experiments with gold wires of ·0006 inch diameter (the smallest size that could be drawn) offer further support to this view. These wires when mounted in the same way as the platinum-rhodium wires and calibrated in the same manner in the furnace, melted when the furnace thermo-couple indicated a temperature of 1160° C., *i. e.*, 95° C. above the generally accepted value for the melting point of gold (1065° C.). They also melted in a gaseous mixture during explosion when the temperature, as measured by a similarly calibrated platinum-rhodium wire, was exactly 1160° C., thus showing that the error due to conduction from the gold wire into the cold leads was the same in the explosion as in the furnace during calibration.

The curves in figs. 6 and 8 show remarkable differences between the measured and calculated temperatures. In the weaker hydrogen mixtures the measured temperatures (both with platinum and with gold wires) were actually greater than the calculated temperatures, and therefore, much greater than the actual temperatures of the gaseous mixtures because of heat loss by radiation, and what is more important, combustion was not complete.

The behaviour of the wire in these mixtures might conceivably be due to the occlusion of hydrogen, which, in the presence of excess air in the gaseous mixture,

* No allowance has been made for radiation loss from the flame in calculating the ideal temperature. This, however, does not account, even appreciably, for the difference between the measured and ideal temperatures. The calculated temperature, in any case, can only be regarded as very approximate, because the specific heat of CO_2 and its degree of dissociation at temperatures of this order are uncertain.

would result in an increased concentration of reacting molecules on the surface of the wire. This, however, seems to us to be unlikely in view of the fact that the high temperature is maintained in the wire for a considerable time, and further we have found that the wire appears to behave in the same way in mixtures containing an excess of hydrogen.

We find it difficult to account for these results other than in terms of the theory we put forward in previous papers *, viz., that the molecules formed after combination in the gaseous phase remain for some time in an abnormal state associated with some latent form of energy which is unloaded on the hot surface of the wire.

The theory would involve the assumption that the mean translational energy of the molecules is considerably lower than that corresponding to the measured temperature. In terms of this theory the difference between the measured temperature and the actual gas temperature corresponding to the mean translation energy of its molecules it to be attributed to the unloading of the latent energy of the molecules upon the surface of the wire.

The results for the carbon-monoxide mixtures and for the stronger hydrogen mixtures in which the measured temperatures were maintained during the pre-pressure period at values much below the calculated temperatures do not appear at first sight to require an explanation involving the theory of abnormal molecules. We feel, however, that it is really equally difficult to account for them except in terms of a theory of this kind, otherwise it would be necessary to assume that chemical combination in any given small volume of mixture proceeds rapidly (though by no means instantaneously) until a certain proportion of the molecules (of the order of 75 per cent. in certain mixtures) had combined, and then practically stops short. Our theory makes it necessary to assume that the temperatures corresponding to the mean molecular translational energy are considerably less than the measured temperatures, and herein lies the difficulty in accepting the theory in connexion with the carbon monoxide mixtures and the stronger hydrogen mixtures, for the measured temperatures were as much as 25 per cent. below the calculated temperatures. As a further test

* Phil. Mag. pp. 398–401 (March 1930).

of the theory, we are now making an attempt to determine the mean molecular translational energy in the inflamed portions of gaseous mixtures at various stages during explosion in closed vessels by making simultaneous measurements of the pressure and the volume of the flame. Preliminary experiments of this kind seem to confirm our view, but they have not been carried far enough to enable us to speak quite definitely as yet.

The work described in this paper is being continued to cover a wider range of combustible gases and of mixture strengths, and also to investigate the behaviour of the wires with different diluent gases. We reserve a fuller discussion until the results of these and of the flame volume experiments are available. Meanwhile we think our present experiments sufficiently prove that platinum thermometry is not to be relied upon for determining the true temperature of flame, if the temperature is defined as the mean translational energy of its molecules. In making this statement we are not unmindful of the fact that the spectral line reversal method yields results in agreement with those obtained by platinum thermometry, and we suggest that in flames the sodium and lithium atoms may be excited to an extent beyond that corresponding to the true flame temperature, due possibly to the unloading upon them, during collision, of the latent molecular energy we have postulated. It is not without interest in this connexion to point out that Jones and others * found that when thallium salts were used in the spectral line method the flame temperatures inferred were about 140° C. lower than with sodium and lithium.

We ought to add that while the experiments described in the present paper seem to us to be most readily explained in terms of the theory that gaseous combustion results in the formation of very stable abnormal molecules, which we developed some time ago as the result of experiments on luminosity and with platinum thermometry, we still feel, as we then stated, that the stability of these molecules may be apparent rather than real, in that it may be due to "continual dissociation and recombination brought about by collision or by continual interchange

* J. Am. Chem. Soc. liii. no. 3, p. 860.

of partners with neighbouring molecules." * Either theory we think would account satisfactorily for all our experimental results though the latter would involve a new conception of the dissociation level in gases immediately after combination.

CI. *On the Analogy between the Electromagnetic Field and a Fluid containing a Large Number of Vortex Filaments.* *By* Sir J. J. Thomson, *O.M., F.R.S.*†

THE lines of electric force have many analogies with vortex filaments ; thus neither the lines nor the filaments can be created or destroyed, neither of them can have their ends in free space, they must either form closed curves or, if they are lines of force, their ends must be on charges of electricity, if they are filaments on a boundary of the liquid. Again, the disposition of the lines of force determines the distribution of energy in the electric field, while that of the filaments determines the distribution in the liquid. These relations are only of a qualitative kind.

My aim in this paper is to show that the analogy is quantitative as well as qualitative and that the Field Equations for a liquid full of vortex filaments are in general of exactly the same type as Maxwell's Equations of the electromagnetic field, and, in special cases, as Schrödinger's Equation ‡.

The following relation holds for a quantity such as a vortex filament or line of force which cannot be created nor destroyed, and where, therefore, the changes in the quantity at any place must be due to the motion of the quantity to or from that place :

$$\frac{d\zeta}{dt}+u\left(\frac{d\xi}{dx}+\frac{d\eta}{dy}+\frac{d\zeta}{dz}\right)=\frac{d}{dy}(u\eta-v\xi)-\frac{d}{dz}(w\xi-u\zeta)\ \S,$$

where ξ, η, ζ are the components of the quantity at (x, y, z), and u, v, w the components of its velocity at this place.

* Phil. Mag. p. 401 (March 1930).

† Communicated by the Author.

‡ Some properties of a turbulent fluid are discussed by Lord Kelvin in the Phil. Mag. xxiv. p. 342 (1887).

§ 'Recent Researches on Electricity and Magnetism,' J. J. Thomson, p. 7.

For a vortex filament

$$\frac{d\xi}{dx}+\frac{d\eta}{dy}+\frac{d\zeta}{dz}=0,$$

so that

$$\frac{d\xi}{dt}=\frac{d}{dy}(u\eta-v\xi)-\frac{d}{dz}(w\xi-u\zeta), \quad . \quad . \quad . \quad (A)$$

with similar equations for $d\eta/dt$, $d\zeta/dt$.

These are purely kinematical relations and can be deduced without using dynamical consideration.

They can be verified at once from the hydrodynamical equation *

$$\frac{du}{dt}=2(v\zeta-w\eta)-\frac{dp}{dx}. \quad . \quad . \quad . \quad . \quad (B)$$

We see from equation (B) that

$$2(v\zeta-w\eta), \qquad 2(w\xi-u\zeta), \qquad 2(u\eta-v\xi)$$

are the components of an acceleration which the filament experiences in virtue of its motion. This acceleration is at right angles both to the direction of the filament and to the direction in which it is moving, and its magnitude is proportional to the product of the strength of the filament and the component of its velocity at right angles to its length. A single straight filament if projected with a velocity at right angles to its length will not move in a straight line but will describe a circle with uniform velocity.

We now proceed to find the value of

$$\frac{d}{dt}(v\zeta-w\eta).$$

The change in the value of any property of the filaments in unit volume of the fluid will be due (1) to the motion of vortex filaments in or out of the element of volume, and (2) to the changes caused by the action of one filament on another inside the unit volume. This is expressed by the "Transference Equation" (Jeans, 'Kinetic Theory of Gases,' p. 249),

$$\frac{d}{dt}\Sigma Q=-\frac{d}{dx}\Sigma(uQ)-\frac{d}{dy}\Sigma(vQ)-\frac{d}{dz}\Sigma(wQ)+\Delta Q,$$

where Q expresses some quality of a single filament, ΣQ the the sum of these for all the filaments in unit volume, and ΔQ the change in ΣQ due to the action between the filaments.

* Lamb's 'Hydrodynamics,' p. 188.

If $Q=v\zeta-w\eta$, ΔQ will vanish, for we know from 'Hydrodynamics' (Lamb, p. 201) that

$$\iiint(v\zeta-w\eta)dx\,dy\,dz=0,$$

so putting $Q=v\zeta-w\eta$, we get

$$\frac{d}{dt}\Sigma(v\zeta-w\eta)=-\frac{d}{dx}\Sigma(uv\zeta-uw\eta)$$
$$-\frac{d}{dy}\Sigma(v^2\zeta-vw\eta)-\frac{d}{dz}\Sigma(wv\zeta-w^2\eta).$$

The components of the velocity may be written in the form

$$u=\mathrm{U}+p,\qquad v=\mathrm{V}+q,\qquad w=\mathrm{W}+r,$$

where from analogy with the motion of the molecules of a gas we may call (U, V, W) the molar velocity, and (p, q, r) the molecular velocity of the filament. If, as in a normal gas, the molecular velocities are equally distributed in all directions

$$\bar{p}=\bar{q}=\bar{r}=\overline{pq}=\overline{pr}=\overline{rq}=0,$$
$$\bar{p}^2=\bar{q}^2=r^2,$$

where a bar over a symbol indicates the mean value of the symbol in unit volume.

Thus
$$\bar{u}=\mathrm{U},\qquad \bar{v}=\mathrm{V},\qquad \bar{w}=\mathrm{W},$$
$$\overline{uv}=\mathrm{UV},\qquad \bar{u}^2=\mathrm{U}^2+\bar{p}^2.$$

We shall suppose that the molar velocity is small compared with the molecular, so that $\bar{u}^2=\bar{p}^2$ approximately.

Since an element of a vortex filament does not contribute anything to the motion of the axis of the element, u, v, w will not depend on ξ, η, ζ, so that

$$\Sigma(uv\zeta)=\Sigma\zeta.\overline{uv},\qquad \Sigma v^2\zeta=\Sigma\zeta.\bar{v}^2=\Sigma\zeta.\bar{q}^2.$$

Thus we get, remembering that the molar velocities are small compared with the molecular,

$$\frac{d}{dt}\Sigma(v\zeta-w\eta)=\frac{d}{dz}\left(\Sigma\eta\bar{r}^2\right)-\frac{d}{dy}(\Sigma\zeta\bar{q}^2),$$

or if
$$s^2=\bar{p}^2=\bar{q}^2=\bar{r}^2,$$

$$\frac{d}{dt}\Sigma(v\zeta-w\eta)=\frac{d}{dz}(\Sigma\eta.s^2)-\frac{d}{dy}(\Sigma\zeta.s^2).\quad .\quad (\mathrm{C})$$

Similarly

$$\frac{d}{dt}\Sigma(w\xi-u\zeta)=\frac{d}{dx}(\Sigma\zeta.s^2)-\frac{d}{dz}(\Sigma\xi s^2),$$

$$\frac{d}{dt}\Sigma(u\eta-v\xi)=\frac{d}{dy}(\Sigma.\xi.s^2)-\frac{d}{dx}(\Sigma\eta.s^2),$$

and from equation (A)

$$\frac{d}{dt}\Sigma\xi=\frac{d}{dy}\Sigma(u\eta-v\xi)-\frac{d}{dz}\Sigma(w\xi-u\zeta).$$

If we write

$$\Sigma\xi=4\pi f,\qquad \Sigma\eta=4\pi g,\qquad \Sigma\zeta=4\pi h,$$
$$\Sigma(v\zeta-w\eta)=\alpha,\qquad \Sigma(w\xi-u\zeta)=\beta,\qquad \Sigma(u\eta-v\xi)=\gamma,$$

these equations become

$$4\pi\frac{df}{dt}=\frac{d\gamma}{dy}-\frac{d\beta}{dz},$$
$$4\pi\frac{dg}{dt}=\frac{d\alpha}{dz}-\frac{d\gamma}{dx},$$
$$4\pi\frac{dh}{dt}=\frac{d\beta}{dx}-\frac{d\alpha}{dy},$$

and
$$\frac{d\alpha}{dt}=\frac{d}{dz}(4\pi gs^2)-\frac{d}{dy}(4\pi hs^2),$$

or if
$$s^2=1/\kappa,$$
$$\frac{d\alpha}{dt}=\frac{d}{dz}\left(\frac{4\pi}{\kappa}g\right)-\frac{d}{dy}\left(\frac{4\pi}{\kappa}h\right),$$
$$\frac{d\beta}{dt}=\frac{d}{dx}\left(\frac{4\pi}{\kappa}h\right)-\frac{d}{dz}\left(\frac{4\pi}{\kappa}f\right),$$
$$\frac{d\gamma}{dt}=\frac{d}{dy}\left(\frac{4\pi}{\kappa}f\right)-\frac{d}{dx}\left(\frac{4\pi}{\kappa}g\right).$$

These, if f, g, h represent the components of electric displacement and α, β, γ those of magnetic force, are exactly Maxwell's equation for a medium whose specific inductive capacity is κ.

It follows from these equations that f, g, h, α, β, γ all satisfy the wave equation

$$\frac{d^2\phi}{dt^2}=\frac{1}{\kappa}\left(\frac{d^2\phi}{dx^2}+\frac{d^2\phi}{dy^2}+\frac{d^2\phi}{dz^2}\right),$$

the velocity of the wave $1/\sqrt{\kappa}=s$.

Thus the fluid filled with vortex filaments can serve as a model of the electromagnetic field, the vortex filaments representing the lines of electric force and the motion of the filaments the magnetic force.

In deducing equations (A) it was assumed that variations in the density of the filaments at any place were due entirely to the motion to or from that place of filaments having a molar velocity superposed on their molecular velocity.

There may, however, in certain cases be alterations in the density of the filaments which arise in another way. There may be a group of these filaments which form a connected system, such as would be formed if they all ended on a common boundary, such as a small hole in the liquid; in the electrical problem the analogue of this would be the system of lines of force starting from an electron or proton. For such systems there would be a certain distribution of the filaments or lines of force which would be in equilibrium or steady motion, and if the distribution were disturbed the system would oscillate with a definite frequency. Consider a portion of one of these systems when the distribution is oscillating; the filaments in it at one time will be approaching each other and the density of their distribution increasing, at another time they will be receding from each other and their density diminishing. Thus from this cause there will be a periodic variation of the density which will not vanish even though the filaments have no molar velocity.

In the absence of this cause we have seen that the variables satisfy the wave equation

$$\frac{d^2\phi}{dt^2} = c^2\left(\frac{d^2\phi}{dx^2} + \frac{d^2\phi}{dy^2} + \frac{d^2\phi}{dz^2}\right).$$

In this equation the left-hand side may be regarded as the acceleration of a quantity fixed by the symbol ϕ, and the right-hand side therefore as a force acting per unit mass on this quantity; this corresponds to the equation of motion of a free particle whose motion does not call into play any forces of restitution. When, as in the case we are considering, the system fixed by ϕ can vibrate, the vibration will call into play an acceleration $-n^2\phi$, if $n/2\pi$ is the frequency of the vibration. Thus for such a system, instead of the wave equation, we have

$$\frac{d^2\phi}{dt^2} = -n^2\phi + c^2\left(\frac{d^2\phi}{dx^2} + \frac{d^2\phi}{dy^2} + \frac{d^2\phi}{dz^2}\right). \quad . \quad . \quad . \quad \text{(D)}$$

To find the velocity of a wave represented by this equation, put

$$\phi = \mathrm{A}\cos p\left(t - \frac{x}{v}\right),$$

where $p/2\pi$ is the frequency of the wave vibration, and v the phase velocity. Substituting the value of ϕ in equation (D) we get

$$\frac{p^2 - n^2}{c^2} = \frac{p^2}{v^2},$$

thus the phase velocity will vary with the period. If u is the group velocity,

$$\frac{1}{u} = \frac{d}{dp}\left(\frac{p}{v}\right),$$

so that

$$u = \frac{c^2}{v},$$

and therefore

$$\frac{p^2 - n^2}{c^2} = \frac{p^2 u^2}{c^4}.$$

Since

$$\frac{d^2\phi}{dt^2} = -p^2\phi,$$

equation (D) becomes

$$\left.\begin{aligned} \frac{n^2 - p^2}{c^2}\,\phi &= \nabla^2\phi, \quad (1) \\ -\frac{p^2 u^2}{c^4}\,\phi &= \nabla^2\phi. \quad (2) \end{aligned}\right\} \quad \ldots\ldots \quad (\mathrm{E})$$

In the case of a moving electron, if E is its total energy, m its mass, and h Planck's constant,

$$\mathrm{E} = mc^2 = h\,.\,\frac{p}{2\pi};$$

so that

$$p^2u^2/c^4 = 4\pi^2 m^2 u^2/h^2.$$

Since the energy is carried by the wave, the velocity of the electron must be the group velocity of the waves at the electron. Thus u^2 must be the velocity of the electron where it reaches the point x, y, z; its kinetic energy is

$$\tfrac{1}{2}mu^2 = (\mathrm{E} - \mathrm{V}),$$

where V is the potential energy of the electron at x, y, z.

Substituting this value of p^2u^2/c^4 in E(2), we get

$$\nabla^2\phi + \frac{8\pi^2 m}{h^2}(\mathrm{E} - \mathrm{V}) = 0,$$

which is Schrödinger's equation.

We see from equation (1, E) that waves cannot be propagated through a medium of this kind unless their frequency is greater than the intrinsic frequency of the medium.

In a fluid containing vortex filaments the energy is not, if the filaments are fine, mainly in the filaments themselves but in the fluid around them—indeed, none of the energy is in the filaments if these are hollow. Each filament makes the fluid in its neighbourhood rotate around it, and some of

this is carried along by the filament. The mass of the filament is the mass of the fluid carried along by it and its kinetic energy that of this fluid. A circular vortex ring, for example, carries with it much more liquid and energy than are in the central core to which the vorticity is confined. The amount of mass and energy carried along by a group of filaments will depend upon filaments in the neighbourhood of the group. If the distribution of filaments in the fluid changes from place to place the quantity of fluid and energy of the group will change too. Suppose, for example, that this diminishes when the group moves from A to B, some of the energy which was attached to the group at A is no longer attached to it at B, and does not count as its kinetic energy. The lost energy is, however, in the fluid and will be regained by the group when this gets back to B. Thus the energy detached may be regarded as potential energy—it is always kinetic energy of the fluid, but acts like potential when it is no longer bound to the group.

CII. *Note on the Physical Significance of Second Order Terms in the Perturbation Theory. By* H. Jones, *H. H. Wills Physical Laboratory, University, Bristol* *.

THE perturbation theory has recently been expressed in a more compact form by Prof. Lennard-Jones †, who obtains a determinantal equation giving the energies to all orders. The present note is an attempt to consider the physical significance of this rather different outlook on the perturbation theory, and in particular to consider those cases which do not appear to fit neatly in the more usual theory. Thus the application of the Schrödinger perturbation theory to the calculation of the forces which exist between atoms separated by great distances, or to the calculation of the effect of a weak electric field on an alkali atom appears unsatisfactory. The result is well known; the first approximations are vanishingly small, while the second approximations are appreciably greater and seem to account (as far as can be judged from numerical calculations) for the actually observed effects. In these cases where the perturbation is very small, one would have expected almost exact

* Communicated by Prof. J. E. Lennard-Jones.

† Proc. Roy. Soc. A, cxxix. 1930. See in particular § 4.

results from the first approximation, and some further discussion of these cases seems necessary.

The roots of the already-mentioned infinite determinant obtained by Lennard-Jones give the exact energy levels of the perturbed system, and in that paper the ways of approximating to these roots are fully discussed. In particular, it was shown how the usual perturbation terms correspond to a certain development and how this was not in all cases the most convenient. This note aims at no more than providing a few simple illustrations of this outlook and the physical picture underlying this mathematical scheme. It is shown, for example, how in the case of an alkali atom in a uniform electric field there are two possible ways of approximating to the roots—one appropriate to weak fields and one appropriate to strong fields. In the general

Fig. 1.

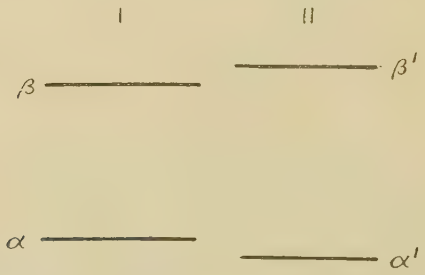

theory the determinant arises through the essential step of expanding the wave-function for the perturbed state as an infinite series of the wave-functions of the unperturbed system.

An elementary consideration, however, allows one to see the physical significance of this step and also to see immediately which are the important terms for special cases. We consider the case of an atom (and suppose for simplicity there is only one electron) perturbed by a uniform electric field. The unperturbed and the perturbed atom form two separate systems, each with their own set of stationary states α, β, γ, etc. and α', β', γ', etc. If I be certainly in α and the field be applied adiabatically, II will certainly be in α' and so on. If now one cuts off the field suddenly (not adiabatically), one observes α' as a state of I, *i.e.* as a superposition of states α, β, γ, etc., because there is not time during the removal of the field for α' to change to α.

Conversely, if we observe I and find it certainly to be in α, then apply the field suddenly, II will be partly in α' and partly in β' etc. Now removing the field adiabatically we have I partly in α partly in β etc. It might seem at first as if this is incompatible with the conservation of energy, so we follow the experiment in detail to show that it is not so.

One can think of an atom in two ways: (1) as an electron having a position lying in a range q to $q+\delta q$, or (2) as the atom being in a definite stationary state. One cannot think of both together without introducing contradictions. Thus one tries to think of the hydrogen atom in the ground state, there is then a finite probability that the electron lies at a great distance from the nucleus. As the kinetic energy is necessarily positive, the energy of the system is then much greater than the energy of the stationary state and a contradiction appears with the conservation of energy.

In order to show that the sudden (not adiabatic) application of a uniform electric field is always capable of providing sufficient energy to cause transitions, one thinks in terms of the first picture. As there is no question of what particular stationary state the atom is in, one can think of the electron as sometimes lying within a small range at a distance r from the nucleus. If the field be switched on suddenly when the electron is in this position, there is an addition of energy equal to $(\mathbf{F}, r)$ which may be either positive or negative, and of any magnitude. Therefore the sudden application of a field allows transitions from any one state to any other without the violation of the conservation of energy.

Calculation of the change of energy of a system consisting of one electron due to the application of an arbitrary electric field.

In calculating the change in the energy of a system consisting of one electron due to the application of an arbitrary electric field, the object is not an attempt to get more accurate results than have already been obtained but rather to use this case as an example of those where the usual outlook of the perturbation theory is not very satisfactory. As in the case of two atoms at great distance apart, so in the case of an alkali atom subject to a weak field there are terms in the second approximation greatly exceeding the terms in the first, and it is in just such cases where the perturbation is small that exact results would be expected

from the first order. For simplicity, let us suppose only two states of the system are involved, an s ground state and an excited p state. The magnetic moment of the electron and relativity effects are neglected. As there are two states of the unperturbed system, there will be two states of the perturbed system each of which corresponds to a state of the unperturbed system partly in s and partly in p. We write it

$$\psi_\kappa = \phi_s + \lambda_\kappa \phi_p, \qquad \kappa = 1, 2, \quad . \quad . \quad . \quad . \quad . \quad (1)$$

where ϕ_s and ϕ_p are the orthogonal and normalized wave-functions of the atom in the s and p states respectively. To determine λ_1 and λ_2 and the energies of the states denoted by ψ_1 and ψ_2, we have equations

$$\left.\begin{aligned} H_0\phi_s &= E_s\phi_s, \\ H_0\phi_p &= E_p\phi_p, \end{aligned}\right\} \quad . \quad . \quad . \quad . \quad . \quad . \quad . \quad (2)$$

$$(H_0 + V)\psi_\kappa = E_\kappa \psi_\kappa, \quad . \quad . \quad . \quad . \quad . \quad . \quad . \quad (3)$$

H_0 being the Hamiltonian operator for the unperturbed system, $(H_0 + V)$ that for the perturbed system. Substituting from (1) for ψ_κ in (3), removing some of the terms by (2), and multiplying throughout on the left of (3) successively by ϕ_s and ϕ_p and integrating, we have

$$\left.\begin{aligned} (E_s + V_{ss} - E_\kappa) + \lambda_\kappa V_{sp} &= 0, \\ V_{ps} + \lambda_\kappa (E + V_{pp} - E_\kappa) &= 0, \end{aligned}\right\} \quad . \quad . \quad . \quad . \quad (4)$$

where

$$V_{sp} = \int \phi_s V \phi_p \, dr, \text{ etc.}$$

Eliminating λ_κ and solving for E_κ gives

$$2E_\kappa = E_s + V_{ss} + E_p + V_{pp} \pm \sqrt{(E_s + V_{ss} - E_p - V_{pp})^2 + 4V_{sp}V_{ps}}. \quad . \quad (5)$$

There are two special cases of importance: (a) when

$$| E_s - E_p + V_{ss} - V_{pp} | >> | V_{sp} |,$$

we have

$$\left.\begin{aligned} E_1 &= E_s + V_{ss} + \frac{V_{sp}V_{ps}}{E + V_{ss} - E_p - V_{pp}}, \\ E_2 &= E_p + V_{pp} - \frac{V_{sp}V_{ps}}{E_s + V_{ss} - E_p - V_{pp}}, \end{aligned}\right\} \quad . \quad . \quad (6)$$

and

$$\left.\begin{aligned}\lambda_1 &= \frac{V_{ps}}{E_s + V_{ss} - E_p - V_{pp}},\\ \lambda_2 &= \frac{E_s + V_{ss} - E_p - V_{pp}}{V_{sp}},\end{aligned}\right\} \quad . \quad . \quad . \quad . \quad . \quad (6.1)$$

Secondly, (*b*) when

$$| E_s + V_{ss} - E_p - V_{pp} | << | V_{sp} | \quad \text{and} \quad V_{sp} = V_{ps},$$

we have

$$E_\kappa = \tfrac{1}{2}(E_s + E_p + V_{ss} + V_{pp}) \pm V_{sp}, \quad . \quad . \quad . \quad (7)$$

and

$$\lambda_\kappa = \pm 1.$$

These results may be applied to the case of an alkali atom in a uniform electric field. This system is equivalent to that of an hydrogen atom subject to a field

$$\mathbf{F} = \mathbf{F}_1 + \mathbf{F}_2,$$

where $\mathbf{F}_1$ is a uniform electric field and $\mathbf{F}_2$ is a spherically symmetrical field such as might arise due to a core. $\mathbf{F}_1$ will not make contributions to V_{ss} or V_{pp}, therefore these are due entirely to $\mathbf{F}_2$, *i. e.* to the influence of the core, and give the first approximation to the Rydberg correction. Thus, for $E_s + V_{ss}$ we write simply E_s the energy of the atom in the ground state in the absence of an external field; similarly for $E_p + V_{pp}$ we write just E_p the energy of the first p state. Also, one sees easily that $\mathbf{F}_2$ does not contribute to V_{sp}; to emphasize this we put $V_{sp} = V_{ps} = f_{sp}$. Again, since we are considering a weak electric field, *i. e.* where the effect of $\mathbf{F}_1$ is much smaller than the effect of $\mathbf{F}_2$, we are dealing with case (*a*). Therefore

$$E_1 = E_s + \frac{f_{sp}^2}{E_s - E_p},$$

$$E_2 = E_p - \frac{f_{sp}^2}{E_s - E_p}.$$

This may be expressed schematically as in fig. 2.

These are to our approximation the expressions for the energies of the ground s and first p states of an alkali atom in an external field, and agree with observations on the quadratic Stark effect. When the effect of $\mathbf{F}_1$ is much greater than that of $\mathbf{F}_2$ as for an alkali atom in a very strong field, or more simply a hydrogen atom in any field, then we have case (*b*). The two states involved, whose

wave-functions are ϕ and ϕ_p, are the $2s$ and the $2p$ states of the atom, and for hydrogen these have the same energy, say E(2). The equation (7) now becomes

$$E_\kappa = E(2) \pm f_{sp}.$$

This gives just the ordinary splitting of the second quantum state of hydrogen in an electric field as in the linear Stark effect. In addition equation (5) gives us the transition from weak to strong fields, *i. e.* from the quadratic to the linear Stark effect for the alkali metals,

$$2E_\kappa = E_s + E_p \pm \sqrt{(E_s - E_p)^2 + 4f_{sp}^2}.$$

These two cases serve to bring out an essential point of the outlook on the perturbation theory taken here, viz., that there is no sharp distinction between the determination of energy changes due to an external perturbation when there

Fig. 2.

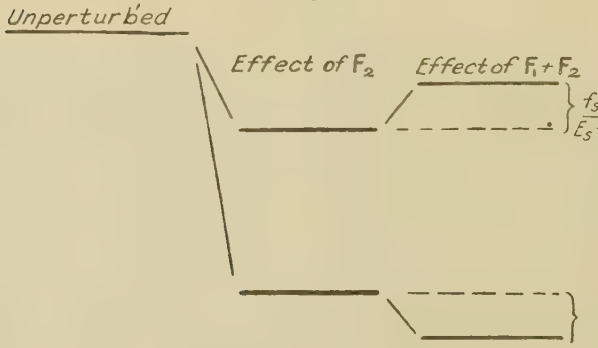

is an initial degeneracy and when there is not an initial degeneracy. When an initial degeneracy does exist, it is obvious that the state of the zero approximation is to be obtained by the superposition of the states with the same energy. When it is realized that the external perturbation can always provide energy for the introduction of other unperturbed states, it becomes equally clear that the true zero approximation to the perturbed state, even when there is no degeneracy, is obtained by superposing those states of the unperturbed system which lie near to the state of the perturbed system whose energy is required. When there is an initial degeneracy in the formation of the zero approximation state by superposition, there is no reason *a priori* for giving one state a greater weight than another. When there is no degeneracy, on the other hand, it appears that those

states which energetically are relatively far from the perturbed state (whose energy is required) should have a less weight than those which are nearer. What the actual values of these weights are, come from the perturbation calculation itself.

Schrödinger charge distributions in the perturbed states.

We consider the wave-functions of the perturbed states of an alkali atom, perturbed by a uniform electric field. The wave-functions of the two unperturbed states, which we consider ϕ_s and ϕ_p, are given in polar coordinates (apart from the normalizing factors) by

$$\phi_s = (\delta - r)e^{-r/2},$$
$$\phi_p = re^{-r/2}\cos\theta,$$

where $\delta = 2$ for hydrogen. When a core is present, a better function is obtained by taking $\delta < 2$. The nodes of the two states ψ_1 and ψ_2 of the perturbed system are given, therefore, by the equations

$$r = \frac{\delta}{1 - \lambda_1 \cos\theta}, \quad \text{where} \quad |\lambda_1| < 1;$$

$$r = \frac{\delta}{1 - \lambda_2 \cos\theta}, \quad \text{where} \quad |\lambda_2| > 1.$$

Equations (6.1) show that

$$\lambda_2 = -1/\lambda_1.$$

When F_1 is very small, $\lambda_1 \to 0$ and the nodal surface is a sphere. When the effect of the core is entirely neglected $\lambda_1 = 1$, and therefore the nodal surface is a parabaloid as to be expected. For intermediate values as for the alkalies in an external field the nodal surfaces are ellipsoids of revolution.

In fig. 3, curve (a) gives a section of the nodal surface for the state ψ_1. This corresponds to the ground s state of an alkali atom perturbed by an electric field, the nodal surface which is a sphere (a') in the unperturbed atom is drawn out into an ellipsoid. Thus the Schrödinger charge distribution of the atom in the ground state is distorted in such a way as to give the atom an electric moment. Curve (b) is the section of the nodal surface of the state ψ_2. When the external field is zero this is a plane through the nucleus (b'), the perturbation changes the plane into a parabaloid, and in this state again the atom possesses an electric moment.

The hydrogen molecular ion.

If E_s be the energy of the ground state of the hydrogen atom and the distance between the two nuclei is great,

there will be a state of the perturbed system lying close to E_s. It is required to calculate the energy of this state.

We ask first to what state of the unperturbed system does this state of the perturbed system belong. To answer this we remove the perturbation in such a short interval of time that the system has not time to change from one to another, and we can observe the perturbed state as a state of the unperturbed system. This will not be a stationary state of the unperturbed system, but one in which it is partly in each

Fig. 3.

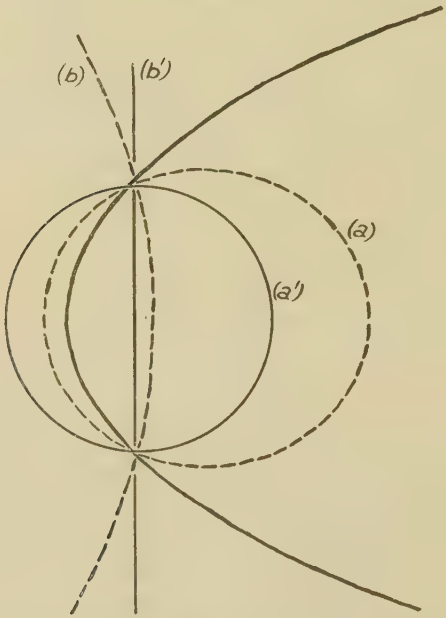

of the stationary states. For simplicity we again suppose that there are only two states involved, the ground s and the first p state. As there are two states for the electron at each nucleus, there will be four states of the perturbed system.

$$\psi_\kappa = \phi_s(a) + \lambda_\kappa \phi_p(a) \pm (\phi_s(b) + \lambda_\kappa \phi_p(b)), \quad \kappa = 1, 2, . \quad (8)$$

where a and b refer to the two nuclei. As in the previous case from equations

$$\left.\begin{aligned} H_0\phi_s &= E_s\phi_s, \\ H_0\phi_p &= E_p\phi_p, \end{aligned}\right\} \quad . \quad . \quad . \quad . \quad . \quad . \quad (9)$$

holding for the states at either nucleus; and

$$(H_0+V)\psi_\kappa=E_\kappa\psi_\kappa, \quad . \quad . \quad . \quad . \quad . \quad (10)$$

there results by left-hand multiplication of equation (10) by $\phi_s(a)$ and $\phi_r(a)$ and integrating, four linear equations

$$\left.\begin{aligned}(E_s-E_\kappa+V^E_{ss})+\lambda_\kappa V^E_{sp}\pm V^P_{ss}\pm\lambda_\kappa V^P_{sp}=0,\\ V^E_{ps}+\lambda_\kappa(E_p-E_s+V_{pp})\pm V^P_{ps}\pm\lambda_\kappa V^P_{pp}=0,\end{aligned}\right\}$$

where the two positive signs or the two negative signs are to be taken together, and where

$$V^E_{sp}=\int\phi_s(a)V\phi_p(a)\,dr,$$
$$V^P_{sp}=\int\phi_s(a)V\phi_p(b)\,dr.$$

These are satisfied if

$$\begin{vmatrix}(E_s+V^E_{ss}\pm V^P_{ss}-E_\kappa), & (V^E_{sp}\pm V^P_{sp})\\ (V^E_{ps}\pm V^P_{ps}), & (E_p+V^E_{pp}\pm V^P_{pp}-E_\kappa)\end{vmatrix}=0. \quad (12)$$

This is a quadratic equation for E_κ, and in the special case when $|E_s-E_p|>>|V^E_{sp}\pm V^P_{sp}|$ the roots may be written

$$\left.\begin{aligned}E_1&=E_s+V^E_{ss}\pm V^P_{ss}+\frac{(V^E_{sp}\pm V^P_{sp})(V^E_{ps}\pm V^P_{ps})}{(E_s+V^E_{ss}\pm V^P_{ss})-(E_p+V^E_{pp}\pm V^P_{pp})},\\ E_2&=E_p+V^P_{pp}\pm V^P_{pp}-\frac{(V^E_{sp}\pm V^P_{sp})(V^E_{ps}\pm V^P_{ps})}{(E_s+V^E_{ss}\pm V^P_{ss})-(E_p+V^E_{pp}\pm V^P_{pp})}.\end{aligned}\right\}$$

The two energy values E_2 bear no significant relation to the actual system H_2, because we have neglected the numerous states which lie close to the $2p$ state, in particular the $2s$ state. The two energies E_1 have more bearing on the actual problem because the $2p$ state is the next nearest to the ground $1s$ state, and may therefore be expected to have next to the $1s$ state the greatest weight in the formation of the non-stationsry state which corresponds to the lowest stationary state of the perturbed system. The two energies are, in fact, built up from the ordinary exchange energies and the first term in the second approximation of the usual perturbation theory.

Finally, two results may be mentioned which do not seem so strange from the present standpoint as they previously appeared to do. First, the outer electron configuration of the atoms of zinc and cadmium in their ground state consists of two electrons in a closed helium-like shell. When these atoms are brought together in the form of a lattice the usual first order perturbation terms gives a repulsion, or for great

separation a very weak attraction. One is led to think, therefore, that the binding forces in the crystal are of the nature of a polarization effect. When only two atoms are concerned it is easy by means of a semi-classical picture of a distortion of the Schrödinger space-charge, by the field of the other atom, to see how each, regarded separately, developed an electric moment and therefore gives rise to a second order term in the usual perturbation theory. When, however, there are many atoms and each is placed symmetrically with respect to the others, it is not so easy to understand how a given atom, considered alone, can acquire an electric moment, which is necessary if the binding is to be of the nature of a polarization effect. The present outlook allows this to be understood immediately. Corresponding to the ground state of the whole system there is a non-stationary state of each atom of the unperturbed system (*i. e.* the atoms infinitely separated). This state is one in which the atom is partly in the ground state and partly in the various excited states, in particular the first p state. As we have seen, the superposition of these states has the effect of giving the atom an electric moment. Thus one sees immediately that there will be binding forces by polarization in the crystal state as well as in the molecular state.

Secondly, when the state of the unperturbed system, which really corresponds to the state considered of the perturbed system, is used, *i. e.* a non-stationary state arising by the superposition of the unperturbed stationary states, terms in the first order arise which can be interpreted by analogy as polarization effects, and the greater these terms the greater the binding energy of the crystal. This means that the greater the weight to be attached to the excited states in the non-stationary state of the unperturbed atom the greater the binding energy. A state of the crystal built up from singlet atomic states would be non-conducting, as such a state would be symmetrical in the momentum space This suggests that the conductivity will be the greater the greater the extent to which the excited states are involved, and therefore the greater the binding energy the greater the conductivity for the metals zinc, cadmium, and mercury. This is actually the case.

It is a pleasure to express my thanks to Prof. Lennard-Jones, with whom each point of this note has been discussed, for much stimulating criticism and advice.

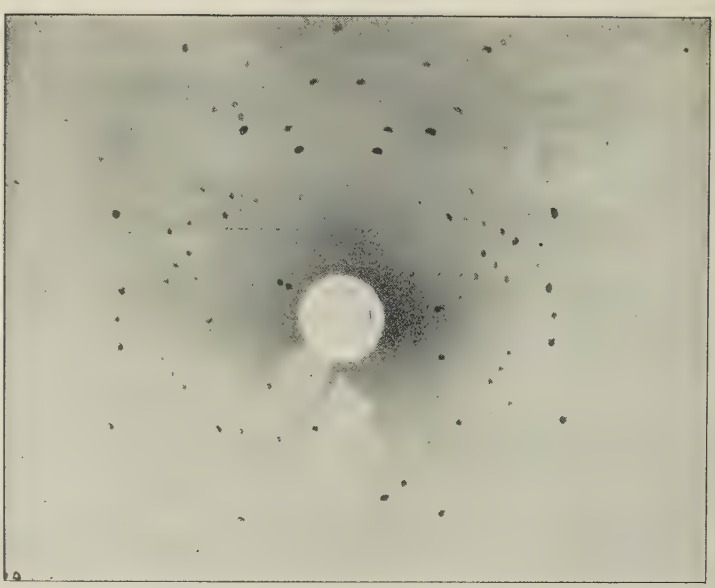

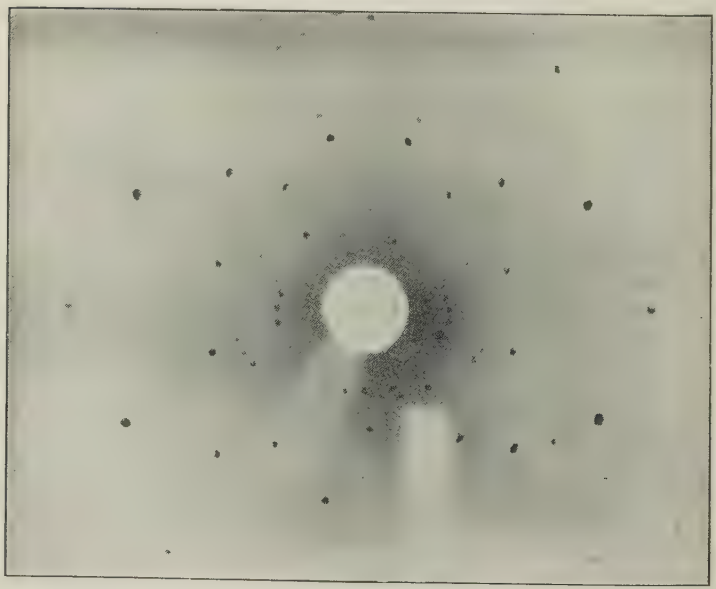

Laue Ph

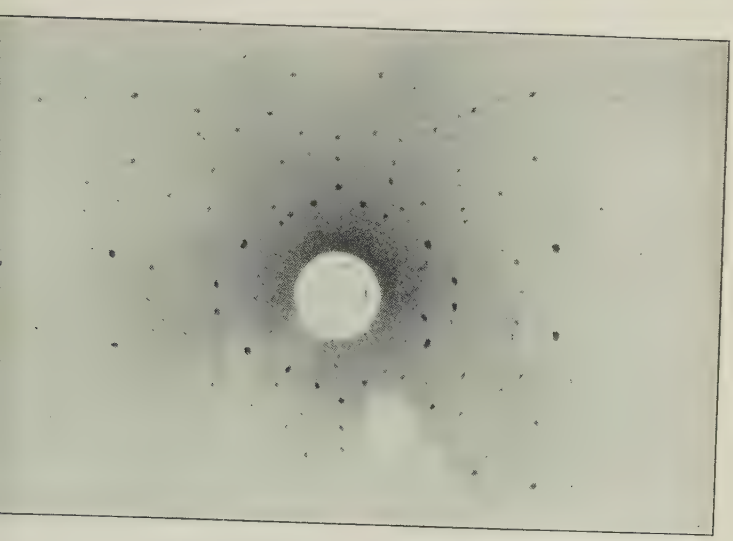

CuAl.

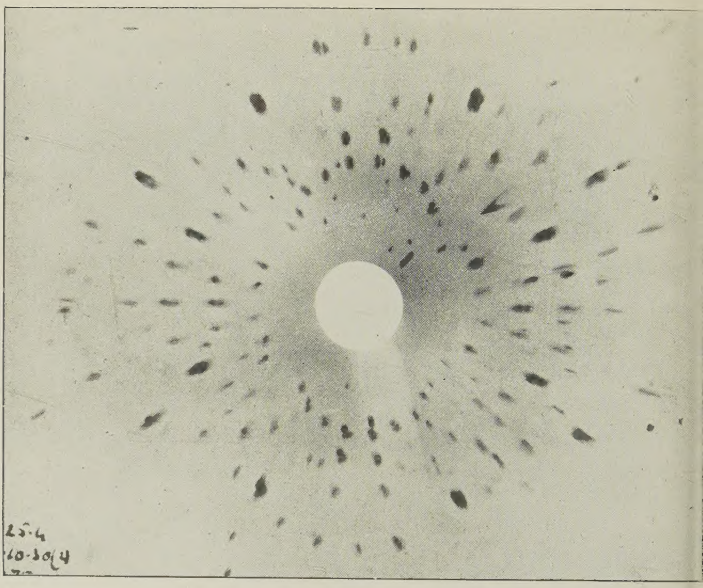

a.

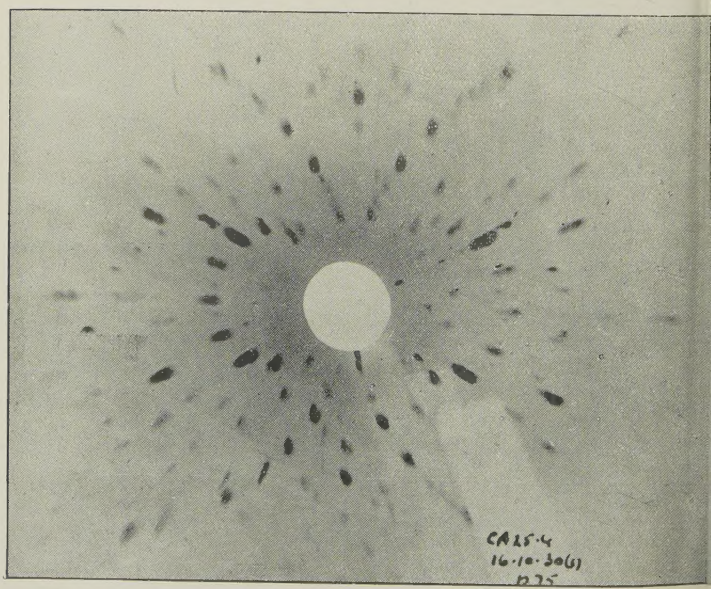

b.

Laue Photographs of a Copp

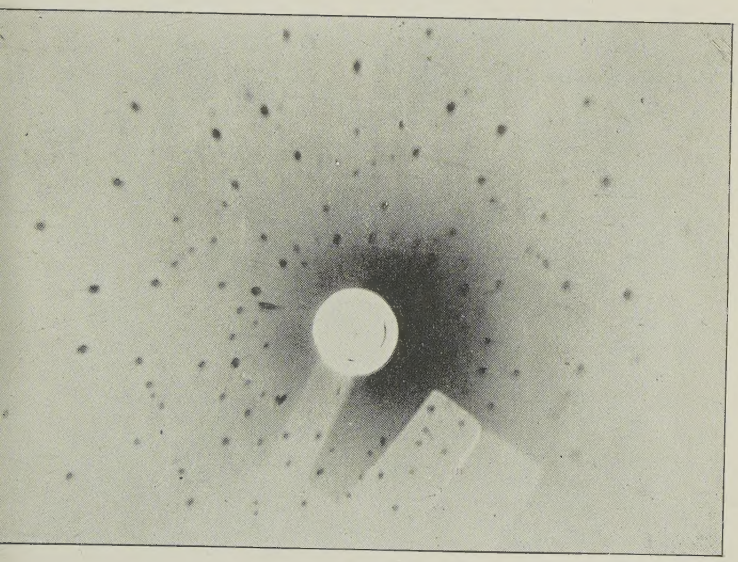

c.

Alloy (25·4 wt. per cent. Al).